IMPROVED CONTROL STRUCTURES AND METHODOLOGIES FOR LINEAR PROCESSES WITH DELAY

DOLA GOBINDA PADHAN

IMPROVED CONTROL STRUCTURES AND METHODOLOGIES FOR LINEAR PROCESSES WITH DELAY

A

Thesis Submitted

in Partial Fulfilment of the Requirements

for the Degree of

DOCTOR OF PHILOSOPHY

By

DOLA GOBINDA PADHAN

Department of Electronics and Electrical Engineering

Indian Institute of Technology Guwahati

Guwahati - 781 039, INDIA.

December, 2012

Certificate

This is to certify that the thesis entitled "**Improved Control Structures and Methodologies for Linear Processes with Delay**", submitted by **Dola Gobinda Padhan** (08610212), a research scholar in the *Department of Electronics & Electrical Engineering, Indian Institute of Technology Guwahati*, for the award of the degree of **Doctor of Philosophy**, has been carried out by him under my supervision and guidance. The thesis has fulfilled all requirements as per the regulations of the institute and in my opinion has reached the standard needed for submission. The results embodied in this thesis have not been submitted to any other University or Institute for the award of any degree or diploma.

Dated:
Guwahati.

Prof. Somanath Majhi
Dept. of Electronics & Electrical Engg.
Indian Institute of Technology Guwahati
Guwahati - 781039, Assam, India.

To my family ...

Acknowledgements

I would like to express my sincere gratitude to my supervisor, Prof. Somanath Majhi, for his helpful discussions, support and encouragement throughout the course for this work. His vision and passion for research influenced my attitude for research work and spurred my creativity. I would particularly like to thank for all his help in patiently and carefully correcting all my manuscripts.

I would like to thank my doctoral committee members Prof. C. Mahanta, Dr. Indrani Kar and Prof. S. K. Dwivedy for sparing their precious time to evaluate the progress of my work. Their suggestions have been valuable. I would also like to thank other faculty members for their kind help carried out during my academic studies. My special thanks to Mr. Sidananda, Mr. Sanjib, Mr. Goswami and all the members of the Control & Instrumentation Laboratory for maintaining an excellent computing facility and providing various resources useful for the research work.

I had a great time with my many friends at IIT Guwahati, including (but not limited to) Sanjoy, Bajarangbali, Utkal, Basudeb and Mandar. I thank them for their support and encouragement.

Specially, I wish to express my deep appreciation to my wife Nibedita for her unconditional support, love and understanding all these moments. I thank my daughter Dhriti for keeping me energetic and reducing my worries. Again, I am grateful to my parents, in-laws, sisters and brothers, whose love and encouragement made this research possible.

I am thankful to IIT Guwahati for providing the research scholarship to undertake my PhD research. Finally, I would like to thank the Almighty God for bestowing me this opportunity and showering his blessings on me to come out successful against all odds.

(Dola Gobinda Padhan)

Abstract

The aim of this thesis is to investigate various control structures and strategies for time delay processes. Time delays (dead times) appear in many processes in industry, economics, biology, communication networks etc. The presence of dead times complicates the control design and exerts severe limitations on the performance of such systems. Hence control structures that can potentially improve the performance of those processes are of central importance. Simple controllers, easy to design and tune, are very important in process industries. In this thesis, some control schemes based on a new but very simple Smith Predictor are presented. A simple modified Smith predictor control scheme with only two controllers is proposed for stable, unstable and integrating processes. The setpoint tracking controller is designed using H_2 optimal control method and an optimal IMC filter structure is proposed to design a PID controller that produces an improved disturbance rejection response. The proposed scheme can, by both analysis and simulation, yield great improvement of both setpoint and load disturbance responses over existing approaches.

In addition to the modified Smith predictor design for improved disturbance rejection, several cascade control structures combined with modified Smith predictor are proposed for processes with time delays. In this thesis, two series and two parallel cascade control structures are presented to improve the closed-loop performances and finally, a control structure and design method are suggested for Load frequency control of power system. A series cascade control structure with modified Smith predictor is presented for controlling open-loop unstable time delay processes. An analytical design method is derived for the disturbance rejection controllers by proposing the desired closed-loop complementary sensitivity functions. The direct synthesis method is used to design the setpoint tracking controller. The internal stability of the scheme is analyzed. For a class of integrating time delayed processes, a novel series cascade control structure to enhance the closed-loop performance is investigated. The inner loop controller is designed based on IMC approach and the primary setpoint filter is based on

optimal performance index. The primary load disturbance rejection controller, a PID controller in series with a lead/lag compensator, is designed on the basis of the desired closed-loop complementary sensitivity function. Next, a new parallel cascade control structure and controller design method are presented for controlling stable, unstable or integrating processes with time delay. The design of the disturbance rejection controller and the setpoint tracking controller are based on loop shaping and ISE performance measures, respectively. The stabilization, robustness and performances of time delay processes are analyzed. Another new parallel cascade control scheme is proposed for controlling stable and unstable processes with time delay. The two main features of the scheme are: the primary process output completely tracks the primary setpoint and the servo response decouples the regulatory response in the nominal system. The inner loop controller is designed based on IMC approach. The outer loop controller is a PID controller in series with lead/lag filter which is designed based on the desired complementary sensitivity function. Finally, a new control structure with a PID load frequency controller for power systems is presented. Initially, the controller is designed for single area power system, then it is extended to multi-area case. The control strategy is based on the desired complementary sensitivity function. The controller parameters are obtained by expanding the controller transfer function using a Laurent series. Relay based identification technique is adopted to estimate the power system dynamics. The control structures and simulation results presented in the thesis have both theoretical contributions and practical values. Simulation results are furnished to illustrate the effectiveness of the proposed approaches.

Contents

List of Figures

List of Tables

Nomenclature

FOPTD	First order plus time delay process model
IPTD	Pure integrating plus time delay process model
ISOPTD	Integrating second order plus time delay process model
UFOPTD	Unstable first order plus time delay process model
SOPTD	Second order plus time delay process model
USOPTD	Unstable second order plus time delay process model
ISE	Integral square error
IAE	Integral absolute error
ITAE	Integral of time weighted absolute error
TV	Total Variation
PD	Proportional derivative controller
PID	Proportional integral derivative controller
PI-PD	Proportional integral - proportional derivative controller
IMC	Internal Model Control
SISO	Single-Input Single-Output
MIMO	Multi Input Multi Output
LFC	Load Frequency Control
NRTWD	Non-reheat turbine without droop
NRTD	Non-reheat turbine with droop
RTWD	Reheat turbine without droop
RTD	Reheat turbine with droop

Mathematical Notations

G_p	Transfer function of a process
G	Transfer function of a process without time delay
θ	Time delay of a process
k	Steady state gain of a process
τ, τ_1, τ_2	Time constants of a process transfer function
G_m	Transfer function of a process model without time delay
θ_m	Time delay of a process model
G_{cs}	Transfer function of setpoint tracking controller
G_{cd}, G_{cd1}, G_{cd2}	Transfer functions of load disturbance rejection controllers
y, y_1, y_2	Output signals
u	Control variable
r, r_1, r_2	Setpoints / reference inputs
e	Error signal
d, d_0, d_1, d_2	Static load disturbances
t_r	Rise time
M_p	Maximum overshoot
t_s	Settling time
λ_{cs}	Tuning parameter of a setpoint controller
λ_{cd}	Tuning parameter of a load disturbance rejection controller
K_c or K_p	Proportional gain
T_i	Integral time
T_d	Derivative time
$a_1, a_2, a_3, b_1, b_2, b_3$	Filter parameters
θ_1	Time delay of primary process

θ_2	Time delay of secondary process
θ_{m1}	Time delay of primary process model
θ_{m2}	Time delay of secondary process model
K_{c1}, K_{c2}	Proportional gains
T_{i1}, T_{i2}	Integral times
T_{d1}, T_{d2}	Derivative times
$a_{f1}, a_{f2}, b_{f1}, b_{f2}, c_{f1}, c_{f2}, d_{f1}, d_{f2}$	Filter parameters
$\Delta_m(s)$	Process multiplicative uncertainty
$T_d(s)$	Closed-loop complementary sensitivity function
ω_{gc}	Gain crossover frequency
ϕ_m	Phase margin
A_m	Gain margin
M_s	Maximum of sensitivity function
M_{s1}	Maximum of sensitivity function for primary loop
M_{s2}	Maximum of sensitivity function for secondary loop
T_G	Time constant of a governor
T_T	Time constant of a turbine
T_P	Time constant of load and machine

List of Publications

Journal Publications

1. Padhan D.G. and Majhi S., "Modified Smith predictor and controller for time delay processes", *IET Electronics letter*, vol. 47(17), pp. 959-961, 2011.

2. Padhan D.G. and Majhi S., "Modified Smith predictor based cascade control of unstable time delay processes", *ISA Transactions, Elsevier*, vol. 51, pp. 95-104, 2012.

3. Padhan D.G. and Majhi S., "An improved parallel cascade control structure for processes with time delay", *IFAC Journal of Process Control, Elsevier*, vol. 22, pp. 884-898, 2012.

4. Padhan D.G. and Majhi S., "Enhanced cascade control for a class of integrating processes with time delay", *ISA Transactions (2012), Elsevier*, http://dx.doi.org/10.1016/j.isatra.2012.08.004

5. Padhan D.G. and Majhi S., "A new control scheme for PID load frequency controller of single-area and multi-area power systems", *ISA Transactions (2012), Elsevier*, http://dx.doi.org/10.1016/j.isatra.2012.10.003

Conference Publications

1. Padhan D.G. and Majhi S.,"Synthesis of PID tuning for a new parallel cascade control structure", *IFAC Conference on Advances in PID Control PID'12*, 28-30 March 2012, Brescia, Italy.

2. Padhan D.G. and Majhi S.,"Improved parallel cascade control structure for time delay processes", *IEEE INDICON*, 16-18th December 2011, Hydrabad, India.

3. Padhan D.G. and Majhi S.,"A two-degree-of-freedom control scheme for improved performance of unstable delay processes", *IEEE ICECE*,18-20 December 2010, Dhaka, Bangladesh.

4. Padhan D.G. and Majhi S.,"Modified Smith predictor and controller for stable and unstable processes ", *4th International Conference CERA09*, 19-21 February 2010, IIT Roorkee, India.

5. Padhan D.G. and Majhi S.,"An improved cascade control structure for time delay processes", *NSC-2011*, 9-11 December 2011, IIT Bhubaneswar, India.

6. Padhan D.G. and Majhi S.,"A two-degree-of-freedom control scheme for improved performance of integrating delay processes ", *NSC-2010*, ,10-12 December 2010, NITK Surathkal, India.

7. Padhan D.G. and Majhi S.,"Modified Smith predictor and controller based on GM(1,1) model", *NCET-2010*, 16-17 April 2010, Goa, India.

1

Introduction

Contents

1.1 Dead time compensator

The control of processes involving time delays has attracted the attention of many researchers in the past few years [1–4]. This is due to the fact that many processes present delay in their input or output and in many cases these delays are responsible for instabilities in closed-loop control systems. A time delay may be defined as the time interval between the start of an event at one point in a system and its resulting action at another point in the system. Delays are also known as transport lags or dead times. Time delays are important phenomena in industrial processes, economical, chemical and biological systems. For instance, they appear as transportation and communication lags and also arise as feedback delays in control loops [5]. Compared to processes without delays, the presence of a delay in the process greatly complicates the analytical aspects of the control system design, making it more difficult to achieve a satisfactory level of control [4, 6]. Conventional controllers, such as Proportional-Integral-Derivative (PID) controllers in simple single-input single-output (SISO) systems, can be used when the delay is small but they show poor performance when the process exhibits long delays, because a significant amount of detuning is required to maintain closed-loop stability [7]. The Smith predictor [8] is a well-known feedback structure and effective dead-time compensator for stable processes. Its attractiveness comes from the fact that it allows design to be performed using techniques which apply to processes with rational transfer functions. In this scheme, a mathematical model of the process is implemented in an internal feedback loop around a conventional controller. The major advantage of the Smith predictor is that the delay is effectively taken outside the control loop in the transfer function relating the process output to setpoint. Therefore, a simple conventional controller (such as PI and PID) can be used in this system. The schematic diagram of the Smith predictor control structure is shown in Figure 1.1, where G_c is a conventional controller, d is an input disturbance, G is a delay-free plant, G_m is a delay-free nominal model of G, θ is a real time delay and θ_m is an estimated time delay. The closed-loop transfer function can be written as

$$\frac{Y(s)}{R(s)} = \frac{G_c G e^{-\theta s}}{1 + G_c G_m [1 - e^{-\theta_m s}] + G_c G e^{-\theta s}} \tag{1.1}$$

If the model of the process $G_m e^{-\theta_m s}$ is exactly equal to the process $G e^{-\theta s}$, then the closed-loop transfer function can be reduced to

$$\frac{Y(s)}{R(s)} = \frac{G_c G}{1 + G_c G} e^{-\theta s} \tag{1.2}$$

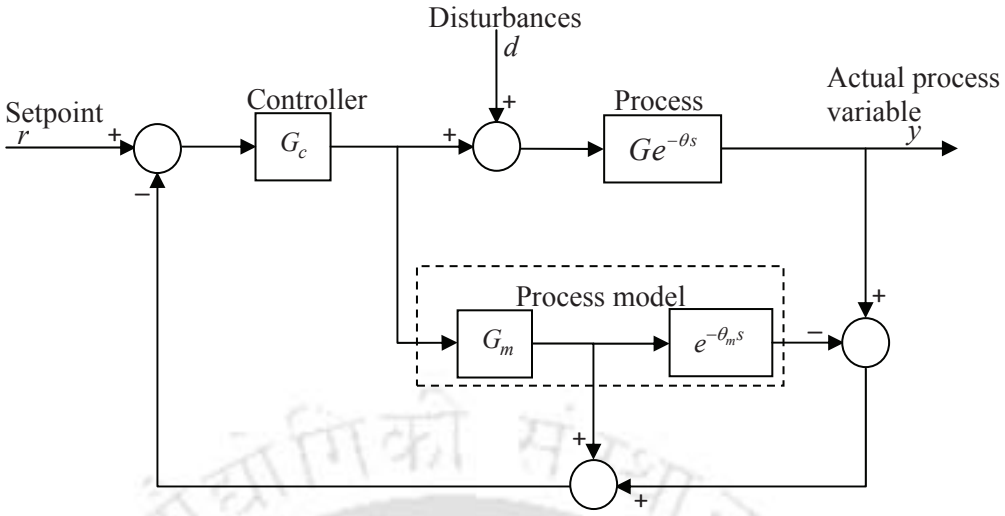

Figure 1.1: Smith predictor control structure

Note that the time delay is no longer in the characteristic equation. Figure 1.2 is an equivalent block diagram of the system in Figure 1.1 when $d = 0$. However, the Smith predictor is sensitive to

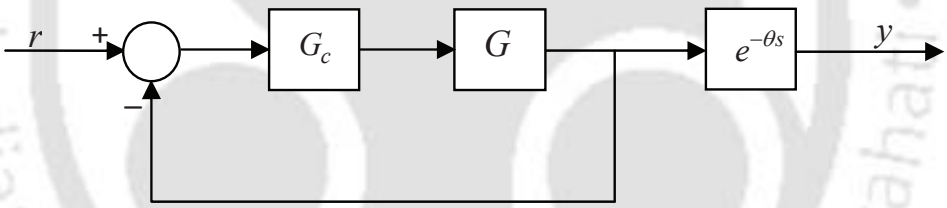

Figure 1.2: Equivalent Smith predictor control structure

model mismatch and has poor disturbance rejection capability. How to overcome these shortcomings is the subject of numerous studies. The Smith Predictor [9] and its many extensions, generally based on process model control schemes [6], and the finite spectrum assignment methodology [10] can be considered as the first control methods for SISO linear processes showing a delay in their input or output [2,4]. A close analysis of these methods and their modifications points out that they all use, in an implicit or explicit manner, a prediction of the state in order to achieve the control of the system. Different modifications have been proposed to simplify and improve the tuning of the controller based on the application of the Smith predictor [6, 7, 11–18], to reject load disturbances for process with integration and long dead-time [19–26], and to control unstable systems with delays [27–34], but they

are either too complex for an industrial implementation or they fail to control unstable systems with very long delays. In an industrial application a simple and easy to tune control structure is always desirable.

1.2 Cascade control structures

The achievement of satisfactory performances in addition to a fast setting-up are essential requirements for a control system to be adopted in the industrial context. PID controllers are widely adopted in industry because acceptable performances can be obtained by adopting one of the many tuning methods, based on a simple modelling of the plant, that have been devised in the last few decades, or even by a trial and error procedure. When more demanding control specifications are required for a given application, PID controllers can be still adopted as a basis of more complex control structures where couplings between simple control systems are exploited. A typical example in this context is cascade control, which is a multi-loop control structure commonly used in process industries [35]. Cascade control structures are very effective when the single-loop PID controller finds difficulty in regulating the output in the face of load disturbances. The idea of cascade structure is that the effect of the disturbance on the main controlled variable is reduced by an internal (or secondary) loop when an intermediate measurement is available. Generally a cascade control structure

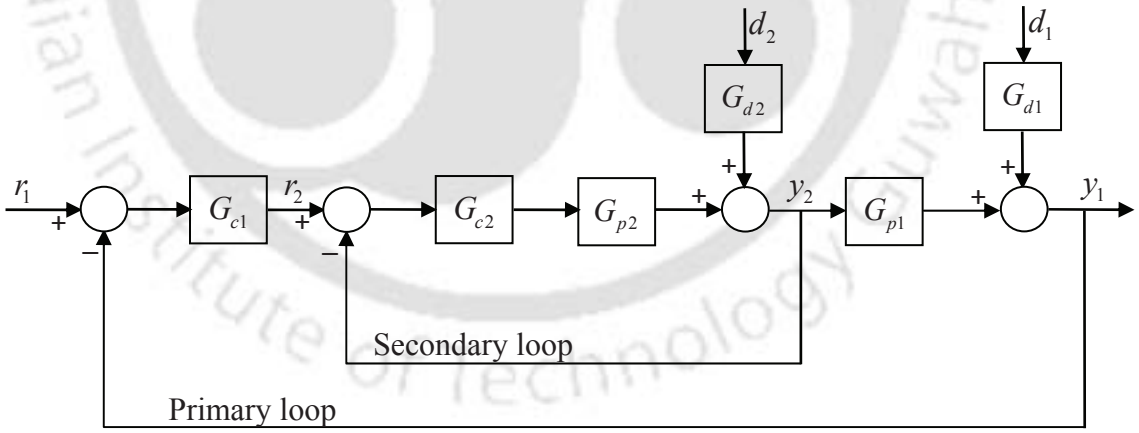

Figure 1.3: Series cascade control structure

is composed of two control loops, i.e. a secondary (inner or slave) loop embedded within a primary (outer or master) loop. Load disturbances that seep into the inner loop are supposed to be reduced or counteracted before they extend to the outer loop. Therefore it is crucial that the inner loop takes

on faster dynamical response in comparison with the outer loop for these load disturbances. Cascade control structures are of two types: series cascade control and parallel cascade control.

In series cascade control (as shown in Figure 1.3), both the manipulated variable and the disturbance affects directly one intermediate (secondary) variable and this in-turn affects the primary controlled variable. The manipulated variable r_2 affects directly one intermediate variable (y_2) and this in-turn affects the primary controlled variable (y_1). The primary loop controls the controlled variable y_1 by manipulating the setpoint of the secondary controller G_{c2}. Thus we have the same controlled variable and setpoint as in a single feedback loop but the control valve has been augmented by an inner control loop. The disturbances G_{d2} are rejected by the secondary loop before they affect the main process, and thus response is quicker and the impact on y_1 is less. The primary loop is necessary to handle the other disturbances, such as G_{d1} that always exist.

A parallel cascade control (as shown in Figure 1.4) is one in which both the manipulated variable and the disturbances affect the primary and secondary outputs simultaneously. In the Figure 1.4, G_{p1} and G_{p2} are the transfer functions of the primary and secondary processes respectively. G_{c1}

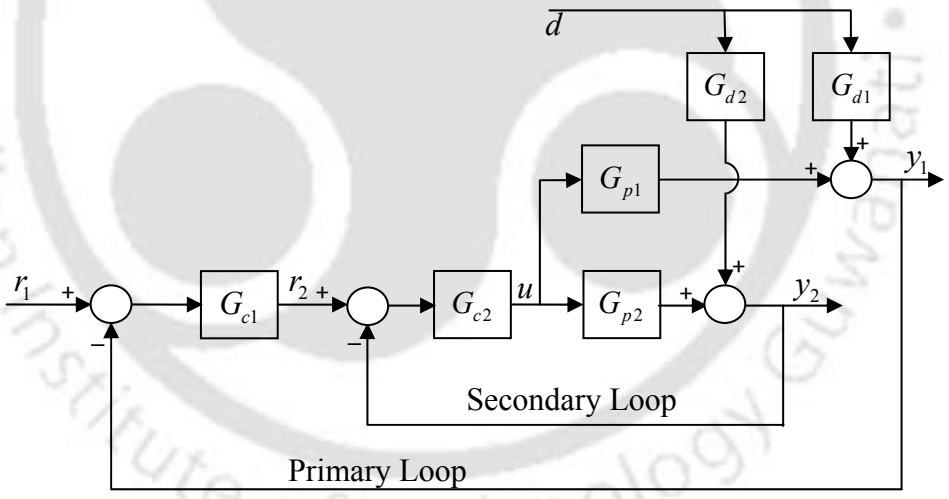

Figure 1.4: Parallel cascade control structure

and G_{c2} are the primary and secondary controllers. G_{d1} and G_{d2} are the transfer functions of the disturbances for primary and secondary loops respectively. Parallel cascade control is appropriate when the secondary loop has a faster dynamic response and the rejection of the disturbance in the secondary output reduces the steady state output error in the primary loop. The parallel cascade

control is also beneficial when measurements of the primary output are sampled infrequently and/or with long time delays. The design of the overall control system involves the tuning of two (PID) controllers. Usually, the secondary controller is tuned first by setting the primary controller in manual mode. Then, the primary controller is tuned while the previously tuned secondary controller is applied to the inner loop. It appears that the design procedure is longer and more complicated than that of a standard single-loop (PID) control. The existence of both series and parallel cascade control systems is discussed by Luyben [36]. Because of the wide applications of cascade control in the process industries, several researchers have focused on series cascade control [37–42] and parallel cascade control [43–49] methodologies.

1.3 Load frequency control

With an increasing demand for electric power, the electric power system becomes more and more complicated. Therefore the supply of electric power with stability and high reliability is required. Normally, the power system operates in normal state which is characterized by constant frequency and voltage profile with certain system reliability. For a successful operation of power system under abnormal conditions, mismatches have to be corrected via supplementary control [50]. Automatic Generation Control (AGC) or Load Frequency Control (LFC) is one of the most important issues in electric power system design and operation for supplying sufficient and reliable electric power with good quality [51].

The main objectives of LFC for a power system are given below

(i) The steady state frequency error following a step load change should vanish. The transient frequency and time errors should be small.

(ii) Unscheduled tie line power flows between neighboring control areas need to be minimised.

(iii) The static change in the tie power following a step load in any area should be zero, provided each area can accommodate its own load change.

(iv) The frequency and tie line power deviations need to be maintained with acceptable overshoot and settling time.

The LFC scheme has evolved over the past few decades and is in use on interconnected power systems. There has been continuing interest in designing LFC with better performance to maintain the frequency and keep tie-line power flows within pre-specified values using various control methodologies.

The load frequency control problem has been investigated by many researchers. The LFC mechanism is well discussed in [52, 53]. An integral controller provides zero steady state frequency deviation but it exhibits poor dynamic performance. To improve the transient response, various control techniques, such as linear feedback, optimal control and variable structure control have been proposed [54–56]. Adaptive controllers with self adjusting gain settings have also been proposed for the LFC problem [57–60]. Artificial neural networks have been successfully applied to the LFC problem with rather promising results [61, 62]. Kothari et al. [63] obtained an optimum integral and proportional integral (PI) controllers by using the concept of stability and techniques with conventional area control error (ACE). Velusami and Chidambaram [64] proposed a decentralized (PI) biased dual mode controllers for two area interconnected thermal power system. Malik et al. [65] developed a generalized approach based on the concepts of discontinuous control, dual-mode control and variable structure systems. Their proposed generalized approach was used to develop an LFC algorithm which was tested on a multi-area interconnected power system. Rao and Ahson [66] examined the use of a two-level control scheme for a two-area power system with nonlinear interactions between the areas. Rubaai and Udo [67] proposed a multilevel adaptive load frequency controller which is based on the self tuning-regulator. Khodabakhshian and Hooshmand [68] proposed a new PID controller design for automatic generation control of hydro power systems. Abraham et al. [69] designed an automatic generation controller for an interconnected hydrothermal power system considering super-conducting magnetic energy storage. Wang et al. [70, 71] proposed a simple, robust controller, which is based on the Riccati equation approach; only the bounds of the system parameters are required to design a robust load frequency controller. Yamashita and Miyagi [59] devised a method for designing a multi variable self tuning-regulator for an LFC system with the inclusion of the interaction of voltage on load demand.

1.4 Motivation

In control engineering, the objective is to achieve a feasible control signal, which based on measurements, affects the controlled process to behave in a desired way, despite disturbances acting from the environment. The control system is an integral part in ensuring the quality and productivity in many process industries. In the rapidly changing world of global competition, control engineers faced with more stringent conditions such as strict environmental regulations and highly integrated processes,

have to design better performance control systems to meet the continuously evolving objectives. As processes tend to become more tightly integrated, the control structure design becomes more important and a more difficult task. Most available control theories and design methods assume that the control structure is given prior to the design. That is, they do not explicitly address the structural decisions involved in the control structure design. This has resulted in a gap between control theory and process control applications. The main objective of this thesis is to provide new theory and tools in order to reduce this gap. Basically, a good control system has to respond fast with minimal overshoot to the input command signal and also show robustness to process uncertainties. The core of a good control system has to be a well-tuned process controller, yet for the many different types of processes encountered in the process industries, a single set of tuning rules does not usually apply to all when achieving good performance is of concern. So, in this thesis, different control structures and approaches are developed to improve existing control techniques and also suggest new ways of tuning process controllers.

In the field of Industrial process control, improved productivity, efficiency and product goals generate a demand for more effective control strategies to be implemented in the production line. From the industrial perspective, the performance, robustness and real constraints of control systems become more important to ensure strong competitiveness. All these requirements call for a strong need for new approaches to improve the performance for industrial process control. Therefore, this thesis is motivated to explore new control schemes and techniques for improved performance of industrial process control systems.

Although advanced control techniques are necessary in many industrial control problems, interestingly the PID control remains a control strategy that has been successfully used over the years. Simplicity in use, robustness, a wide range of applicability and near-optimal achievable performance are some of the factors that have made PID control so attractive in both the academic and industry sectors. For these reasons, in industrial process control applications, more than 90% of the controllers are of PID type [72]. PID controller exhibits good performance for linear and small time delay systems. In process industries many control loops show long dead-time characteristics. However, processes with long time-delays can not be controlled effectively using a simple PID controller. This is due to the additional phase lag contributed by the time delay which tends to destabilize the closed-loop system. The stability problem can be solved by decreasing the controller gain. However, in this case the

response obtained is very sluggish.

Many control designs focus on setpoint response, but overlook disturbance rejection performance. However, in industrial control practice, there is no doubt that disturbance rejection is much more important than setpoint tracking [72], since the setpoint reference signal may be kept unchanged for years, and the system performance is mainly affected by varying disturbances [73]. In fact, countermeasure of disturbance is one of the key factors for successful and failed applications. In view of the great importance of disturbance rejection in process control, good solutions have been sought for a long time. To cope with the disturbance, one possible way is to design the single controller in the feedback system, where trade-off has to be made between the setpoint response and disturbance rejection performance. As for conventional PI or PID methods within the framework of a unity feedback control structure, many improved tuning rules have been provided [74–78]. However, owing to the water-bed effect between the setpoint response and the load disturbance response, the improvement of the disturbance response is not significant. The setpoint response is usually accompanied with excessive overshoot and large settling time when the time delay is significant. A better approach is to introduce an additional controller to manipulate the disturbance rejection. Thus, it is highly appealing for a new control scheme and controller design method to provide substantial improvement on disturbance rejection.

In control industries, unstable systems are fundamentally and quantifiably more difficult to control than stable ones. This is mainly due to the facts that controllers for unstable systems are operationally critical, and that closed-loop systems with unstable components are only locally stable. Therefore, unstable process control has been an active research area in recent years. It is therefore motivated to devise a new control scheme for unstable time delay processes, which could enable manipulation of disturbance transient response without causing any loss of the existing benefits of the previous schemes and is robust against modelling errors.

Controlling processes with long time delays and subjected to strong disturbances with the standard feedback control loop sometimes does not result in good enough performance [79]. Cascade control [37] is one strategy that can be used to improve disturbance rejection performance in several situations. The idea of cascade control structure is that the effect of the disturbance on the main controlled variable is reduced by an internal (or secondary) loop when an intermediate measurement is available. Control strategies that combine cascade control with dead-time compensation structures

are interesting solutions to control unstable or integrating processes with significant dead times and subjected to strong disturbances in the inner loop. Because of this, in the past few years this subject has attracted the attention of several researchers [42, 80–82]. However, the control structures involve many controllers, and the design methods are difficult to be used.

The LFC scheme has evolved over the past few decades and is in use on interconnected power systems. There has been continuing interest in designing LFC with better performance to maintain the frequency and keep tie-line power flows within prespecified values using various control methodologies. Operating the power system in a new environment will certainly be more complex than in the past, due to the considerable degree of interconnection, and to the presence of technical constraints to be considered together with the traditional requirements of system reliability. In response to the new challenges, novel modeling and control approaches are required to get a new trade off between efficiency and robustness. At present, the power system utilities participate in LFC task with simple, heuristically tuned controllers. In response to the new technical control demands for large scale power systems, the main motivation of the present thesis is to develop new LFC synthesis methodologies for multi-area power systems based on fundamental LFC concepts and generalized well-tested traditional LFC scheme, to meet all or a combination of following specifications: robustness, decentralized property, simplicity of structure, cover all the specified LFC objectives, formulation of uncertainties and constraints.

1.5 Contributions of this Thesis

This thesis aims at improving existing control techniques and developing new approaches for tuning process controllers. Several new control schemes are addressed for single variable linear processes in industrial process control, aiming to improve the performance, disturbance response and system robustness. In particular, the thesis has investigated the following areas:

I. Design of Modified Smith Predictor Controllers

A simple method of designing the controllers for the modified Smith predictor scheme with improved closed-loop performances is proposed for time delay processes. The proposed structure consists of two controllers that are meant for different objectives, namely, the setpoint tracking and the load disturbance rejection. The H_2 optimal control method is used to design the setpoint tracking controller, and an optimal IMC filter structure is proposed to design a PID controller that produces an

improved disturbance rejection response. The control structure gives two-degrees-of-freedom control and correspondingly the setpoint and load disturbance responses can each be tuned conveniently by a single control parameter. Robustness studies on the stability and performance are provided, with respect to the uncertainties in the process model parameters. The effectiveness of the proposed technique is verified by simulation results.

II. Enhanced Series Cascade Control Structure for Unstable Delay Processes

A series cascade control structure with modified Smith predictor is presented for controlling open-loop unstable time delay processes. The proposed structure has three controllers of which one is meant for servo response and the other two are for regulatory responses. An analytical design method is derived for the two disturbance rejection controllers by proposing the desired closed-loop complementary sensitivity functions. These two closed-loop controllers are considered in the form of PID controller cascaded with a second order lead/lag filter. The direct synthesis method is used to design the setpoint tracking controller. By virtue of the enhanced structure, the proposed control scheme decouples the servo response from the regulatory response in case of nominal systems i.e., the setpoint tracking controller and the disturbance rejection controllers can be tuned independently. Internal stability of the proposed cascade structure is analyzed. Kharitonov's theorem is used for the robustness analysis. The disturbance rejection capability of the proposed scheme is superior as compared to some existing methods.

III. Improved Series Cascade Control Structure for Integrating Delay Processes

Unlike self-regulating processes, cascade control strategies for control of integrating processes with time delay are limited. A novel series cascade control structure to enhance the closed loop performance is proposed for integrating and time delay processes. It realizes two-degree-of-freedom control in the primary loop. The proposed control structure has only two controllers and a setpoint filter. The inner loop controller is designed based on IMC approach and the primary setpoint filter is based on optimal performance index. The primary load disturbance rejection controller, a PID controller in series with a lead/lag compensator, is designed on the basis of the desired closed-loop complementary sensitivity function. The robustness analysis is carried out using Kharitonov's theorem. Simulation results demonstrate the efficacy of the proposed method by showing satisfactory nominal and robust performances.

IV. Modified Smith Predictor based Parallel Cascade Control Structure

To improve the dynamic performance of a control system, parallel cascade control strategies have been proposed earlier mainly for control of stable processes. In this thesis, further results are presented for a new parallel cascade control structure and controller design for controlling stable, unstable or integrating processes with time delay. The design of the disturbance rejection controller and the setpoint tracking controller are based on loop shaping and ISE performance measures, respectively. A modified Smith predictor scheme is used in the primary loop to enhance the closed-loop performance of the system. Based on the Nyquist stability theorem, the stabilization of typical time delay processes is investigated. For each process, the maximum stabilizable normalized time delay for different controllers is derived. The robustness and performances of time delay processes are analyzed. Examples are given to illustrate the usefulness of the proposed method and its superiority over some parallel cascade control schemes.

V. A New Parallel Cascade Control Scheme for Unstable Delay Processes

A new parallel cascade control scheme is proposed for controlling stable and unstable processes with time delay. The two main features of the proposed scheme are: the primary process output completely tracks the primary setpoint and the servo response decouples the regulatory response in the nominal system. The control structure has only two controllers. The inner loop controller is designed based on IMC approach. The outer loop controller is a PID controller in series with lead/lag filter which is designed based on the desired complementary sensitivity function. Significant improvement in the load disturbance rejection performances are obtained when compared to some recent methods in the literature.

VI. A New Control Scheme for PID Load Frequency Controller of Power Systems

A new control structure with a PID load frequency controller for power systems is presented. Initially, the controller is designed for single-area power system, then it is extended to multi-area case. The control strategy is based on the desired complementary sensitivity function. The controller parameters are obtained by expanding the controller transfer function using a Laurent series. Relay based identification technique is adopted to estimate the power system dynamics. Robustness studies on the stability and performance are provided, with respect to the uncertainties in the plant parameters. The proposed scheme ensures that the overall system remains asymptotically stable for all bounded uncertainties and for system oscillations.

1.6 Thesis Organization

The thesis is organized as follows. Chapter 2 presents a new modified Smith predictor control structure for time delay processes. Chapter 3 discusses the use of modified Smith predictor in the outer loop of series cascade control structure to enhance the closed-loop performances for unstable time delay processes. Chapter 4 is devoted to a new series cascade control structure for a class of integrating time delay processes, where the novel design of the disturbance rejection controller enables significantly improved disturbance rejection. In Chapter 5, a control strategy that combines a parallel cascade control structure with modified Smith predictor to enhance the closed-loop performances of time delayed processes is presented. Chapter 6 is concerned with a PID controller design for a new parallel cascade control structure for unstable delay processes. Chapter 7 addresses a new control structure for PID load frequency controller of single-area and multi-area power systems. Finally in Chapter 8, general conclusions are given and suggestions for further works are presented.

2

Design of Modified Smith Predictor Controllers

Contents

Resume

This chapter presents a simple dead time control structure with less number of controller to improve the closed-loop performances for processes with delay. The H_2 optimal control method and IMC approach are used to design the setpoint tracking controller and the load disturbance rejection controller, respectively. The regulatory response controller parameters are obtained by expanding the controller transfer function using a Maclaurin series. The overall control structure has only two physically meaningful tuning parameters. One is used to set the speed of the closed-loop servo response and the other tuning parameter is used to set the speed of the closed-loop load response. An advantage of the structure is that setpoint tracking and disturbance rejection can be designed separately. The comparative analysis shows that particularly the disturbance rejection capability of the proposed control structure is superior than the other methods. Six examples are included to demonstrate the improved closed-loop performance of the proposed controller design.

The work presented in this chapter is published [83], [84] and [85].

2.1 Introduction

Plants with long time delays can mostly not be controlled effectively using a PID controller in the conventional single feedback loop structure because a significant amount of detuning is required to maintain closed-loop stability. The stability problem can be solved by decreasing the controller gain. However, in this case the response obtained is very sluggish. The Smith predictor is a popular and very effective control system structure which was proposed for controlling of the stable processes with long dead-time firstly. However, this approach fails in a very significant way for an unstable process due to the problem of stabilization. Furukawa et al. [86] augmented the scheme with an observer, Watanabe et al. [6] pointed out that a Smith predictor results in a steady-state error for integrating processes if a disturbance enters into the system and De Paor's [87] approach has a severe constraint on the ratio of dead-time to the time constant. Later on, De Paor et al. [88] extended and partially optimized the modified Smith predictor and controller [87] to relax the constraint on the ratio, but there is no significant extension to the ranges of that ratio for which closed loop asymptotic stability can be achieved. These cited authors have thus solved the stabilization problem by involving greater complexity than the Smith predictor. Since then, a number of methods have been proposed to overcome the problem of controlling a process with an integrator and long dead time. A modified

structure to decouple the setpoint response from the disturbance response, improving the last one, is presented by Åström et al. [19]. Mataušek et al. [20] proposed a structure similar to that of Åström et al. [19] but having an additional feedback path from the difference of the plant output and the model output to the reference input. The modified Smith predictor structure suggested by Majhi and Atherton [27] has three controllers as shown in Fig. 2.1. When the plant model perfectly matches the plant dynamics i.e. $G_m = G$ and $\theta_m = \theta$, the closed-loop transfer function for setpoint and disturbance inputs are, respectively

$$Y_r(s) = \frac{GG_c e^{-\theta s}}{1 + G(G_c + G_{c1})} \tag{2.1}$$

$$Y_d(s) = \frac{Ge^{-\theta s}}{1 + G(G_c + G_{c1})} \frac{1 + G(G_c + G_{c1}) - GG_c e^{-\theta s}}{1 + GG_{c2} e^{-\theta s}} \tag{2.2}$$

The characteristic polynomial of the setpoint transfer function $Y_r(s)$ $(= Y(s)/R(s))$ under the model

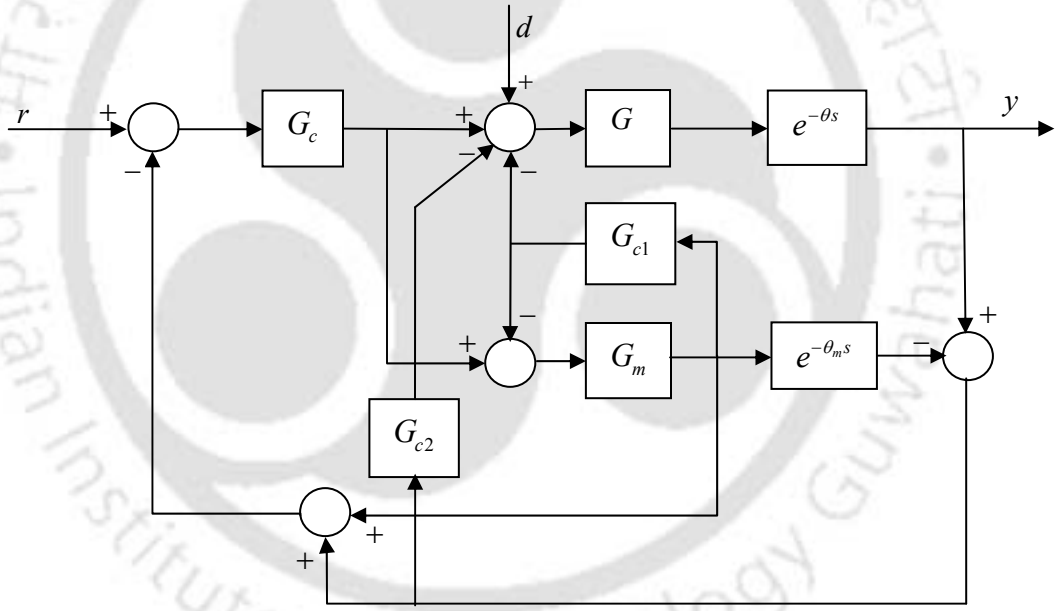

Figure 2.1: Majhi and Atherton's Smith predictor structure

matching condition is free from time delay term and therefore contribute to obtaining the smooth setpoint response. However, the load disturbance transfer function $Y_d(s)(= Y(s)/D(s))$ is rather complicated and involves all three controllers. It is a considerable challenge to tune the three controllers simultaneously to reject the load disturbances in an optimal way. Moreover, the setpoint response is coupled with the load disturbance response when tuning the controllers G_c and G_{c1}. In addition, how

to compromise between the setpoint and load disturbance response is another challenge, which is not explicitly interpreted in [27]. Recently, Lu et al. [31] have proposed a double two-degrees-of-freedom control scheme with four controllers as shown in Fig. 2.2. In the nominal case, the closed-loop transfer

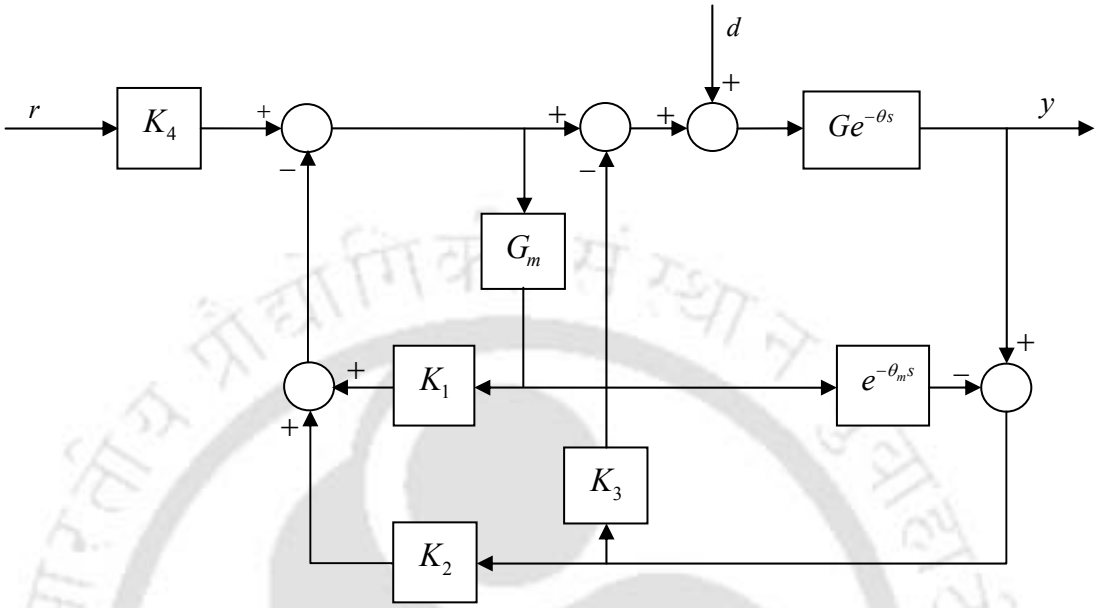

Figure 2.2: Lu et al.'s Smith predictor structure

function for the setpoint input is given by

$$Y_r(s) = \frac{GK_4}{1 + GK_1} e^{-\theta s} \tag{2.3}$$

and for the load disturbance input, the transfer function is

$$Y_d(s) = \frac{Ge^{-\theta s}(1 + GK_1 - Ge^{-\theta s}K_2)}{(1 + GK_1)(1 + Ge^{-\theta s}K_3)} \tag{2.4}$$

In Lu et al.'s method also the disturbance rejection transfer function contains three controllers and simultaneous tuning of three controllers is difficult. Kaya [89] and Liu et al. [32, 90] have proposed modified Smith predictor schemes with three controllers. However, many existing methods are sensitive to the model uncertainty and thus, it is tough to achieve the desired closed-loop response. Most of the methods discussed above have complicated control structures with a number of controllers. Practically, a simple control structure with less number of controllers is desirable for ease in plant operations.

In this chapter, to overcome the above deficiencies a new Smith predictor structure is presented. Tun-

ing rules are derived for controllers of the proposed structure for effective control of stable, unstable and integrative plants. Disturbance rejection in process industries is commonly much more important than setpoint tracking for many process control applications [72]. This innovative scheme leads to substantial control performance improvement, especially for the disturbance rejection. Several simulation examples are provided to show the superiority of the proposed design method, compared with recently reported methods.

The rest of the chapter is organized as follows. Section 2.2 describes the new Smith predictor structure. In Section 2.3, the controller design methods are discussed for six typical industrial processes followed by Section 2.4 in which the selection of tuning parameter is given. Section 2.5 deals with robustness analysis and performances. Simulation results are presented in Section 2.6. The chapter ends with the conclusions.

2.2 Modified Smith predictor

The structure of the modified Smith predictor for controlling stable, unstable and integrating processes is shown in Fig. 2.3. In the figure, G_{cs} is the setpoint tracking controller and G_{cd} is the disturbance rejection controller. Even though G_{cd} is meant for load disturbance rejection, it also takes part in stabilizing the unstable and integrating processes with time delay. Obviously, both G_{cs} and G_{cd} take independent responsibility for overall system performances. Most importantly, by virtue of the enhanced structure, the setpoint response is apparently decoupled from the load disturbance response. This is a dominant advantage of the proposed control structure. The closed-loop response to setpoint and disturbance inputs can be given by

$$Y(s) = Y_r(s)R(s) + Y_d(s)D(s) \tag{2.5}$$

where

$$Y_r(s) = \frac{G_{cs}Ge^{-\theta s}(1 + G_m G_{cd}e^{-\theta_m s})}{(1 + G_m)(1 + G_{cd}Ge^{-\theta s})} \tag{2.6}$$

$$Y_d(s) = \frac{Ge^{-\theta s}}{1 + G_{cd}Ge^{-\theta s}} \tag{2.7}$$

and $G_m e^{-\theta_m s}$ and $Ge^{-\theta s}$ are the transfer functions of the plant model and the plant, respectively. Based on the assumption that the model used perfectly matches the plant dynamics that is $G_m = G$

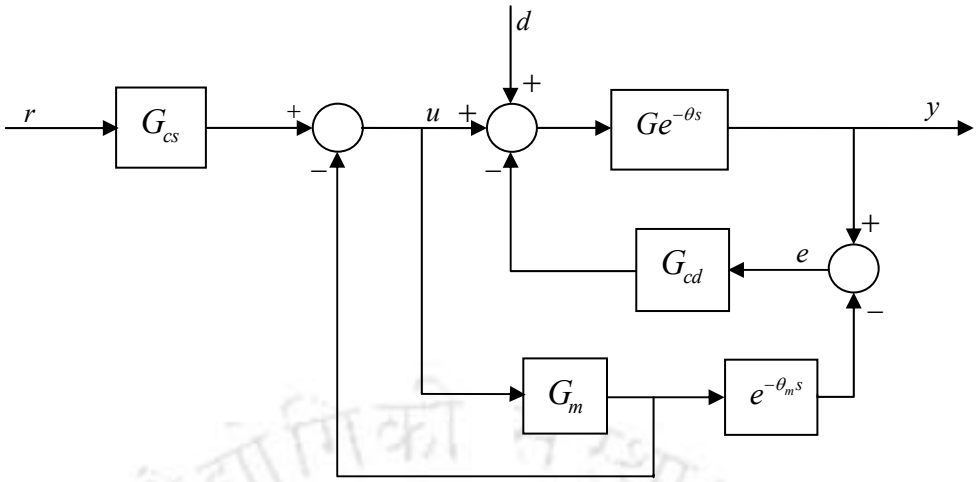

Figure 2.3: New Smith predictor structure

and $\theta_m = \theta$, (2.6) and (2.7) reduce to

$$Y_r(s) = \frac{G_{cs}Ge^{-\theta s}}{1+G} \tag{2.8}$$

$$Y_d(s) = \frac{Ge^{-\theta s}}{1+G_{cd}Ge^{-\theta s}} \tag{2.9}$$

It is apparent from (2.8) and (2.9) that the new Smith predictor has decoupled the load disturbance response from the setpoint response. (2.9) shows that the load disturbance response will be unstable when $G_{cd} = 0$ and the plant is unstable.

2.3 Controller design procedures

The dynamics of a large number of industrial processes with time delay can be represented by the following typical transfer function models:

- pure integrating process plus time delay,

$$G_p = \frac{ke^{-\theta s}}{s} \tag{2.10}$$

- first order plus time delay,

$$G_p = \frac{ke^{-\theta s}}{\tau s + 1} \tag{2.11}$$

- integrating second order plus time delay,

$$G_p = \frac{ke^{-\theta s}}{s(\tau s + 1)} \tag{2.12}$$

- unstable first order plus time delay,

$$G_p = \frac{ke^{-\theta s}}{\tau s - 1} \tag{2.13}$$

- stable second order plus time delay,

$$G_p = \frac{ke^{-\theta s}}{(\tau_1 s + 1)(\tau_2 s + 1)} \tag{2.14}$$

- unstable second order plus time delay,

$$G_p = \frac{ke^{-\theta s}}{(\tau_1 s - 1)(\tau_2 s + 1)} \tag{2.15}$$

Again when a process is of higher order, it can be reduced to any of the above mentioned process models by using the relevant model reduction method.

2.3.1 Design of G_{cs}

The setpoint tracking controller (G_{cs}) is designed based on H_2 optimal control specification method, $\min\|e\|_2^2$. The system performance objective is achieved by implementing $\min\|W(s)(1 - Y_r(s))\|_2^2$ for the proposed structure, where $W(s)$ is a setpoint input weight function. $W(s)$ is selected as $\frac{1}{s}$ for the step changes of the setpoint input and load disturbances in industrial and chemical practice.

Consider a process $G_p = ke^{-\theta s}/(\tau_1 s \pm 1)(\tau_2 s + 1)$. Using the n/n order all-pass Padé approximation of the time delay $e^{-\theta s}$, it becomes

$$G_p = \frac{kP_{nn}(-\theta s)}{(\tau_1 s \pm 1)(\tau_2 s + 1)P_{nn}(\theta s)} \tag{2.16}$$

where

$$P_{nn}(\theta s) = \sum_{j=0}^{n} \frac{(2n-j)!n!}{(2n)!j!(n-j)!}(\theta s)^j \tag{2.17}$$

and n is chosen to be an integer large enough to guarantee that the approximation error can be neglected in comparison with the process model mismatch in practice. Again, using (2.8) when there is no model mismatch, it follows that

$$\begin{aligned} \|W(s)(1-Y_r(s))\|_2^2 &= \left\| \frac{1}{s}\left(1 - \frac{kG_{cs}(s)P_{nn}(-\theta s)}{[(\tau_1 s \pm 1)(\tau_2 s+1)+k]\,P_{nn}(\theta s)}\right)\right\|_2^2 \\ &= \left\| \frac{P_{nn}(\theta s)}{sP_{nn}(-\theta s)} - \frac{kG_{cs}(s)}{s\,[(\tau_1 s \pm 1)(\tau_2 s+1)+k]}\right\|_2^2 \end{aligned} \tag{2.18}$$

It is noted that $P_{nn}(0) = 1$ and all zeros of $P_{nn}(-\theta s)$ are in the right hand side of the s plane. Using the orthogonality property of the H_2 norm, we get

$$\begin{aligned} \|W(s)(1-Y_r(s))\|_2^2 &= \left\| \frac{P_{nn}(\theta s) - P_{nn}(-\theta s)}{sP_{nn}(-\theta s)}\right\|_2^2 \\ &\quad + \left\| \frac{[(\tau_1 s \pm 1)(\tau_2 s+1)+k] - kG_{cs}(s)}{s\,[(\tau_1 s \pm 1)(\tau_2 s+1)+k]}\right\|_2^2 \end{aligned} \tag{2.19}$$

In order to obtain a optimal controller, minimizing the right hand side of the above expression (equating its second term to zero) i.e.

$$\frac{[(\tau_1 s \pm 1)(\tau_2 s+1)+k] - kG_{cso}(s)}{s\,[(\tau_1 s \pm 1)(\tau_2 s+1)+k]} = 0 \tag{2.20}$$

we obtain the optimal controller

$$G_{cso} = \frac{(\tau_1 s \pm 1)(\tau_2 s+1)+k}{k} \tag{2.21}$$

For ease in implementation a low pass filter of the form

$$f_{cs}(s) = \frac{1}{(\lambda_{cs}s+1)^2} \tag{2.22}$$

is introduced where λ_{cs} is the filter time constant. Then, the setpoint tracking controller becomes

$$G_{cs}(s) = G_{cso}f_{cs}(s) = \frac{(\tau_1 s \pm 1)(\tau_2 s+1)+k}{k(\lambda_{cs}s+1)^2} \tag{2.23}$$

When the tuning parameter λ_{cs} tends to zero, $G_{cs}(s)$ becomes optimal. λ_{cs} which is an adjustable closed-loop design parameter is always positive. A faster speed of response is achievable by a small value of λ_{cs}, and robustness is improved by a large value of λ_{cs}. Hence, there is a tradeoff in selecting

the tuning parameter λ_{cs}. Thus, λ_{cs} should be selected such that there is a good compromise between faster speed of the responses and improved robustness. The guidelines to choose such a parameter given in Majhi and Atherton [27], is adopted here. The setpoint tracking controllers obtained using similar analysis for different processes are summarized in Table 2.1.

Table 2.1: Setpoint tracking controller G_{cs}

Process	G_{cs}	
FOPTD	$\frac{\tau s+k+1}{k(\lambda_{cs}s+1)}$	$\tau_1=\tau,\ \tau_2=0$
IPTD	$\frac{s+k'}{k'(\lambda_{cs}s+1)}$	$\tau_1\to\infty,\ k'=\frac{k}{\tau_1}\to finite,\ \tau_2=0$
ISOPTD	$\frac{\tau s^2+s+k}{k(\lambda_{cs}s+1)^2}$	$\tau_1\to\infty,\ \tau_2=\tau$
UFOPTD	$\frac{\tau s+k-1}{k(\lambda_{cs}s+1)}$	$\tau_1=\tau,\ \tau_2=0$
SOPTD	$\frac{\tau_1\tau_2 s^2+(\tau_1+\tau_2)s+k+1}{k(\lambda_{cs}s+1)^2}$	
USOPTD	$\frac{\tau_1\tau_2 s^2+(\tau_1-\tau_2)s+k-1}{k(\lambda_{cs}s+1)^2}$	$\tau_1>\tau_2$

2.3.2 Design of G_{cd}

The disturbance rejection controller (G_{cd}) is designed based on IMC-PID approach [91]. The IMC controller design involves the following two steps.

Step 1: The process model G_m is factored as $G_m(s)=G_{m+}(s)G_{m-}(s)$, where G_{m+} is the invertible portion of the model and G_{m-} is the portion of the model having non-minimum phase characteristics and generally contains dead times and/or right half plane zeros and giving $G_{m-}(0)=1$.

Step 2: The idealized IMC controller is the inverse of the invertible portion of the process model i.e. $Q_m=G_{m+}^{-1}$

To make the IMC controller proper, it is mandatory to add a low-pass filter f_{cd} with a steady state gain of 1. The filter is introduced for physical realisability of the IMC controller. Thus, the IMC controller is designed as

$$Q=Q_m f_{cd}=G_{m+}^{-1}f_{cd} \tag{2.24}$$

The ideal feedback controller that is equivalent to the IMC controller can be expressed in terms of the internal model, G_m and the IMC controller, Q as

$$G_{cd}=\frac{Q}{1-G_mQ} \tag{2.25}$$

Since the resulting controller does not have a standard PID controller form, the remaining issue is to design the PID controller that approximates the equivalent feedback controller most closely. Therefore, the mathematical Maclaurin series expansion formula is employed to produce the desired disturbance estimator in a simple way. In practice the desired disturbance estimator should possess an integral characteristic to eliminate any system output deviation arising from load disturbances. Therefore, let

$$G_{cd} = \frac{f(s)}{s} \tag{2.26}$$

Expanding G_{cd} in Maclaurin series in s gives

$$G_{cd} = \frac{1}{s}(f(0) + f'(0)s + \frac{f''(0)}{2!}s^2 + ...) \tag{2.27}$$

The first three terms of (2.27) can be interpreted as exactly a standard PID controller given by

$$G_{cd} = K_p + \frac{1}{T_i s} + T_d s \tag{2.28}$$

where $K_p = f'(0)$, $T_i = \frac{1}{f(0)}$ and $T_d = \frac{f''(0)}{2}$.

Now consider a FOPTD process model $G_p = \frac{ke^{-\theta s}}{\tau s+1}$ where k is the process gain, τ is the time constant and θ is the time delay. The optimum IMC filter structure is given by

$$f_{cd} = \frac{(\alpha s + 1)^2}{(\lambda_{cd} s + 1)^3} \tag{2.29}$$

The resulting IMC controller becomes

$$Q = \frac{(\tau s + 1)(\alpha s + 1)^2}{k(\lambda_{cd} s + 1)^3} \tag{2.30}$$

Therefore, the disturbance rejection controller, which is equivalent to the IMC controller, is

$$G_{cd} = \frac{(\tau s + 1)(\alpha s + 1)^2}{k[(\lambda_{cd} s + 1)^3 - e^{-\theta s}(\alpha s + 1)^2]} \tag{2.31}$$

where α calculated by solving

$\left[1 - (\alpha s + 1)^2 e^{-\theta s} / (\lambda_{cd} s + 1)^3\right]\big|_{s=-1/\tau} = 0$, becomes $\alpha = \tau \left[1 - \left(\left(1 - \frac{\lambda_{cd}}{\tau}\right)^3 e^{-\theta/\tau}\right)^{1/2}\right]$

When the process model is IPTD, it is not possible to apply the aforementioned IMC procedure as the terms including α disappear at $s = 0$. Usually, the controller based on the model with a stable pole near zero can give a more robust closed-loop response than that based on the model with an integrator or unstable pole near zero, as suggested by Lee et al [92]. Thus, IPTD can be approximated

to FOPTD as given below,

$$G_p = \frac{ke^{-\theta s}}{s} = \frac{ke^{-\theta s}}{s+\frac{1}{\phi}} = \frac{\phi k e^{-\theta s}}{\phi s+1} \tag{2.32}$$

where ϕ is a constant with sufficiently large value. The optimum filter structure for IPTD is same as that for the FOPTD. Following a similar calculation procedure, the disturbance rejection controller can be obtained in the form

$$G_{cd} = \frac{(\phi s+1)(\alpha s+1)^2}{k\phi[(\lambda_{cd}s+1)^3 - e^{-\theta s}(\alpha s+1)^2]} \tag{2.33}$$

where α is calculated by solving $\left[1-(\alpha s+1)^2 e^{-\theta s}/(\lambda_{cd}s+1)^3\right]\big|_{s=-1/\phi}$ $= 0$, i.e. $\alpha = \phi\left[1-\left((1-\lambda_{cd}/\phi)^3 e^{-\theta/\phi}\right)^{1/2}\right]$

The ISOPTD process model can be approximated as SOPTD i.e. $G_p = \frac{ke^{-\theta s}}{(s+1/\phi)(\tau s+1)} = \frac{\phi k e^{-\theta s}}{(\phi s+1)(\tau s+1)}$, where ϕ is a constant with sufficiently large value. The optimum IMC filter is considered as

$$f_{cd} = \frac{(\alpha_2 s^2+\alpha_1 s+1)}{(\lambda_{cd}s+1)^4} \tag{2.34}$$

The disturbance rejection controller is obtained in the form

$$G_{cd} = \frac{(\tau s+1)(\phi s+1)(\alpha_2 s^2+\alpha_1 s+1)}{k\phi\left[(\lambda_{cd}s+1)^4 - e^{-\theta s}(\alpha_2 s^2+\alpha_1 s+1)\right]} \tag{2.35}$$

The value of α_1, α_2 are calculated by solving $\left[1-(\alpha_2 s^2+\alpha_1 s+1)e^{-\theta s}/(\lambda_{cd}s+1)^4\right]\big|_{s=-\frac{1}{\phi},-\frac{1}{\tau}} = 0$, i.e.

$\alpha_1 = \frac{\phi^2\left[\left(1-\frac{\lambda_{cd}}{\phi}\right)^4 e^{-\theta/\phi}-1\right]-\tau^2\left[\left(1-\frac{\lambda_{cd}}{\tau}\right)^4 e^{-\theta/\tau}-1\right]}{\tau-\phi}$ and $\alpha_2 = \tau^2\left[\left(1-\frac{\lambda_{cd}}{\tau}\right)^4 e^{-\theta/\tau}-1\right] + \tau\alpha_1$.

For UFOPTD, the optimum IMC filter is considered as that of FOPTD. The disturbance rejection controller becomes

$$G_{cd} = \frac{(\tau s-1)(\alpha s+1)^2}{k\left[(\lambda_{cd}s+1)^3 - e^{-\theta s}(\alpha s+1)^2\right]} \tag{2.36}$$

where α is calculated by solving $\left[1-(\alpha s+1)^2/(\lambda_{cd}s+1)^3\right]\big|_{s=\frac{1}{\tau}} = 0$, $\alpha = \tau\left[\left(\left(1+\frac{\lambda_{cd}}{\tau}\right)^3 e^{\theta/\tau}\right)^{1/2}-1\right]$

For the SOPTD process model type (2.14), the optimum IMC filter is same as that of ISOPTD and the disturbance rejection controller becomes

$$G_{cd} = \frac{(\tau_1 s+1)(\tau_2 s+1)(\alpha_2 s^2+\alpha_1 s+1)}{k[(\lambda_{cd}s+1)^4 - e^{-\theta s}(\alpha_2 s^2+\alpha_1 s+1)]} \tag{2.37}$$

Table 2.2: Disturbance Rejection controller G_{cd}

Process	Parameters of G_{cd}
FOPTD	$K_p = \frac{1}{T_i}\left[\tau + 2\alpha - \frac{3\lambda_{cd}^2 - \theta^2/2 + 2\alpha\theta - \alpha^2}{3\lambda_{cd} - 2\alpha + \theta}\right]$ $T_i = k(3\lambda_{cd} - 2\alpha + \theta)$ $T_d = \frac{1}{T_i}\left[2\tau\alpha + \alpha^2 - \frac{\lambda_{cd}^3 + \theta^3/6 - \alpha\theta^2 + \alpha^2\theta}{3\lambda_{cd} - 2\alpha + \theta}\right] - \frac{K_p(3\lambda_{cd}^2 - \theta^2/2 + 2\alpha\theta - \alpha^2)}{3\lambda_{cd} - 2\alpha + \theta}$
IPTD	$K_p = \frac{\phi + 2\alpha}{T_i} - \frac{3\lambda_{cd}^2 - \frac{\theta^2}{2} + 2\alpha\theta - \alpha^2}{T_i(3\lambda_{cd} - 2\alpha + \theta)}$ $T_i = \phi k(3\lambda_{cd} - 2\alpha + \theta)$ $T_d = \frac{1}{T_i}\left[(2\phi\alpha + \alpha^2) - \frac{\lambda_{cd}^3 + \frac{\theta^3}{6} - \alpha\theta^2 + \alpha^2\theta}{3\lambda_{cd} - 2\alpha + \theta}\right] - \frac{K_p(3\lambda_{cd}^2 - \frac{\theta^2}{2} + 2\alpha\theta - \alpha^2)}{3\lambda_{cd} - 2\alpha + \theta}$
ISOPTD	$K_p = \frac{1}{T_i}\left[\phi + \tau + \alpha_1 - \frac{6\lambda_{cd}^2 - \theta^2/2 + \theta\alpha_1 - \alpha_2}{4\lambda_{cd} - \alpha_1 + \theta}\right]$ $T_i = \phi k(4\lambda_{cd} - \alpha_1 + \theta)$ $T_d = \frac{1}{T_i}\left[\phi\tau + (\tau + \phi)\alpha_1 + \alpha_2 - \frac{4\lambda_{cd}^3 + \theta^3/6 - \alpha_1\theta^2/2 + \theta\alpha_2}{4\lambda_{cd} - \alpha_1 + \theta}\right] - \frac{K_p(6\lambda_{cd}^2 - \theta^2/2 + \theta\alpha_1 - \alpha_2)}{4\lambda_{cd} - \alpha_1 + \theta}$
UFOPTD	$K_p = \frac{1}{T_i}\left[-\tau + 2\alpha - \frac{3\lambda_{cd}^2 - \theta^2/2 + 2\alpha\theta - \alpha^2}{3\lambda_{cd} - 2\alpha + \theta}\right]$ $T_i = -k(3\lambda_{cd} - 2\alpha + \theta)$ $T_d = \frac{1}{T_i}\left[-2\tau\alpha + \alpha^2 - \frac{\lambda_{cd}^3 + \theta^3/6 - \alpha\theta^2 + \alpha^2\theta}{3\lambda_{cd} - 2\alpha + \theta}\right] - \frac{K_p(3\lambda_{cd}^2 - \theta^2/2 + 2\alpha\theta - \alpha^2)}{3\lambda_{cd} - 2\alpha + \theta}$
SOPTD	$K_p = \frac{1}{T_i}\left[\tau_1 + \tau_2 + \alpha_1 - \frac{6\lambda_{cd}^2 - \theta^2/2 + \theta\alpha_1 - \alpha_2}{4\lambda_{cd} - \alpha_1 + \theta}\right]$ $T_i = k(4\lambda_{cd} - \alpha_1 + \theta)$ $T_d = \frac{1}{T_i}\left[\tau_1\tau_2 + (\tau_1 + \tau_2)\alpha_1 + \alpha_2 - \frac{4\lambda_{cd}^3 + \theta^3/6 - \alpha_1\theta^2/2 + \theta\alpha_2}{4\lambda_{cd} - \alpha_1 + \theta}\right] - \frac{K_p(6\lambda_{cd}^2 - \theta^2/2 + \theta\alpha_1 - \alpha_2)}{4\lambda_{cd} - \alpha_1 + \theta}$
USOPTD	$K_p = \frac{1}{T_i}\left[\tau_2 - \tau_1 + 2\alpha - \frac{6\lambda_{cd}^2 - \theta^2/2 + 2\alpha\theta - \alpha^2}{4\lambda_{cd} - 2\alpha + \theta}\right]$ $T_i = -k(4\lambda_{cd} - 2\alpha + \theta)$ $T_d = \frac{1}{T_i}\left[-\tau_2\tau_1 - 2\alpha(-\tau_2 + \tau_1) + \alpha^2 - \frac{4\lambda_{cd}^3 + \theta^3/6 - \alpha\theta^2 + \alpha^2\theta}{4\lambda_{cd} - 2\alpha + \theta}\right] - \frac{K_p(6\lambda_{cd}^2 - \theta^2/2 + 2\alpha\theta - \alpha^2)}{4\lambda_{cd} - 2\alpha + \theta}$

Here $\alpha_1 = \frac{\tau_1^2\left[\left(1 - \frac{\lambda_{cd}}{\tau_1}\right)^4 e^{-\theta/\tau_1} - 1\right] - \tau_2^2\left[\left(1 - \frac{\lambda_{cd}}{\tau_2}\right)^4 e^{-\theta/\tau_2} - 1\right]}{\tau_2 - \tau_1}$ and $\alpha_2 = \tau_2^2\left[\left(1 - \frac{\lambda_{cd}}{\tau_2}\right)^4 e^{-\theta/\tau_2} - 1\right] + \tau_2\alpha_1$.

Analogously, the optimum IMC filter for USOPTD is considered as

$$f_{cd} = \frac{(\alpha s + 1)^2}{(\lambda_{cd} s + 1)^4} \tag{2.38}$$

and the disturbance rejection controller obtained in the form

$$G_{cd} = \frac{(\tau_1 s - 1)(\tau_2 s + 1)(\alpha s + 1)^2}{k[(\lambda_{cd} s + 1)^4 - e^{-\theta s}(\alpha s + 1)^2]} \tag{2.39}$$

where solving the inequality
$\left[1 - e^{-\theta s}(\alpha s + 1)^2/(\lambda_{cd} s + 1)^4\right]\big|_{s=\frac{1}{\tau_1}} = 0$, $\alpha = \tau_1 \left[\left(\left(\frac{\lambda_{cd}}{\tau_1} + 1\right)^4 e^{\theta/\tau_1}\right)^{1/2} - 1\right]$.
Expanding G_{cd} in a Maclaurin series in s, enables one to express the PID tuning rules as given in Table 2.2.

2.4 Selection of the tuning parameter λ_{cd}

The tuning of the control parameter λ_{cd} aims at the trade-off between nominal performance of the closed loop and its robust stability. That is, decreasing λ_{cd} improves the disturbance rejection performance of the closed loop but degrades its robust stability in the presence of process uncertainty. In contrast, increasing λ_{cd} tends to strengthen the robust stability of the closed loop but degrades its disturbance rejection performance. The primary requirement for selection of λ_{cd} is that the resulting controller gains should be positive for positive values of the process model gain. As none of the constraints (2.40)-(2.45) for tuning the control parameter λ_{cd} can be solved analytically, numerical simulation tests based on the MATLAB toolbox have been performed to ascertain the tuning rule of thumb for the control parameter λ_{cd}. For IPTD, it is observed that the initial value of the tuning parameter can be taken as $0.8\theta_m$. If good control performances are not achieved with this value, then the tuning parameter can be increased gradually from this value till good nominal and robust control performances are achieved. Quantitatively, for IPTD, the range of the tuning parameter λ_{cd} that gives good control performances is $0.8\theta_m - 2.2\theta_m$. Theoretically, to obtain robust stability and robust performance λ_{cd} should be selected such that the robust stability and performance conditions (2.40)-(2.45) are satisfied. The suggested range for the selection of tuning parameter λ_{cd} for remaining processes are given in Table 2.3.

Table 2.3: Selection of λ_{cd}

Process	Suggested range for λ_{cd}
FOPTD	$(0.08\theta_m)$ - (θ_m)
ISOPTD	$(0.47\theta_m)$ - $(1.9\theta_m)$
UFOPTD	(θ_m) - $(2\theta_m)$
SOPTD	$(0.48\theta_m)$ - $(1.09\theta_m)$
USOPTD	$(0.94\theta_m)$ - $(1.6\theta_m)$

2.5 Robustness analysis and performance

2.5.1 Robustness analysis

For any closed loop control system, it is necessary to analyze the stability and robustness for uncertainties in the process and for the load disturbances. According to the Small gain theorem [93], the closed-loop system for the load disturbance rejection is robustly stable if and only if

$$\|\Delta_m(j\omega)T(j\omega)\| < 1 \qquad \forall\omega \in (-\infty, \infty) \tag{2.40}$$

where $T(s = j\omega)$ is the closed-loop complementary sensitivity function and $\Delta_m(j\omega)$ is the process multiplicative uncertainty i.e. $\Delta_m(j\omega) = \left|\left(G_p(j\omega) - \tilde{G}_m(j\omega)\right)\Big/\tilde{G}_m(j\omega)\right|$ where $\tilde{G}_m(j\omega) = G_m(j\omega)e^{-\theta_m s}$. To show the stability and robustness analysis more qualitatively, consider the IPTD process for which the complementary sensitivity function using (2.10), (2.28) and Table 2.2 is

$$T(s) = \frac{k(1 + K_pT_is + T_iT_ds^2)e^{-\theta s}}{T_is^2 + k(1 + K_pT_is + T_iT_ds^2)e^{-\theta s}} \tag{2.41}$$

where the controller parameters K_p, T_i and T_d are the functions of the tuning parameter λ_{cd}. For the process gain uncertainty [26], the tuning parameter should be selected in such a way that

$$\|T(j\omega)\|_\infty < \frac{1}{|\Delta k|/k} \qquad \forall\omega > 0 \tag{2.42}$$

For the process time delay uncertainty [26], the tuning parameter should be selected in such a way that

$$\|T(j\omega)\|_\infty < \frac{1}{|e^{-j\Delta\theta\omega} - 1|} \qquad \forall\omega > 0 \tag{2.43}$$

If uncertainty exists in both process gain and time delay, the tuning parameter should be selected in such a way that

$$\|T(j\omega)\|_\infty < \frac{1}{\left|(1+\frac{\Delta k}{k})e^{-j\Delta\theta\omega}-1\right|} \qquad \forall\omega > 0 \tag{2.44}$$

According to the robust control theory [91], the constraint for robust closed loop performance for load disturbance rejection is

$$\|\Delta_m(j\omega)T(j\omega) + w_1(j\omega)(1-T(j\omega))\|_\infty < 1 \tag{2.45}$$

where $w_1(j\omega)$ is the weight function of the sensitivity function, $S(j\omega) = 1 - T(j\omega)$. Therefore, the tuning parameter λ_{cd} should be selected such that the resulting controller satisfy the robust nominal performance and robust stability constraints. Similar robustness and stability analysis can be done for the remaining type of time delay processes.

2.5.2 Performance

Many performance criteria can be used to determine the desired closed-loop responses. Simple performance criteria such as overshoot, settling time, decay ratio, rise time, and gain/phase margin criteria can be used to select the controller settings. Because simple performance criteria use only the isolated characteristics of the dynamic response, time integral performance criteria such as integral square error (ISE= $\int_0^\infty e(t)^2 dt$), integral absolute error (IAE= $\int_0^\infty |e(t)|\, dt$), and integral of the time-weighted absolute error (ITAE= $\int_0^\infty t\,|e(t)|\, dt$) are used. Among the three integral performance criteria, selecting the right one is important. The ISE criterion penalizes large errors (resulting in the most-aggressive settings) and the ITAE criterion penalizes persistent errors (resulting in the most-conservative settings), the IAE criterion tends to produce moderate settings that are between those for the ISE and ITAE criteria. Hence, in this study, IAE and ISE criteria are selected as the matrices to evaluate the closed-loop controller performance.

Another measure of the controller performance is the smoothness of the generated control signal and is computed by calculating the total variation (TV) of the manipulated input, u i.e. TV= $\sum_{i=1}^{\infty} |u_{i+1} - u_i|$. The TV of u is the sum of all of the control moves, both up and down. Thus, it is also a good measure of the smoothness of the manipulated input signal. It is desired that TV be as small as possible [94].

2.6 Simulation study

Example-2.1: Consider an integrating plus time delay process, $G_p(s) = \frac{1}{s}e^{-5s}$. Rao et al.'s method [26] gives the parameters for the setpoint tracking controller as $k_c = 0.4$, $\tau_i = 10$ and the disturbance rejection PD controller as $(0.12 + 0.45s)$. Similarly by Lu et al.'s method [31] the parameters of the four controller are $K_1 = 0.5$, $K_2 = (0.5 + 0.934s)$, $K_3 = 0.105$ and $K_4 = 0.5$. In the case of Majhi and Atherton's method [27] the controller parameters are $K_p = 0.5$, $T_i = 1$, $K_f = 1$ and $K_d = 0.105$. In the proposed method, $\lambda_{cs} = 2$ in order to maintain the same speed of response as those of the Rao et al., Lu et al. and Majhi and Atherton. In this case in order to achieve good nominal and robust control performances, tuning parameter for the load disturbance rejection, $\lambda_{cd} = 0.9\theta_m$. Thus, the controllers $G_{cs} = \frac{s+1}{2s+1}$ and $G_{cd} = (0.2295 + \frac{1}{54.4554s} + 0.4541s)$ are obtained using Tables 2.1-2.2. A unit-step setpoint is introduced at time $t = 0$ and a load disturbance $d = -0.1$ at time t = 70 sec. The closed-loop responses for all the above controller settings are shown in Figure 2.4 and the corresponding control signals are shown in Figure 2.5.

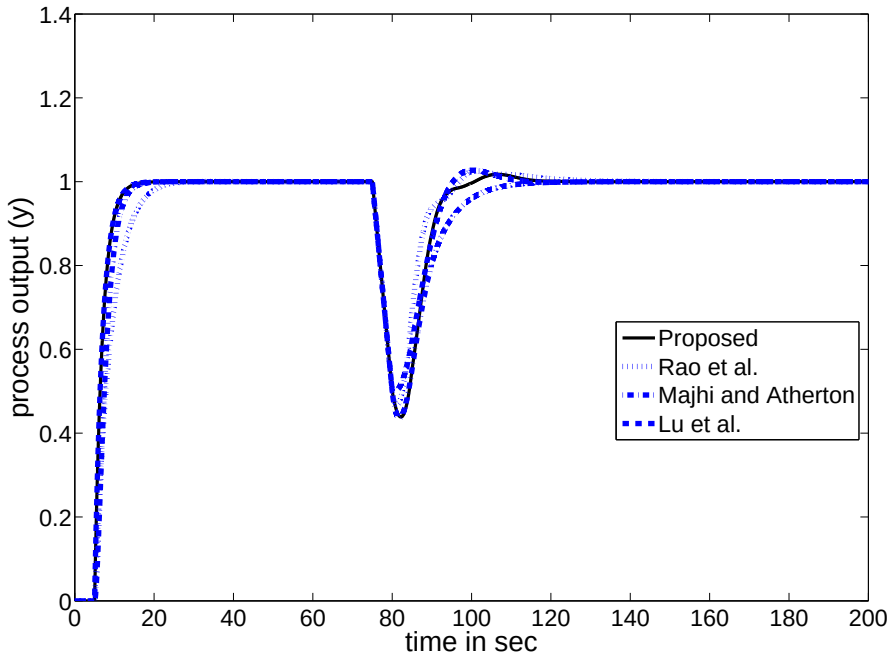

Figure 2.4: Nominal responses for Example 2.1

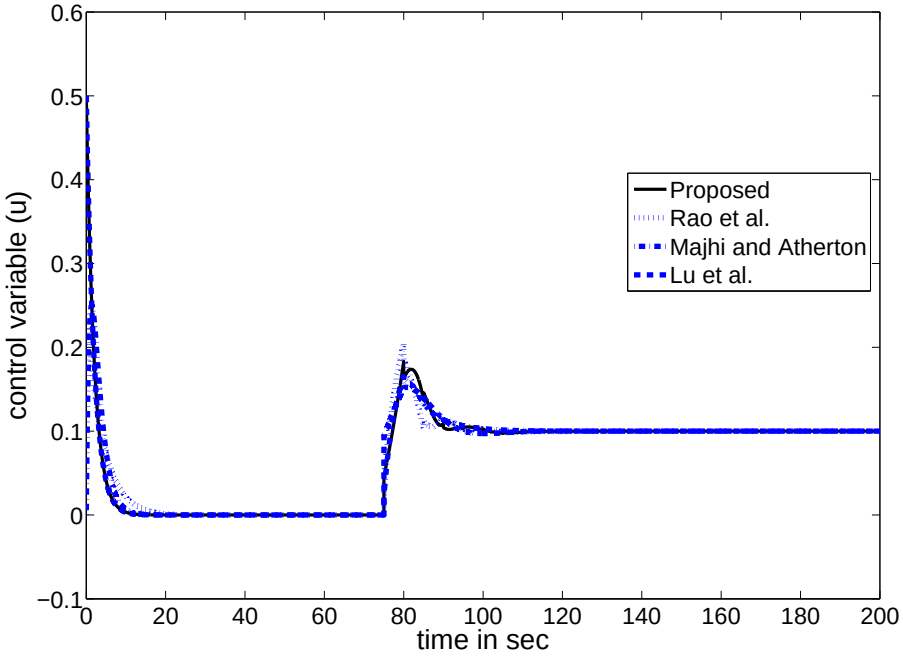

Figure 2.5: Control variables for nominal responses for Example 2.1

From the responses it can be observed that the proposed method does not give inferior performances than when compared with the other responses. But particularly for disturbance rejection, the proposed method gives comparatively superior performances to other methods. In the present work a +30% error in estimating the dead time is considered. The method proposed by Lu et al. shows completely unstable responses for infinitesimal perturbation in time delay and hence it is not shown in the Figure 2.6. From the simulations it is seen that Rao et al.'s method yields oscillatory responses when there exist process model mismatches. Figure 2.6 shows that the proposed method gives satisfactory overall performances compared to the other methods. Comparatively smooth control signal is obtained using proposed scheme (see Figure 2.7). To show the effect of λ_{cd}, the robust stability and performance of the closed loop system are carried out using (2.41) and (2.43). Here, the robustness is checked by considering λ_{cd}= 4, 4.5 and 5.5, respectively.

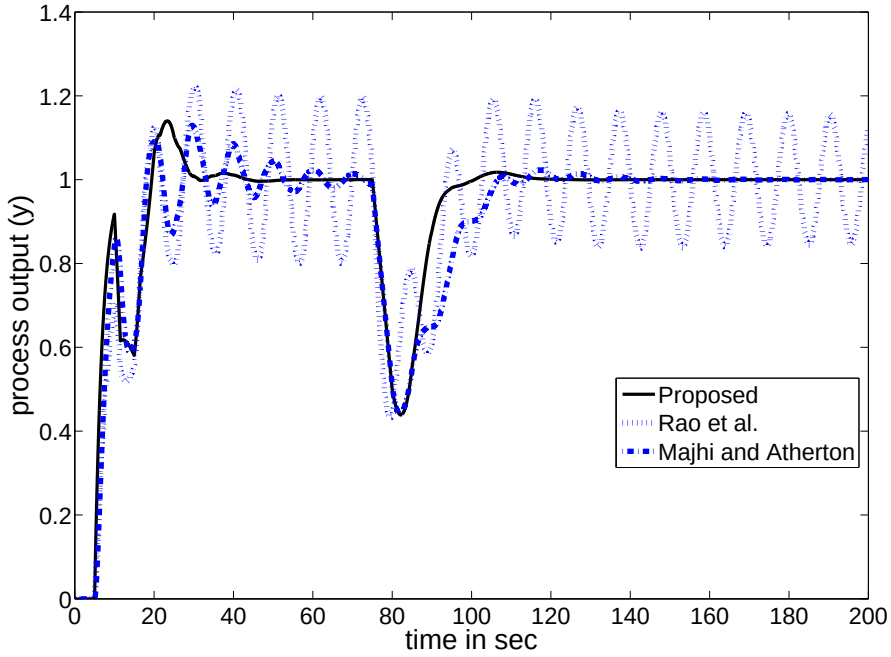

Figure 2.6: Responses for +30% estimation error in process time delay for Example 2.1

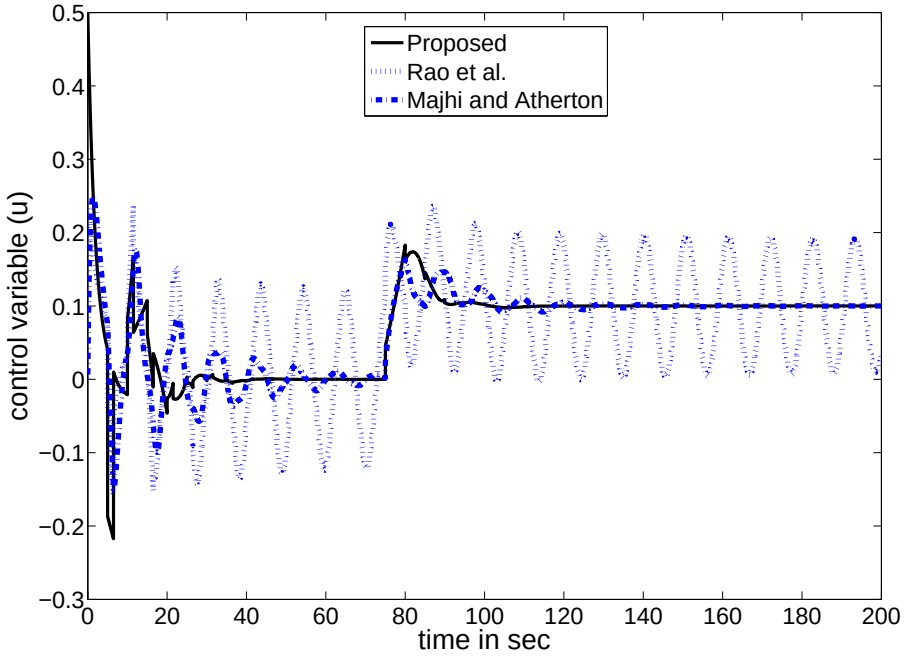

Figure 2.7: Control variables for +30% estimation error in process time delay for Example 2.1

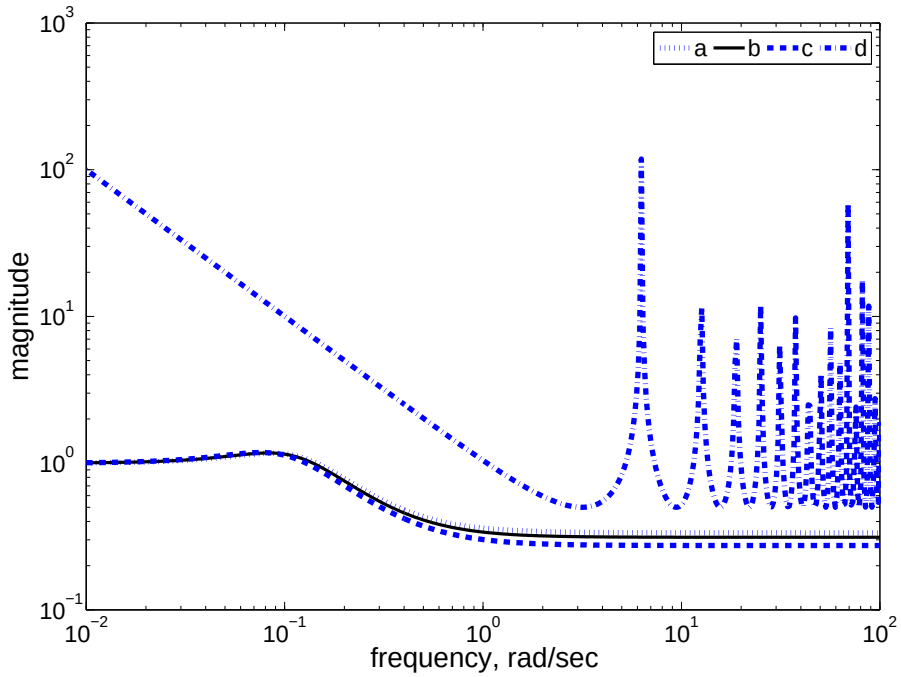

Figure 2.8: Magnitude plot of the complementary sensitivity function and uncertainty bound for Example-2.1: (a) $\lambda_{cd} = 4$, (b) $\lambda_{cd} = 4.5$, (c) $\lambda_{cd} = 5.5$ and (d) $\frac{1}{e^{-s}-1}$

Figure 2.8 shows the magnitude of the complementary sensitivity function and the magnitude of $1/(e^{-s} - 1)$ for $+20\%$ perturbation in time delay over a frequency range. Only delay uncertainty is considered here, as the delay compensators are sensitive to time delay mismatches. From Figure 2.8, it is concluded that the robust stability margin increases as λ_{cd} increases, i.e. for $\lambda_{cd} = 4$, the stability margin is less compared to that of $\lambda_{cd} = 4.5$ and $\lambda_{cd} = 5.5$. The closed loop performance is also evaluated for different values of λ_{cd} for both nominal conditions and for a estimation error of $+30\%$ in time delay and the corresponding responses are shown in Figure 2.9 and Figure 2.10, respectively. The performance specifications of disturbance responses for nominal and model mismatch cases are summarized in Table 2.4. The proposed method gives same performance specifications both for nominal and perturbation systems. It is obvious that the proposed method has robust and superior control performances. The proposed controllers provide a faster closed-loop response to a unit-step input and improved disturbance rejection.

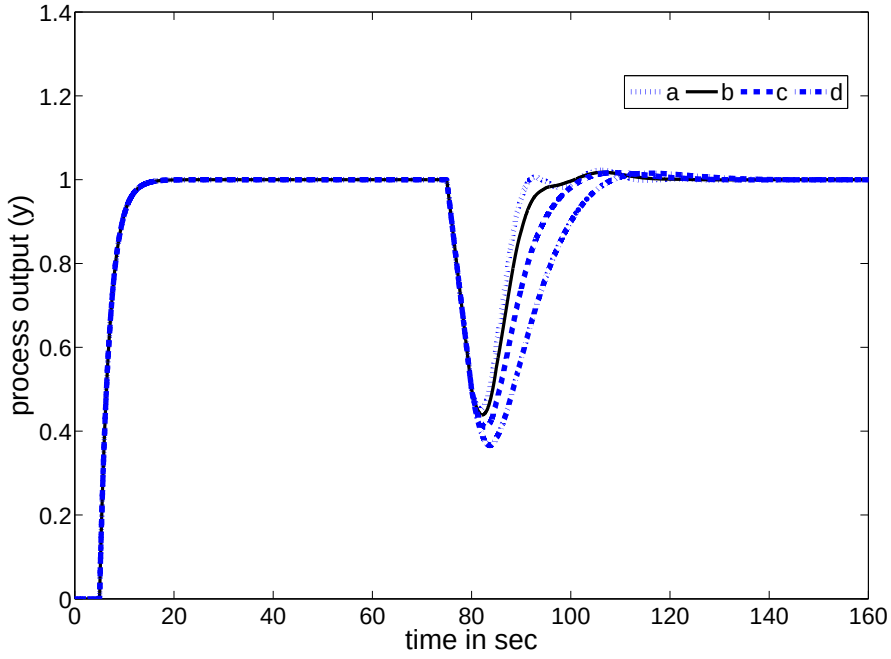

Figure 2.9: Nominal responses for (a) $\lambda_{cd} = 4$, (b) $\lambda_{cd} = 4.5$, (c) $\lambda_{cd} = 5.5$ and (d) $\lambda_{cd} = 7$ for Example 2.1

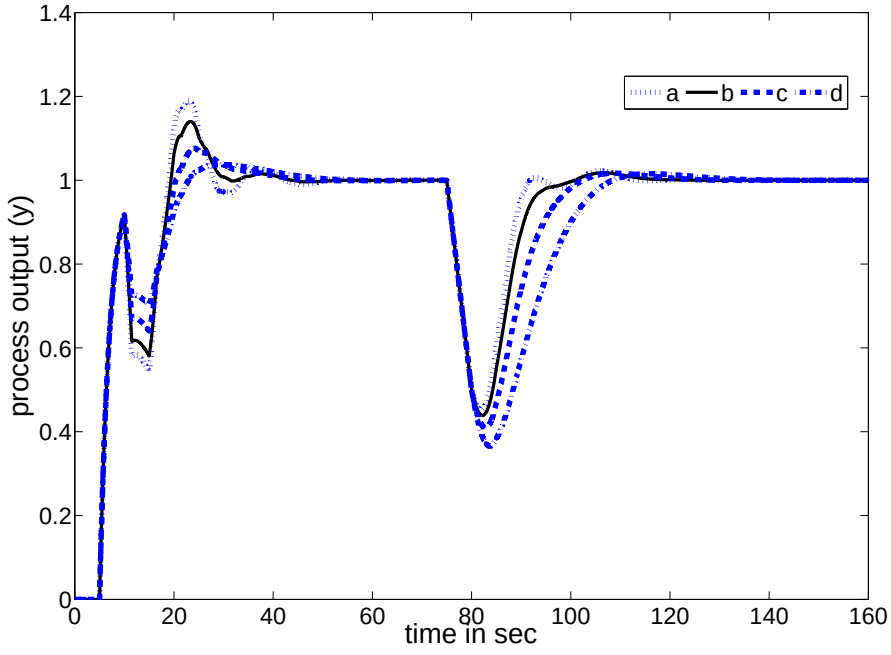

Figure 2.10: Responses for +30% estimation error in process time delay for (a) $\lambda_{cd} = 4$, (b) $\lambda_{cd} = 4.5$, (c) $\lambda_{cd} = 5.5$ and (d) $\lambda_{cd} = 7$ for Example 2.1

Table 2.4: Performance specifications of disturbance responses

	Scheme	Nominal System			Perturbed system		
		IAE	ISE	TV	IAE	ISE	TV
Example-2.1	Proposed	5.79	2.28	0.83	5.79	2.28	2.05
	Rao et al.	5.04	1.702	0.61	12.77	2.66	8.76
	Majhi and Atherton	7.32	3.130	0.73	9.58	3.81	1.48
	Lu et al.	5.44	1.883	0.71	-	-	-
Example-2.2	Proposed	0.71	0.05	4.24	0.71	0.05	15.10
	Kaya	0.76	0.06	5.18	0.95	0.06	68.34
Example-2.3	Proposed	16.99	10.9	0.55	16.99	10.9	0.77
	Rao et al.	19.01	8.32	0.51	27.58	11.43	1.97
Example-2.4	Proposed	4.43	0.85	2.30	4.43	0.85	4.92
	Lu et al.	5.40	1.13	1.84	21.57	4.73	6.49
Example-2.5	Proposed	7.04	0.88	5.04	7.04	0.88	6.73
	Kaya	9.07	1.09	3.91	10.35	1.37	5.34
Example-2.6	Proposed	3.56	0.45	2.05	3.56	0.45	4.98
	Majhi and Atherton	5.48	1.03	4.12	14.58	2.59	6.91
	Lu et al.	2.61	0.26	2.52	13.97	1.74	162.85

(-)Unstable responses

From the time domain specifications (see Table 2.5), it is observed that the proposed method has lesser rise time, lesser or zero overshoot and lesser settling time.

Example-2.2: Consider the FOPTD plant studied by Camacho et al. [95], $G_p(s) = \frac{1}{1.3s+1}e^{-5.68s}$ where $\theta/\tau = 4.37$. The parameters of Kaya's [96] modified Smith predictor for this process are $K_c = 1$, $T_i = 0.25$ and $K_f = 6.5784$. In the proposed design method, $\lambda_{cs} = 1$ in order to maintain the same set-point rising speed as Kaya's method. By the proposed method, the set-point tracking controller is obtained in the form $G_{cs}(s) = \frac{1.3s+2}{s+1}$. Tuning parameter for the load disturbance rejection, $\lambda_{cd} = 0.22\theta_m$. We obtain the disturbance rejection controller in the form $G_{cd}(s) = (0.5358 + \frac{1}{6.8310s} + 0.6105s)$. With these controller settings, the performances of the closed loop system is evaluated by introducing a unit step input in the setpoint at time $t = 0$ and a negative step load input of 0.1 at $t = 30$ sec. The step responses for no mismatch in the plant model are shown in Figure 2.11.

Table 2.5: Time domain specifications

	Scheme	Nominal System			Perturbed system		
		t_r	$M_p(\%)$	t_s	t_r	$M_p(\%)$	t_s
Example-2.1	Proposed	4.4	0	13.2	4.4	14.15	29.1
	Rao et al.	8.7	0	20.4	11.6	22.19	*
	Majhi and Atherton	5.2	0	14.7	12.5	6.89	43.2
	Lu et al.	4.4	0	13.2	4.4	-	-
Example-2.2	Proposed	4.4	0	18.3	4.4	13.43	59.5
	Kaya	3.2	5.59	19.7	3.2	48.05	*
Example-2.3	Proposed	11.8	0	27.4	24.8	9.99	55.1
	Rao et al.	27.7	0	54.5	35.4	3.95	147.1
Example-2.4	Proposed	4.4	0	13.2	8.1	31.03	57.3
	Lu et al.	4.4	0	13.2	11	30.40	281.8
Example-2.5	Proposed	12.1	0	36.2	33.4	9.04	87.2
	Kaya	13.4	0	38.6	30.6	2.84	94
Example-2.6	Proposed	12.1	0	26.4	15.5	34.59	85.3
	Majhi and Atherton	4.8	1.13	21.9	18.7	30.99	204.4
	Lu et al.	8.4	0	20.1	17.6	32.37	*

(-)Unstable responses, (*)Oscillatory responses

Now suppose that there exists a 40% error in estimating the process time delay θ such that it is actually 40% larger. The perturbed system responses are shown in Figure 2.12. The proposed method shows comparatively smooth responses. From the Figure 2.11 and Figure 2.12, it can be observed that particularly the load disturbance response of the proposed method is excellent. From the Table 2.4, it can be observed that the proposed method gives low IAE, ISE and TV values for both nominal system and perturbed system. As stated earlier, the disturbance rejection is more important than set point tracking for industrial practice. It is evident that the proposed controller provides robust performance particularly in the load disturbance rejection.

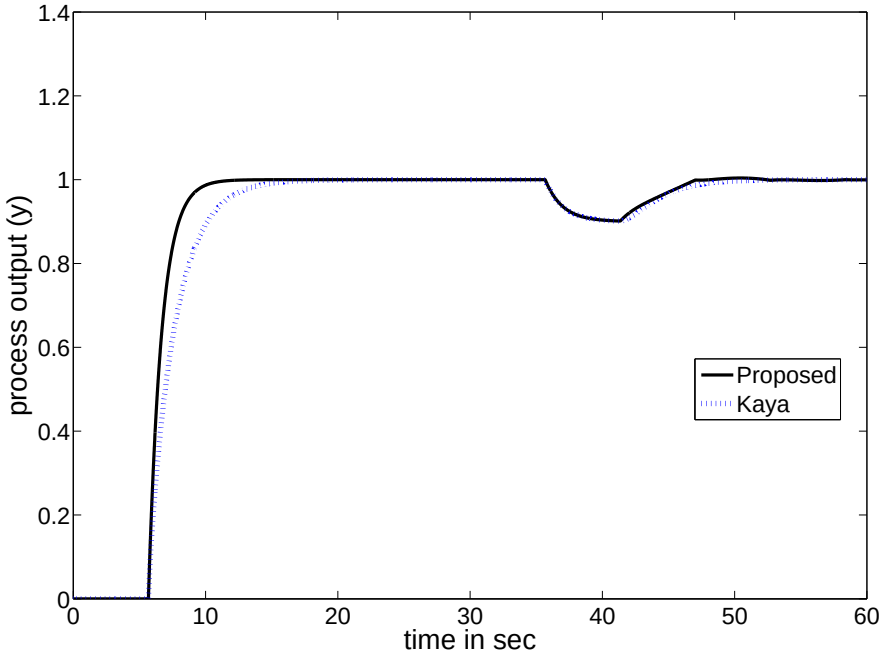

Figure 2.11: Nominal responses for Example 2.2

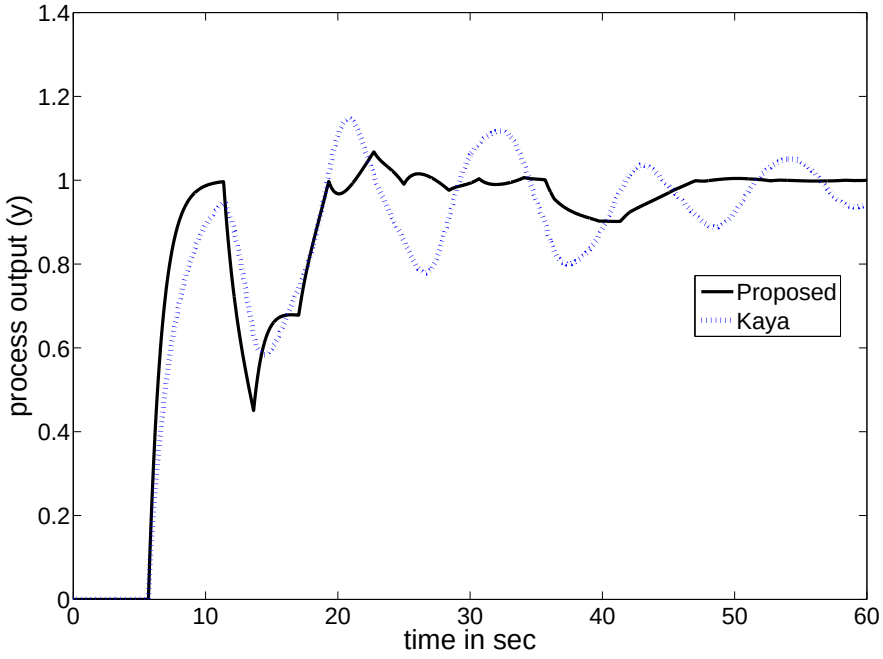

Figure 2.12: Responses for +40% estimation error in process time delay for Example 2.2

Example-2.3: A higher-order integrating process with time delay [27], $G_p(s) = \frac{1}{(s(s+1)^2(3s+1))}e^{-5s}$ is considered here. Majhi and Atherton [27] have shown that this process can be identified as an ISOPTD process as $G_p(s) = \frac{1}{s(3.4945s+1)}e^{-6.5672s}$. The proposed controller design technique is applied to this identified model. Rao et al. [26] already showed that their method gives superior control performances than Kaya's [97] and Liu et al.'s [90] methods. The parameters for Rao et al.'s setpoint tracking controller are $k_c = 0.124$, $\tau_i = 27.58$, and $\tau_d = 1.130$ and the disturbance rejection controller is given in the form $G_{cd} = 0.035 + 1.12s$. In the proposed method, $\lambda_{cs} = 3.5$ is chosen in order to obtain the same setpoint rising speed as that of the Rao et al.'s method. Using the design formula, the setpoint tracking controller is obtained as $G_{cs}(s) = \frac{3.4945s^2+s+1}{12.25s^2+7s+1}$. The disturbance rejection tuning parameter $\lambda_{cd} = 0.65\theta_m$ is chosen in order to get good nominal and robust performances and the disturbance rejection controller is obtained in the form $G_{cd}(s) = (0.1424 + \frac{1}{166.333s} + 0.5880s)$. A unit step input in the setpoint at $t = 0$ and a load disturbance at $t = 150$ sec are introduced. The magnitude of the step load disturbance $d = -0.1$. The responses of the closed-loop system for these controller settings are given in Figure 2.13 for the actual plant.

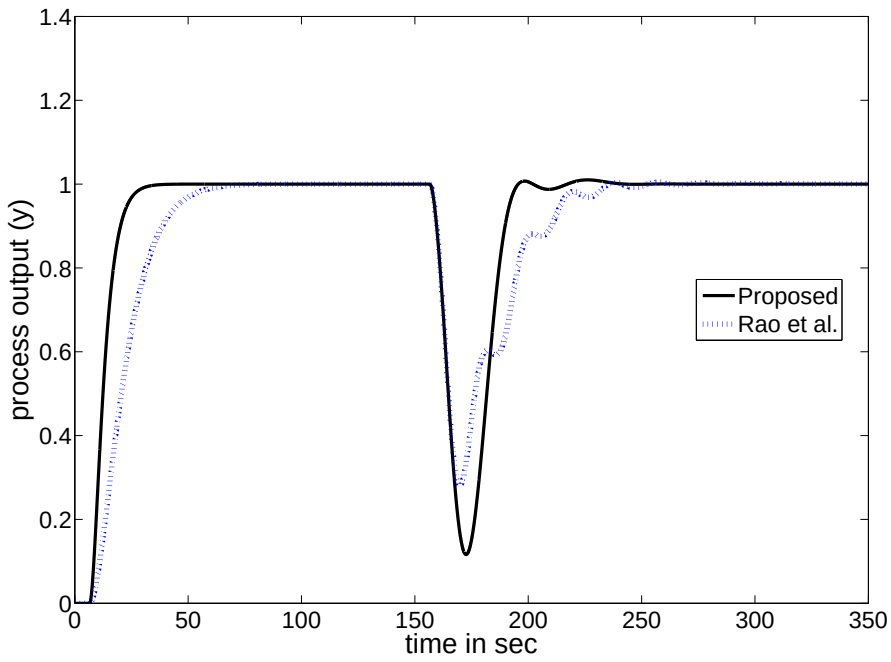

Figure 2.13: Nominal responses for Example 2.3

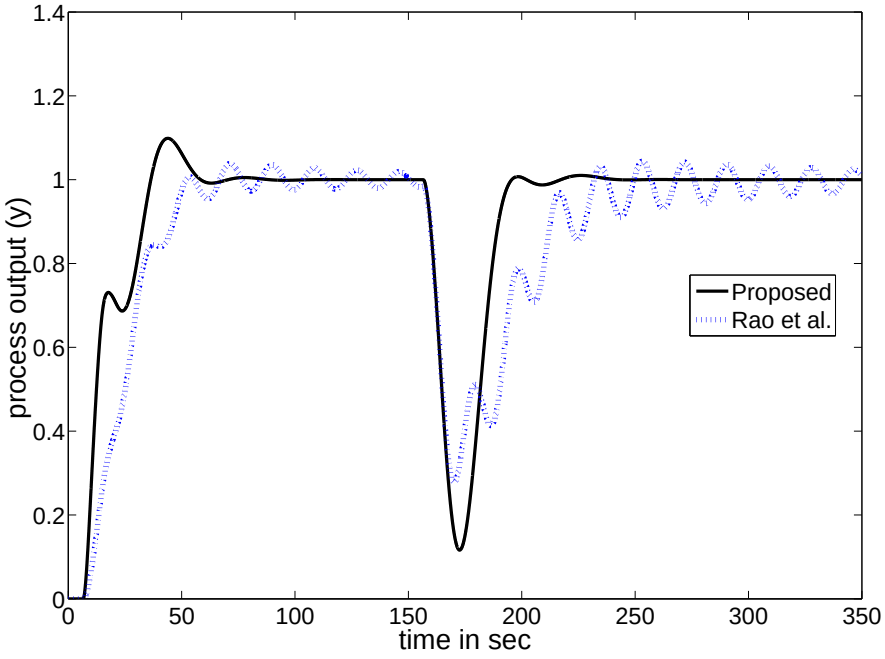

Figure 2.14: Responses for +35% estimation error in process time delay for Example 2.3

The response is superior to that obtainable by Rao et al.'s method. The step setpoint response and load disturbance response of the proposed method are excellent. Now suppose that there exists a +35% error in estimating the process time delay θ. The perturbed system responses are shown in Figure 2.14. It can be observed that the robustness of the proposed design technique towards assumed parameter perturbation is satisfactory. The time domain specifications are given in the Table 2.5. The Table 2.4 shows that the proposed method has low performance indices which indicates the method gives better control performances. The performance of the proposed technique found to be superior because of the modeling, the new Smith predictor structure and the design method used.

Example-2.4: Consider an unstable FOPTD process studied by Majhi and Atherton [27], $G_p(s) = \frac{4}{10s-1}e^{-5s}$. The parameters of Lu et al.'s controller [31] are $K_1 = 1.5$, $K_2 = (1.25+3.16s)$, $K_3 = 0.35$, and $K_4 = 1.25$. In the proposed method, the setpoint tracking tuning parameter $\lambda_{cs} = 2$ is chosen in order to maintain the same setpoint rising speed as that of Lu et al.. The load disturbance rejection tuning parameter λ_{cd} is assumed as $1.2\theta_m$. By employing the design formulae the two controllers become $G_{cs}(s) = \frac{10s+3}{8s+4}$ and $G_{cd}(s) = (0.6115 + \frac{1}{35.8948s} + 1.6600s)$. The closed-loop performances are evaluated with these controller settings for a unit step input in the setpoint at $t = 0$, and a negative

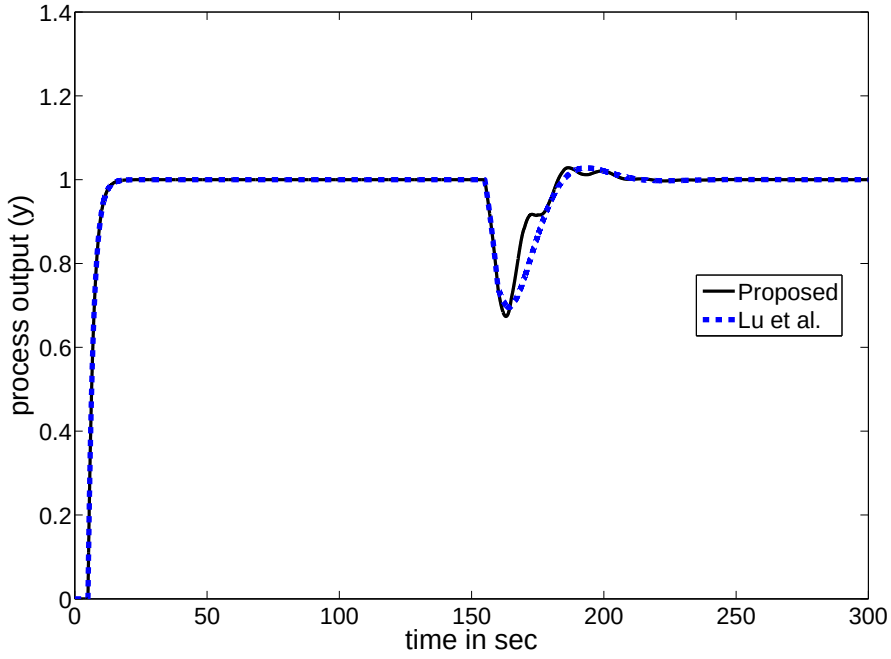

Figure 2.15: Nominal responses for Example 2.4

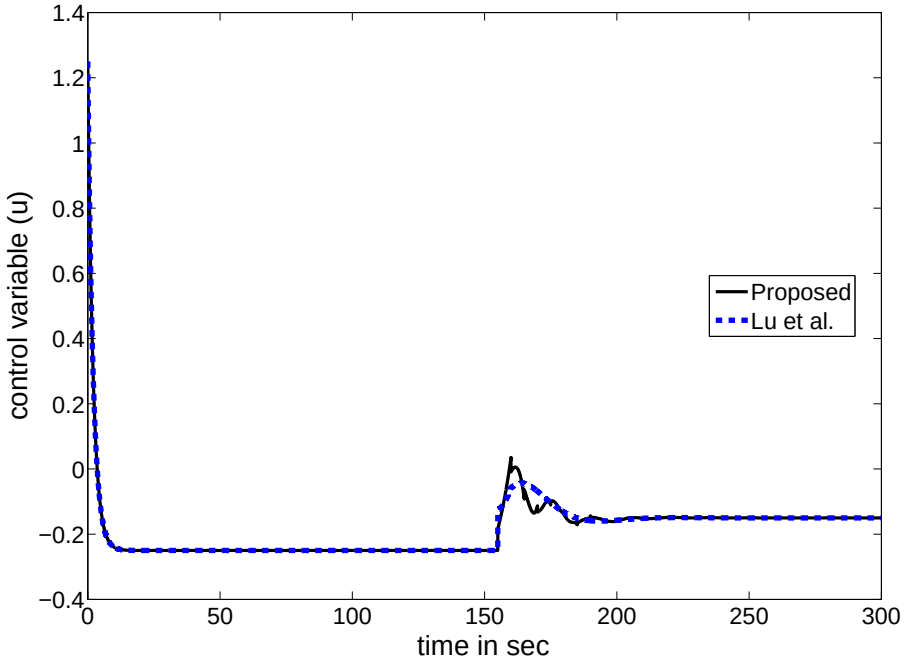

Figure 2.16: Control variables for nominal responses for Example 2.4

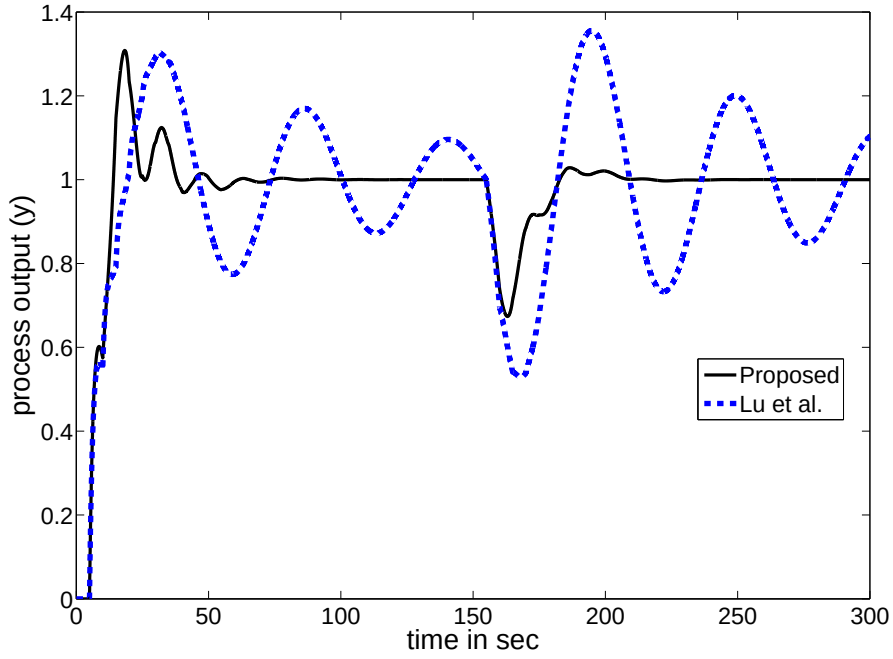

Figure 2.17: Responses for -30% estimation error in process time constant for Example 2.4

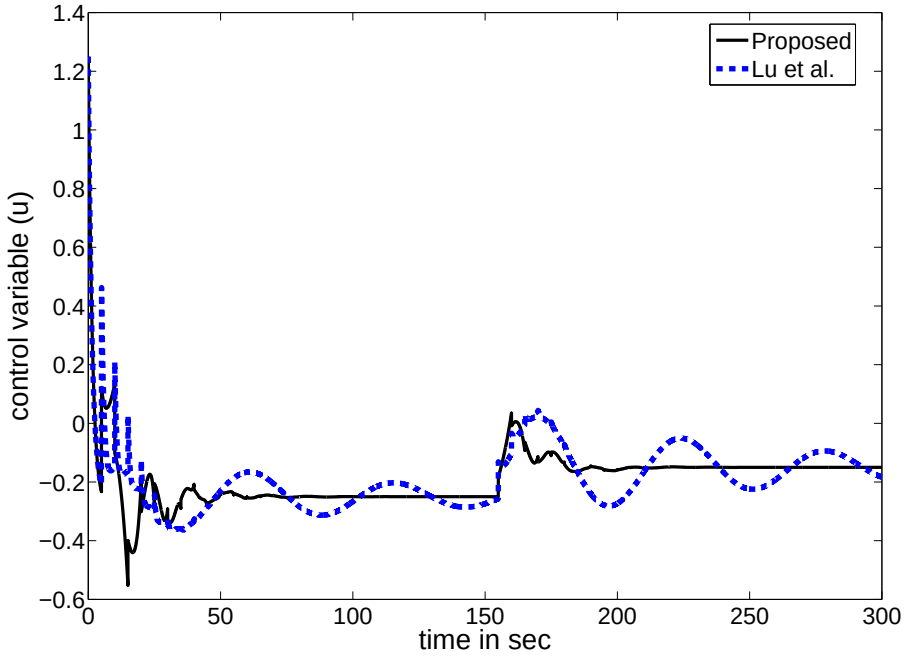

Figure 2.18: Control variables for -30% estimation error in process time constant for Example 2.4

step load input of 0.1 at $t = 150$ sec. The responses are shown in Figure 2.15 and the corresponding control signals are in Figure 2.16. The proposed method gives the same setpoint tracking speed as that of Lu et al. However, for the load disturbance rejection, the proposed method gives significantly improved performances. A -30% error in estimating in the process time constant is considered and the corresponding responses are shown in Figure 2.17. The perturbed systems control signals are shown in Figure 2.18. From the figures it is clear that the responses of Lu et al.'s method are oscillatory. The proposed method gives improved performances for both setpoint tracking and load disturbance rejection. From the Table 2.4, it is observed that the performance indices are very much low as compared to Lu et al.'s. The Table 2.5 and the simulation results show that the proposed method gives a superior settling time and load disturbance rejection.

Example-2.5: Consider a higher order plant studied by Kaya [89], $G_p(s) = \frac{4e^{-10s}}{(20s+1)(10s+1)(5s+1)(s+1)}$. Kaya [89] has shown that this process can be reduced as an SOPTD model as $G_p(s) = \frac{4e^{-14.69s}}{(21.62s+1)(11.34s+1)}$. The proposed controller design technique is applied to the reduced model. Here $k = 4$, $\theta = 14.69$, $\tau_1 = 21.62$ and $\tau_2 = 11.34$. The parameters of Kaya's controllers are $K_p = 3.81$, $K_f = 1.16$, $T_i = 21.6$ and $T_f = 21.6$. Kaya has shown that his design method is superior to Majhi and Atherton's [27] , Hang et al.'s [98], and Hägglund's [11] design methods. The tuning parameters are $\lambda_{cs} = 3.6$ and $\lambda_{cd} = 0.55\theta_m$ for the proposed design method. By employing the controllers design formulae, the setpoint tracking and load disturbance rejection controllers are obtained in the form of $G_{cs}(s) = \frac{245.1708s^2+32.96s+5}{51.84s^2+28.8s+4}$ and $G_{cd}(s) = (0.4804 + \frac{1}{69.3372s} + 4.4978s)$ respectively. The magnitude of the load disturbance is assumed to be $d = -0.1$. The responses due to the controller settings are shown in Figure 2.19. The proposed method gives the same setpoint tracking speed as that of Kaya's method. However, for the load disturbance rejection, the proposed method gives an improved performance. Now suppose that there exists a $+20\%$ error in estimating the process time delay and -20% in process time constant τ_1, the perturbed system responses are shown in Figure 2.20. It is observed from the Table 2.4, the IAE and ISE values are low. The proposed method is more robust to the system parameters variations particularly for disturbance rejection.

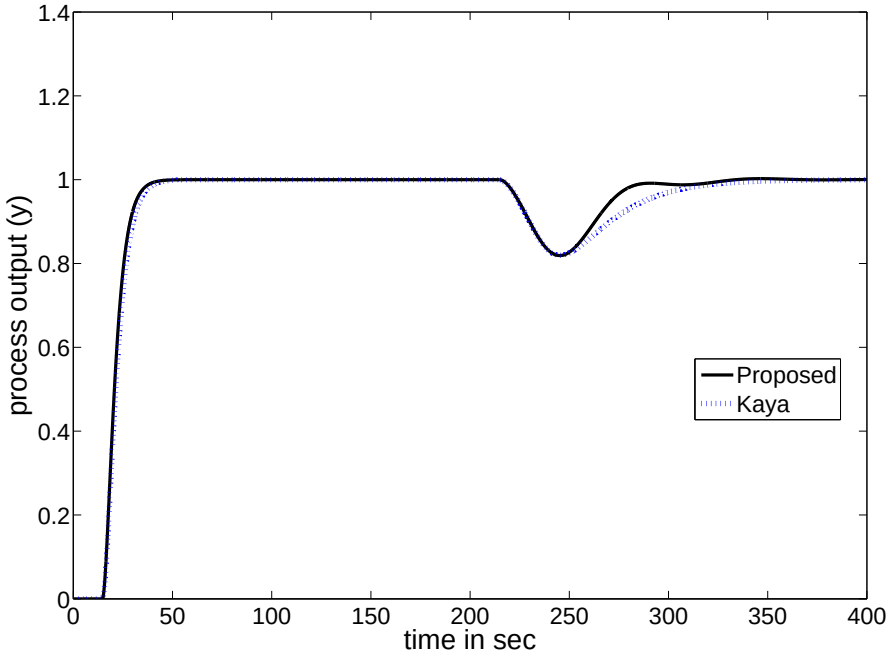

Figure 2.19: Nominal responses for Example 2.5

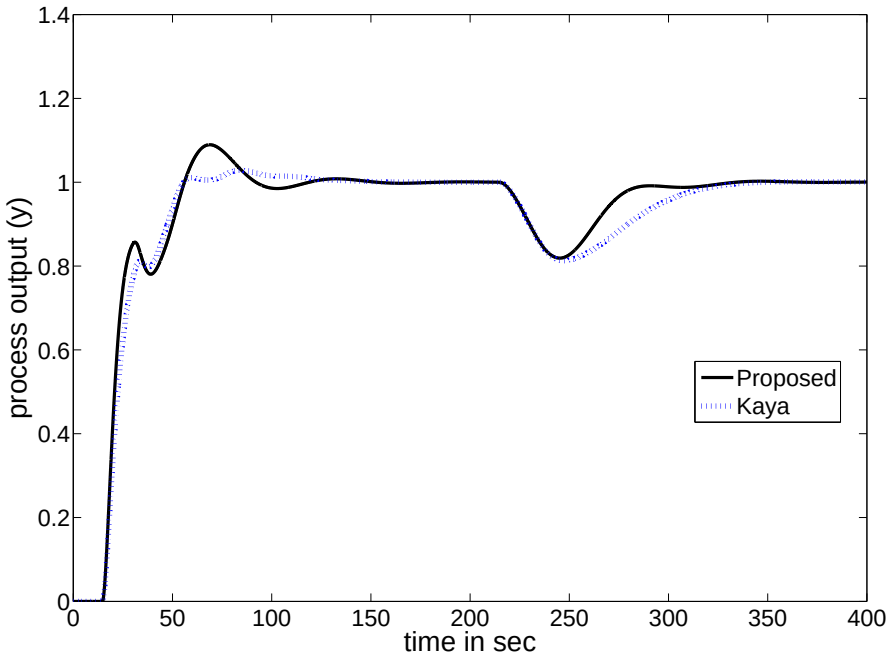

Figure 2.20: Responses for +20% estimation error in process time delay and −20% in process time constant for Example 2.5

Example-2.6: Consider an unstable SOPTD process [99] whose parameters are $k = 2$, $\tau_1 = 10$, $\tau_2 = 2$ and $\theta = 5$. The parameters of the controllers from Majhi and Atherton [99] method are $K_p = 0.1$, $T_i = 0.1$, $K_f = 5.017$, $T_f = 3.408$, $T_d = 2$ and $K_d = 0.707$. The controllers of Lu et al.'s [31] method are given as $K_1 = 2.1 + 4s$, $K_2 = 1.6 + 10.44s$, $K_3 = 0.707 + 1.414s$ and $K_4 = 1.6$. For the proposed method, choose $\lambda_{cs} = 2.5$ and $\lambda_{cd} = 1.02\theta_m$. By using the controllers design formulae the setpoint tracking controller and the disturbance rejection controller are obtained in the form of $G_{cs}(s) = \frac{20s^2+8s+1}{12.5s^2+10s+2}$ and $G_{cd}(s) = (1.0595 + \frac{1}{26.3083s} + 4.3698s)$ respectively.

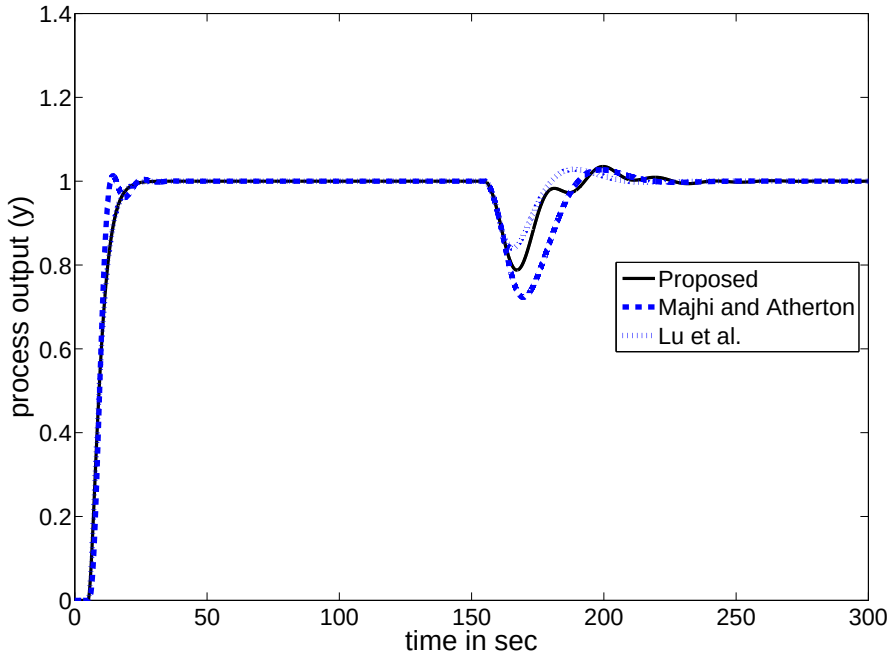

Figure 2.21: Nominal responses for Example 2.6

Using these controller settings the performance is evaluated by giving unit step input in the setpoint at $t = 0$ and a negative step load input of 0.1 at $t = 150$ sec. Figure 2.21 and Figure 2.22 show the responses for the nominal system. It can be observed that the proposed method gives better control performances for the load disturbance rejection. An estimation error of $+20\%$ in process time delay and -20% in process time constant τ_1 is considered and the corresponding responses are shown in Figure 2.23 and Figure 2.24. It is clear that the proposed method yields significantly better performances. It is observed that the proposed controllers provide robust performance for both nominal and perturbed system.

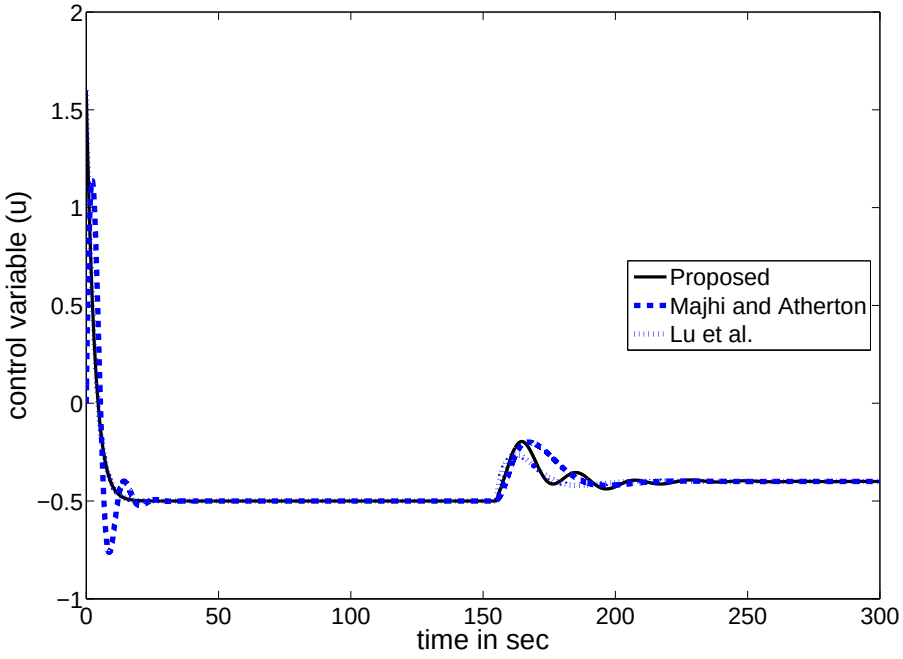

Figure 2.22: Control variables for nominal responses for Example 2.6

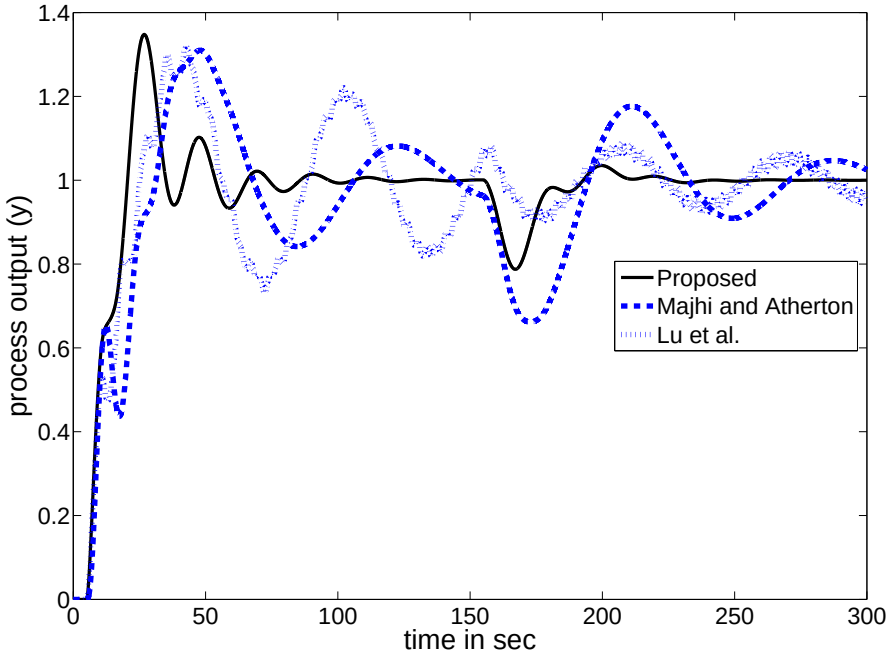

Figure 2.23: Responses for +20% estimation error in process time delay and −20% in process time constant τ_1 for Example 2.6

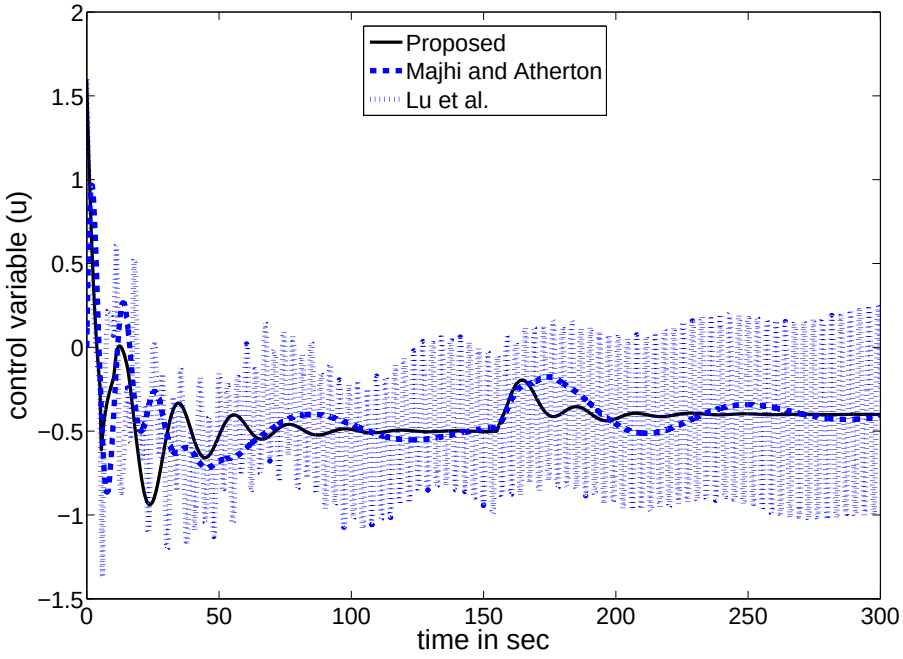

Figure 2.24: Control variables for +20% estimation error in process time delay and −20% in process time constant τ_1 for Example 2.6

Table 2.6: Robustness margins for regulatory responses

	Scheme	Nominal System		Perturbed system	
		GM	PM	GM	PM
Example-2.1	Proposed	2.56	40.15^o	1.85	30.3^o
Example-2.2	Proposed	2.13	60.87^o	1.92	52.13^o
Example-2.3	Proposed	1.88	38.16^o	1.68	30.57^o
Example-2.4	Proposed	1.94	35.6^o	1.78	30.2^o
Example-2.5	Proposed	2.6	47.81^o	1.71	44.48^o
Example-2.6	Proposed	1.89	35.42^o	1.69	31.3^o

GM: Gain Margin, PM: Phase Margin

The robustness margins for the six examples are given in Table 2.6. From the Table 2.6, it is concluded that the proposed controller gives robust response for load disturbances.

Remark 1. *Consider a non-minimum phase stable process studied by S. Skogestad [94],* $G_p(s) = \frac{(-s+1)}{(6s+1)(2s+1)^2}e^{-s}$. *Its approximate first order process model is given by* $G_p(s) = \frac{1}{7s+1}e^{-5s}$. *By the proposed method,* $\lambda_{cs} = 5$ *and* $\lambda_{cd} = \theta_m$ *have been chosen. The setpoint tracking controller and the disturbance rejection controller are obtained in the form of* $G_{cs}(s) = \frac{7s+2}{5s+1}$ *and* $G_{cd}(s) = (1.0726 + \frac{1}{7.4960s} + 1.3031s)$ *respectively. With these controller settings, the performances of the closed loop system is evaluated by introducing a unit step input in the setpoint at time* $t = 0$ *and a negative step load disturbance of* 0.1 *at* $t = 70$ *sec. From the responses of Figure 2.25 and Figure 2.26, it is concluded that the proposed structure is capable of successfully controlling non-minimum phase stable processes.*

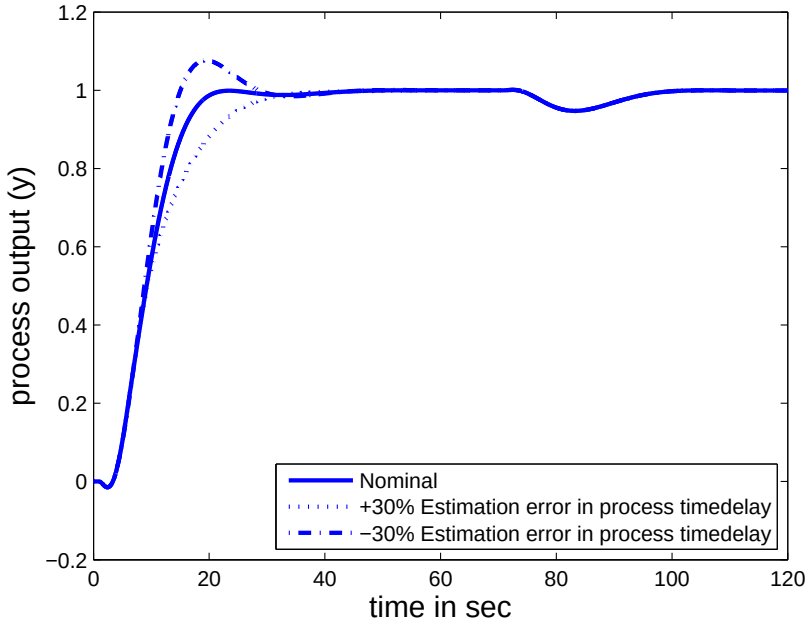

Figure 2.25: Process output responses for Non-minimum phase stable process

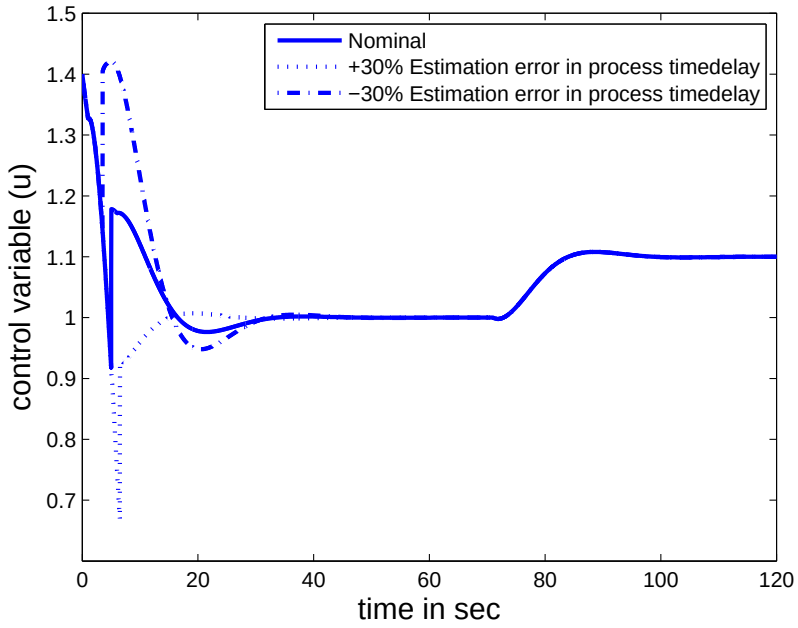

Figure 2.26: Control variable responses for Non-minimum phase stable process

2.7 Conclusions

In this chapter, the problem of controlling stable, unstable and integrating processes incorporating time delay has been tackled by proposing a new Smith predictor. The proposed Smith predictor is capable of successfully controlling a stable process and an integrator with a long time delay and the design approach can be used to control higher order integrating, minimum and non-minimum phase stable processes. The proposed control structure has two-degrees-of-freedom and correspondingly the setpoint and the load disturbance responses can be improved independently by the setpoint tracking controller and disturbance rejection controller. Hence, the setpoint tracking is decoupled from the load disturbance rejection under ideal conditions which is a dominant advantage of the proposed control scheme. It is convenient to make a trade-off between nominal performance and robust stability of the proposed control structure, and the tuning procedures for setpoint tracking and load disturbance rejection can be implemented separately, which is very attractive in practice. From the IAE and ISE values, it is shown that both nominal and robust control performances are obtained with the designed controllers. It has been demonstrated by simulation that the control strategy and the design procedure are a promising tool for controlling stable, unstable and integrating processes.

3

Enhanced Series Cascade Control Structure for Unstable Delay Processes

Contents

Resume

Control of unstable processes with dead time is a challenging problem. Series cascade controllers are used in process industries to improve the dynamic performance of a control system in the presence of disturbances. This chapter shows how to tackle unstable processes with delay using a new series cascade control structure. A delay compensator scheme has been incorporated in the primary loop of the series cascade control system. The two disturbance rejection controllers are designed by proposing the desired closed-loop complementary sensitivity functions. The direct synthesis method is used to design the setpoint tracking controller. The proposed control structure gives two-degrees-of-freedom control and correspondingly the setpoint and load disturbance responses can each be tuned conveniently by a single control parameter. Several case studies are considered to show the advantage of the proposed method when compared to other recently reported methods.

The content in this chapter is published recently in [100].

3.1 Introduction

Cascade control (which was first introduced by [37]) is one of the popular multi-loop control methods commonly used in the process control industries for the control of physical parameters such as temperature, flow and pressure. Cascade controllers are effective when the single loop PID controller finds difficulty in regulating the output in the face of load disturbances. Figure 3.1 shows a typical example of cascade control, a stirred chemical reactor where cooling water flows through the reactor jacket to regulate the reactor temperature [101, 102]. The reactor temperature is affected by changes in disturbance variables such as reactant feed temperature or feed composition. The simplest control strategy would handle such disturbances by adjusting a control valve on the cooling water inlet stream. However, an increase in the inlet cooling water temperature, an unmeasured disturbance, may cause unsatisfactory performance. The resulting increase in the reactor temperature, owing to a reduction in heat removal rate, may occur slowly. If appreciable dynamic lags occur in the jacket as well as in the reactor, the corrective action taken by the controller will be delayed. To overcome this disadvantage, a feedback controller for the jacket temperature, whose setpoint is determined by the reactor temperature controller, can be added to provide cascade control, as shown in Figure 3.1. The reactor temperature controller is the primary controller; the jacket temperature controller is the secondary controller. The control system measures the jacket temperature, compares it to a setpoint, and uses the resulting error

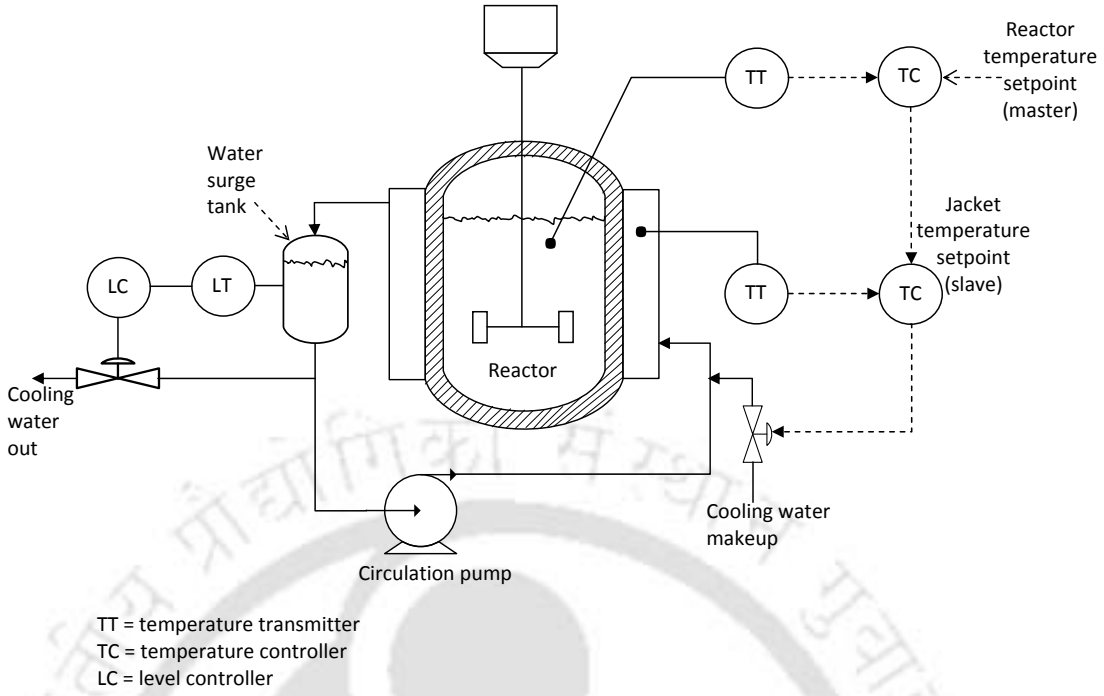

Figure 3.1: A stirred chemical reactor with cascade control

signal as the input to a controller for the cooling water makeup. The temperature setpoint and both measurements are used to adjust a single manipulated variable, the cooling water makeup rate.

The principal advantage of the cascade control strategy is that a second measured variable is located close to a potential disturbance and its associated feedback loop can react quickly, thus improving the closed-loop response.

A cascade control scheme can be used to achieve better regulatory response than that existing in the slave loop; however, if a long time delay exists in the master loop, the cascade control may not give satisfactory closed-loop responses to setpoint changes. To overcome this problem, a Smith predictor scheme can be used in the outer loop of the cascade control system. Kaya [41] proposed a cascade control scheme combined with a Smith predictor for stable cascade processes with dominant time delay and achieved better control performance when compared to some existing conventional PID tuning methods. Later on Kaya [96] suggested an improved cascade control scheme for stable processes. The design and analysis of cascade control strategies for stable processes are addressed by many researchers [40, 92, 103–105]. However, limited research has been carried out for the design of cascade control strategies for unstable processes. The control of open-loop unstable processes are

much more difficult than the control of stable processes. Liu et al. [80] proposed IMC based cascade control scheme for unstable processes with four controllers. Kaya and Atherton [81] proposed a cascade control structure for controlling unstable and integrating processes with four controllers. Very recently, Uma et al. [42] proposed an improved cascade control scheme for unstable processes using a modified Smith predictor with three controllers and one filter in the outer feedback path. In the work of Kaya and Atherton [81] and Liu et al. [80], one of the controllers is used only for stabilization and Uma et al.'s [42] scheme has one filter in the feedback path to improve the performance of the unstable processes. But in the proposed structure, there is no special controller for stabilization, rather the closed-loop controllers are used for rejecting the load disturbances as well as for stabilizing the unstable processes. Most of the methods discussed above involve many controllers with complex design methods. In practice, a simple control structure with fewer number of controllers is desirable. This chapter shows how to overcome the above deficiencies using a new cascade control structure with three controllers. Disturbance rejection in process industries is commonly much more important than setpoint tracking for many process control applications. This is because setpoint changes are often only made when the production rate is altered [72]. The proposed scheme leads to substantial control performance improvement, especially for the disturbance rejection. As the modified Smith predictor has been used in the outer loop of the cascade control structure, the proposed scheme takes advantage of modified Smith predictor and cascade control structure. Tuning rules are derived for the controllers used in the proposed structure for effective control of open-loop unstable plants. Internal stability, robustness and performance of the proposed method have been analyzed. Simulation examples are provided to show how the proposed design method compares with recently reported methods.

For clear interpretation, the chapter is organized as follows. Section 3.2 describes the proposed cascade control structure. In Section 3.3, the controller design methods are discussed followed by Section 3.4 in which the selection of tuning parameters is given. Section 3.5 deals with internal stability analysis. Robustness analysis and performance are discussed in Section 3.6. Simulation results are presented in Section 3.7 followed by the conclusions at the end.

3.2 Proposed cascade control scheme

A new cascade control structure is proposed for open-loop unstable processes as shown in Figure 3.2 where a modified Smith predictor scheme is incorporated in the outer loop. $G_{p1}(= \tilde{G}_{p1}e^{-\theta_1 s})$ and

$G_{p2}(= \tilde{G}_{p2}e^{-\theta_2 s})$ are the outer and the inner loop processes and $\tilde{G}_{p1}$ and $\tilde{G}_{p2}$ are the delay free parts and θ_1 and θ_2 are the time delays of G_{p1} and G_{p2}, respectively. $G_{m1} = \tilde{G}_{m1}e^{-\theta_{m1}s}$ is the primary process model and $G_{m2} = \tilde{G}_{m2}e^{-\theta_{m2}s}$ is the secondary process model in which $\tilde{G}_{m1}$ and $\tilde{G}_{m2}$ are the delay free parts. The overall process transfer function for the outer loop is

$$G_{po} = G_{p1}G_{p2} = \tilde{G}_{p1}\tilde{G}_{p2}e^{-(\theta_1+\theta_2)s} = G_p e^{-\theta_p s} \tag{3.1}$$

and the overall process model transfer function for the outer loop is given by

$$G_{mo} = G_{m1}G_{m2} = \tilde{G}_{m1}\tilde{G}_{m2}e^{-(\theta_{m1}+\theta_{m2})s} = G_m e^{-\theta_m s} \tag{3.2}$$

where $G_m = \tilde{G}_{m1}\tilde{G}_{m2}$ is the overall delay free part and $\theta_m = \theta_{m1} + \theta_{m2}$ is the overall time delay of the process model transfer function. The proposed scheme has three controllers : G_{cs}, G_{cd2} and G_{cd1}. The setpoint tracking controller G_{cs} is responsible for the overall servo performances, G_{cd2} is the inner loop disturbance rejection controller for rejecting the load disturbances entering into secondary process and G_{cd1} is the outer loop disturbance rejection controller for rejecting the load disturbances entering into the primary unstable process. Even though G_{cd2} and G_{cd1} are meant for load disturbance rejection, they also take part in stabilizing the unstable processes with time delay. It is to be noted that by virtue of the enhanced structure, the setpoint response is decoupled from the load disturbance response. The controllers G_{cd2} and G_{cd1} are assumed to have the forms (PID controller in series with first/second order lead/lag compensator)

$$G_{cd2} = K_{c2}\left(1 + \frac{1}{T_{i2}s} + T_{d2}s\right)\left(\frac{a_{f2}s^2 + a_{f1}s + 1}{b_{f2}s^2 + b_{f1}s + 1}\right) \tag{3.3}$$

and

$$G_{cd1} = K_{c1}\left(1 + \frac{1}{T_{i1}s} + T_{d1}s\right)\left(\frac{c_{f2}s^2 + c_{f1}s + 1}{d_{f2}s^2 + d_{f1}s + 1}\right) \tag{3.4}$$

where K_{c1} and K_{c2} are the proportional gains, T_{i1} and T_{i2} are the integral time constants and T_{d1} and T_{d2} are the derivative time constants of the PID controllers, and a_{f1}, a_{f2}, b_{f1}, b_{f2}, c_{f1}, c_{f2}, d_{f1} and d_{f2} are the filter parameters. The closed-loop transfer function of the master loop for servo response is given by

$$\frac{y_1}{r_1} = \frac{G_{cs}G_{p1}G_{p2}(1 + G_{m2}G_{cd2})(1 + G_m G_{cd1}e^{-\theta_m s})}{(1 + G_m)(1 + G_{p1}G_{p2}G_{cd1} + G_{p2}G_{cd2} + G_{m2}G_{cd1}G_{cd2}G_{p1}G_{p2})} \tag{3.5}$$

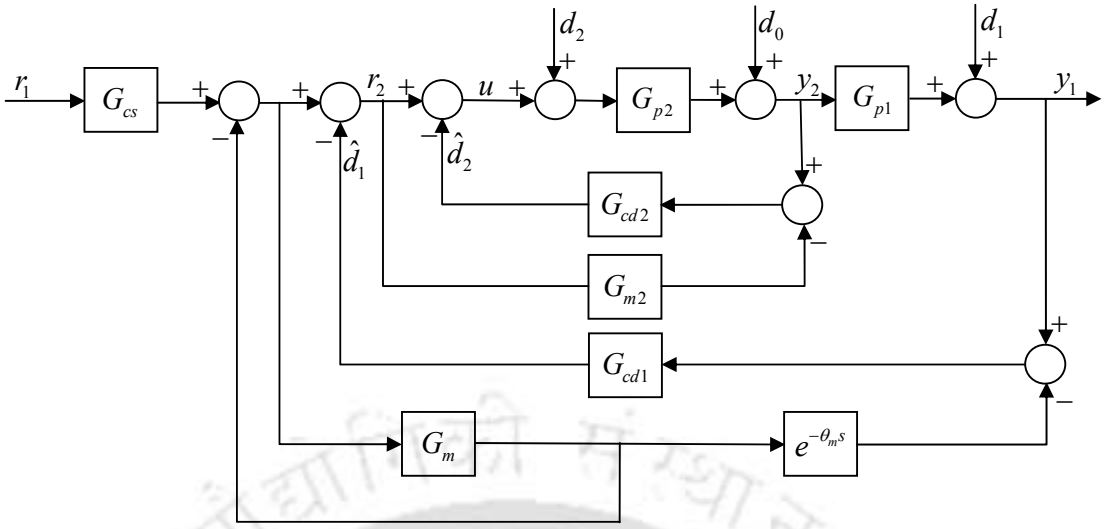

Figure 3.2: Proposed cascade scheme with modified Smith predictor

Similarly, the closed-loop transfer function of the master loop for regulatory responses are given by

$$\frac{y_1}{d_2} = \frac{G_{p1}G_{p2}}{1 + G_{p2}G_{cd2} + G_{p1}G_{p2}G_{cd1} + G_{m2}G_{cd1}G_{cd2}G_{p1}G_{p2}} \tag{3.6}$$

$$\frac{y_1}{d_0} = \frac{G_{p1}}{1 + G_{p2}G_{cd2} + G_{p1}G_{p2}G_{cd1} + G_{m2}G_{cd1}G_{cd2}G_{p1}G_{p2}} \tag{3.7}$$

$$\frac{y_1}{d_1} = \frac{1 + G_{p2}G_{cd2}}{1 + G_{p2}G_{cd2} + G_{p1}G_{p2}G_{cd1} + G_{m2}G_{cd1}G_{cd2}G_{p1}G_{p2}} \tag{3.8}$$

Assuming exact matching between the process and the model parameters, (3.5–3.8) reduce to

$$\frac{y_1}{r_1} = \frac{G_{cs}G_{p1}G_{p2}}{1 + G_m} \tag{3.9}$$

$$\frac{y_1}{d_2} = \frac{G_{p1}G_{p2}}{(1 + G_{p2}G_{cd2})(1 + G_{p1}G_{p2}G_{cd1})} \tag{3.10}$$

$$\frac{y_1}{d_0} = \frac{G_{p1}}{(1 + G_{p2}G_{cd2})(1 + G_{p1}G_{p2}G_{cd1})} \tag{3.11}$$

and

$$\frac{y_1}{d_1} = \frac{1}{1 + G_{p1}G_{p2}G_{cd1}} \tag{3.12}$$

From (3.9–3.12), it is concluded that the new cascade structure has decoupled the regulatory response from the servo response for nominal systems which is an important feature of the proposed control scheme.

3.3 Controller design procedures

Generally, in process control the dynamics of inner loop process are stable while the outer loop process dynamics may be stable or unstable. Hence, the dynamics of the inner loop process and the corresponding process model can be represented by

$$G_{p2} = \frac{k_2 e^{-\theta_2 s}}{\tau_2 s + 1} \tag{3.13}$$

and

$$G_{m2} = \frac{k_{m2} e^{-\theta_{m2} s}}{\tau_{m2} s + 1} \tag{3.14}$$

where k_2 and k_{m2} are the steady state gains, θ_2 and θ_{m2} are the time delays and τ_2 and τ_{m2} are the time constants of the secondary loop process and process model, respectively.
Similarly, the dynamics of the outer loop process and the corresponding process model can be represented by

$$G_{p1} = \frac{k_1 e^{-\theta_1 s}}{\tau_1 s - 1} \tag{3.15}$$

and

$$G_{m1} = \frac{k_{m1} e^{-\theta_{m1} s}}{\tau_{m1} s - 1} \tag{3.16}$$

where, k_1 and k_{m1} are the steady state gains, θ_1 and θ_{m1} are the time delays and τ_1 and τ_{m1} are the time constants of the primary loop process and process model, respectively. An analytical procedure is presented for determining parameters of the disturbance rejection controllers and the setpoint tracking controller is designed using the direct synthesis method. Design of the three controllers (G_{cs}, G_{cd2} and G_{cd1}) are explained in the following.

3.3.1 Design of slave loop controller, G_{cd2}

In order to design the load disturbance rejection controllers analytically and independently, the inner loop and outer loop dynamics are considered separately. From the Figure 3.2, the nominal regulatory response transfer functions for the inner loop are

$$H_{d2}(s) = \frac{y_2}{d_2} = \frac{G_{p2}}{1 + G_{cd2} G_{p2}} \tag{3.17}$$

$$H_{d0}(s) = \frac{y_2}{d_0} = \frac{1}{1 + G_{cd2} G_{p2}} \tag{3.18}$$

The nominal complementary sensitivity function of the inner loop for disturbance rejection can be obtained as

$$T_{d_{slave}} = \frac{\hat{d}_2}{d_2} = \frac{G_{cd2}G_{p2}}{1 + G_{cd2}G_{p2}} \tag{3.19}$$

In order to reject step load disturbances injected into the secondary process input, the asymptotic constraint

$$\lim_{s \to 1/\tau_2} (1 - T_{d_{slave}}) = 0 \tag{3.20}$$

should be satisfied so that the closed-loop internal stability can be achieved. According to robust IMC theory [93], the desired closed-loop complementary sensitivity function is proposed as

$$T_{d_{slave}} = \frac{\alpha_2 s + 1}{(\lambda_2 s + 1)^2} e^{-\theta_2 s} \tag{3.21}$$

where λ_2 is a tuning parameter for obtaining the desirable regulatory performance of the inner loop. Now substituting (3.21) in (3.20), gives

$$\lim_{s \to 1/\tau_2} \left[1 - \frac{\alpha_2 s + 1}{(\lambda_2 s + 1)^2} e^{-\theta_2 s} \right] = 0 \tag{3.22}$$

By following a simple calculation, we get

$$\alpha_2 = \tau_2 \left[\left(1 + \frac{\lambda_2}{\tau_2} \right)^2 e^{\theta_2/\tau_2} - 1 \right] \tag{3.23}$$

Using (3.19), the inner loop controller G_{cd2} can be obtained as

$$G_{cd2} = \frac{T_{d_{slave}}}{1 - T_{d_{slave}}} \frac{1}{G_{p2}} \tag{3.24}$$

Substituting (3.13) and (3.21) into (3.24), we get

$$G_{cd2} = \frac{(\alpha_2 s + 1)(\tau_2 s + 1)}{k_2[(\lambda_2 s + 1)^2 - (\alpha_2 s + 1)e^{-\theta_2 s}]} \tag{3.25}$$

Due to the symmetrical pole-zero configuration, the phase of the standard Padé approximation ($R_{n,n}(s)$) goes to $-n\pi$ and its amplitude remains constant at all frequencies. On the other hand, the step-response of $R_{n,n}(s)$ exhibits a jump at $t = 0$ which is not very desirable. To avoid this phenomenon the Padé approximation $R_{n-1,n}(s)$ where the numerator's degree is one less than that of the denominator has been suggested. This gives a better approximation of the step-response [106]. Using $R_{n-1,n}(s)$ (where $n = 2$) Padé approximation for time delay term of (3.25) i.e. $e^{-\theta_2 s} = \frac{6 - 2\theta_2 s}{6 + 4\theta_2 s + \theta_2^2 s^2}$,

now (3.25) becomes

$$G_{cd2} = \frac{(\alpha_2 s+1)(\tau_2 s+1)(6+4\theta_2 s+\theta_2^2 s^2)}{k_2[(\lambda_2 s+1)^2(6+4\theta_2 s+\theta_2^2 s^2)-(\alpha_2 s+1)(6-2\theta_2 s)]} \tag{3.26}$$

Simplifying (3.26), we get

$$G_{cd2} = \frac{6+4\theta_2 s+\theta_2^2 s^2}{k_2 x_1 s} \times \frac{(\alpha_2 s+1)(\tau_2 s+1)}{1+p_1 s+p_2 s^2+p_3 s^3} \tag{3.27}$$

where,

$x_1 = 6\theta_2 + 12\lambda_2 - 6\alpha_2$, $x_2 = 6\lambda_2^2 + 8\lambda_2\theta_2 + \theta_2^2 + 2\alpha_2\theta_2$, $x_3 = 4\lambda_2^2\theta_2 + 2\lambda_2\theta_2^2$, $x_4 = \lambda_2^2\theta_2^2$, $p_1 = x_2/x_1$, $p_2 = x_3/x_1$ and $p_3 = x_4/x_1$.

Comparing (3.27) and (3.3), the parameters of the slave loop controller G_{cd2} are expressed as

$$\begin{cases} K_{c2} = -4\theta_2/k_2 x_1,\ T_{i2} = 2\theta_2/3,\ T_{d2} = \theta_2/4 \\ a_{f1} = \tau_2 + \alpha_2,\ a_{f2} = \tau_2\alpha_2,\ b_{f1} = -p_1,\ b_{f2} = -p_2 \end{cases} \tag{3.28}$$

It is to be noted that all the parameters in (3.28) become positive since the expression of x_1 gives a negative value (see Appendix-A.1).

3.3.2 Design of master loop controller, G_{cd1}

From (3.12), the nominal regulatory response transfer function of the outer loop is given by

$$H_{d1}(s) = \frac{y_1}{d_1} = \frac{1}{1+G_{cd1}G_{p1}G_{p2}} \tag{3.29}$$

The nominal complementary sensitivity function of the master loop for disturbance rejection is

$$T_{d_{master}} = \frac{\hat{d}_1}{d_2} = \frac{G_{cd1}G_{p1}G_{p2}}{1+G_{cd1}G_{p1}G_{p2}} \tag{3.30}$$

Like the previous subsection, an asymptotic constraint in order to reject the load disturbances injected into the primary process is

$$\lim_{s\to 1/\tau_1}(1-T_{d_{master}}) = 0 \tag{3.31}$$

The desired closed-loop complementary sensitivity function is proposed as

$$T_{d_{master}} = \frac{\alpha_1 s+1}{(\lambda_1 s+1)^3} e^{-\theta_m s} \tag{3.32}$$

where $\theta_m = \theta_1 + \theta_2$ and λ_1 is a tuning parameter for obtaining the desirable regulatory performance of the outer loop. Substitution of (3.32) in (3.31) results in

$$\lim_{s \to 1/\tau_1} \left[1 - \frac{\alpha_1 s + 1}{(\lambda_1 s + 1)^3} e^{-\theta_m s} \right] = 0 \tag{3.33}$$

which upon simplification gives

$$\alpha_1 = \tau_1 \left[\left(\frac{\lambda_1}{\tau_1} + 1 \right)^3 e^{\theta_m / \tau_1} - 1 \right] \tag{3.34}$$

Using (3.30), expression for the outer loop controller G_{cd1} can be written as

$$G_{cd1} = \frac{T_{d_{master}}}{1 - T_{d_{master}}} \frac{1}{G_{p1} G_{p2}} \tag{3.35}$$

Hence, from (3.13), (3.15), (3.32) and (3.35), the expression for the master loop controller G_{cd1} becomes

$$G_{cd1} = \frac{(\alpha_1 s + 1)(\tau_1 s - 1)(\tau_2 s + 1)}{k_1 k_2 [(\lambda_1 s + 1)^3 - (\alpha_1 s + 1) e^{-\theta_m s}]} \tag{3.36}$$

Using Padé approximation $R_{n-1,n}(s)$ (where $n = 2$) for the time delay term of (3.36),

$$G_{cd1} = \frac{(\alpha_1 s + 1)(\tau_1 s - 1)(\tau_2 s + 1)(6 + 4\theta_m s + \theta_m^2 s^2)}{k_1 k_2 [(\lambda_1 s + 1)^3 (6 + 4\theta_m s + \theta_m^2 s^2) - (\alpha_1 s + 1)(6 - 2\theta_m s)]} \tag{3.37}$$

By following a simple calculation, we have

$$G_{cd1} = -\frac{6 + 4\theta_m s + \theta_m^2 s^2}{k_1 k_2 m_1 s} \times \frac{(\alpha_1 s + 1)(\tau_2 s + 1)}{(1 + l_1 s + l_2 s^2 + l_3 s^3 + l_4 s^4)/(-\tau_1 s + 1)} \tag{3.38}$$

where,

$m_1 = 6\theta_m + 18\lambda_1 - 6\alpha_1$, $m_2 = 2\alpha_1\theta_m + \theta_m^2 + 12\lambda_1\theta_m + 18\lambda_1^2$, $m_3 = 3\lambda_1\theta_m^2 + 12\lambda_1^2\theta_m + 6\lambda_1^3$, $m_4 = 3\lambda_1^2\theta_m^2 + 4\lambda_1^3\theta_m$, $m_5 = \lambda_1^3\theta_m^2$, $l_1 = m_2/m_1$, $l_2 = m_3/m_1$, $l_3 = m_4/m_1$ and $l_4 = m_5/m_1$.

Since the resulting controller does not have a standard PID controller form, the remaining issue is to design the PID controller that approximates the controller most closely. Therefore, the following procedure is employed to produce the desired disturbance estimator in a simple way. The filter parameters d_{f1} and d_{f2} can be determined from the second part of the denominator of (3.38) i.e. $(1 + l_1 s + l_2 s^2 + l_3 s^3 + l_4 s^4)/(-\tau_1 s + 1)$. d_{f1} can be obtained by taking first derivative of the above term and setting $s = 0$ i.e.

$$\frac{d}{ds} \left(d_{f2} s^2 + d_{f1} s + 1 \right) \Big|_{s=0} = \frac{d}{ds} \left(\frac{1 + l_1 s + l_2 s^2 + l_3 s^3 + l_4 s^4}{-\tau_1 s + 1} \right) \Big|_{s=0}$$

Similarly, taking second derivative and substituting $s = 0$ give the expression for d_{f2}. The filter parameters d_{f1} and d_{f2} can also be obtained using the Taylor series expansion as given in Appendix-A.2.

(3.38) and (3.4) gives the parameters of master loop controller G_{cd1} as

$$\begin{cases} K_{c1} = -4\theta_m/k_1k_2m_1,\ T_{i1} = 2\theta_m/3,\ T_{d1} = \theta_m/4 \\ c_{f1} = \tau_2 + \alpha_1,\ c_{f2} = \tau_2\alpha_1,\ d_{f1} = l_1 + \tau_1,\ d_{f2} = l_2 + \tau_1 d_{f1} \end{cases} \tag{3.39}$$

It is to be noted that in (3.39) all the controller parameters become positive as the expression of m_1 gives a negative value (see Appendix-A.3).

3.3.3 Design of setpoint tracking controller, G_{cs}

In a feedback system with a stable/unstable process with time delay, often the setpoint response transfer function is chosen in the form of low pass filter with time delay for a unit step setpoint. In order to obtain good setpoint response for the nominal system, the setpoint tracking controller is designed to be rational and stable. G_{cs} is designed for the trajectory problem. The idea of direct synthesis is to specify the desired closed-loop response and solve for the corresponding controller. We use the following transfer function to obtain the desired response

$$H_{r1}(s) = \frac{1}{(\lambda_{cs}s + 1)^2}e^{-\theta_m s} \tag{3.40}$$

where $\theta_m = \theta_1 + \theta_2$, and λ_{cs} is the time constant of setpoint controller, or equivalently

$$h_{r1}(t) = \begin{cases} 0, & t < \theta_m \\ 1 - \left(1 + \frac{t}{\lambda_{cs}}\right) e^{-(t-\theta_m)/\lambda_{cs}}, & t \geq \theta_m \end{cases} \tag{3.41}$$

(3.41) corresponds to a smooth setpoint response with no overshoot.

Using (3.9) and (3.40), the setpoint tracking controller can be obtained as

$$G_{cs}(s) = \frac{\tau_1\tau_2 s^2 + (\tau_1 - \tau_2)s + k_1k_2 - 1}{k_1k_2(\lambda_{cs}s + 1)^2} \tag{3.42}$$

When the tuning parameter λ_{cs} tends to zero, $G_{cs}(s)$ becomes optimal. λ_{cs} is an adjustable closed-loop design parameter that is always positive. A fast speed of response is favored by a small value of λ_{cs}, and robustness is favored by a large value of λ_{cs}. Hence, there is a tradeoff in selecting the tuning

parameter λ_{cs}. Thus, λ_{cs} should be selected such that there is a good compromise between the speed of response and the robustness. Guidelines for selection of the tuning parameters (λ_{cs}, λ_1 and λ_2) are presented in the section 3.4.

3.4 Selection of tuning parameters λ_{cs}, λ_2 and λ_1

The setpoint controller tuning parameter λ_{cs} is selected so as to achieve good performance and robustness. The response speed is determined by the parameter λ_{cs}. The choice of a higher value of λ_{cs} slows down the system and makes it more robust while small values of λ_{cs} may cause instability of the cascade control structure in the presence of unmodelled dynamics. $\lambda_{cs} > 0$ is an adjustable closed-loop design parameter whose initial value is typically chosen as half of the overall process model time delay. If good control performances are not achieved with this value, then λ_{cs} can be varied gradually from this value till good nominal and robust control performances are achieved. Quantitatively, the suggested range of λ_{cs} is $0.1\theta_m - \theta_m$. As the secondary controller mainly takes care of the regulatory performance of the inner loop and the primary controller takes care of the outer loop regulatory performance, λ_2 and λ_1 can be selected independently. The tuning of the control parameters λ_2 and λ_1 aims at the trade-off between nominal performance of the closed-loop and its robust stability. That is, decreasing λ_2 and λ_1 improves the disturbance rejection performance of the closed-loop but degrades its robust stability in the presence of process uncertainty. In contrast, increasing λ_2 and λ_1 tends to strengthen the robust stability of the closed-loop but degrades its disturbance rejection performance. On the basis of simulation studies based on the MATLAB toolbox, it is observed that the initial value of λ_2 is twice of the inner loop process model time delay and that of λ_1 is equal to overall process model time delay. If good control performances are not achieved with these values, then the tuning parameters can be varied gradually from these values till good nominal and robust control performances are achieved. The suggested range of tuning parameters are $\lambda_2 = 1.5\theta_{m2} - 3.6\theta_{m2}$ and $\lambda_1 = 0.5\theta_m - 1.5\theta_m$.

For clarity, the detail tuning procedure is summarized below.

I. With the known secondary process model (G_{m2}), select the tuning parameter λ_2 in the range of $1.5\theta_{m2} - 3.6\theta_{m2}$ and find the secondary loop disturbance rejection controller (G_{cd2}) parameters using (3.28).

II. Then from the known primary process (G_{p1}), obtain the overall primary loop process model

(G_m) and overall primary loop time delay (θ_m) from (3.2)

III. Find the primary loop disturbance rejection controller (G_{cd1}) parameters from (3.39) after selecting the tuning parameter λ_1 in the range of $0.5\theta_m - 1.5\theta_m$.

IV. Then determine the setpoint tracking controller (G_{cs}) using (3.42) after selecting the tuning parameter λ_{cs} in the range of $0.1\theta_m - \theta_m$.

3.5 Internal stability analysis

A system with unstable pole-zero cancellations renders internally unstable closed-loop system. The input/output stability analysis may not be sufficient for the practical control system analysis and design. Therefore, the internal stability analysis is the basic requirement for any interconnected control systems. A linear time-invariant interconnected system consisting of single input and single output (SISO) plants is internally stable if and only if

$$p_c(s) = \Delta \prod_{i=1}^{n} p_i(s) \tag{3.43}$$

has all its roots in the left half of the complex plane [107]. In (3.43), Δ = determinant of the systems as defined in the Mason's gain formula for signal flow graph analysis i.e. $\Delta = 1 - \sum_i L_{1i} + \sum_j L_{2j} - \sum_k L_{3k} + \cdots$, (L_{1i} is the loop gains, L_{2j} is the products of two non-touching loop gains and L_{3k} is the products of three non-touching loop gains), n = number of subsystems, and $p_i(s)$ = characteristic polynomial of the respective subsystem transfer function.

The proposed control scheme has eight subsystems such as G_{cs}, G_{cd1}, G_{cd2}, G_{p1}, G_{p2}, G_{m2}, G_m and $e^{-\theta_m s}$. Let $G_{cs} = f_1(s)/g_1(s)$, $G_{cd1} = f_2(s)/g_2(s)$, $G_{cd2} = f_3(s)/g_3(s)$ and $G_{p1} = G_{p2} = G_{m2} = \delta(s)/\gamma(s)$ be coprime polynomial fractions. Their respective characteristic polynomials are $p_1 = g_1(s)$, $p_2 = g_2(s)$, $p_3 = g_3(s)$, $p_4 = p_5 = p_6 = \gamma(s)$, $p_7 = \gamma^2(s)$ and $p_8 = 1$.

Using (3.43), $p_c(s)$ can be expressed as

$$\begin{aligned} p_c(s) &= \Delta \prod_{i=1}^{8} p_i(s) \\ &= [\gamma^2(s) + \delta^2(s)][\gamma(s)g_3(s) + \delta(s)f_3(s)][\gamma^2(s)g_2(s) + \delta^2(s)f_2(s)]g_1(s) \end{aligned} \tag{3.44}$$

The stabilization of G_{p2} depends on the polynomial $[\gamma(s)g_3(s) + \delta(s)f_3(s)]$. The slave loop controller G_{cd2} must be stable for the stability of $g_3(s)$ and is used to achieve best disturbance response. Similarly, the stabilization of the primary process G_{p1} depends on the polynomial $[\gamma^2(s)g_2(s) + \delta^2(s)f_2(s)]$. In

order to achieve the best disturbance response, the master loop controller G_{cd1} must be stable for the stability of $g_2(s)$. The controller G_{cs} must be stable for the stability of $g_1(s)$ in order to achieve the best setpoint response. With these constraints, the overall system is internally stable if and only if G_{p1} and G_{p2} are stabilized by the controllers G_{cd1} and G_{cd2} respectively.

3.6 Robustness analysis and performance

3.6.1 Robustness analysis

Since no mathematical model of a system will be a perfect representation of the actual system, a study of robustness analysis is an important task in control system design. There are two most important adverse effects of modeling uncertainties such as degradation of the system performance and destabilization. In practical situations, there are at least two types of uncertainties. First, unmodeled dynamics which represent high frequency uncertainties, and second, parametric uncertainty representing lack of precise knowledge of the actual system parameters. Recent developments in the analysis of systems with parametric uncertainty have been inspired by Kharitonov's theorem. Kharitonov's theorem is probably the most well-known and simplest tool for robust stability analysis [108–112].

Interval polynomial may be written as

$$\Gamma = \left\{ p(s,q) | p(s,q) = \sum_{i=0}^{n} q_i s^i \ , \ q_i \in [q_i^-, q_i^+], i = 0, 1, \cdots, n \right\} \tag{3.45}$$

where q_i^- and q_i^+ represent lower and upper bounds for the continuous set q_i. The variations of polynomial coefficients in 3.45 must be independent of each other. Kharitonov's theorem states that $p(s,q) = 0$ is robustly stable if and only if the following four Kharitonov's polynomials are stable

$$K_1(s) = q_0^- + q_1^- s + q_2^+ s^2 + q_3^+ s^3 + q_4^- s^4 + q_5^- s^5 + q_6^+ s^6 + q_7^+ s^7 + \cdots$$

$$K_2(s) = q_0^+ + q_1^+ s + q_2^- s^2 + q_3^- s^3 + q_4^+ s^4 + q_5^+ s^5 + q_6^- s^6 + q_7^- s^7 + \cdots$$

$$K_3(s) = q_0^+ + q_1^- s + q_2^- s^2 + q_3^+ s^3 + q_4^+ s^4 + q_5^- s^5 + q_6^- s^6 + q_7^+ s^7 + \cdots$$

$$K_4(s) = q_0^- + q_1^+ s + q_2^+ s^2 + q_3^- s^3 + q_4^- s^4 + q_5^+ s^5 + q_6^+ s^6 + q_7^- s^7 + \cdots$$

The geometric meaning of this theorem is that if the origin point of the complex plane is outside the boundary of the Kharitonov rectangles then the system is robustly stable. If the family of n^{th}-degree

polynomials is robustly stable, the value sets will move in a counter-clockwise direction through n quadrants of the complex plane without passing through or touching the origin of the plane. The analytical meaning of this theorem is that the robust stability of an interval polynomial family can be determined by forming the four Kharitonov polynomials, factoring them, and examining the roots. If all the roots are in the left-half plane, then the family is robustly stable. If any of those polynomials has roots on the imaginary axis or in the right-half plane, the family is not robustly stable.

For example, consider a system with the following outer and inner loop plant transfer functions $G_{p1} = \frac{e^{-0.339s}}{5s-1}$ and $G_{p2} = \frac{e^{-0.6s}}{2.07s+1}$.

From (3.29), the closed-loop characteristic equation of the outer loop is given by

$$1 + G_{cd1}G_{p1}G_{p2} = 0$$

Now, the interval polynomial of this system is given by

$$\begin{aligned} p(s,q) = {} & [2.2750 \;\; 2.7806] + [14.3827 \;\; 17.5789]s + [36.9524 \;\; 45.1640]s^2 + [50.9606 \;\; 62.2852]s^3 \\ & + [41.8061 \;\; 51.0963]s^4 + [21.2444 \;\; 25.9654]s^5 + [5.8279 \;\; 7.1229]s^6 + [0.7445 \;\; 0.9099]s^7 \end{aligned} \tag{3.46}$$

The four Kharitonov polynomials are obtained as

$$K_1(s) = 2.2750 + 14.3827s + 45.1640s^2 + 62.2852s^3 + 41.8061s^4 + 21.2444s^5 + 7.1229s^6 + 0.9099s^7$$

$$K_2(s) = 2.7806 + 17.5789s + 36.9524s^2 + 50.9606s^3 + 51.0963s^4 + 25.9654s^5 + 5.8279s^6 + 0.7445s^7$$

$$K_3(s) = 2.7806 + 14.3827s + 36.9524s^2 + 62.2852s^3 + 51.0963s^4 + 21.2444s^5 + 5.8279s^6 + 0.9099s^7$$

$$K_4(s) = 2.2750 + 17.5789s + 45.1640s^2 + 50.9606s^3 + 41.8061s^4 + 25.9654s^5 + 7.1229s^6 + 0.7445s^7$$

Table 3.1: The roots of Kharitonov polynomials

$K_1(s)$	$K_2(s)$	$K_3(s)$	$K_4(s)$
-3.9185	$-2.4605 + j3.3704$	$-0.8300 + j2.7856$	$-3.8328 + j1.7493$
-2.3321	$-2.4605 - j3.3704$	$-0.8300 - j2.7856$	$-3.8328 - j1.7493$
$-0.1947 + j1.8466$	-1.6326	-2.6051	$-0.0634 + j1.2189$
$-0.1947 - j1.8466$	$-0.1122 + j0.7888$	-1.3674	$-0.0634 - j1.2189$
-0.7410	$-0.1122 - j0.7888$	$-0.1780 + j0.4606$	-1.1263
$-0.2236 + j0.2390$	-0.7869	$-0.1780 - j0.4606$	-0.3750
$-0.2236 - j0.2390$	-0.2630	-0.4165	-0.2735

The coefficients of Kharitonov polynomials ($K_1(s)$, $K_2(s)$,$K_3(s)$ and $K_4(s)$) are checked for Hurwitz

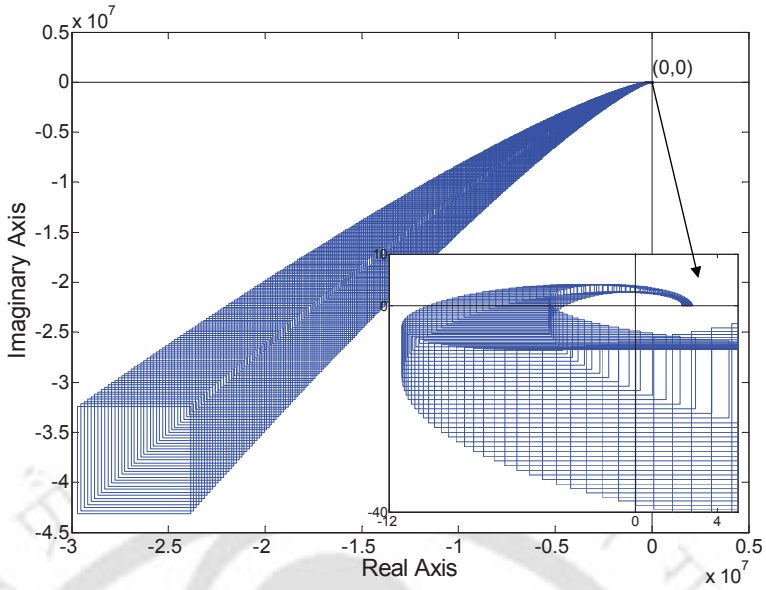

Figure 3.3: Kharitonov's rectangle (Nominal system) for $G_{p1} = e^{-0.339s}/(5s-1)$ and $G_{p2} = e^{-0.6s}/(2.07s+1)$

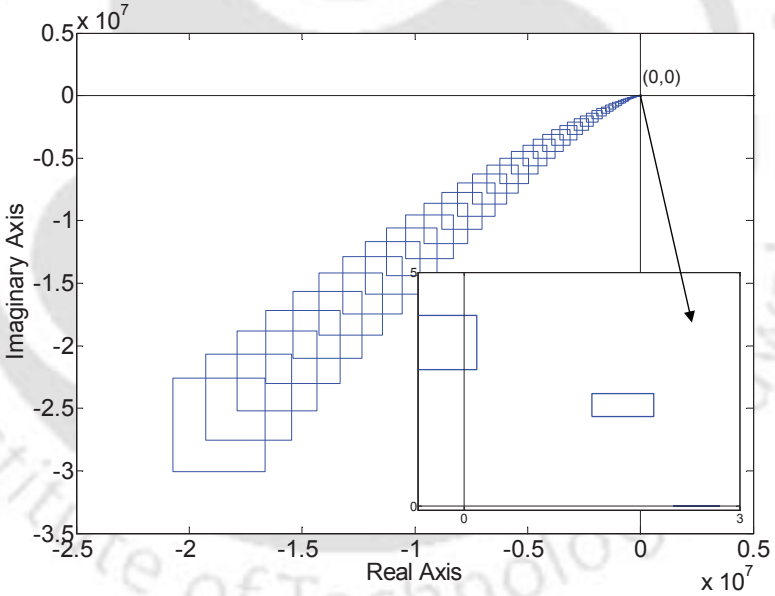

Figure 3.4: Kharitonov's rectangle for $+10\%$ perturbation in both time delays and -10% in both time constants for $G_{p1} = e^{-0.339s}/(5s-1)$ and $G_{p2} = e^{-0.6s}/(2.07s+1)$

condition. It is observed that all the roots of the Kharitonov polynomials (Table 3.1) have negative real part i.e. all roots are in the left half of the complex plane. The Kharitonov rectangles of the closed-loop system for nominal and perturbed systems are shown in Figure 3.3 and Figure 3.4

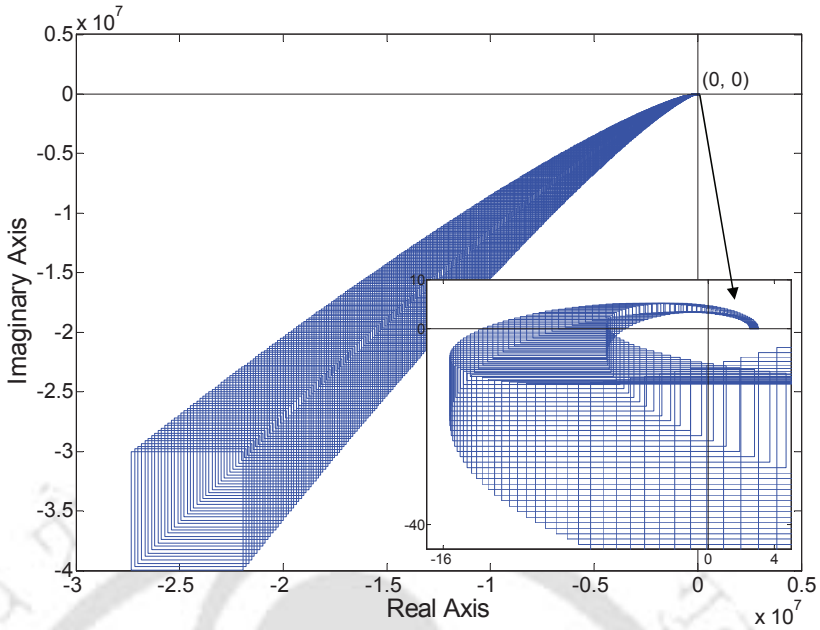

Figure 3.5: Kharitonov's rectangle (Nominal system) for $G_{p1} = e^{-4s}/(20s-1)$ and $G_{p2} = 2e^{-2s}/(20s+1)$

respectively. From the Figure 3.3 and Figure 3.4, it is clear that Kharitonov rectangles move about the origin in counterclockwise sense in order to have the monotonic phase increase property of Hurwitz polynomials. The graphs are zoomed to show what is happening in the neighborhood of the point $(0, 0)$. It is observed that the closed-loop characteristic equation of the system is stable in complex plane in Mikhailov's sense. Since the origin is excluded from the Kharitonov rectangles (Figure 3.3, Figure 3.4) it is concluded that the closed-loop control system is robustly stable. By following a similar procedure as above the robustness analysis for other processes can be checked. Figure 3.5 shows the Kharitonov rectangles for the closed-loop system for $G_{p1} = e^{-4s}/(20s-1)$ and $G_{p2} = 2e^{-2s}/(20s+1)$.

3.6.2 Performance

To evaluate the closed-loop performance, the indices IAE, ISE and TV are considered.

3.7 Simulation study

The results of simulations of three examples to illustrate the value of the proposed cascade control design method are given in this section.

Example-3.1: Consider the plant parameters of master and slave loop studied by Liu et al. [80] where $k_1 = 1$, $\tau_1 = 5$, $\theta_1 = 0.339$ and $k_2 = 1$, $\tau_2 = 2.07$, $\theta_2 = 0.6$. Choosing the tuning parameter

$\lambda_{cs} = 0.852\theta_m = 0.8$, the setpoint tracking controller becomes $G_{cs} = \frac{10.35s^2+2.93s}{0.64s^2+1.6s+1}$. The parameters of G_{cd2} are $a_{f1} = 3.9850$, $a_{f2} = 3.9641$, $b_{f1} = 1.9558$, $b_{f2} = 0.2294$, $K_{c2} = 0.5337$, $T_{i2} = 0.2260$ and $T_{d2} = 0.0848$ by selecting the tuning parameter $\lambda_2 = 1.7\theta_{m2} = 0.5763$. The parameters of G_{cd1} are obtained as $c_{f1} = 7.4950$, $c_{f2} = 11.2297$, $d_{f1} = 0.4757$, $d_{f2} = 0.1448$, $K_{c1} = 0.4213$, $T_{i1} = 0.6260$ and $T_{d1} = 0.2348$ by selecting $\lambda_1 = 1.065\theta_m = 1$. Uma et al. [42] has shown the superiority of their control scheme over Liu et al.'s [80] and Kaya and Atherton's [81] schemes. In the case of Uma et al.'s method, the parameters for setpoint tracking controllers are $k_{cs} = 9.1554$, $k_{is} = 2.8953$, $k_{ds} = 4.4519$, $\beta_s = 0.2373$ and the tuning parameters are $\lambda_s = 0.7042$ and $\lambda_2 = 0.6$. The disturbance rejection controller parameters are $k_{cd} = 4.5867$, $k_{id} = 0.8488$, $k_{dd} = 2.4639$, $\alpha_d = 0.4695$ and $\beta_d = 0.022$. The setpoint weighting and filter parameters are $\varepsilon = 0.3$ and $\tau_f = 5.6340$, respectively. A unit-step setpoint is introduced at time $t = 0$, a unit negative step input load disturbance d_2 at time $t = 20$ sec and a load disturbance $d_1 = -0.2$ at time $t = 40$ sec. The closed-loop nominal responses for all the above controller settings are shown in the Figure 3.6 and the corresponding control signals are given in the Figure 3.7.

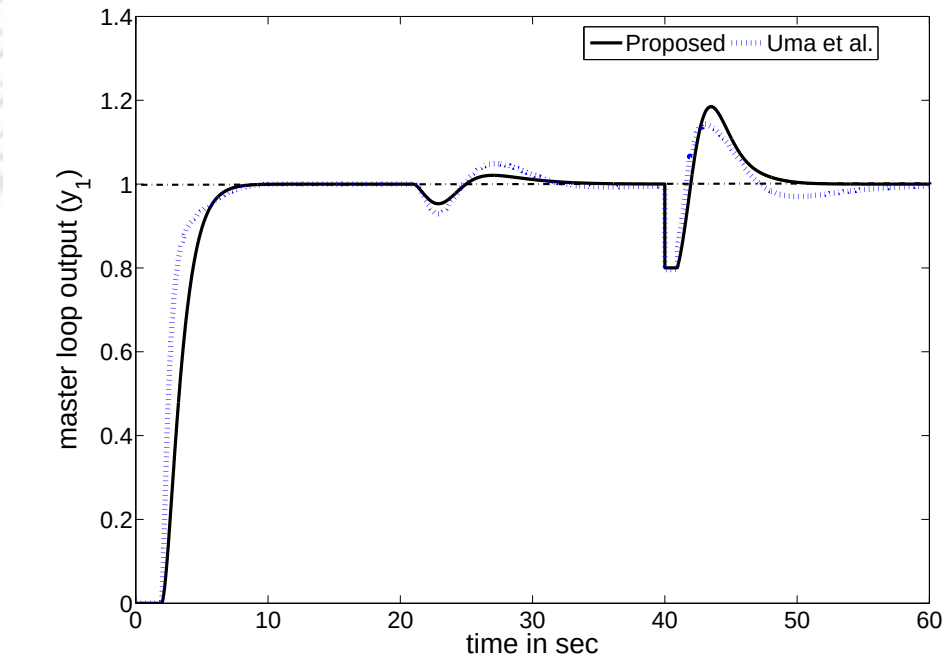

Figure 3.6: Nominal responses for example 3.1

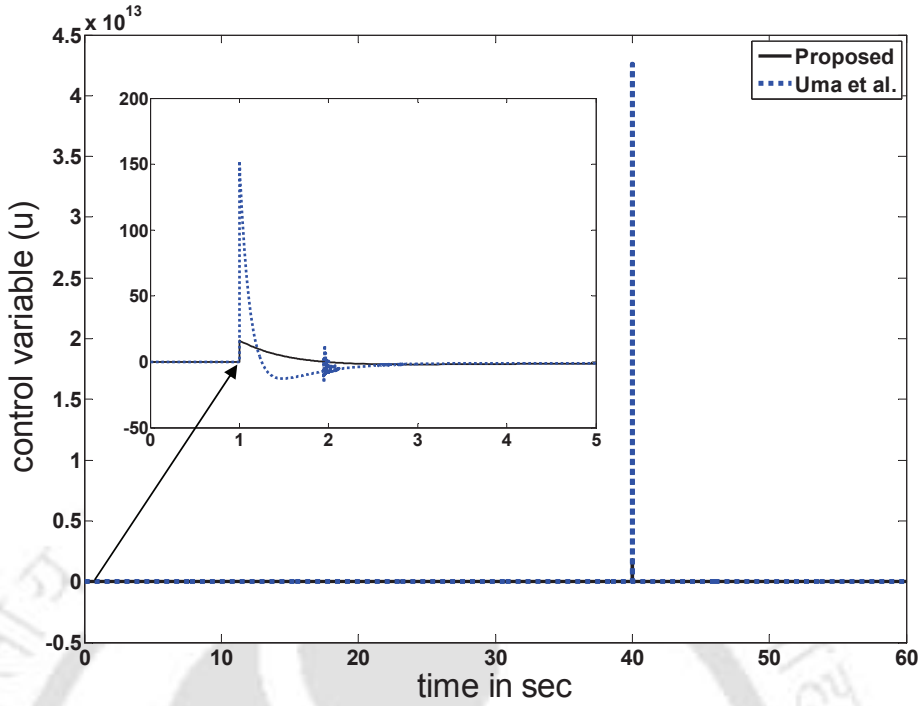

Figure 3.7: Nominal control signals for example 3.1

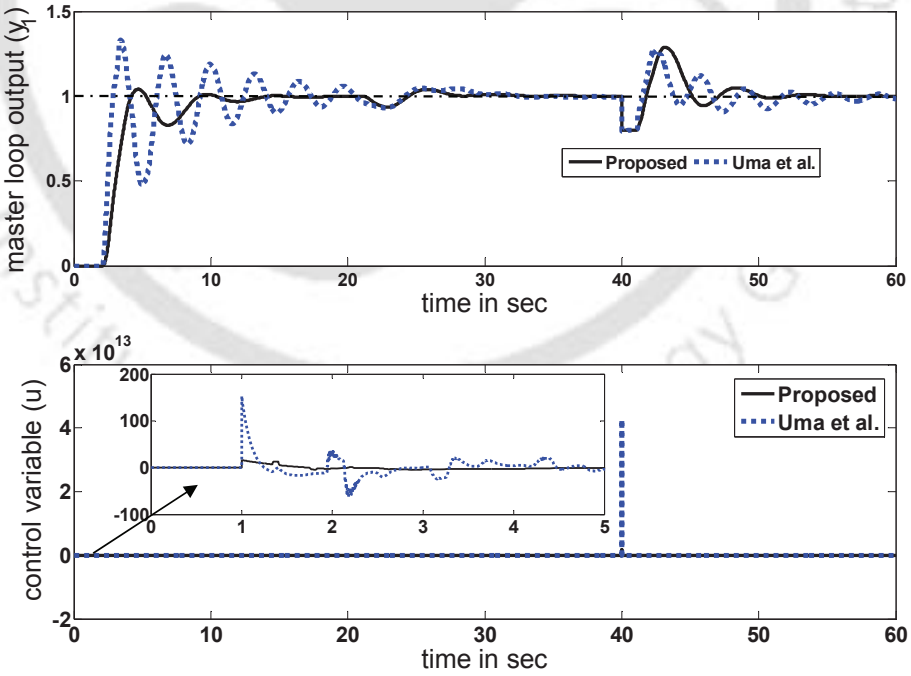

Figure 3.8: +20% perturbation in both the time delays and −20% in both the time constants for example 3.1

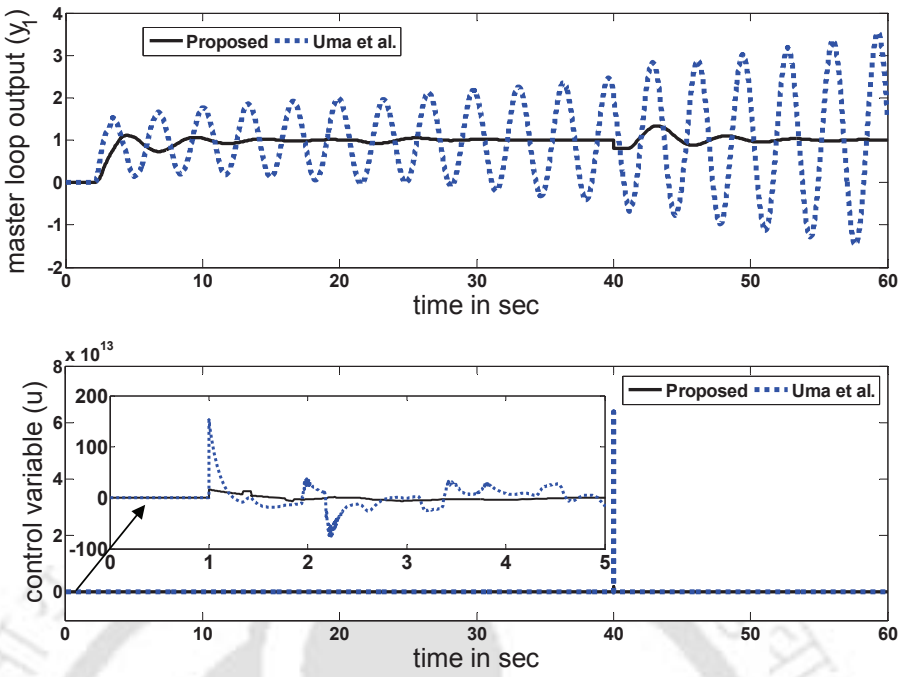

Figure 3.9: +25% perturbation in both the time delays and −25% in both the time constants for example 3.1

From the responses, it is observed that the proposed method gives almost similar setpoint response when compared with the other method. But particularly for disturbance rejection, the proposed method gives less settling time and comparatively superior performances to Uma et al.'s method. In the present work, to illustrate the robustness to parameter variations, a +20% perturbations in both the process time delays and −20% in both the process time constants are considered and corresponding responses are shown in Figure 3.8. From the Figure 3.8, it is seen that the proposed cascade control structure gives improved responses both in setpoint as well as load disturbance rejection. Figure 3.9 shows the responses for +25% perturbations in both the time delays and −25% in both the time constants. In Figure 3.9, it is observed that Uma et al.'s method gives unbounded response. Also, it is seen from Figure 3.8, Figure 3.9 and Table 3.3 that the proposed method gives smooth control signal as compared to Uma et al.'s method. From the Table 3.2, it is observed that the proposed control scheme gives low value of performance specifications.

Example-3.2: Consider a system with the following master and slave loop plant transfer functions $G_{p1} = \frac{e^{-4s}}{20s-1}$ and $G_{p2} = \frac{2e^{-2s}}{20s+1}$, respectively, studied by Liu et al. [80] and Uma et al. [42]. For the proposed method, taking $\lambda_{cs} = 0.334\theta_m = 2$ results in the setpoint controller of the form $G_{cs} = \frac{400s^2+1}{8s^2+8s+2}$ using (3.42). The parameters of G_{cd2} are $a_{f1} = 31.8289$, $a_{f2} = 236.5784$, $b_{f1} = 19.2568$,

$b_{f2} = 14.5805$, $K_{c2} = 0.3645$, $T_{i2} = 1.3333$ and $T_{d2} = 0.5$ by selecting $\lambda_2 = 2\theta_{m2} = 4$. The parameters of G_{cd1} are obtained as $c_{f1} = 46.6511$, $c_{f2} = 533.0224$, $d_{f1} = 2.0483$, $d_{f2} = 3.0520$, $K_{c1} = 0.2312$, $T_{i1} = 4$ and $T_{d1} = 1.5$ by selecting $\lambda_1 = 0.667\theta_m = 4$. In Liu et al.'s method, the controllers are $P_c = 1 + s$, $C(s) = (400s^2 + 2s + 1)/2(6s + 1)^2$, $F_{10}(s) = (20s + 1)/2(0.5s + 1)$ and $F_2(s) = 1.9785 + (1/30.6256s) + 28.0736s$. In Uma et al.'s method, the settings are given by $k_{cs} = 4.6571$, $k_{is} = 0.1829$, $k_{ds} = 12.2857$, $\beta_s = 2.8571$, $k_{cd} = 3.1190$, $k_{id} = 0.0921$, $k_{dd} = 6.6156$, $\alpha_d = 3$, $\beta_d = 0.1440$, $\varepsilon = 0.3$ and $\tau_f = 36$. With these controller settings, the performances of

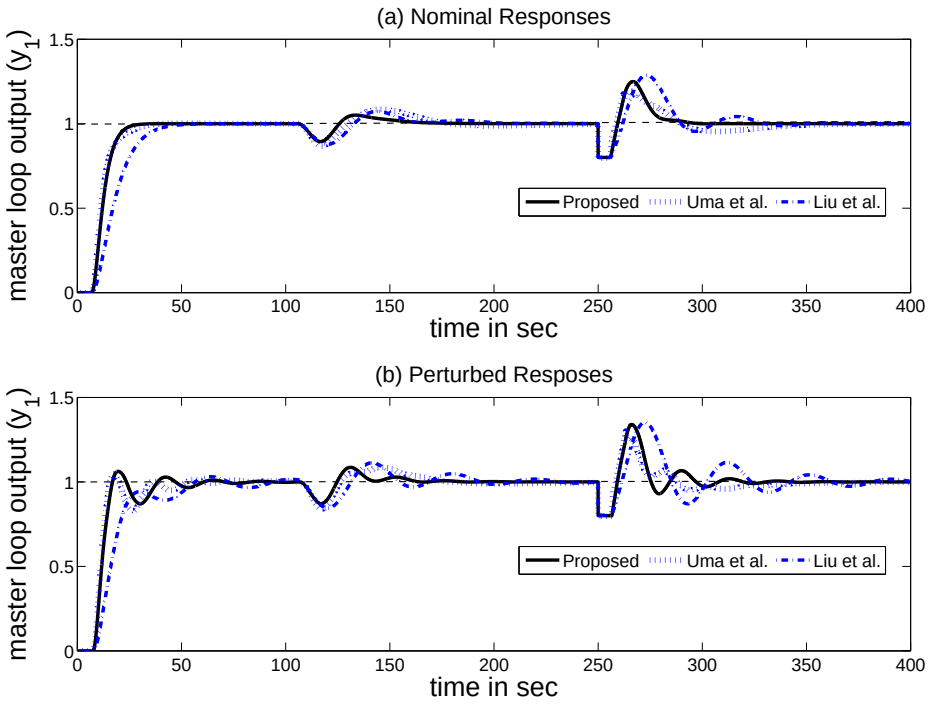

Figure 3.10: Responses for example 3.2

the closed-loop system is evaluated by introducing a unit step input in the setpoint at time $t = 0$, a negative step load input(d_2) at $t = 100$ sec and a negative disturbance (d_1) of magnitude 0.2 at $t = 250$ *sec* . The step responses for no mismatch in the plant models are shown in Figure 3.10(a). Now suppose that there exists a 10% error in estimating the process time delays and time constants i.e. both process time delays are 10% larger and both process time constants are 10% smaller, the perturbed system responses are shown in Figure 3.10(b). From the Table 3.2, it can be observed that the proposed method gives low IAE and ISE values for both nominal system and perturbed system.

It is seen from the Table 3.3, the proposed scheme gives smoother control signals compared to Uma et al.'s as the TV value of proposed method is low. Often, the disturbance rejection is more important than setpoint tracking for industrial practice. It is evident that the proposed controller provides robust performance particularly in the load disturbance rejection.

Example-3.3: Let the primary and secondary plant transfer functions be $G_{p1} = \frac{e^{-3s}}{10s-1}$ and $G_{p2} = \frac{2e^{-2s}}{s+1}$, respectively, studied by Kaya and Atherton [81] and Uma et al. [42]. For the proposed method, the setpoint tracking controller is obtained in the form $G_{cs} = \frac{10s^2+9s+1}{4.5s^2+6s+2}$ using (3.42) by selecting the tuning parameter $\lambda_{cs} = 0.3\theta_m = 1.5$. Using the design formulae the disturbance rejection controller parameters are obtained as $a_{f1} = 449.5502$, $b_{f1} = 0.8409$, $K_{c2} = 0.0015$, $T_{i2} = 1.3333$, $T_{d2} = 0.5$, $c_{f1} = 36.2409$, $c_{f2} = 35.2409$, $d_{f1} = 1.7273$, $d_{f2} = 2.2519$, $K_{c1} = 0.0914$, $T_{i1} = 3.3333$ and $T_{d1} = 1.25$ by selecting $\lambda_2 = 3.4\theta_{m2} = 6.8$ and $\lambda_1 = 0.8\theta_m = 4$. In Kaya and Atherton's method, the controllers are $G_{c1} = 0.5(1 + 1/0.1s)$, $G_{c2} = (s+1)/(2s+2)$, $G_{c3} = 14.25 + 5.58s$ and $G_d = 1.414(1+s)$. The controller settings of Uma et al.'s method are $k_{cs} = 7.7086$, $k_{is} = 1.1181$, $k_{ds} = 6.6604$, $\beta_s = 0.566$, $k_{cd} = 2.0907$, $k_{id} = 0.059$, $k_{dd} = 3.3963$, $\alpha_d = 2.5$, $\beta_d = 0.1509$, $\varepsilon = 0.3$ and $\tau_f = 30$. A unit step input in the setpoint at $t = 0$ and a unit negative load disturbance(d_0) at $t = 50$ sec are introduced. The closed-loop responses for nominal system is shown in the Figure 3.11(a).

Table 3.2: Performance specifications of regulatory responses

	Scheme	Nominal System		Perturbed system	
		IAE	ISE	IAE	ISE
Example-3.1	Proposed	1.115	0.1045	1.708	0.2581
	Uma et al.	1.276	0.1105	4.141	0.6681
Example-3.2	Proposed	7.123	0.9748	8.751	1.213
	Uma et al.	11.14	1.082	11.48	1.258
	Liu et al.	11.83	1.689	16.68	2.477
Example-3.3	Proposed	6.258	1.277	7.236	2.102
	Uma et al.	6.22	1.163	7.829	2.125
	Kaya and Atherton	7.976	2.005	11	3.756

Now suppose that there exists a +10% perturbation in the primary process time delay and −10% in primary time constant.

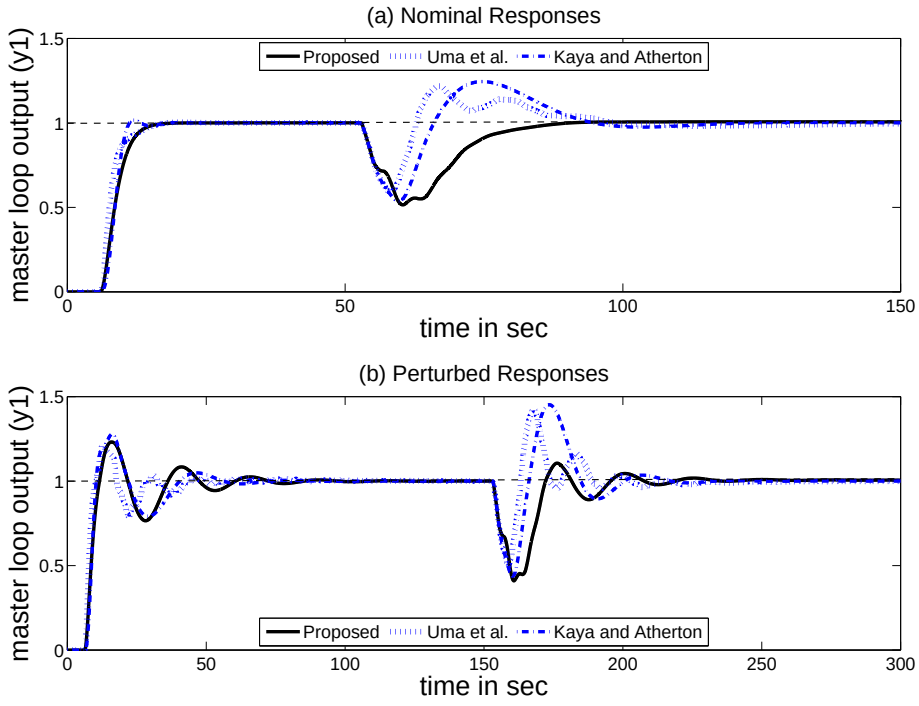

Figure 3.11: Responses for example 3.3

Table 3.3: Performance specifications of manipulated input

	Scheme	Nominal System	Perturbed system
		TV	TV
Example-3.1	Proposed	35.245	74.618
	Uma et al.	90.66	1.388×10^3
Example-3.2	Proposed	50.568	87.958
	Uma et al.	71.228	180.380
	Liu et al.	12.742	19.861
Example-3.3	Proposed	3.000	4.585
	Uma et al.	12.320	52.836
	Kaya and Atherton	4.704	5.940

The closed-loop performances of perturbed systems are evaluated by introducing a unit step input at $t = 0$ and a unit negative disturbance (d_0) at $t = 150$ sec as shown in Figure 3.11(b). From the Table

3.2 and 3.3, it is observed that the performance specifications are low for the proposed method. The proposed cascade control structure gives much improved performance especially for load disturbance rejection. It can be observed that the robustness of the proposed design technique towards assumed parameter perturbation is satisfactory. The performance of the proposed technique is found to be superior because of the modeling, the new cascade control structure and the design method used.

3.8 Conclusions

In this chapter, the problem of controlling an open-loop unstable process with time delay has been tackled by proposing an enhanced cascade control scheme. Cascade control structure improves regulatory response while the modified Smith predictor isolates and compensates the dead time. The proposed control structure combines the merits of the cascade control and the modified Smith predictor structure. The setpoint tracking is decoupled from the load disturbance rejection under ideal conditions which is an important feature of the proposed control scheme. It is demonstrated by Kharitonov's theorem that the controllers are robust and stable. The control method is very simple and has given improved results when compared with some recently published results.

4

Improved Series Cascade Control Structure for Integrating Delay Processes

Contents

Resume

This chapter presents a simple and effective modified Smith predictor based control structure which can be used to control a class of integrating processes with delay. The proposed control structure consists of only two controllers and a setpoint filter. The secondary loop controller is designed based on IMC approach, the setpoint filter is based on optimal performance index and the primary load disturbance rejection controller is designed on the basis of the desired closed-loop complementary sensitivity function. The present method gives significant disturbance rejection performance. Simulation comparative results with some of the schemes recently presented in the literature are presented, showing the simplicity of the proposed design.

The work presented in this chapter is published in [113].

4.1 Introduction

The design and analysis of cascade control strategies for stable processes are addressed by many researchers such as [38, 40, 79, 92, 103, 105, 114–119]. However, limited research has been carried out for the design of cascade controllers for integrating processes. The control of integrating processes is much more difficult than the control of self-regulating processes. Again, a simple cascade control structure may not give a satisfactory regulatory performance for integrating processes if the time delay incorporated is dominant. It is widely known that the process time delay can be compensated effectively by the use of Smith predictor. A control structure which possesses the features of both cascade control and the Smith predictor together can drastically improve the closed-loop performances. Recently, Kaya and Atherton [81] have proposed a control structure for controlling integrating processes using modified Smith predictor, but their control structure involves four controllers. Later on Uma et al. [82] proposed a control structure for integrating processes with three controllers and a filter. In the present work, a modified Smith predictor [83] is used in the outer loop of the cascade control structure for control of integrating processes with time delay. This chapter shows how the proposed cascade control enhances the closed-loop performances with only two controllers and a filter. The two main advantages of the proposed control structure are: firstly, it suppresses the load disturbance and compensates the dead time and secondly, the servo response decouples the regulatory response in nominal case. Furthermore, to improve the practical utility of cascade control structures, we conduct a more in-depth analysis of the effect of load disturbances on closed-loop performance with the help of

simulation tool. This will provide support for control engineers in designing more effective strategies for multi-loop or MIMO (multi input and multi output) control systems.

For clear interpretation, the proposed cascade control structure is presented in Section 4.2. The controller design procedures are given in Section 4.3. Selection of tuning parameters is addressed in Section 4.4 followed by robustness analysis in Section 4.5 and the simulation results in section 4.6. The conclusions are drawn in Section 4.7.

4.2 Series cascade control structure

The proposed series cascade control structure for integrating processes with time delay is shown in Fig. 4.1. G_{p1} and G_{p2} are the dynamics of primary and secondary processes, respectively. The proposed structure has two controllers (namely, G_{c2} and G_{c3}) and a setpoint filter (G_{c1}). G_{c2} in the inner loop stabilizes the process by rejecting the disturbances entering the inner loop. G_{c3} is the outer loop disturbance rejection controller and also takes part in stabilizing the integrating processes with time delay. G_{c1} is responsible for the overall servo performances. The closed-loop primary process

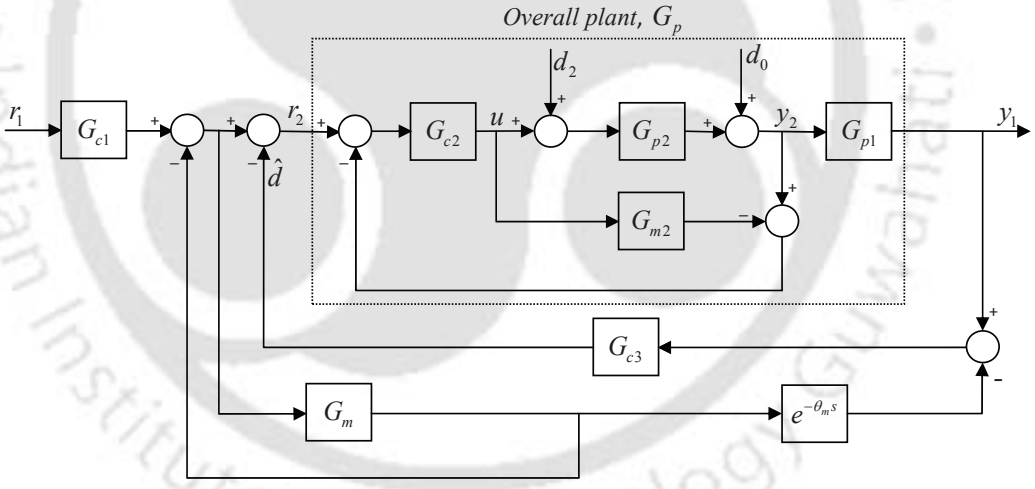

Figure 4.1: Proposed series cascade control structure

response (y_1) to primary setpoint (r_1) and disturbance (d_0 and d_2) inputs is given by

$$y_1 = \frac{G_{c1}G_{c2}G_{p2}G_{p1}\left(1+G_{c3}G_m e^{-\theta_m s}\right)}{(1+G_m)(1+G_{c2}G_{p2}G_{p1}G_{c3}+G_{c2}G_{p2}-G_{c2}G_{m2})} r_1 + \frac{G_{p1}(1-G_{c2}G_{m2})}{1+G_{c2}G_{p2}G_{p1}G_{c3}+G_{c2}G_{p2}-G_{c2}G_{m2}} d_0 + \frac{G_{p2}G_{p1}(1-G_{c2}G_{m2})}{1+G_{c2}G_{p2}G_{p1}G_{c3}+G_{c2}G_{p2}-G_{c2}G_{m2}} d_2 \tag{4.1}$$

where $G_m e^{-\theta_m s}$ is the transfer function model of the overall process dynamics (G_p), G_m is the delay free model of G_p and G_{m2} is the model of G_{p2}. Based on the assumption that the model used perfectly matches the process dynamics, (4.1) reduces to

$$y_1 = \frac{G_{c1} G_m e^{-\theta_m s}}{1 + G_m} r_1 + \frac{G_{p1}\left(1 - G_{c2} G_{m2}\right)}{1 + G_{c2} G_{p2} G_{p1} G_{c3}} d_0 + \frac{G_{p2} G_{p1}\left(1 - G_{c2} G_{m2}\right)}{1 + G_{c2} G_{p2} G_{p1} G_{c3}} d_2 \tag{4.2}$$

It concludes from (4.2) that the proposed series cascade control structure decouples the load response from the setpoint response for the nominal case.

4.2.1 Process models

Generally, in the industrial applications, the dynamics of secondary process is stable and that of the primary process is stable or unstable or integrating [82]. Therefore, the slave loop process transfer function is assumed to be a first order plus time delay (FOPTD):

$$G_{p2} = \frac{k_2 e^{-\theta_2 s}}{\tau_2 s + 1} \tag{4.3}$$

The secondary process model is given by

$$G_{m2} = \frac{k_{m2} e^{-\theta_{m2} s}}{\tau_{m2} s + 1} \tag{4.4}$$

The master loop process transfer functions are assumed in the following form

$$G_{p1} = \frac{k_1 e^{-\theta_1 s}}{s} \tag{4.5}$$

for an integrating plus time delay (IPTD) process,

$$G_{p1} = \frac{k_1 e^{-\theta_1 s}}{s^2} \tag{4.6}$$

for a double integrating plus time delay (DIPTD) process and

$$G_{p1} = \frac{k_1 e^{-\theta_1 s}}{s\left(\tau_1 s + 1\right)} \tag{4.7}$$

for an integrating second order plus time delay (ISOPTD) process.

4.3 Controller design procedures

The proposed cascade control structure has two controllers and a setpoint filter: G_{c2}, G_{c3} and G_{c1} and the design methods are explained in this section.

4.3.1 Design of the inner loop controller G_{c2}

The inner loop controller (G_{c2}) is an IMC controller and is designed based on IMC approach [91]. The IMC approach is already discussed in Chapter 2 therefore the detail of the design procedure has not been given here. Using the IMC approach, the secondary loop controller is obtained as

$$G_{c2} = \frac{\tau_2 s + 1}{k_2(\lambda_2 s + 1)} \tag{4.8}$$

where λ_2 is the desired closed-loop time constant of the controller.

4.3.2 Design of G_{c1} and G_{c3}

4.3.2.1 Design of setpoint filter G_{c1} :

G_{c1} is designed for servo tracking. Consider a primary process with transfer function

$$G_{p1} = \frac{k_1 e^{-\theta_1 s}}{s^n (\tau_1 s + 1)} \tag{4.9}$$

where n is a positive integer. The overall process dynamics is given by

$$G_p = G_{c2} G_{p2} G_{p1} = \frac{k_1 e^{-\theta_p s}}{s^n (\tau_1 s + 1)(\lambda_2 s + 1)} \tag{4.10}$$

where $\theta_p = \theta_1 + \theta_2$. Using the (1, 2) Padé approximation of the time delay, (4.10) reduces to

$$G_p = \frac{k_1 (6 - 2s\theta_p)}{s^n (\tau_1 s + 1)(\lambda_2 s + 1)\left(6 + 4s\theta_p + s^2\theta_p^2\right)} \tag{4.11}$$

We adopt the optimal performance index [120] $\min \|W(s)(1 - Y_{r1}(s))\|_\infty$ to design the setpoint tracking controller G_{c1}, where $Y_{r1}(s) = y_1/r_1$, $W(s)$ is a weighting function and it usually can be selected as $1/s$ for a unit step setpoint. According to the maximum modulus theorem, a bounded function $|W(s)(1 - Y_{r1}(s))|$ cannot attain its maximum value at the interior point of the open right half plane. On the other hand, the G_p has a zero at $3/\theta_p$ in the open right half plane. Thus, we obtain

$$\|W(s)(1 - Y_{r1}(s))\|_\infty \geq |W(3/\theta_p)| \tag{4.12}$$

Minimizing (4.12), we get

$$W(s)(1 - Y_{r1}(s)) = \theta_p/3 \tag{4.13}$$

Using (4.2) and (4.13), we obtain the optimal controller as

$$G_{com} = \frac{s^n (\tau_1 s + 1)(\lambda_2 s + 1) + k_1}{k_1} \tag{4.14}$$

However, the above controller may not be realizable. So a low pass filter

$$f_1 = \frac{1}{(\lambda_1 s + 1)^x} \tag{4.15}$$

is introduced and the index x should be selected such that the resulting controller becomes realizable. Thus, the setpoint filter is obtained in the form of

$$G_{c1} = G_{com} f_1 = \frac{s^n (\tau_1 s + 1)(\lambda_2 s + 1) + k_1}{k_1 (\lambda_1 s + 1)^x} \tag{4.16}$$

where λ_1 is an adjusting tuning parameter. As λ_1 tends to zero, the G_{c1} tends to be optimal. λ_1 is a closed loop tuning parameter which is always positive. For smaller value of λ_1, the speed of response is faster whereas good robustness is achieved by a larger value of λ_1.

Remark 2. *The order of the numerator and denominator polynomials of G_{c1} is considered as same. x is selected based on the order of the numerator polynomials. In order to make the controller realizable, it is suggested that $x = 2$ for IPTD, $x = 3$ for DIPTD and ISOPTD processes.*

4.3.2.2 Design of the outer loop controller G_{c3} :

Based on the nature of the integrating process, the desired closed-loop complementary sensitivity function is chosen and correspondingly the controller is designed. In fact, for all the cases PID controller in series with lead/lag compensator is obtained. The detailed design procedure is explained below.

The nominal complementary sensitivity function of the primary loop for disturbance rejection is

$$T_{d_{outer}} = \frac{\hat{d}}{d_2} = \frac{G_{c2} G_{p1} G_{p2} G_{c3}}{1 + G_{c2} G_{p1} G_{p2} G_{c3}} \tag{4.17}$$

(4.17) can be written as

$$T_{d_{outer}} = \frac{G_p G_{c3}}{1 + G_p G_{c3}} = \frac{G_m e^{-\theta_m s} G_{c3}}{1 + G_m e^{-\theta_m s} G_{c3}} \tag{4.18}$$

where G_m and θ_m are the delay free part and the time delay of the overall process model respectively. By following a simple calculation, we get

$$G_{c3} = \frac{T_{d_{outer}}}{1 - T_{d_{outer}}} \frac{1}{G_m e^{-\theta_m s}} \tag{4.19}$$

4.3.2.3 For IPTD primary process:

If the primary process dynamics is $G_{p1} = \left(k_1 e^{-\theta_1 s}\right)/s$, according to robust IMC theory, the desired closed-loop complementary sensitivity function can be written as

$$T_{d_{outer}} = \frac{\alpha_1 s + 1}{(\lambda_3 s + 1)^2} e^{-\theta_m s} \tag{4.20}$$

From (4.3), (4.5), (4.8), (4.19) and (4.20), we get

$$G_{c3} = \frac{s\,(\alpha_1 s + 1)\,(\lambda_2 s + 1)}{k_1 \left[(\lambda_3 s + 1)^2 - (\alpha_1 s + 1)\, e^{-\theta_m s}\right]} \tag{4.21}$$

As the resulting controller G_{c3} does not have a standard PID controller form, the remaining issue is to design the PID controller that approximates the controller most closely. Therefore, the following procedure is employed to get the desired outer loop disturbance rejection controller in a simple way. Padé approximations are the most frequently used methods to approximate a time delay by a rational function. Due to the symmetrical pole-zero configuration, the phase of standard Padé approximation ($R_{n,n}(s)$) goes to $-n\pi$ and its amplitude remains constant at all frequencies. The step-response of the standard Padé approximation with equal numerator and denominator degree, exhibits a jump at time t=0 which is highly undesirable in simulating time delays [106]. To avoid this phenomenon, the Padé approximation with different degrees ($R_{n-1,n}(s)$, the numerator's degree is one less than that of the denominator) is considered. This gives a better approximation of the step-response.

Using the (1, 2) Padé approximation for the time delay (i.e. $e^{-\theta_m s} = (6 - 2s\theta_m)/\left(6 + 4s\theta_m + s^2\theta_m^2\right)$), (4.21) reduces to

$$G_{c3} = \frac{(\alpha_1 s + 1)\,(\lambda_2 s + 1)\left(6 + 4s\theta_m + s^2\theta_m^2\right)}{k_1\left[x_3 s^3 + x_2 s^2 + x_1 s + x_0\right]} \tag{4.22}$$

where $x_3 = \lambda_3^2\theta_m^2$, $x_2 = 4\lambda_3^2\theta_m + 2\lambda_3\theta_m^2$, $x_1 = 2\alpha_1\theta_m + 6\lambda_3^2 + \theta_m^2 + 8\lambda_3\theta_m$ and $x_0 = -6\alpha_1 + 6\theta_m + 12\lambda_3$. (4.22) can be approximated as a PID controller in series with lead/lag compensator in the form of

$$G_{c3} = K_c\left(1 + \frac{1}{T_i s} + T_d s\right)\left(\frac{a_2 s^2 + a_1 s + 1}{b_2 s^2 + b_1 s + 1}\right) \tag{4.23}$$

where

$$\begin{cases} K_c = \frac{6(\alpha_1+\lambda_2)}{k_1 x_1}, T_i = \alpha_1 + \lambda_2, T_d = \frac{\alpha_1\lambda_2}{\alpha_1+\lambda_2} \\ a_2 = \frac{\theta_m^2}{6}, a_1 = \frac{2\theta_m}{3} \\ b_2 = \frac{x_3}{x_1}, b_1 = \frac{x_2}{x_1} \end{cases} \tag{4.24}$$

with $\alpha_1 = \theta_m + 2\lambda_3$.

4.3.2.4 For DIPTD primary process:

If the process dynamics is of $G_{p1} = \left(k_1 e^{-\theta_1 s}\right)/s^2$, the desired closed-loop complementary sensitivity function is considered as

$$T_{d_{outer}} = \frac{\alpha_2 s^2 + \alpha_1 s + 1}{(\lambda_3 s + 1)^4} e^{-\theta_m s} \tag{4.25}$$

From (4.3), (4.6), (4.8), (4.19) and (4.25), the controller becomes

$$G_{c3} = \frac{s^2 \left(\alpha_2 s^2 + \alpha_1 s + 1\right)(\lambda_2 s + 1)}{k_1 \left[(\lambda_3 s + 1)^4 - (\alpha_2 s^2 + \alpha_1 s + 1) e^{-\theta_m s}\right]} \tag{4.26}$$

Again, using the (1, 2) Padé approximation for the time delay
(i.e. $e^{-\theta_m s} = (6 - 2s\theta_m)/\left(6 + 4s\theta_m + s^2\theta_m^2\right)$), (4.26) reduces to

$$G_{c3} = \frac{s \left(\alpha_2 s^2 + \alpha_1 s + 1\right)(\lambda_2 s + 1)\left(6 + 4s\theta_m + s^2\theta_m^2\right)}{k_1 \left[m_5 s^5 + m_4 s^4 + m_3 s^3 + m_2 s^2 + m_1 s + m_0\right]} \tag{4.27}$$

where $m_5 = \lambda_3^4\theta_m^2$, $m_4 = 4\lambda_3^4\theta_m + 4\lambda_3^3\theta_m^2$, $m_3 = 6\lambda_3^4 + 16\lambda_3^3\theta_m + 6\lambda_3^2\theta_m^2$, $m_2 = 24\lambda_3^2\theta_m + 2\alpha_2\theta_m + 4\lambda_3\theta_m^2 + 24\lambda_3^3$, $m_1 = 36\lambda_3^2 + \theta_m^2 - 6\alpha_2 + 16\lambda_3\theta_m + 2\alpha_1\theta_m$ and $m_0 = 6\theta_m + 24\lambda_3 - 6\alpha_1$.
By taking $\alpha_1 = \theta_m + 4\lambda_3$ and $\alpha_2 = 6\lambda_3^2 + \theta_m^2/6 + 8\lambda_3\theta_m/3 + \alpha_1\theta_m/3$, (4.27) can be written in the form of a PID controller in series with compensator as

$$G_{c3} = K_c \left(1 + \frac{1}{T_i s} + T_d s\right)\left(\frac{a_3 s^3 + a_2 s^2 + a_1 s + 1}{b_3 s^3 + b_2 s^2 + b_1 s + 1}\right) \tag{4.28}$$

where

$$\begin{cases} K_c = \frac{6\alpha_1}{k_1 m_2},\ T_i = \alpha_1,\ T_d = \frac{\alpha_2}{\alpha_1} \\ a_3 = \frac{\lambda_2\theta_m^2}{6},\ a_2 = \frac{\theta_m^2}{6} + \frac{2\lambda_2\theta_m}{3}, a_1 = \frac{2\theta_m}{3} + \lambda_2 \\ b_3 = \frac{m_5}{m_2},\ b_2 = \frac{m_4}{m_2},\ b_1 = \frac{m_3}{m_2} \end{cases} \tag{4.29}$$

4.3.2.5 For ISOPTD primary process:

In case of ISOPTD process i.e. $G_{p1} = k_1 e^{-\theta_1 s}/s\,(\tau_1 s + 1)$, the desired closed-loop complementary sensitivity function is considered as

$$T_{d_{outer}} = \frac{(\alpha_1 s + 1)}{(\lambda_3 s + 1)^3} e^{-\theta_m s} \tag{4.30}$$

From (4.3), (4.7), (4.8), (4.19) and (4.30), the resulting controller becomes

$$G_{c3} = \frac{s\,(\tau_1 s + 1)(\alpha_1 s + 1)(\lambda_2 s + 1)}{k_1 \left[(\lambda_3 s + 1)^3 - (\alpha_1 s + 1) e^{-\theta_m s}\right]} \tag{4.31}$$

(4.31) is further simplified by using (1, 2) Padé approximation for the time delay as

$$G_{c3} = \frac{(\tau_1 s + 1)(\alpha_1 s + 1)(\lambda_2 s + 1)\left(6 + 4s\theta_m + s^2\theta_m^2\right)}{k_1\left[l_4 s^4 + l_3 s^3 + l_2 s^2 + l_1 s + l_0\right]} \tag{4.32}$$

where $l_4 = \lambda_3^3\theta_m^2$, $l_3 = 4\lambda_3^3\theta_m + 3\lambda_3^2\theta_m^2$, $l_2 = 6\lambda_3^3 + 12\lambda_3^2\theta_m + 3\lambda_3\theta_m^2$, $l_1 = 2\alpha_1\theta_m + \theta_m^2 + 18\lambda_3^2 + 12\lambda_3\theta_m$ and $l_0 = 6\theta_m + 18\lambda_3 - 6\alpha_1$.

By taking $\alpha_1 = \theta_m + 3\lambda_3$, (4.32) can be approximated in the form of a PID controller in series with lead/lag compensator as (4.28). With that the controller settings are obtained as

$$\begin{cases} K_c = \frac{6(\alpha_1+\lambda_2)}{k_1 l_1},\ T_i = \alpha_1 + \lambda_2,\ T_d = \frac{\alpha_1\lambda_2}{\alpha_1+\lambda_2} \\ a_3 = \frac{\tau_1\theta_m^2}{6},\ a_2 = \frac{4\tau_1\theta_m+\theta_m^2}{6},\ a_1 = \frac{3\tau_1+2\theta_m}{3} \\ b_3 = \frac{l_4}{l_1},\ b_2 = \frac{l_3}{l_1},\ b_1 = \frac{l_2}{l_1} \end{cases} \tag{4.33}$$

The detail of the tuning rules for G_{c3} are summarized in Table 4.1.

Table 4.1: Summary of tuning rules for G_{c3}

Primary Process	Parameters of G_{c3}
IPTD	$K_c = \frac{6(\alpha_1+\lambda_2)}{k_1 x_1}, T_i = \alpha_1 + \lambda_2, T_d = \frac{\alpha_1\lambda_2}{\alpha_1+\lambda_2}$, $a_2 = \frac{\theta_m^2}{6}, a_1 = \frac{2\theta_m}{3}, b_2 = \frac{x_3}{x_1}, b_1 = \frac{x_2}{x_1}$
DIPTD	$K_c = \frac{6\alpha_1}{k_1 m_2},\ T_i = \alpha_1,\ T_d = \frac{\alpha_2}{\alpha_1}$ $a_3 = \frac{\lambda_2\theta_m^2}{6},\ a_2 = \frac{\theta_m^2}{6} + \frac{2\lambda_2\theta_m}{3}, a_1 = \frac{2\theta_m}{3} + \lambda_2$ $b_3 = \frac{m_5}{m_2},\ b_2 = \frac{m_4}{m_2},\ b_1 = \frac{m_3}{m_2}$
ISOPTD	$K_c = \frac{6(\alpha_1+\lambda_2)}{k_1 l_1},\ T_i = \alpha_1 + \lambda_2,\ T_d = \frac{\alpha_1\lambda_2}{\alpha_1+\lambda_2}$ $a_3 = \frac{\tau_1\theta_m^2}{6},\ a_2 = \frac{4\tau_1\theta_m+\theta_m^2}{6},\ a_1 = \frac{3\tau_1+2\theta_m}{3}$ $b_3 = \frac{l_4}{l_1},\ b_2 = \frac{l_3}{l_1},\ b_1 = \frac{l_2}{l_1}$

4.4 Selection of the tuning parameters

In the proposed control structure, there are three adjustable tuning parameters: λ_1, λ_2 and λ_3. λ_2 is the tuning parameter of secondary loop controller. In order to achieve good performance of a cascade control system, the inner loop should be faster than the outer loop. The smaller the value of λ_2 the better the performance of the cascade control system. Hence, it is suggested that λ_2 can be chosen equal to the secondary loop process time delay, θ_2. If it is required to get faster response, λ_2 can be chosen as one-half the time delay and so on. Choice of λ_2 is also suggested by [81], whose control scheme has been used for comparison.

For smaller value of λ_1, the speed of response is faster whereas good robustness is achieved by a larger

value of λ_1. So, λ_1 should be selected such that faster speed of response and good robustness can be achieved. Hence, as a rule of thumb, the initial value of λ_1 can be chosen equal to the overall process time delay.

The tuning of the control parameter λ_3 aims at the trade-off between nominal performance of the closed loop and its robust stability. That is, decreasing λ_3 improves the disturbance rejection performance of the closed loop but degrades its robust stability in the presence of process uncertainty. In contrast, increasing λ_3 tends to strengthen the robust stability of the closed loop but degrades its disturbance rejection performance. On the basis of simulation studies based on the MATLAB toolbox, it is observed that the initial value of λ_3 is equal to overall process time delay. If good control performances are not achieved with the initial values of λ_1 and λ_3, then the tuning parameters can be varied gradually from these values till good nominal and robust control performances are achieved. The suggested range of tuning parameters are $\lambda_1 = 0.1\theta_m - 1.4\theta_m$, $\lambda_2 = 0.1\theta_2 - \theta_2$ and $\lambda_3 = 0.8\theta_m - 2.5\theta_m$.

4.5 Robustness analysis and performance

4.5.1 Robustness analysis

A study of robustness analysis is an important task in control system design because the behaviour of the real system is almost always different from the behavior of the model. The notion of robustness expresses the capability of a system to be insensitive to the effects of parameters variability. It can be observed from (4.2) that the robust control performances can be studied by analyzing G_{c3} as if it affects the process model ($G_m e^{-\theta_m s}$) in a single feedback path. The type of uncertainties affecting the design of G_{c3} are the parametric uncertainties such as uncertainty in process gain, time constant and time delay.

According to the Small gain theorem [93], the closed-loop system for the load disturbance rejection is robustly stable if and only if

$$\left\| \Delta_m(s)\, T_d(s) \right\|_\infty < 1 \tag{4.34}$$

where $T_d(s)$ is the closed-loop complementary sensitivity function and $\Delta_m(s)$ is the process multiplicative uncertainty i.e. $\Delta_m(s) = \left| \left(G_p(s) - \tilde{G}_m(s) \right) \Big/ \tilde{G}_m(s) \right|$ where $\tilde{G}_m(s) = G_m(s) e^{-\theta_m s}$. To show the stability and robustness analysis more qualitatively, consider the cascade control system with IPTD primary process for which the complementary sensitivity function of the closed-loop system with the

designed controller (4.23) is

$$T_{d_{outer}}(s) = \frac{k_1 K_c \left(1 + T_i s + T_i T_d s^2\right)\left(a_2 s^2 + a_1 s + 1\right) e^{-\theta_m s}}{s^2 T_i \left(\lambda_2 s + 1\right)\left(b_2 s^2 + b_1 s + 1\right) + k_1 K_c \left(1 + T_i s + T_i T_d s^2\right)\left(a_2 s^2 + a_1 s + 1\right) e^{-\theta_m s}} \quad (4.35)$$

where the controller parameters K_c, T_i and T_d are functions of the tuning parameters λ_2 and λ_3. b_1 and b_2 are functions of λ_3.

Now, substituting (4.20) into (4.34) yields the robust stability constraint

$$\left\| \frac{\Delta_{m1}(s)\ (\alpha_1 s + 1)}{(\lambda_3 s + 1)^2} \right\|_\infty < 1 \quad (4.36)$$

for the outer loop of the proposed cascade control structure. where $\Delta_{m1}(s)$ is the multiplicative uncertainty bound of the primary process G_{p1}. For the primary process gain uncertainty, the tuning parameter should be selected in such a way that

$$\frac{\lambda_3^2\omega^2 + 1}{\sqrt{\alpha_1^2\omega^2 + 1}} > \frac{|\Delta k_1|}{k_1}, \qquad \forall \omega > 0 \quad (4.37)$$

For the primary process time delay uncertainty $\Delta\theta_1$, the robust stability constraint for tuning λ_3 is

$$\frac{\lambda_3^2\omega^2 + 1}{\sqrt{\alpha_1^2\omega^2 + 1}} > \left| e^{-j\Delta\theta_1\omega} - 1 \right|, \qquad \forall \omega > 0 \quad (4.38)$$

If uncertainty exists in both primary process gain and time delay, the tuning parameter should be selected in such a way that

$$\frac{\lambda_3^2\omega^2 + 1}{\sqrt{\alpha_1^2\omega^2 + 1}} > \left| \left(1 + \frac{\Delta k_1}{k_1}\right) e^{-j\Delta\theta_1\omega} - 1 \right|, \qquad \forall \omega > 0 \quad (4.39)$$

According to robust control theory [91], the closed-loop performance for load disturbance rejection is robust, the following constraints have to be followed by the sensitivity and complementary sensitivity functions

$$\left\| \Delta_{m1}(s)\, T_{d_{outer}}(s) + w_1(s)\left(1 - T_{d_{outer}}(s)\right) \right\|_\infty < 1 \quad (4.40)$$

where $w_1(s)$ is the weight function of the sensitivity function, $S_{d_{outer}}(s) = 1 - T_{d_{outer}}(s)$. Therefore, the tuning parameters λ_2 and λ_3 should be selected such that the resulting controller satisfies the robust nominal performance and robust stability constraints. Similar robustness and stability analysis can be done for the remaining type of time delay processes.

For more clarity, the Kharitonov's theorem is used to conduct the robustness analysis for the proposed control scheme. Consider the Example-4.1 of the chapter i.e. the outer and inner loop plant transfer

functions $G_{p1} = 2e^{-2s}/s$ and $G_{p2} = 4e^{-s}/(s+1)$.

From (4.2), the closed-loop characteristic equation of the outer loop is given by

$$1 + G_{c2}G_{p2}G_{p1}G_{c3} = 0$$

Now, the interval polynomial of this system is given by

$$\begin{aligned} p(s,q) = {} & [0.1178 \;\; 0.1963] + [1.413 \;\; 2.355]s + [5.976 \;\; 9.96]s^2 \\ & + [11.0395 \;\; 18.3992]s^3 + [9.9359 \;\; 16.5598]s^4 + [3.577 \;\; 5.9617]s^5 \end{aligned} \tag{4.41}$$

The four Kharitonov polynomials are obtained as

$$K_1(s) = 0.1178 + 1.413s + 9.96s^2 + 18.3992s^3 + 9.9359s^4 + 3.577s^5$$

$$K_2(s) = 0.1963 + 2.355s + 5.976s^2 + 11.0395s^3 + 16.5598s^4 + 5.9617s^5$$

$$K_3(s) = 0.1963 + 1.413s + 5.976s^2 + 18.3992s^3 + 16.5598s^4 + 3.577s^5$$

$$K_4(s) = 0.1178 + 2.355s + 9.96s^2 + 11.0395s^3 + 9.9359s^4 + 5.9617s^5$$

Table 4.2: The roots of Kharitonov polynomials

$K_1(s)$	$K_2(s)$	$K_3(s)$	$K_4(s)$
$-1.0294 + j1.5806$	-2.0759	-3.1550	$-0.1380 + j1.0490$
$-1.0294 - j1.5806$	$-0.0419 + j0.5351$	-1.1182	$-0.1380 - j1.0490$
-0.5595	$-0.0419 - j0.5351$	$-0.0587 + j0.2483$	-1.0843
$-0.0796 + j0.1010$	-0.5101	$-0.0587 - j0.2483$	-0.2380
$-0.0796 - j0.1010$	-0.1079	-0.2390	-0.0684

The coefficients of Kharitonov polynomials are checked for Hurwitz condition. It is observed that all the roots of the Kharitonov polynomials (see Table 4.2) have negative real part. In order to check the robustness, 25% uncertainties in the plant parameters have been considered. The Kharitonov rectangles of the closed-loop system are shown in Figure 4.2. From the Figure 4.2, it is clear that Kharitonov rectangles move about the origin in counterclockwise sense in order to have the monotonic phase increase property of Hurwitz polynomials. The graph is zoomed to show the zero exclusion condition. It is observed that the closed-loop characteristic equation of the system is stable in complex plane in Mikhailov's sense. Since the origin is excluded from the Kharitonov rectangles (Fig 4.2) it is

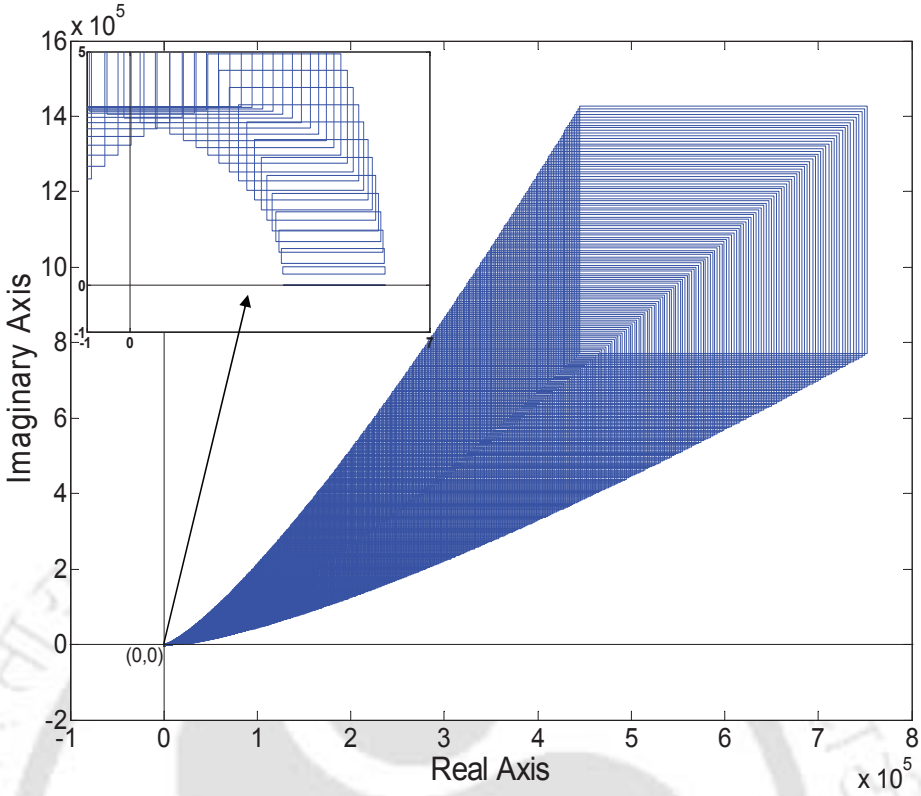

Figure 4.2: Kharitonov's rectangles for $G_{p1} = 2e^{-2s}/s$ and $G_{p2} = 4e^{-s}/(s+1)$

concluded that the closed-loop control system is robustly stable. By following a similar procedure as above the robustness analysis for Example-4.2 and Example-4.3 can be checked.

4.5.2 Performance

Two popular performance indices are considered to evaluate the closed-loop performance such as IAE and ISE. TV is computed to show the smoothness of a control signal.

4.6 Simulation results

Example-4.1: Consider a cascade control system discussed by [82] and [81] with plant models of $G_{p1} = 2e^{-2s}/s$ and $G_{p2} = 4e^{-s}/(s+1)$. For the proposed method, the inner loop controller is $G_{c2} = (s+1)/(2s+4)$ by taking $\lambda_2 = 0.5\theta_2$. $G_{c1} = \left(s^2+s+2\right)/\left(4.5s^2+6s+2\right)$ by choosing $\lambda_1 = 0.4\theta_m = 1.2$. λ_3 is chosen as $1.5\theta_m$. Using (4.24), the parameters of G_{c3} are obtained as $K_c = 0.1208$, $T_i = 12.5$, $T_d = 0.48$, $a_2 = 1.5$, $a_1 = 2$, $b_2 = 0.5870$ and $b_1 = 1.0435$. With these controller settings, the performances of the closed loop system is evaluated by introducing a unit step

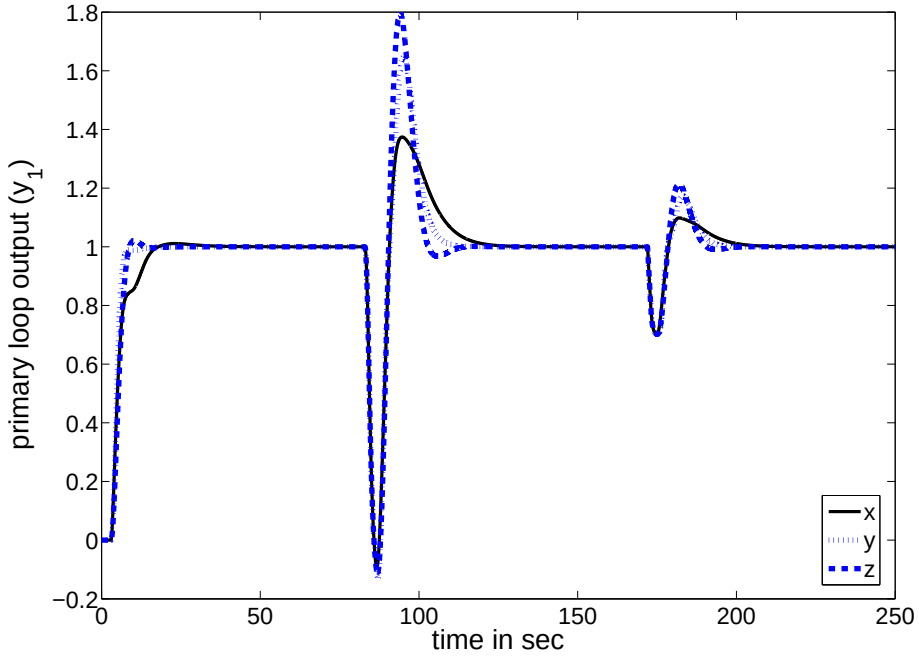

Figure 4.3: Nominal process outputs for example 4.1: (x) Proposed, (y) Uma et al. and (z) Kaya and Atherton

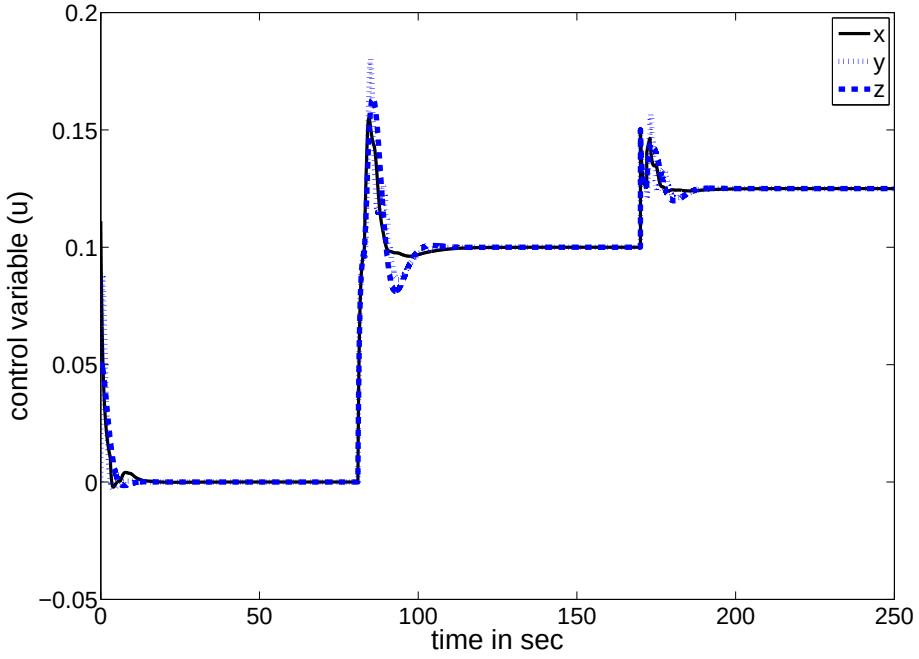

Figure 4.4: Nominal control signals for example 4.1: (x) Proposed, (y) Uma et al. and (z) Kaya and Atherton

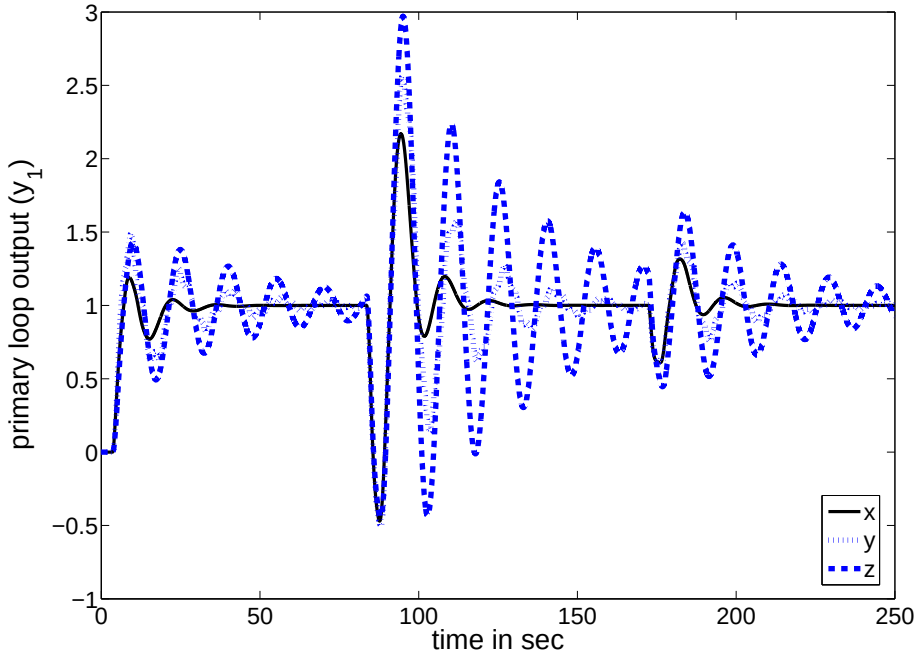

Figure 4.5: Perturbed responses for example 4.1: (x) Proposed, (y) Uma et al. and (z) Kaya and Atherton

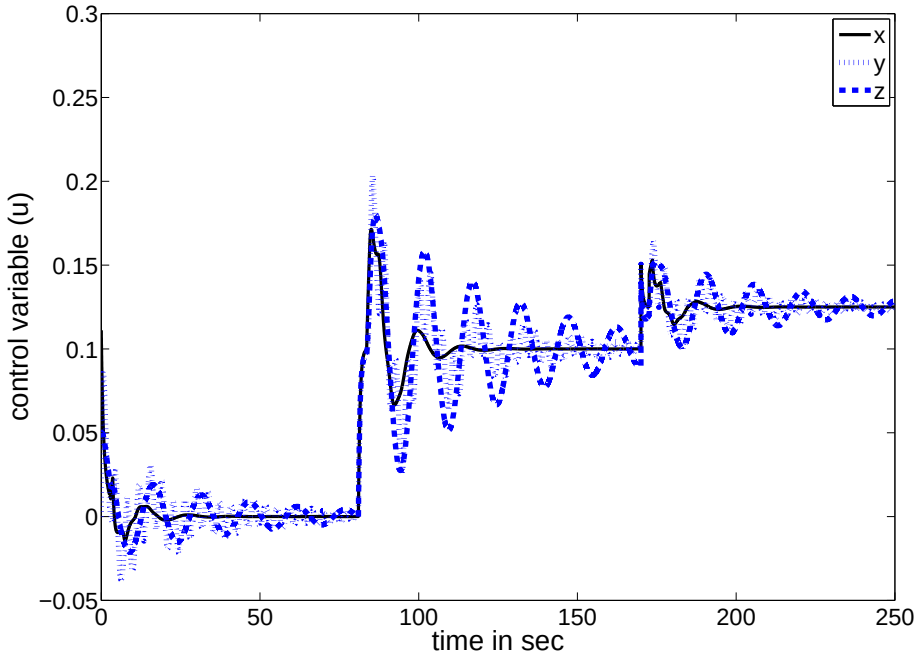

Figure 4.6: Perturbed control signals for example 4.1: (x) Proposed, (y) Uma et al. and (z) Kaya and Atherton

Table 4.3: Performance specifications

	Scheme	Nominal System			Perturbed system		
		IAE	ISE	TV	IAE	ISE	TV
Regulatory							
Example-4.1	Proposed	2.47	0.38	0.09	3.9	0.98	0.17
	Uma et al.	2.54	0.47	0.17	7.27	1.69	0.77
	Kaya and Atherton	2.71	0.54	0.12	13.58	3.68	0.32
Example-4.2	Proposed	8.05	4.08	2.52	8.97	5.81	5.37
	Uma et al.	10.72	6.58	3.21	18.78	12.60	16.48
Example-4.3	Proposed	50.44	16.19	0.22	67.15	36.87	0.29
	Conventional	524.6	993.5	0.37	454.3	1090	0.39
Servo							
Example-4.1	Proposed	5.92	4.59	0.12	7.39	5.04	0.18
	Uma et al.	5	4.37	0.18	12.03	6.27	1.24
	Kaya and Atherton	5.55	4.71	0.11	20.58	8.37	0.37
Example-4.2	Proposed	4	3.06	1.30	4.85	3.09	2.33
	Uma et al.	4.66	3.53	2.73	6.13	3.45	6.04
Example-4.3	Proposed	34.27	26.24	0.03	35.6	24.67	0.04
	Conventional	82.81	42.72	0.04	66.94	39.04	0.06

input in the set-point at time $t = 0$, a negative step load input (d_2) of magnitude 0.1 at $t = 80$ sec and a negative disturbance (d_0) of magnitude 0.1 at $t = 170$ sec. The methods proposed by Kaya and Atherton [81] and Uma et al. [82] are considered for comparison. The closed-loop responses for these controllers setting are shown in Figure 4.3 and the corresponding control signals are given in Figure 4.4. In the present work a +30% perturbation in the primary process time delay and gain has been considered and the corresponding responses are shown in Figure 4.5 and 4.6. The performance indices (IAE and ISE) are less and the TV is also small for the proposed method (see Table 4.3). Thus, the proposed method gives smooth control signal. It is evident from the simulation results that the proposed method yields robust and superior control performances.

Example-4.2: Let the outer and inner loop process transfer functions studied by Uma et al. [82] be $G_{p1} = e^{-0.7s}/s^2$ and $G_{p2} = e^{-0.3s}/(s+1)$, respectively. For the proposed method, taking $\lambda_2 =$

$\theta_2 = 0.3$, $G_{c2} = (s+1)/(0.3s+1)$. $G_{c1} = \left(0.3s^3 + s^2 + 1\right)/\left(s^3 + 3s^2 + 3s + 1\right)$ by choosing $\lambda_1 = \theta_m = 1$. The parameters of the controller G_{c3} can be obtained using (4.29). By taking $\lambda_3 = 2\theta_m$, the parameters of G_{c3} are $K_c = 0.1496$, $T_i = 9$, $T_d = 3.6111$, $a_3 = 0.05$, $a_2 = 0.3667$, $a_1 = 0.9667$, $b_3 = 0.0443$, $b_2 = 0.2659$ and $b_1 = 0.6870$. For the purpose of comparison, method proposed by Uma et al. [82] is considered. The transfer functions of the three controllers proposed by Uma et al. method are given by $G_{c2} = (s+1)/(0.5s+1)$, $G_{cs} = 0.5\left(1 + \frac{1}{5s} + 2s\right)\left(\frac{s+1}{0.1s^2+0.5s+1}\right)$ and $G_{cd} = (0.0789 + 0.4342s)\left(\frac{0.0833s^3+0.5833s^2+1.5s+1}{0.0789s^3+0.3947s^2+0.7533s+1}\right)$.

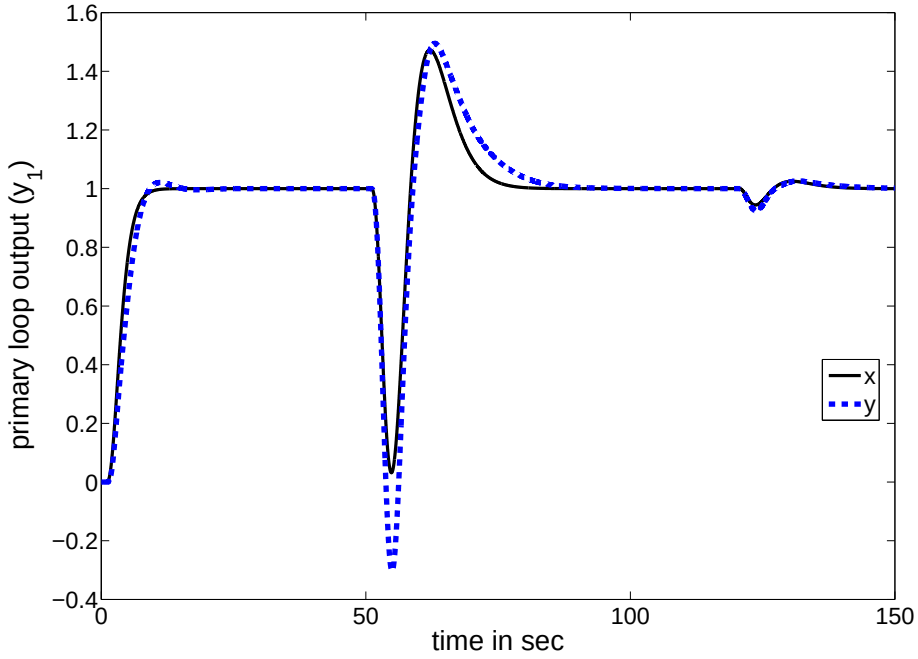

Figure 4.7: Nominal process outputs for example 4.2: (x) Proposed, (y) Uma et al.

The setpoint weighting parameter and the filter parameter in the case of Uma et al.'s method are 0.4 and 5, respectively. With these controller settings a unit step input in the setpoint at $t = 0$, a unit step negative disturbance in the inner loop(d_2) at $t = 50$ sec and a negative disturbance of magnitude 0.05 in d_0 at $t = 120$ sec are introduced and the corresponding closed-loop responses are shown in Figure 4.7 and 4.8. A perturbation of +35% in primary process gain and time delay has been considered in order to analyze the robustness of the controllers (see Figure 4.9 and 4.10). From the simulation results, it is seen that the proposed method gives satisfactory closed-loop performances. The values of IAE, ISE, and TV are given in Table 4.3.

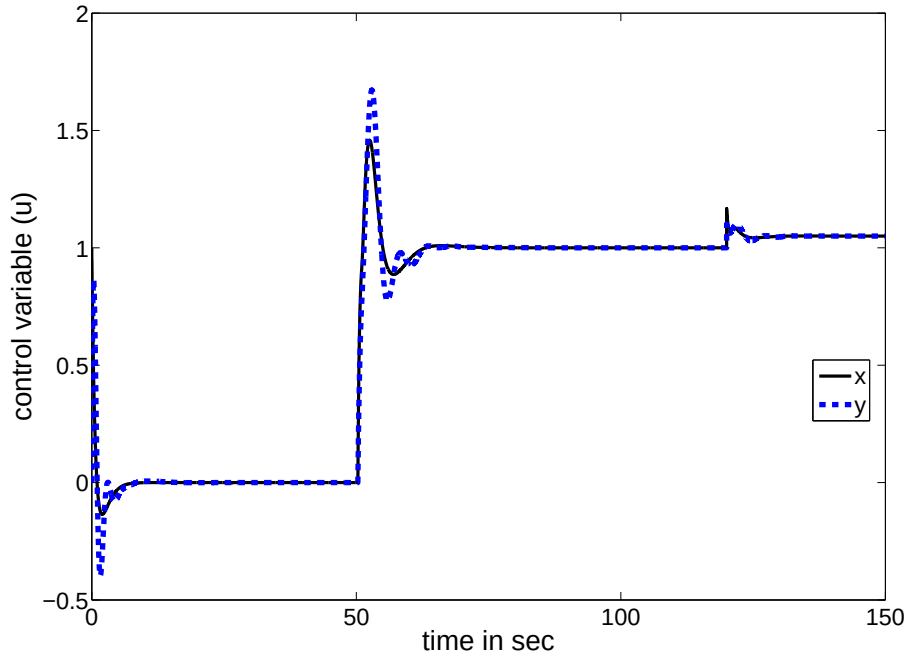

Figure 4.8: Nominal control signals for example 4.2: (x) Proposed, (y) Uma et al.

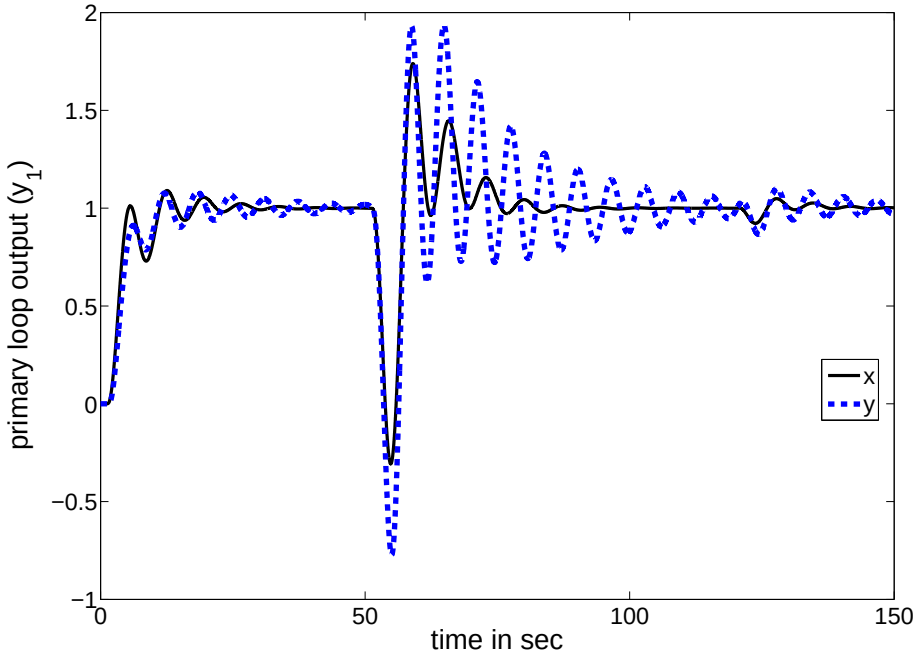

Figure 4.9: Perturbed responses for example 4.2: (x) Proposed, (y) Uma et al.

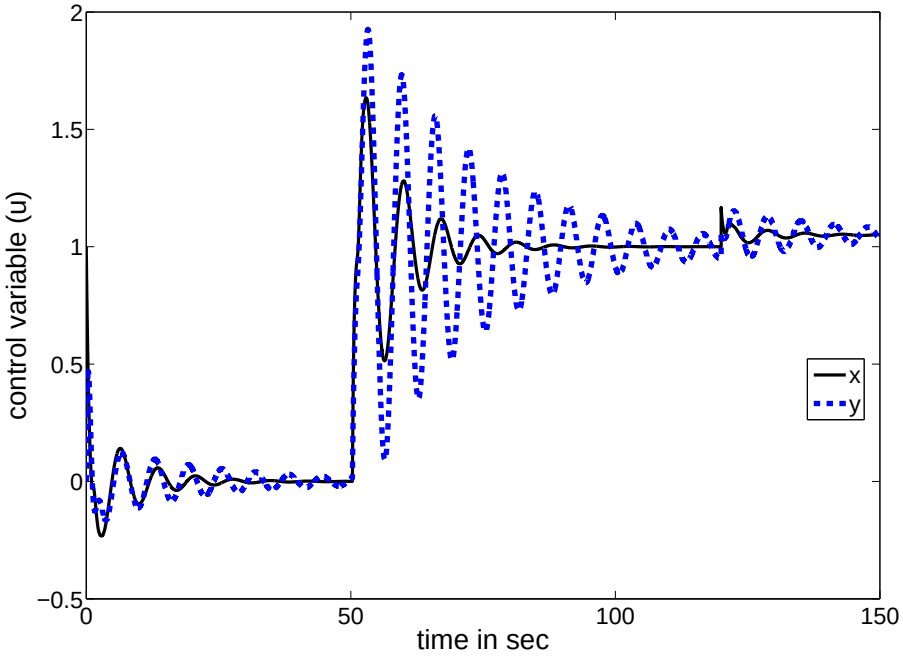

Figure 4.10: Perturbed control signals for example 4.2: (x) Proposed, (y) Uma et al.

Example-4.3: Consider a cascade control system with the following primary and secondary loop process transfer functions $G_{p1} = e^{-6.5672s}/(s\,(3.4945s+1))$ and $G_{p2} = 2e^{-2s}/(s+1)$, respectively. By choosing $\lambda_3 = 2\theta_m$ and using the design formulae (4.33), the parameters of controller G_{c3} are obtained as $K_c = 0.0456$, $T_i = 61.9704$, $T_d = 1.9355$, $a_3 = 42.7476$, $a_2 = 32.1915$, $a_1 = 9.2060$, $b_3 = 45.3194$, $b_2 = 29.0943$ and $b_1 = 7.8726$. The inner loop controller is obtained as $G_{c2} = (s+1)/(4s+2)$ by taking $\lambda_2 = \theta_2 = 2$. Choosing $\lambda_1 = \theta_m$ results in the setpoint filter as $G_{c1} = \big(6.989s^3 + 5.4945s^2 + s + 1\big)/\big(628.806s^3 + 220.1907s^2 + 25.7016s + 1\big)$. For the purpose of comparison, the conventional series cascade control structure is considered. For the conventional control structure, the inner loop controller is considered as P only controller and the outer loop controller is in the form of an ideal PID controller in series with a first order lag. Using Ziegler-Nichols tuning method, the parameter of inner controller is obtained as 0.38. The outer loop controller is designed for the overall plant, $G_p = \frac{0.76e^{-8.5672s}}{s(3.4945s^2+4.4945s+1)}$. The ISOPTD model is $G_p = \frac{0.76e^{-9.341s}}{s(4.0961s+1)}$ using [121]. The parameters of the outer loop controller ($K_c = 0.0598$, $T_i = 55.2797$, $T_d = 3.7926$ and the filter time constant is 4.6072) are obtained using Tan et al. method [122].

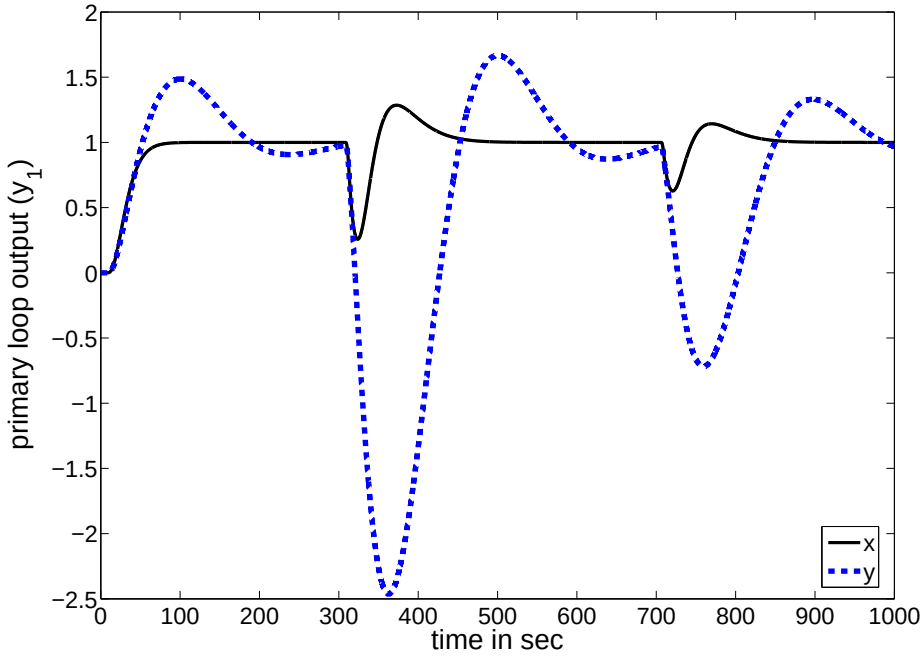

Figure 4.11: Nominal process outputs for example 4.3: (x) Proposed, (y) Conventional

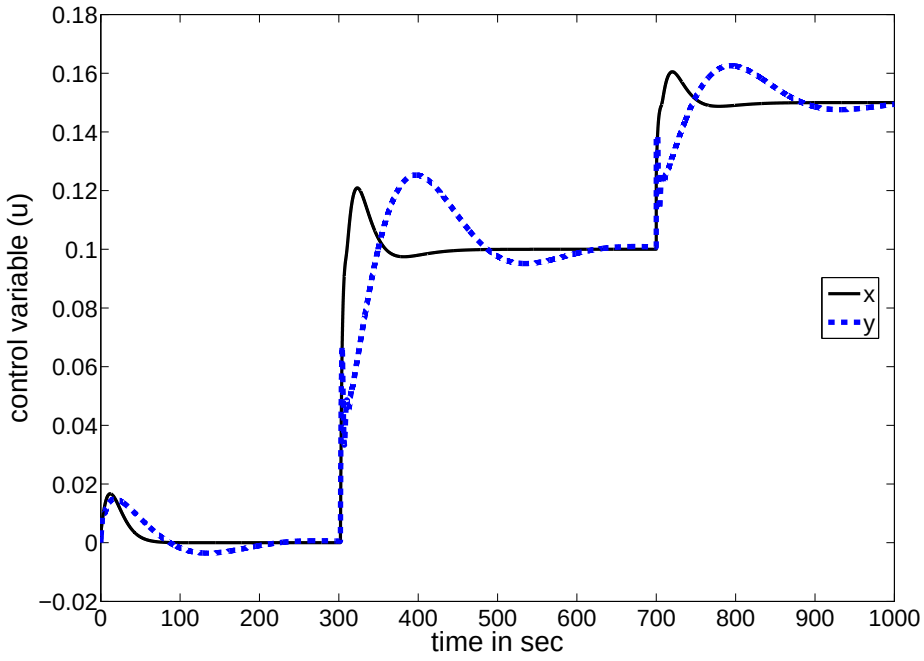

Figure 4.12: Nominal control signals for example 4.3: (x) Proposed, (y) Conventional

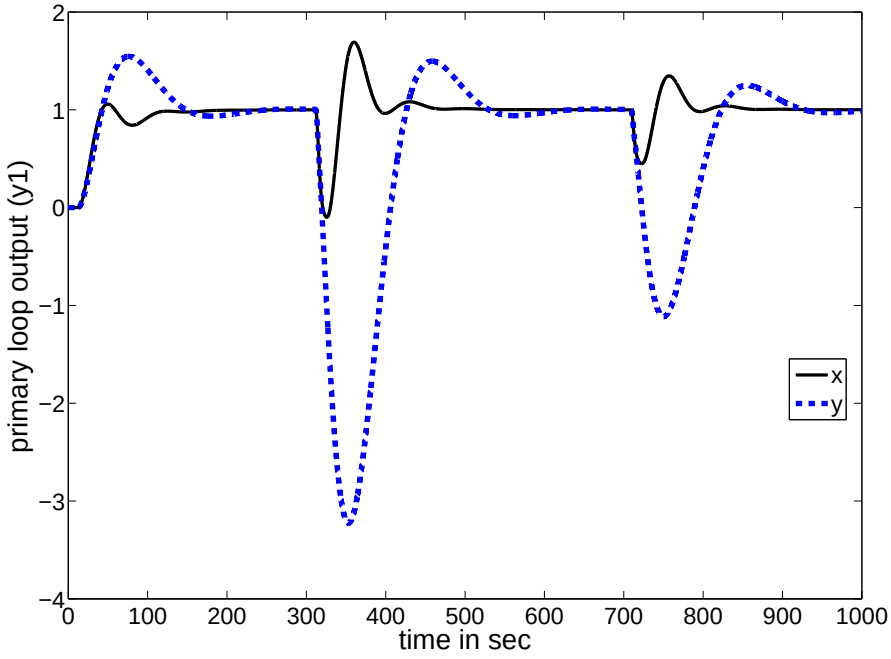

Figure 4.13: Perturbed responses for example 4.3: (x) Proposed, (y) Conventional

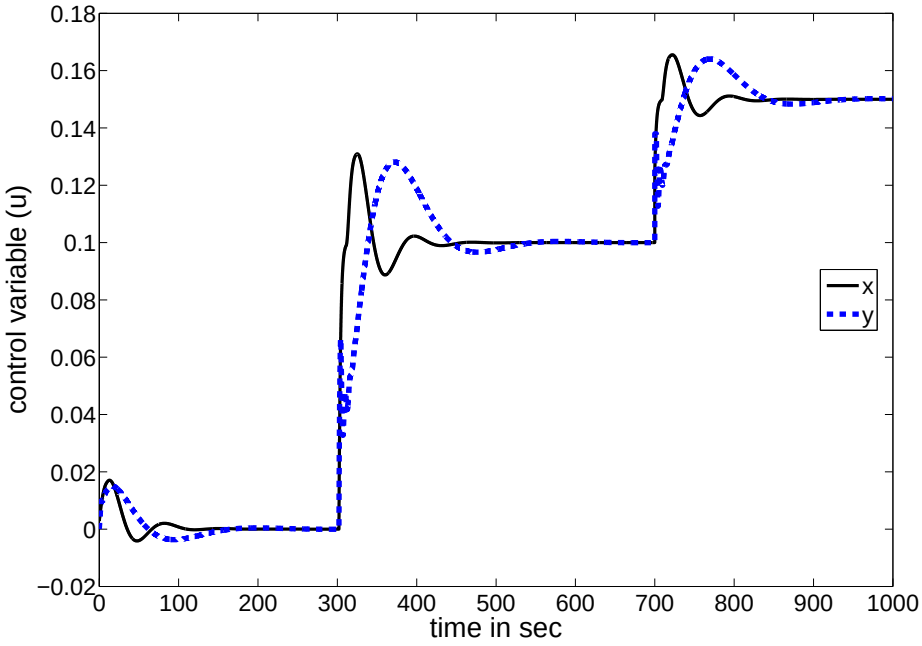

Figure 4.14: Perturbed control signals for example 4.3: (x) Proposed, (y) Conventional

With these controller settings a unit-step setpoint is introduced at time $t = 0$, a negative step input load disturbance d_2 with magnitude 0.1 at time $t = 300$ sec and a load disturbance $d_0 = -0.1$ at time $t = 700$ sec. The corresponding closed-loop responses are shown in Figure 4.11 and 4.12. To illustrate the robustness to parameter variations, perturbations of +40% in the primary process time delay, +40% in the primary process gain and −40% in the primary process time constant have been considered simultaneously and the corresponding closed-loop responses are shown in Figure 4.13 and 4.14. It is apparent from the simulation results that the proposed control scheme gives robust closed-loop performances in terms of the setpoint tracking and the load disturbance rejection. For quantitative comparison, IAE and ISE are considered and the corresponding values are given in Table 4.3 for all the three examples. It is observed that the proposed method has smaller errors. The TV values for the proposed method are small. Thus, using the proposed control scheme, smooth control signal and satisfactory closed-loop performances can be achieved.

4.7 Conclusions

In this chapter, the problem of controlling a class of integrating time delayed processes has been tackled by proposing a new cascade control structure. The proposed cascade structure takes the advantage of the cascade control structure and the modified Smith predictor. With the proposed structure, the setpoint tracking is decoupled from the load disturbance rejection under ideal conditions. By the help of simulation results, it is shown that both nominal and robust control performances are obtained with the designed controllers. The proposed structure gives significant improvement in the closed-loop performances with less number of controllers when compared with some recently reported methods.

5

Modified Smith Predictor based Parallel Cascade Control Structure

Contents

Resume

This chapter presents a new parallel cascade control structure and controller design for controlling stable, unstable or integrating processes with time delay. The present scheme combines the features of both the parallel cascade control and modified Smith predictor structures. The proposed new parallel cascade control structure possesses only two controllers and a setpoint filter. The disturbance rejection controller and the setpoint filter are designed based on loop shaping and ISE performance measures, respectively. Due to the predictor structure used in the proposed scheme, which do not need any extra controller to obtain an internal stable system. Simulation results show that the proposed approach offers a satisfactory closed-loop performance.

The paper [123] contains the work presented in this chapter.

5.1 Introduction

Time delay in a process may complicate analytical aspects of control system design because of limitations introduced by the time delay on system performance [6]. Time delays appear due to transport phenomena, computation of the control input, time-consuming information processing in measurement devices, etc. From a control point of view, time delays produce an increase in the system phase lag, thereby decreasing the phase and gain margins and limiting the response speed of the system which often leads to instability of the control system limiting the achievable closed loop performance. In process control, cascade system is desirable to reduce the effects of possible disturbances and to improve the dynamic performance of the closed-loop system. In series cascade control, both the manipulated variable and the disturbance affect directly an intermediate (secondary) variable and this in-turn affects the primary controlled variable, whereas, in parallel cascade control, the manipulated variable and the disturbances affect both the primary and secondary outputs simultaneously. Unlike the series cascade control, the secondary process plays a major role in contributing in disturbance rejection and improving the dynamic performance of the parallel cascade control system. The overhead composition control of a distillation column, cascaded onto the control of tray temperature, is a typical example of a parallel cascade control system [36]. The reflux flow rate (manipulated variable) and the feed flow or composition (disturbance) affect, both, the purity of the overhead product (primary output) and the tray temperature (secondary output). The control objective is to maintain the overhead composition at the setpoint. The output of the composition controller resets the setpoint for

the temperature controller. By controlling the tray temperature in the cascade manner, the variation in the feed can be compensated before it disturbs the product composition.

Parallel cascade control was first introduced by Luyben [36]. Yu [43] proposed an efficient interaction measure to determine whether the parallel cascade control is advantageous or detrimental to regulatory response. Later, Shen and Yu [44] proposed a method for selection of secondary measurement for parallel cascade control. Semino and Brambilla [45] introduced a nonlinear filter in order to improve the closed-loop control performances and developed a combined structure to avoid interactions between the primary and secondary loops. Using optimal control theory Pottmann et al. [46] developed a parallel control strategy for a biological control system that regulates arterial blood pressure. Chen et al. [47] addressed on the performance assessment of parallel cascade control using the methodology of univariate control loop performance, minimum variance and Diophantine decomposition principles. Lee et al. [48] proposed an analytical method of PID controller design for parallel cascade control. Parallel cascade control structure with Smith predictor for enhanced performance for stable systems has been discussed by Rao et al. [49]. The parallel cascade control structures proposed by Lee et al. [48] and Rao et al. [49] require four controllers. In spite of clear benefits of the parallel cascade control and its wide-spread use in process industries, the design on the parallel cascade control systems has not attracted the attention it deserves. Moreover, parallel cascade control techniques are to be made available for controlling integrating and unstable processes with time delay. In this chapter, a modified Smith predictor [83] combined with parallel cascade control is proposed for the control of stable, unstable and integrating processes with time delay. The proposed scheme combines the features of both the parallel cascade control and modified Smith predictor structures.

The proposed new parallel cascade control structure possesses only two controllers and a setpoint filter. In the proposed method, Karimi et al.'s [124] loop shaping technique has been extended to design the disturbance rejection controllers and ISE performance specification method is used to design the setpoint filter. Especially, unstable and integrating processes coupled with time delay makes the control system design a difficult task, therefore in this chapter, the stabilization, robustness analysis and performances of time delay processes have been investigated. Simulation results are provided to show how the proposed design method outperforms some conventional and recently reported methods. The chapter is organized as follows. Section 5.2 introduces the general problem formulation with the proposed parallel cascade control structure. Section 5.3 presents the details of the controller design

procedures. Stability analysis is presented in Section 5.4. In Section 5.5, the robustness analysis and performances are discussed followed by simulation examples in Section 5.6. The conclusions are drawn in Section 5.7.

5.2 Problem formulation

5.2.1 Parallel cascade control structure

A parallel cascade control scheme is shown in Figure 1.4 where both the manipulated variable and the disturbance affect the primary and the secondary loop outputs through parallel actions. Again, the structure consists of a primary (outer) and a secondary (inner) controllers. The output of the primary controller resets the setpoint of the secondary loop and the output of the secondary controller affects two output variables. In parallel cascade control, the secondary loop dynamics response should be much faster than the primary loop because the disturbances entering in to the secondary loop should be rejected immediately to reduce steady state error in the primary loop subsequently. Therefore, the secondary controller is tuned first and then the primary controller with the secondary controller in action. The parallel cascade control is also beneficial when measurements of the primary output are sampled infrequently and/or with time delays. It can be used to achieve better disturbance rejections existing in the inner loop. However, if a long time delay exists in the outer loop, the parallel cascade control may not give satisfactory closed-loop responses for setpoint changes. To overcome this difficulty, a delay compensation technique is incorporated in the outer loop.

5.2.2 Proposed parallel cascade control structure

A new parallel cascade control structure as shown in Figure 5.1, is proposed for controlling stable, unstable and integrating processes with time delay. The modified Smith predictor [83] is incorporated in the primary loop. The outer and inner loop processes are G_{p1} and G_{p2} respectively and $G_{m1} = G_m e^{-\theta_m s}$ and G_{m2} are the corresponding process models. G_m is the primary process model without time delay and θ_m is the overall time delay of the primary process model. G_{d1} and G_{d2} are the transfer functions of the disturbances for primary and secondary loops respectively. The proposed structure has two controllers: G_{cd1} and G_{cd2}. G_{cd2} is the inner loop disturbance rejection controller for rejecting the load disturbances entering into secondary process and G_{cd1} is the outer loop disturbance rejection controller for rejecting the load disturbances entering into the primary process. Even though G_{cd2} and G_{cd1} are meant for load disturbance rejection, they also help in stabilizing the integrating and

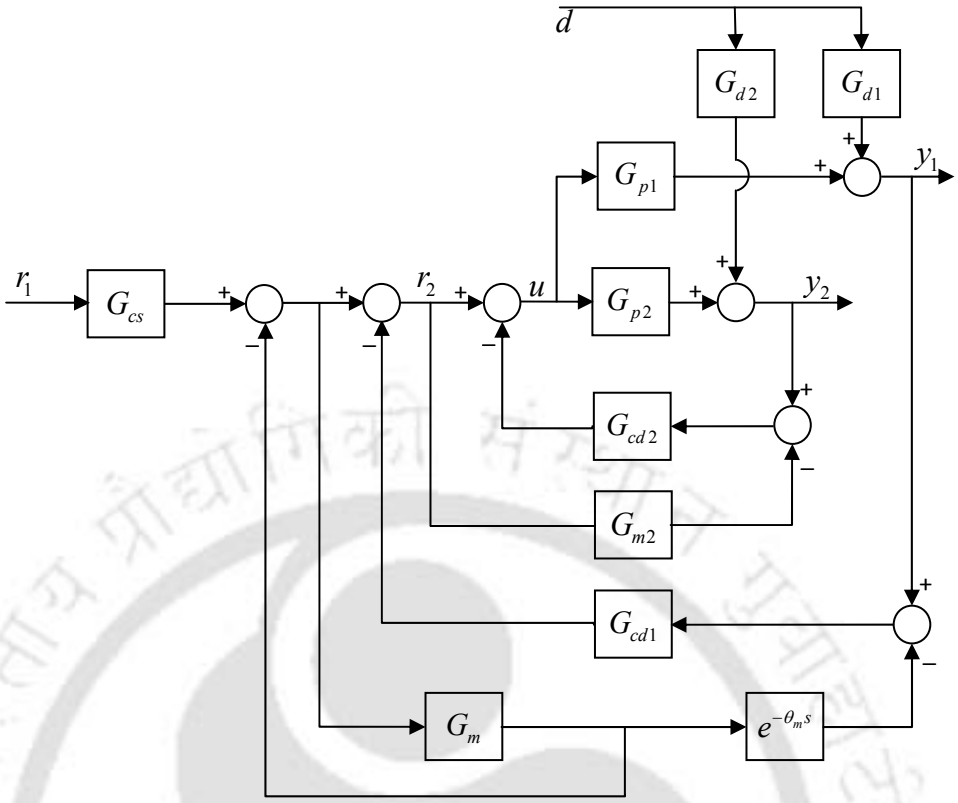

Figure 5.1: Proposed cascade scheme with modified Smith predictor

unstable processes with time delay. G_{cs} is the setpoint filter for the primary setpoint r_1.

The closed-loop transfer function of the primary loop for servo response is given by

$$\frac{y_1}{r_1} = \frac{G_{cs}G_{p1}\left(1+G_{m2}G_{cd2}\right)\left(1+G_{cd1}G_m e^{-\theta_m s}\right)}{\left(1+G_m\right)\left(1+G_{p1}G_{cd1}+G_{p2}G_{cd2}+G_{p1}G_{cd1}G_{m2}G_{cd2}\right)} \tag{5.1}$$

Similarly, the closed-loop transfer function of the primary loop for regulatory responses are given by

$$\frac{y_1}{d} = \frac{G_{d1}\left(1+G_{p2}G_{cd2}\right)-G_{d2}G_{cd2}G_{p1}}{1+G_{p1}G_{cd1}+G_{p2}G_{cd2}+G_{p1}G_{cd1}G_{m2}G_{cd2}} \tag{5.2}$$

Assuming exact matching between the process and the model parameters, (5.1–5.2) reduce to

$$\frac{y_1}{r_1} = \frac{G_{cs}G_{p1}}{1+G_m} \tag{5.3}$$

$$\frac{y_1}{d} = \frac{G_{d1}\left(1+G_{p2}G_{cd2}\right)-G_{d2}G_{cd2}G_{p1}}{\left(1+G_{p1}G_{cd1}\right)\left(1+G_{p2}G_{cd2}\right)} \tag{5.4}$$

(5.3–5.4) shows that the proposed control structure decouples the nominal setpoint response from the regulatory response which is an important feature of the proposed control scheme. Thus, the scheme

is of two-degree-of-freedom and the loops can be tuned independently.

5.2.3 PID controller

The controllers G_{cd2} and G_{cd1} are assumed to have the following transfer functions

$$G_{cd2} = K_{c2}\left(1 + \frac{1}{T_{i2}s} + \frac{T_{d2}s}{\alpha_2 T_{d2}s + 1}\right) \tag{5.5}$$

and

$$G_{cd1} = K_{c1}\left(1 + \frac{1}{T_{i1}s} + \frac{T_{d1}s}{\alpha_1 T_{d1}s + 1}\right) \tag{5.6}$$

where the derivative filter constants are typically fixed by the manufacture [125] and $\alpha_1 = \alpha_2 = 0.1$ throughout the chapter.

5.2.4 Process models

The dynamics of inner loop process and the corresponding disturbance are represented as

$$G_{p2} = G_{d2} = \frac{k_2 e^{-\theta_2 s}}{\tau_2 s + 1} \tag{5.7}$$

and that of inner loop process model is

$$G_{m2} = \frac{k_{m2} e^{-\theta_{m2} s}}{\tau_{m2} s + 1} \tag{5.8}$$

where k_2 and k_{m2} are the steady state gains, θ_2 and θ_{m2} are the time delays and τ_2 and τ_{m2} are the time constants of the secondary loop process and process model, respectively.

For controller design purposes, the commonly used low order process model transfer functions for the outer loop dynamics and the corresponding disturbances are

first order plus time delay (FOPTD) model,

$$G_{p1} = G_{d1} = \frac{k_1 e^{-\theta_1 s}}{\tau_1 s + 1} \tag{5.9}$$

second order plus time delay (SOPTD) model,

$$G_{p1} = G_{d1} = \frac{k_1 e^{-\theta_1 s}}{(\tau_1 s + 1)(\tau_2 s + 1)} \tag{5.10}$$

unstable first order plus time delay (UFOPTD) model,

$$G_{p1} = G_{d1} = \frac{k_1 e^{-\theta_1 s}}{\tau_1 s - 1} \tag{5.11}$$

integrating plus time delay (IPTD) model,

$$G_{p1} = G_{d1} = \frac{k_1 e^{-\theta_1 s}}{s} \tag{5.12}$$

and double integrating plus time delay (DIPTD) model,

$$G_{p1} = G_{d1} = \frac{k_1 e^{-\theta_1 s}}{s^2} \tag{5.13}$$

where, k_1, θ_1, τ_1 and τ_2 are the model parameters of the class of primary loop processes. Again when a primary loop process is of higher order, its dynamics can be represented in the form of any of the above mentioned process models by using the relevant model order reduction techniques.

5.3 Controller design procedures

The parameters of the disturbance rejection controllers and the setpoint filter are designed using the Nyquist curve slope criterion and the ISE performance specification, respectively. The details of the design procedures for G_{cs}, G_{cd2} and G_{cd1} are explained in the following subsections.

5.3.1 Design of Secondary loop controller, G_{cd2}

For ease in presentation, the controller G_{cd2} is described by the transfer function

$$G_{cd2} = K_{c2}\left(1 + \frac{1}{T_{i2}s} + T_{d2}s\right) = \frac{K_{c2}\left(T_{i2}T_{d2}s^2 + T_{i2}s + 1\right)}{T_{i2}s} \tag{5.14}$$

assuming the derivative filter constant to be zero. Now, G_{p2} and G_{cd2} in the frequency domain become $G_{p2}(j\omega) = |G_{p2}(j\omega)|\, e^{j \arg G_{p2}(j\omega)}$ and $G_{cd2}(j\omega) = |G_{cd2}(j\omega)|\, e^{j \arg G_{cd2}(j\omega)} = \mathrm{M}(\omega)e^{j\gamma(\omega)}$

The inner loop transfer function $\mathscr{L}_2(j\omega)$ can be written as

$$\mathscr{L}_2(j\omega) = G_{p2}(j\omega)G_{cd2}(j\omega) = |G_{p2}(j\omega)|\, \mathrm{M}(\omega)e^{j(\arg G_{p2}(j\omega) + \gamma(\omega))} \tag{5.15}$$

At the gain crossover frequency ω_{gc},

$$|\mathscr{L}_2(j\omega_{gc})| = 1 \tag{5.16}$$

$$\arg \mathscr{L}_2(j\omega_{gc}) = \phi_m - \pi \tag{5.17}$$

where ϕ_m is the phase margin of the loop transfer function $\mathscr{L}_2(j\omega)$. From (5.15), (5.16) and (5.17), we get

$$\mathrm{M}(\omega_{gc}) = \frac{1}{|G_{p2}(j\omega_{gc})|} \tag{5.18}$$

$$\gamma(\omega_{gc}) = \phi_m - \pi - \arg\, G_{p2}(j\omega_{gc}) \tag{5.19}$$

In order to find the PID parameters of G_{cd2}, (5.14) is expressed as

$$\mathrm{M}(\omega_{gc})e^{j\gamma(\omega_{gc})} = \frac{K_{c2}\left[\omega_{gc}T_{i2} - j\left(1 - T_{i2}T_{d2}\omega_{gc}^2\right)\right]}{\omega_{gc}T_{i2}} \tag{5.20}$$

Now, by equating the real and imaginary parts of both sides of (5.20), we obtain

$$K_{c2} = \mathrm{M}(\omega_{gc})\cos\gamma(\omega_{gc}) \tag{5.21}$$

and

$$T_{d2} = \frac{1 + \omega_{gc}T_{i2}\tan\gamma(\omega_{gc})}{\omega_{gc}^2 T_{i2}} \tag{5.22}$$

In order to achieve $K_{c2} > 0$ and $T_{d2} > 0$, $\gamma(\omega_{gc})$ must be such that $\cos\gamma(\omega_{gc}) > 0$ and $\omega_{gc}T_{i2}\tan\gamma(\omega_{gc}) > -1$. These two conditions are simultaneously satisfied only if $0 < \gamma(\omega_{gc}) < \frac{\pi}{2}$. The slope of the Nyquist curve of the secondary loop transfer function $\mathscr{L}_2(j\omega)$ at frequency ω_{gc} is equal to the phase of the derivative of $\mathscr{L}_2(j\omega)$ at frequency ω_{gc}. But, the derivative of loop transfer function with respect to ω_{gc} is given by

$$\frac{d\mathscr{L}_2(j\omega_{gc})}{d\omega_{gc}} = G_{p2}(j\omega_{gc})\frac{dG_{cd2}(j\omega_{gc})}{d\omega_{gc}} + G_{cd2}(j\omega_{gc})\frac{dG_{p2}(j\omega_{gc})}{d\omega_{gc}} \tag{5.23}$$

The slope of the Nyquist curve denoted by Ψ_2 at ω_{gc} is given by

$$\Psi_2 = \varphi_{gc} + \arctan\left(\frac{(T_{d2}T_{i2}\omega_{gc}^2 + 1) + (T_{d2}T_{i2}\omega_{gc}^2 - 1)\psi_m(\omega_{gc}) + \psi_p(\omega_{gc})T_{i2}\omega_{gc}}{\psi_m(\omega_{gc})T_{i2}\omega_{gc} - (T_{d2}T_{i2}\omega_{gc}^2 - 1)\psi_p(\omega_{gc})}\right) \tag{5.24}$$

where $\varphi_{gc} = \arg G_{p2}(j\omega_{gc})$, $\psi_m(\omega_{gc}) = \omega_{gc}\frac{d\ln|G_{p2}(j\omega_{gc})|}{d\omega_{gc}}$ and $\psi_p(\omega_{gc}) = \omega_{gc}\frac{d\arg G_{p2}(j\omega_{gc})}{d\omega_{gc}}$.
The expression for T_{d2} in terms of T_{i2} can be obtained by simplifying (5.24)

$$T_{d2} = \frac{\psi_m(\omega_{gc}) - 1 + \psi_p(\omega_{gc})\tan(\Psi_2 - \varphi_{gc}) - T_{i2}\omega_{gc}\left(\psi_p(\omega_{gc}) - \psi_m(\omega_{gc})\tan(\Psi_2 - \varphi_{gc})\right)}{\omega_{gc}^2 T_{i2}\left(1 + \psi_m(\omega_{gc}) + \psi_p(\omega_{gc})\tan(\Psi_2 - \varphi_{gc})\right)} \tag{5.25}$$

By comparing (5.22) and (5.25), we get the expression for T_{i2}

$$T_{i2} = \frac{2}{\omega_{gc}\left[\psi_m(\omega_{gc})\tan(\Psi_2 - \varphi_{gc}) - \psi_p(\omega_{gc}) - \tan\gamma(\omega_{gc})\left(1 + \psi_m(\omega_{gc}) + \psi_p(\omega_{gc})\tan(\Psi_2 - \varphi_{gc})\right)\right]} \tag{5.26}$$

5.3.1.1 Selection of gain crossover frequency, ω_{gc}

The gain crossover frequency ω_{gc} is obtained using the Åström's design inequality [126]. For a system with a time delay θ , n real RHP zeros, a_i, and m real RHP poles, b_i, the design inequality is

given by

$$\sum_{i=1}^{n} \arctan \frac{\omega_{gc}}{a_i} + \sum_{i=1}^{m} \arctan \frac{b_i}{\omega_{gc}} + \frac{\omega_{gc}\theta}{2} \leq \frac{\pi}{2} - \frac{\phi_m}{2} + n_{gc}\frac{\pi}{4} \tag{5.27}$$

where ϕ_m is the phase margin and n_{gc} is the slope of open loop transfer function at the crossover frequency. For the LHP poles with a time delay, the design inequality (5.27) becomes

$$\omega_{gc}\theta \leq \pi - \phi_m + n_{gc}\frac{\pi}{2} \tag{5.28}$$

For the RHP poles with a time delay, the design inequality (5.27) reduces to

$$\sum_{i=1}^{m} \left(\frac{\pi}{2} - \arctan \frac{\omega_{gc}}{b_i} \right) + \frac{\omega_{gc}\theta}{2} \leq \frac{\pi}{2} - \frac{\phi_m}{2} + n_{gc}\frac{\pi}{4} \tag{5.29}$$

Assuming $\frac{\omega_{gc}}{b_i}$ as small value, (5.29) becomes

$$\frac{m\pi}{2} - \sum_{i=1}^{m} \frac{\omega_{gc}}{b_i} + \frac{\omega_{gc}\theta}{2} \leq \frac{\pi}{2} - \frac{\phi_m}{2} + n_{gc}\frac{\pi}{4} \tag{5.30}$$

It is required that the value of n_{gc} must be negative as the magnitude of the loop transfer function must decrease at gain crossover frequency. For the minimum phase systems, the typical values of n_{gc} are between -1.7 and -1.3 [126]. Larger values should be selected for non-minimum phase systems. In order to have the steeper slopes before and after the crossover frequency, n_{gc} is assumed as -1 throughout the chapter. In the proposed cascade control structure shown in Figure 5.1, to evaluate the achievable load disturbance rejection performance of the secondary loop separately, it is suggested to leave out the primary loop initially so that the load disturbance response of the inner loop can be taken into account independently, which will allow the selection of the gain crossover frequency of the loop in a simple way. However, this will inevitably result in actual system performance degradation for the load disturbance rejection due to the interaction arising from the primary loop, such as the load disturbance response oscillation caused by the load disturbances that seep into the inner loop, which also inherently occurs in a conventional cascade control structure. As the primary and secondary loops are interlinked with each other, the selection of the gain crossover frequency for the individual loop can be done by minimizing the performance indices. For the single loop control, the typical values of phase margin is between 30^o and 60^o. For the present work, three values of phase margins i.e. 30^o, 45^o and 60^o have been considered and using (5.28), the corresponding values of $\omega_{gc}\theta$ are 1.05, 0.78 and 0.52, respectively. Therefore, for the primary and secondary loop, we get nine pairs of $\omega_{gc}\theta$. The $\omega_{gc}\theta$ pair is selected by minimizing the performance indices (See Table 5.1). In the Table 5.1, A_{m1}

and A_{m2} are the gain margins for primary and secondary loops, respectively. Corresponding to the minimum values of performance indices (i.e. third entry for the present case), the values obtained for A_{m1} and A_{m2} are satisfactory.

5.3.1.2 Formulae for the parameters of G_{cd2}

For a stable inner loop process, ω_{gc} is obtained from Table 5.1 as $1.05/\theta_2$. The value Ψ_2 is selected based on the simulation studies and the value of Ψ_2 that gives satisfactory closed loop performance is 30^o. The expressions for the parameters of secondary loop controller G_{cd2} in terms of plant model

Table 5.1: Performance specifications of closed loop system for FOPTD primary process

Sl. No.	$\theta_2\omega_{gc}$	$\theta_1\omega_{gc}$	IAE_1	ISE_1	A_{m1}	A_{m2}
1.	0.52	0.52	94.48	59.72	3.15	1.61
2.	0.78	0.52	71.56	47.59	3.15	1.51
3.	1.05	0.52	57.38	41.36	3.15	1.79
4.	0.52	0.78	101.9	63.19	3.02	1.61
5.	0.78	0.78	77.14	50.39	3.02	1.51
6.	1.05	0.78	70.01	47.15	3.02	1.79
7.	0.52	1.05	126.6	77.1	2.02	1.61
8.	0.78	1.05	90.75	55.36	2.02	1.51
9.	1.05	1.05	78.65	49.6	2.02	1.79

parameters obtained using MATLAB curve fitting toolbox are summarized as:

$$\begin{cases} k_2K_{c2} = 1.05\frac{\tau_2}{\theta_2} + 0.0028 \\ \frac{T_{i2}}{\tau_2} = 3.1796\left(\frac{\theta_2}{\tau_2}\right)^{1.09} \\ \frac{T_{d2}}{\tau_2} = 0.1317\left(\frac{\theta_2}{\tau_2}\right)^{0.42} \end{cases} \tag{5.31}$$

for $0 < \theta_2/\tau_2 \leq 1$ and

$$\begin{cases} k_2K_{c2} = 0.52\frac{\tau_2}{\theta_2} - 0.0036 \\ \frac{T_{i2}}{\tau_2} = 0.1316\left(\frac{\theta_2}{\tau_2}\right)^{2.869} \\ \frac{T_{d2}}{\tau_2} = 0.147\left(\frac{\theta_2}{\tau_2}\right)^{1.338} \end{cases} \tag{5.32}$$

for $1 < \theta_2/\tau_2 < 3$ by assuming $\omega_{gc} = 0.52/\theta_2$ and $\Psi_2 = 86^o$.

5.3.2 Design of primary loop controller, G_{cd1}

By following the design procedure outlined in subsection 5.3.1, the primary loop controller G_{cd1} can be designed. For the FOPTD plant model, ω_{gc} is assumed as $0.52/\theta_1$ and the value of Ψ_1 that gives satisfactory closed loop performance is 87^o. Similarly, the values for ω_{gc} and Ψ_1 are $0.52/\theta_1$

and 86^o for the SOPTD model, $0.78/\theta_1$ and 60^o for the IPTD model, $0.52/\theta_1$ and 20^o for the DIPTD model and $2.3562/(2\tau_1 - \theta_1)$ and 16^o for the UFOPTD model. The expressions for the parameters of primary loop controller G_{cd1} in terms of plant model parameters have been obtained using MATLAB curve fitting toolbox and summarized in Table 5.2.

Table 5.2: Expressions for the parameters of G_{cd1}

Process	G_{cd1}
FOPTD	$k_1K_{c1} = 0.1844\frac{\tau_1}{\theta_1} - 0.0036$
	$\frac{T_{i1}}{\tau_1} = 14.3298\left(\frac{\theta_1}{\tau_1}\right)^{1.6}$
	$\frac{T_{d1}}{\tau_1} = 0.354\left(\frac{\theta_1}{\tau_1}\right)^{0.33}$
SOPTD	$k_1K_{c1} = 9.7311\times10^{-4}\frac{\tau_1\tau_2}{\theta_1^2} + 0.51999\left(\frac{\tau_1+\tau_2}{\theta_1}\right) - 0.003599$
	$\frac{T_{i1}}{\tau_1} = 4.0988\left(\frac{\theta_1}{\tau_1}\right)^{1.02}\tau_2^{-0.02}$
	$\frac{T_{d1}}{\tau_1} = 0.1858\left(\frac{\theta_1}{\tau_1}\right)^{0.67}\tau_2^{0.33}$
IPTD	$k_1K_{c1} = 0.78/\theta_1$
	$T_{i1} = 4.9623\theta_1$
	$T_{d1} = 0.3243\theta_1$
DIPTD	$k_1K_{c1} = 0.1847/\theta_1^2$
	$T_{i1} = 12.6557\theta_1$
	$T_{d1} = 3.0457\theta_1$
UFOPTD	$k_1K_{c1} = 0.7945\frac{\tau_1}{\theta_1} + 0.0054$
	$\frac{T_{i1}}{\tau_1} = 84.42\left(\frac{\theta_1}{\tau_1}\right)^{0.1554}$
	$\frac{T_{d1}}{\tau_1} = 1.274\left(\frac{\theta_1}{\tau_1}\right)^{1.79}$

Generally, the processes with the normalized time delay in the range $(0 < \theta_1/\tau_1 \leq 1)$ and $(\theta_1/\tau_1 > 1)$ are called small time delay and large time delay processes, respectively. The graphs of normalized proportional gain, normalized integral time constant and normalized derivative time constant versus normalized time delay are shown in Figure 5.2, 5.3 and 5.4, respectively. From the figures, it is observed that larger proportional gain, smaller integral and derivative time constants are necessary for the control of processes with small normalized dead time than those of the large time delay processes. (Note: The controllers (G_{cd1} and G_{cd2}) have been designed in terms of process parameters (G_{p1} and G_{p2}) assuming $G_{p1} = G_{d1}$ and $G_{p2} = G_{d2}$ (Model matching case). If $G_{p1} \neq G_{d1}$ and $G_{p2} \neq G_{d2}$, a difference in the pole location in G_{p1} (or G_{p2}) and G_{d1} (or G_{d2}) causes a mismatch in pole-zero cancelation.)

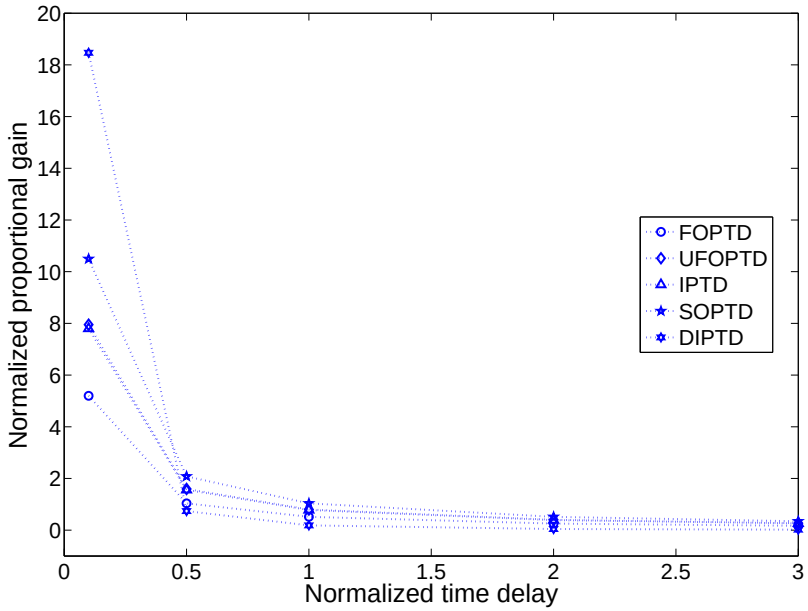

Figure 5.2: Proportional gain of primary loop controller

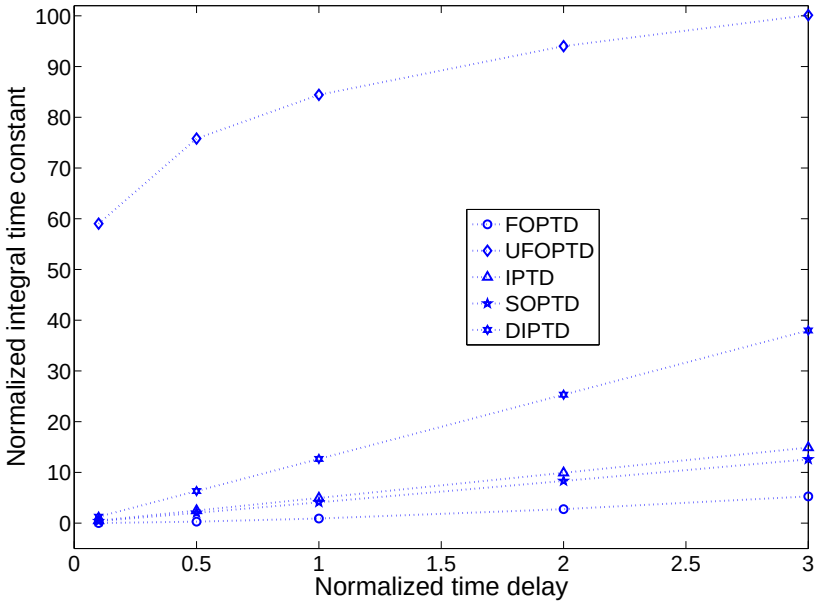

Figure 5.3: Integral time constant of primary loop controller

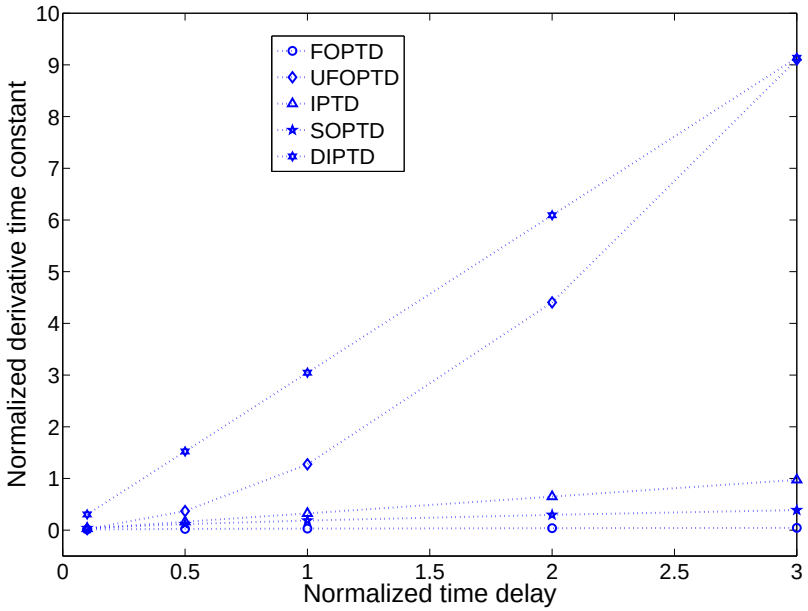

Figure 5.4: Derivative time constant of primary loop controller

5.3.3 Design of setpoint filter, G_{cs}

The ISE performance specification method [32, 83] is adopted to design the filter G_{cs}. In order to ensure the system performance objective, $min \, \|W(s)(1 - Y_{r1}(s))\|_2^2$ is implemented where the setpoint input weight function $W(s)$ is selected as $\frac{1}{s}$ for the step changes of the setpoint input and load disturbances.

Considering a second order primary process with time delay, $G_{p1} = k_1 e^{-\theta_1 s}/(\tau_1 s \pm 1)(\tau_2 s + 1)$, n/n order all-pass Pade approximation of the time delay $e^{-\theta_1 s}$ gives

$$G_{p1} = \frac{k_1 P_{nn}(-\theta_1 s)}{(\tau_1 s \pm 1)(\tau_2 s + 1) P_{nn}(\theta_1 s)}$$

where

$$P_{nn}(\theta_1 s) = \sum_{j=0}^{n} \frac{(2n-j)!n!}{(2n)!j!(n-j)!} (\theta_1 s)^j$$

and n is chosen to be an integer large enough to guarantee that the approximation error can be neglected in comparison with the process model mismatch in practice. Using (5.3) when there is no

model mismatch, it follows that

$$\begin{aligned}\|W(s)(1-Y_{r1}(s))\|_2^2 &= \left\|\frac{1}{s}\left(1-\frac{k_1G_{cs}(s)P_{nn}(-\theta_1 s)}{[(\tau_1 s\pm 1)(\tau_2 s+1)+k_1]\,P_{nn}(\theta_1 s)}\right)\right\|_2^2 \\ &= \left\|\frac{P_{nn}(\theta_1 s)}{sP_{nn}(-\theta_1 s)}-\frac{k_1G_{cs}(s)}{s\,[(\tau_1 s\pm 1)(\tau_2 s+1)+k_1]}\right\|_2^2 \end{aligned} \tag{5.33}$$

Using the orthogonality property of the H_2 norm, we get

$$\begin{aligned}\|W(s)(1-Y_{r1}(s))\|_2^2 &= \left\|\frac{P_{nn}(\theta_1 s)-P_{nn}(-\theta_1 s)}{sP_{nn}(-\theta_1 s)}\right\|_2^2 \\ &\quad+\left\|\frac{[(\tau_1 s\pm 1)(\tau_2 s+1)+k_1]-k_1G_{cs}(s)}{s\,[(\tau_1 s\pm 1)(\tau_2 s+1)+k_1]}\right\|_2^2 \end{aligned} \tag{5.34}$$

The right hand side of (5.34) is minimized (equating its second term to zero) in order to obtain an optimal controller i.e.

$$\frac{[(\tau_1 s\pm 1)(\tau_2 s+1)+k_1]-kG_{csom}(s)}{s\,[(\tau_1 s\pm 1)(\tau_2 s+1)+k_1]}=0 \tag{5.35}$$

or,

$$G_{csom}=\frac{(\tau_1 s\pm 1)(\tau_2 s+1)+k_1}{k_1} \tag{5.36}$$

The resulting controller in (5.36) may not be practically implementable. For ease in implementation a low pass filter of the form $f_{cs}(s)=\frac{1}{(\lambda_{cs}s+1)^{n_{cs}}}$ is introduced where λ_{cs} is the filter time constant, the index n_{cs} ($n_{cs}=1,2,...$) should be selected such that the resulting controller will be realizable. Thus, the setpoint filter is obtained as

$$G_{cs}(s)=G_{csom}f_{cs}(s)=\frac{(\tau_1 s\pm 1)(\tau_2 s+1)+k_1}{k_1(\lambda_{cs}s+1)^{n_{cs}}} \tag{5.37}$$

The tuning parameter λ_{cs} represents the performance degree. The smaller λ_{cs} is, the better the nominal tracking performance. The relationship is monotonic. When $\lambda_{cs}\to 0$, the performance tends to be optimal. $\lambda_{cs}>0$ is tuned for a compromise between overshoot and rise time. Based on the simulation studies, it is suggested that λ_{cs} in the range $(0.4\theta_m-\theta_m)$ for FOPTD, $(0.5\theta_m-1.5\theta_m)$ for UFOPTD, $(0.7\theta_m-1.2\theta_m)$ for IPTD, $(0.8\theta_m-3\theta_m)$ for DIPTD and $(0.1\theta_m-1.3\theta_m)$ for SOPTD process models. In general, λ_{cs} can be fixed around primary loop process model time delay θ_m in the first place. If the closed-loop performance and the robust stability are not satisfactory, then monotonously increase or decrease the adjustable parameter λ_{cs} on-line till the trade-off between the close-loop nominal performance and its robust stability is achieved. The setpoint filter for different processes are summarized in Table 5.3.

Table 5.3: Setpoint filter G_{cs}

Process	G_{cs}	
FOPTD	$\frac{\tau s+k_1+1}{k_1(\lambda_{cs}s+1)}$	$\tau_1=\tau,\ \tau_2=0$
SOPTD	$\frac{\tau_1\tau_2 s^2+(\tau_1+\tau_2)s+k_1+1}{k_1(\lambda_{cs}s+1)^2}$	
IPTD	$\frac{s+k_1'}{k_1'(\lambda_{cs}s+1)}$	$\tau_1\to\infty,\ k_1'=\frac{k_1}{\tau_1}\to finite,\ \tau_2=0$
DIPTD	$\frac{s^2+k_1''}{k_1''(\lambda_{cs}s+1)^2}$	$\tau_1\to\infty,\tau_2\to\infty,k_1''=\frac{k_1}{\tau_1\tau_2}\to finite$
UFOPTD	$\frac{\tau s+k_1-1}{k_1(\lambda_{cs}s+1)}$	$\tau_1=\tau,\ \tau_2=0$

5.4 Stability analysis

Since most of the processes are often operated under diverse disturbances and uncertainties; it is difficult to develop accurate models for the processes and their disturbances. The stability analysis is therefore an important feature of the closed loop system.

5.4.1 Stabilization of primary loop controller, G_{cd1}

The primary open-loop transfer function $\mathscr{L}_1(s)$ can be expressed in the form of

$$\mathscr{L}_1(s)=G_{p1}(s)\,G_{cd1}(s)=K\frac{N(s)}{s^x D(s)}e^{-\theta_{n1}s} \tag{5.38}$$

where K is the normalized gain, θ_{n1} is the normalized time delay and x is a positive integer representing type of the loop. $N(s)$ and $D(s)$ are both rational polynomials of s with $N(0)=D(0)=1$. The Nyquist stability criterion when applied to the open-loop $\mathscr{L}_1(s)$ leads to following points([127], [128]):

- The open-loop transfer function $\mathscr{L}_1(s)$ in (5.38) with m unstable poles, the closed-loop system is stable if and only if the Nyquist plot of $\mathscr{L}_1(s)$ encircles the critical point $(-1,j0)$, m times counterclockwise.
- For the open-loop $\mathscr{L}_1(s)$, $\lim\limits_{\omega\to\infty}|\mathscr{L}_1(j\omega)|<1$ is necessary for the closed-loop stability.
- The necessary condition for closed-loop stability for $\mathscr{L}_1(s)$ is that
  - for $x=0$: $K>-1$ if $m=0$; and $K<-1$ if $m=1$
  - for $x=1,2$: $K>0$ if $m=0$; and $K<0$ if $m=1$.
- The closed-loop system is stable if and only if the polynomial,

$$H(s)=e^{-\theta_{n1}s}\frac{d^{p+1}}{ds^{p+1}}\left[s^x D(s)e^{\theta_{n1}s}\right] \tag{5.39}$$

has all its roots in the open left half plane (LHP), where p is the degree of $N(s)$.

For the SOPTD process, it follows from (5.39) that the closed-loop stability requires $H(s) = s^3\theta_{n1}^3 T + (9\theta_{n1}^2 T + \theta_{n1}^3 + \theta_{n1}^3 T)s^2 + (18T\theta_{n1} + 6\theta_{n1}^2 + 6\theta_{n1}^2 T + \theta_{n1}^3)s + 6T + 6\theta_{n1} + 6T\theta_{n1} + 3\theta_{n1}^2$ be stable where $T = \tau_2/\tau_1$. Then, the constant term $\left(6T + 6\theta_{n1} + 6T\theta_{n1} + 3\theta_{n1}^2\right) > 0$ is necessary, which leads to $\theta_{n1} > \sqrt{1+T^2} - T - 1$. Thus, the controller G_{cd1} could stabilize G_{p1} if and only if $\theta_{n1} > \sqrt{1+T^2} - T - 1$. Similarly, for UFOPTD process, it follows from (5.39) that the the closed-loop stability requires $H(s) = s^2\theta_{n1}^3 + (6\theta_{n1}^2 - \theta_{n1}^3)s + 6\theta_{n1} - 3\theta_{n1}^2$ be stable. Then, the zero order term $\left(6\theta_{n1} - 3\theta_{n1}^2\right) > 0$ is necessary, which requires $\theta_{n1} < 2$. Therefore, the controller G_{cd1} can stabilize G_{p1} if and only if $\theta_{n1} < 2$.

Using the same technique, the stabilization conditions for the remaining primary loop processes are derived and summarized in the Table 5.4.

Table 5.4: Stabilizability results

Sl. No.	Process	Condition on the normalized time delay
1.	FOPTD	$\forall\theta_{n1} > 0$
2.	SOPTD	$\theta_{n1} > \sqrt{1 + (\tau_2/\tau_1)^2} - (\tau_2/\tau_1) - 1$
3.	UFOPTD	$\theta_{n1} < 2$
4.	IPTD	$\forall\theta_{n1} > 0$
5.	DIPTD	$\forall\theta_{n1} > 0$

5.4.2 Stabilization of secondary loop controller, G_{cd2}

As the secondary process is considered as FOPTD, $\forall\theta_{n2} > 0$ the secondary process is stabilizable by the PID controller G_{cd2}.

5.5 Robustness analysis and performances

The robust stability of the closed loop can be analyzed taking into account that $G_{p1}(s)$ belongs to a family of linear models described as $G_{p1}(s) = G_{pn1}(s)\left(1 + \delta G_{p1}(s)\right)$ [129]. The nominal model is represented by $G_{pn1}(s)$ and $\delta G_{p1}(s)$ is a multiplicative description of the modeling errors. Consider the closed-loop characteristic equation

$$1 + G_{cd1}(s)G_{p1}(s) = 1 + G_{cd1}(s)\left(G_{pn1}(s)\left(1 + \delta G_{p1}(s)\right)\right) = 0$$

For all the plants, it is necessary that

$$|\delta G_{p1}(j\omega)| < dG_{p1}(\omega) = \frac{|1 + G_{cd1}(j\omega)G_{pn1}(j\omega)|}{|G_{pn1}(j\omega)|} \qquad \forall\omega \geq 0 \tag{5.40}$$

for the bounds of the multiplicative uncertainties ($\overline{\delta G}_{p1}(\omega)$) and where

$$\overline{\delta G}_{p1}(\omega) < dG_{p1}(\omega) \quad \forall\omega \geq 0 \tag{5.41}$$

The function $dG_{p1}(\omega)$ is the upper bound of the multiplicative modelling error of the plant to guarantee stability and it can be used as a measure of the controller robustness. Here, $dG_{p1}(\omega)$ is a rational function because the Smith predictor has eliminated the dead time. This, in general, allows a better trade-off to be achieved between robustness and performance. The types of uncertainties considered here are the parametric uncertainties such as uncertainty in process gain, time constant and time delay. According to the Small gain theorem [93], the closed loop system for the load disturbance rejection is robustly stable if and only if

$$\|\delta_m(j\omega)T_d(j\omega)\| < 1 \qquad \forall\omega \in (-\infty, \infty) \tag{5.42}$$

where $T_d(s = j\omega)$ is the closed loop complementary sensitivity function and $\delta_m(j\omega)$ is the process multiplicative uncertainty bound i.e. $\delta_m(j\omega) = |(G_p(j\omega) - G_m(j\omega))/G_m(j\omega)|$. The complementary sensitivity function of the closed loop system consists of G_{cd1} whose parameters K_{c1}, T_{i1} and T_{d1} are functions of the tuning parameters ω_{gc} and Ψ_1. For the process gain uncertainty, the tuning parameter should be selected in such a way that

$$\|T_d(j\omega)\|_\infty < \frac{1}{|\Delta k|/k} \qquad \forall\omega > 0 \tag{5.43}$$

For the process time dealy uncertainty, the tuning parameter should be selected in such a way that

$$\|T_d(j\omega)\|_\infty < \frac{1}{|e^{-j\Delta\theta\omega} - 1|} \qquad \forall\omega > 0 \tag{5.44}$$

If uncertainty exists in both process gain and time delay, the tuning parameter should be selected in such a way that

$$\|T_d(j\omega)\|_\infty < \frac{1}{|(1 + \frac{\Delta k}{k})e^{-j\Delta\theta\omega} - 1|} \qquad \forall\omega > 0 \tag{5.45}$$

According to robust control theory [91], the closed loop performance for load disturbance rejection is robust, if

$$\|\delta_m(j\omega)T_d(j\omega) + w_1(j\omega)(1 - T_d(j\omega))\|_\infty < 1 \tag{5.46}$$

where $w_1(j\omega)$ is the weight function of the sensitivity function, $S_d(j\omega) = 1 - T_d(j\omega)$. Therefore, the tuning parameters should be selected such that the resulting controller satisfy the robust nominal performance and robust stability constraints.

5.5.1 Maximum sensitivity (M_s) to modeling error

The maximum sensitivity has a nice geometrical interpretation in the Nyquist diagram for robustness and stability. M_s is the inverse of the shortest distance from the Nyquist curve of the loop transfer function to the critical point (-1, 0) on the complex plane. The maximum sensitivity

$$M_{s1} = \max_{\omega} |S_1(j\omega)| = \max_{\omega} \frac{1}{|1 + G_{cd1}G_{p1}|} \tag{5.47}$$

for primary loop and

$$M_{s2} = \max_{\omega} |S_2(j\omega)| = \max_{\omega} \frac{1}{|1 + G_{cd2}G_{p2}|} \tag{5.48}$$

for secondary loop. For a single loop system, the recommended values for M_s are typically within the range 1-2 [130]. The use of the maximum sensitivity as a robustness measure, has the advantage that lower bounds to the gain and phase margins can be assured according to

$$A_m > \frac{M_s}{M_s - 1} \tag{5.49}$$

$$\phi_m > 2\arcsin\left(\frac{1}{2M_s}\right) \tag{5.50}$$

A small value of M_s indicates that the stability margin of the control system is large. Responses obtained with $M_s \approx 1$ show little or no overshoot, as is desirable in process control. Faster responses are obtained with $M_s \approx 2$. The settling time at load disturbances is significantly shorter with the larger value of M_s. On the other hand, these responses are oscillatory with larger overshoots.

5.5.2 Model mismatch consideration

As the modified Smith predictor has been used in the outer loop of parallel cascade control structure, it is necessary to analyze the model mismatch condition. The over sensitivity problem during model mismatch condition is one of the most criticized drawbacks of the Smith predictor controller

design. If the controller tuning is too tight, the closed-loop system may become unstable with a small model mismatch in the model parameters. Now, we will examine the closed-loop stability property of the proposed controller design with some model mismatch of G_{m1} and G_{m2}.

Assuming the true transfer function of the secondary process is $G_{p2} = \frac{k_2 e^{-\theta_2 s}}{\tau_2 s+1}$ and that of primary IPTD process is $G_{p1} = \frac{k_1 e^{-\theta_1 s}}{s}$. Due to lack of precise knowledge of the actual system parameters, the model transfer functions are guessed wrong with gains, time constants and time delays: $G_{m2} = \frac{(k_2+\Delta k_2)e^{-(\theta_2+\Delta\theta_2)s}}{(\tau_2+\Delta\tau_2)s+1}$ and $G_{m1} = \frac{(k_1+\Delta k_1)e^{-(\theta_1+\Delta\theta_1)s}}{s}$. Kharitonov's theorem is the well-known and simplest tool for robust stability analysis [110, 112]. This theorem has been used for the robustness analysis considering parametric uncertainties in the model parameters. Now, consider a cascade system with primary and secondary process transfer functions (see Example-5.3): $G_{p1} = \frac{2e^{-2s}}{s}$ and $G_{p2} = \frac{4e^{-s}}{s+1}$. The model transfer functions are assumed with +10% change in gains, time constants and time delays simultaneously: $G_{m1} = \frac{2.2e^{-2.2s}}{s}$ and $G_{m2} = \frac{4.4e^{-1.1s}}{1.1s+1}$. From (5.1), the closed-loop characteristic equation of the primary loop is given by

$$(1 + G_m)\,(1 + G_{p1}G_{cd1} + G_{p2}G_{cd2} + G_{p1}G_{cd1}G_{m2}G_{cd2}) = 0$$

The four Kharoitonov polynomials are obtained as

$$K_1(s) = 0.0001 + 0.007s + 0.2196s^2 + 2.6045s^3 + 16.2225s^4 + 66.8261s^5 + 197.5344s^6 + 405.2495s^7 + 582.2001s^8 + 620.8209s^9 + 477.2083s^{10} + 234.4039s^{11} + 68.5753s^{12} + 11.0409s^{13} + 0.7056s^{14}$$

$$K_2(s) = 0.0001 + 0.0073s + 0.2109s^2 + 2.5023s^3 + 16.8847s^4 + 69.5537s^5 + 189.7879s^6 + 389.3573s^7 + 605.9633s^8 + 646.1606s^9 + 458.4943s^{10} + 225.2116s^{11} + 71.3743s^{12} + 11.4915s^{13} + 0.6779s^{14}$$

$$K_3(s) = 0.0001 + 0.007s + 0.2109s^2 + 2.6045s^3 + 16.8847s^4 + 66.8261s^5 + 189.7879s^6 + 405.2495s^7 + 605.9633s^8 + 620.8209s^9 + 458.4943s^{10} + 234.4039s^{11} + 71.3743s^{12} + 11.0409s^{13} + 0.6779s^{14}$$

$$K_4(s) = 0.0001 + 0.0073s + 0.2196s^2 + 2.5023s^3 + 16.2225s^4 + 69.5537s^5 + 197.5344s^6 + 389.3573s^7 + 582.2001s^8 + 646.1606s^9 + 477.2083s^{10} + 225.2116s^{11} + 68.5753s^{12} + 11.4915s^{13} + 0.7056s^{14}$$

The coefficients of Kharitonov polynomials are checked for Hurwitz condition. It is observed that all the roots of the Kharitonov polynomials (Table 5.5) have negative real part i.e. all roots are in the left half of the complex plane. From the Figure 5.5, it is clear that Kharitonov rectangles move about the origin in counter-clockwise sense in order to have the monotonic phase increase property of Hurwitz polynomials. The graph is zoomed to show what is happening in the neighborhood of the

point $(0, 0)$. Since the origin is excluded from the Kharitonov rectangles (Figure 5.5) it is concluded that the closed-loop control system is robustly stable. By following a similar procedure as above the robustness analysis considering parametric uncertainties in the model parameters for FOPTD, UFOPTD, DIPTD and SOPTD can be checked.

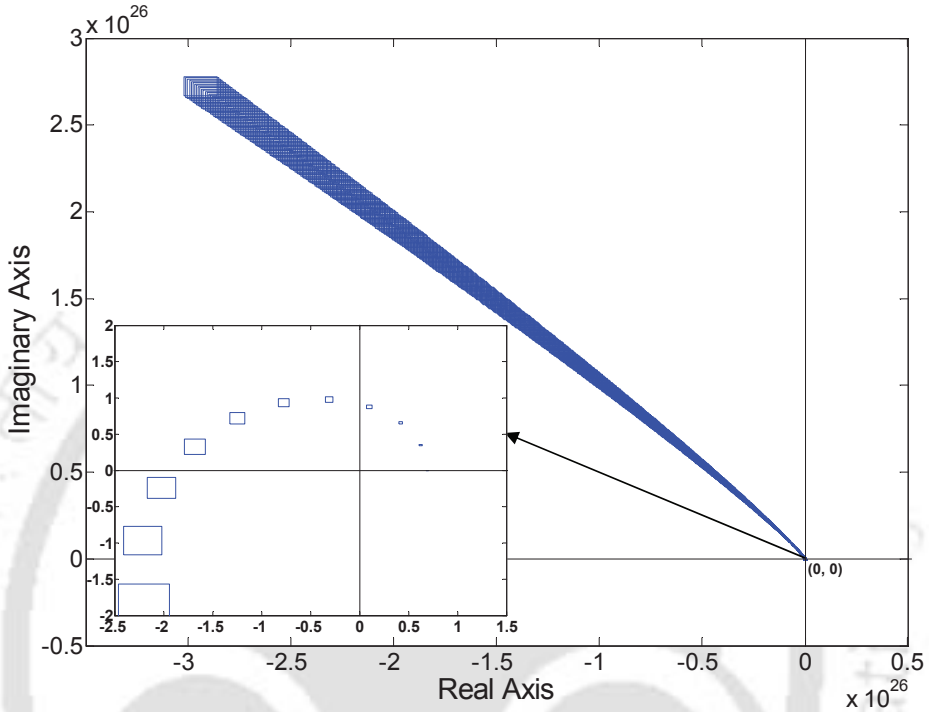

Figure 5.5: Kharitonov's rectangle for +10% estimation error in the parameters of G_{m1} and G_{m2}

Table 5.5: The roots of Kharitonov polynomials

$K_1(s)$	$K_2(s)$	$K_3(s)$	$K_4(s)$
-6.60	-7.41	$-5.19 + j1.65$	-8.01
$-2.35 + j2.03$	-4.76	$-5.19 - j1.65$	-3.28
$-2.35 - j2.03$	$-0.53 + j1.58$	-2.62	$-1.10 + j1.98$
-2.14	$-0.53 - j1.58$	-1.33	$-1.10 - j1.98$
$-0.12 + j0.84$	-1.72	$-0.27 + j1.17$	-1.21
$-0.12 - j0.84$	-0.92	$-0.27 - j1.17$	$-0.03 + j0.63$
-0.84	$-0.01 + j0.50$	-0.62	$-0.03 - j0.63$
-0.51	$-0.01 - j0.50$	$-0.03 + j0.39$	-0.67
$-0.07 + j0.30$	-0.49	$-0.03 - j0.39$	-0.39
$-0.07 - j0.30$	-0.27	-0.38	$-0.10 + j0.20$
-0.27	$-0.12 + j0.12$	$-0.16 + j0.06$	$-0.10 - j0.20$
-0.16	$-0.12 - j0.12$	$-0.16 - j0.06$	-0.19
$-0.02 + j0.02$	$-0.03 + j0.02$	$-0.02 + j0.02$	$-0.02 + j0.02$
$-0.02 - j0.02$	$-0.03 - j0.02$	$-0.02 - j0.02$	$-0.02 - j0.02$

5.5.3 Performance

To evaluate the closed-loop performance, we consider three popular performance specifications based on integral error ($e(t) = r(t) - y(t)$) such as the integral absolute error (IAE= $\int_0^\infty |e(t)|\,dt$), the integral time-weighted absolute error (ITAE= $\int_0^\infty t\,|e(t)|\,dt$) and the integral square error (ISE= $\int_0^\infty e(t)^2 dt$) criteria.
To evaluate the manipulated input, we compute the total variation (TV) of the input $u(t)$ i.e.TV= $\sum_{i=1}^{\infty} |u_{i+1} - u_i|$, which should be as small as possible. The TV is a good measure of smoothness of a signal [94].

5.6 Simulation study

Five examples are given to illustrate the use of the proposed cascade control method. In the first example, the proposed method is compared with Lee et al.'s [48] and Rao et al.'s [49] methods as they have proposed parallel cascade control schemes for controlling stable FOPTD processes. In the remaining examples, results of the proposed method are compared with that of a conventional parallel cascade structure. For the conventional cascade control, a proportional controller for the inner loop and a PI/PID controller for the outer loop are used. For comparison with a conventional cascade control, the difficulty arises as to how to choose the PID parameters. When a cascade control system is tuned after installation, the secondary controller should be tuned first with the primary controller in the manual mode. Then the primary controller is transferred to automatic mode.

Example-5.1: The FOPTD process models studied by Semino and Brambilla [45] are $G_{p1} = G_{d1} = \frac{1.24}{30s+1}e^{-33s}$ and $G_{p2} = G_{d2} = \frac{3.1}{30s+1}e^{-9s}$. Using the proposed method, $K_{c2} = 1.13$, $T_{i2} = 25.678$, $T_{d2} = 2.383$, $K_{c1} = 0.1323$, $T_{i1} = 500.7135$ and $T_{d1} = 10.9597$ are estimated. The setpoint filter is obtained as $G_{cs} = (30s + 2.24)/(30.69s + 1.24)$ by choosing $\lambda_{cs} = 0.75\theta_m$. For Lee et al.'s [48] method, the primary controller settings are $K_{cp} = 2.3$, $\tau_{Ip} = 45.9$, $\tau_{Dp} = 11.6$, $q_{f1} = 1/(30s + 1)$ and the secondary controller settings are $K_{cs} = 1.35$, $\tau_{Is} = 18.5$, $\tau_{Ds} = 3.27$, $q_{f2} = 1/(14.6s + 1)$. For Rao et al.'s [49] method, the secondary loop controllers are $C_2 = (30s + 1)(14.6s + 1)\big/3.1(5s + 1)^2$, $q_{f2} = 1/(14.6s + 1)$ and the primary controller settings are $k_c = 0.625$, $k_i = 0.1302$, $\tau_f = 35.5$. With these controller settings, a unit step setpoint is introduced at time $t = 0$ and a unit negative step input load disturbance at time $t = 350$ sec. The nominal responses of the closed-loop system are given in Figure 5.6 and 5.7.

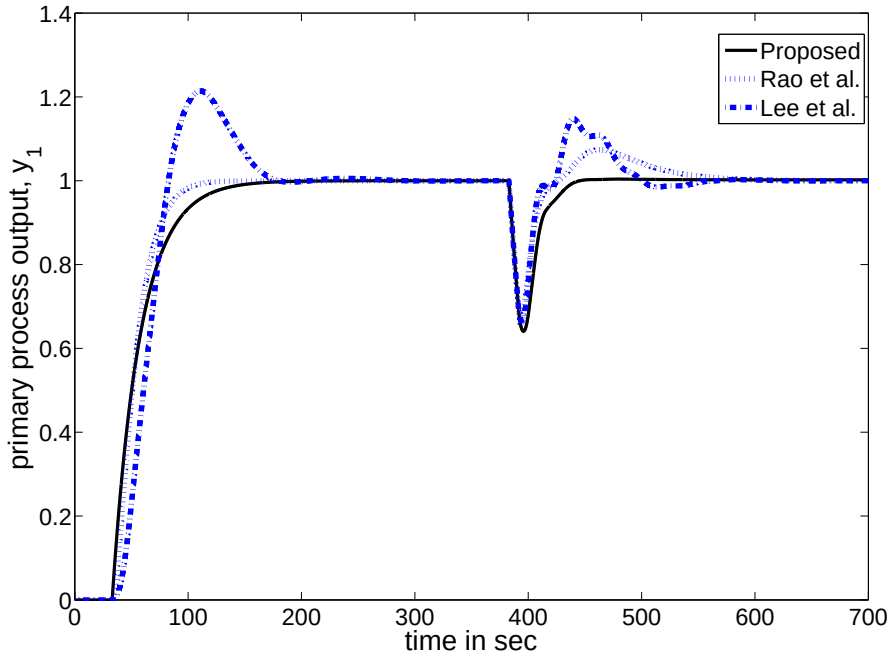

Figure 5.6: Nominal process outputs for example 5.1

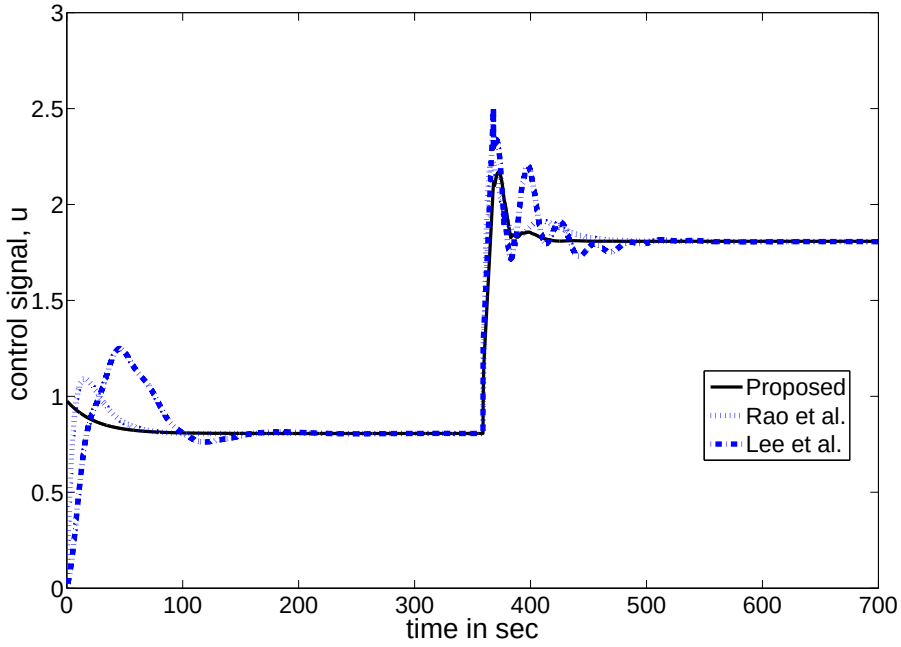

Figure 5.7: Nominal process inputs for example 5.1

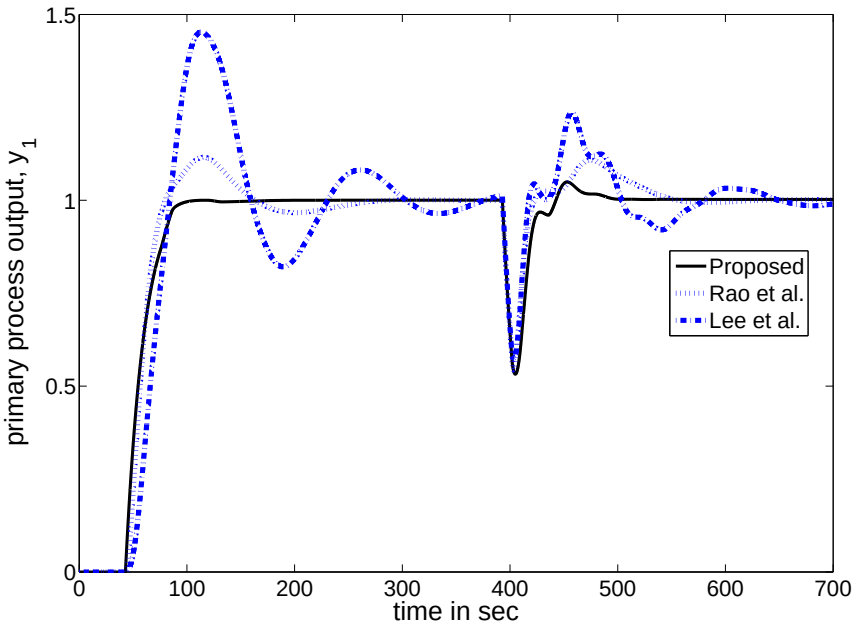

(a) Process outputs

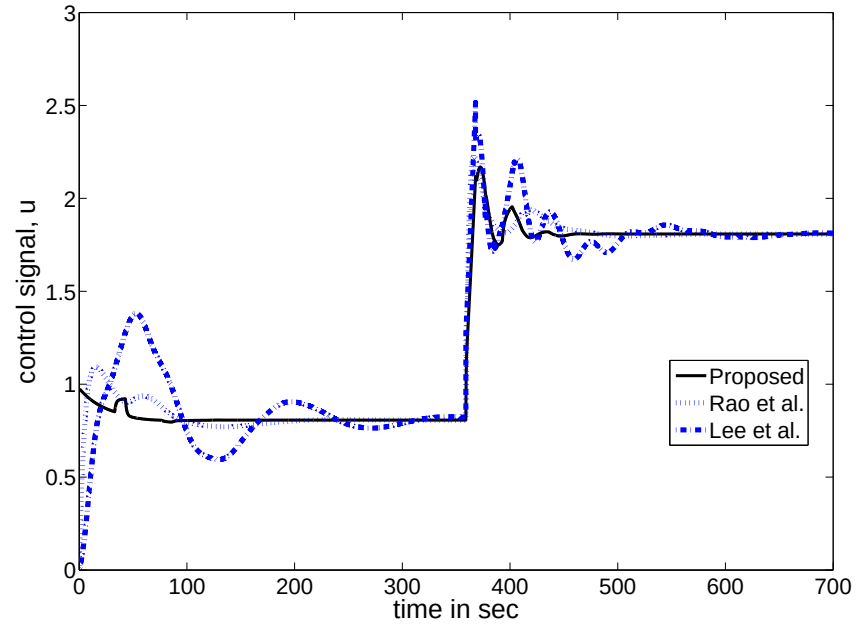

(b) Process inputs

Figure 5.8: Perturbed responses for example 5.1

In the present work, to illustrate the robustness to parameter variations, a +30% perturbations in time delays and −30% in the time constants of both the primary process and disturbance transfer functions and the corresponding responses are shown in Figure 5.8.

Table 5.6: Performance specifications for servo problem

	Scheme	Nominal System				Perturbed system			
		IAE	ISE	ITAE	TV	IAE	ISE	ITAE	TV
Example-5.1	Proposed	53.75	45.38	1604	0.17	58.53	51.25	1845	0.33
	Rao et al.	54.7	46.25	1629	1.38	65.78	53.51	2877	1.53
	Lee et al.	71.86	55.45	3283	1.81	102.2	69.49	8416	2.74
Example-5.2	Proposed	7	5.7	32.5	3.5	6.79	5.38	38.85	6.67
	Conventional	44.58	33.27	1566	8.82	47.73	39.29	1613	9.19
Example-5.3	Proposed	4	3	10	0.25	4.26	3.34	12.1	0.45
	Conventional	10.29	4.71	146.2	0.30	11.25	5.43	163.1	0.46
Example-5.4	Proposed	4.7	3.2	15.05	0.32	4.73	3.21	15.66	0.43
	Conventional	15.76	7.12	331.5	0.78	16.36	7.45	353.6	0.71
Example-5.5	Proposed	18.69	17.19	178.7	7.33	21.74	18.71	307	8.09
	Conventional	155.4	146.2	1.54×10^4	9.42	197.9	244	2.11×10^4	12.34

Table 5.7: Performance specifications for regulatory problem

	Scheme	Nominal System				Perturbed system			
		IAE	ISE	ITAE	TV	IAE	ISE	ITAE	TV
Example-5.1	Proposed	9.10	1.38	886.8	1.86	11.21	2.33	1122	2.27
	Rao et al.	10.89	1.52	1001	1.99	13.22	2.48	1320	2.71
	Lee et al.	11.88	1.90	984.8	4.26	21.2	3.70	2879	4.69
Example-5.2	Proposed	3.25	0.60	174.9	3.45	3.58	0.82	106.3	4.66
	Conventional	18.17	6.16	621.8	5.50	18.84	6.91	633	5.25
Example-5.3	Proposed	1.99	0.25	24.44	0.17	2.25	0.32	26.76	0.22
	Conventional	6.21	1.59	97.08	0.17	6.53	1.75	106.4	0.25
Example-5.4	Proposed	0.35	0.01	2.15	0.57	0.52	0.02	4.60	0.76
	Conventional	13.66	6.21	285.8	2.49	14.03	6.39	302.1	2.74
Example-5.5	Proposed	3.50	0.15	231.1	0.21	3.64	0.16	243.8	0.20
	Conventional	12.78	1.09	1398	0.87	16.39	1.88	1958	1.03

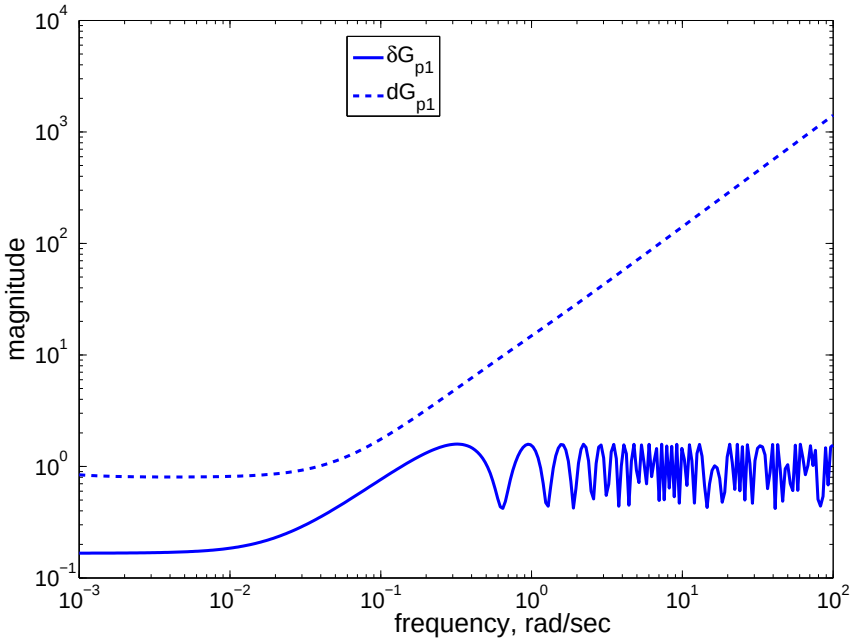

(a) Magnitude plots for modeling error and uncertainty norm bound under perturbations of $+20\%$ in k_1 and $+30\%$ in θ_1 and -30% in τ_1

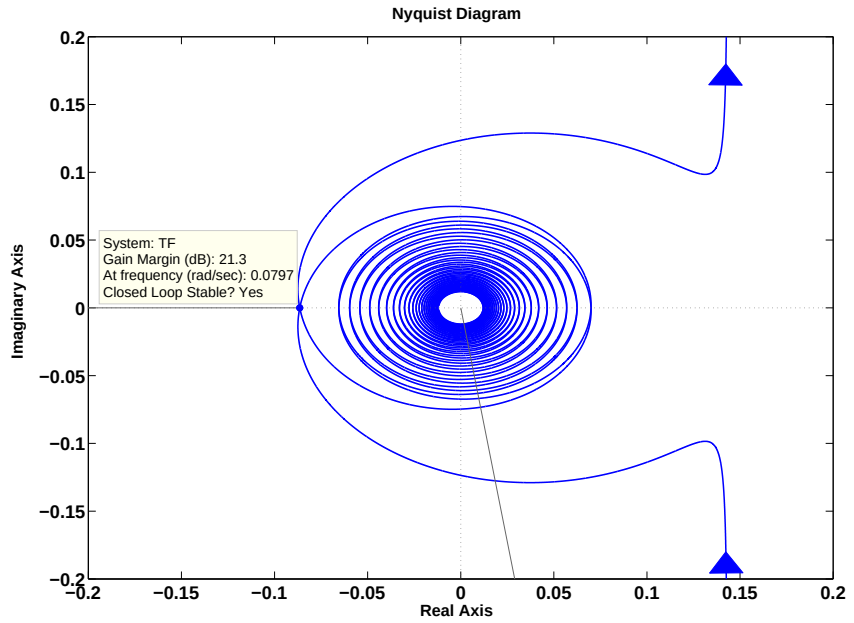

(b) Stabilization of G_{p1}

Figure 5.9: Magnitude plot and Nyquist plot for example 5.1

The responses of the proposed method is superior to that of Rao et al. and Lee et al.. The performance indices of proposed method are low as compared to other methods (Table 5.6 and 5.7).

The proposed method gives smooth control signal. To analyze further robustness conditions, an uncertainty of +30% in the primary process time delay, +20% in primary process gain and −30% in the primary process time constant is considered. The magnitude plots for the modeling error and uncertainty norm bound are shown in Figure. 5.9(a). It is observed from Figure. 5.9(a) that the modeling error is less than the uncertainty bound at all frequencies. Since $\theta_{n1} = 1.1 > 0$, it follows from Table 5.4 that the primary process G_{p1} is stabilizable by the proposed PID controller. The Nyquist plot shown in Figure. 5.9(b) gives stable closed-loop response.

Example-5.2: Consider the UFOPTD primary process (or primary load disturbance) parameters $k_1 = 1$, $\tau_1 = 10$, $\theta_1 = 3$ and the FOPTD secondary process (or secondary load disturbance) parameters $k_2 = 2$, $\tau_2 = 1$, $\theta_2 = 2$ (Kaya and Atherton [81]). (5.32) gives the parameters for inner loop controller, $K_{c2} = 0.1282$, $T_{i2} = 0.9614$, $T_{d2} = 0.3717$ and Table 5.2 for outer loop controller, $K_{c1} = 2.6536$, $T_{i1} = 700.1482$ and $T_{d1} = 1.4766$. By choosing $\lambda_{cs} = 1.33\theta_m$, the setpoint filter is obtained as $G_{cs} = 10s/(4s + 1)$. For the conventional cascade structure, the popular Ziegler-Nichols(ZN) tuning method [131] is used to find the inner loop controller parameter, which is found to be $K_{c2} = 0.38$ and Majhi and Atherton's method [132] is used to find the outer loop PI controller parameters such as $K_{c1} = 7.2889$, $T_{i1} = 27.7656$. The magnitude of the load disturbance is $d = -1$. The responses of the closed-loop system for these controller settings are shown in Figure 5.10 and Figure 5.11 for the actual process. A +20% perturbation in primary process and primary disturbance time delays is considered and the corresponding responses are given in Figure 5.12 and Figure 5.13. The conventional cascade structure gives the worst result in the sense of maximum overshoot and settling time. The TV of proposed method is smaller than that of conventional case (Table. 5.6 and 5.7), which indicates the proposed method gives smooth control signal. The normalized time delay, θ_{n1} is 0.3 which is less than 2. From the stabilizability condition in Table 5.4, it confirms that the primary process is stabilizable by the proposed PID controller. The Nyquist plot shown in Figure 5.14(a) indicates a stable closed loop. Let the primary time delay increases to 30 i.e. $\theta_{n1} = 3$ with other settings unchanged. The Nyquist plot given in Figure 5.14(b) indicates an unstable closed-loop. Magnitude plots for the modeling error and the uncertainty (uncertainty of +30% in k_1, θ_1 and −30% in τ_1) are considered for further analysis of robust stability and shown in Figure.5.15.

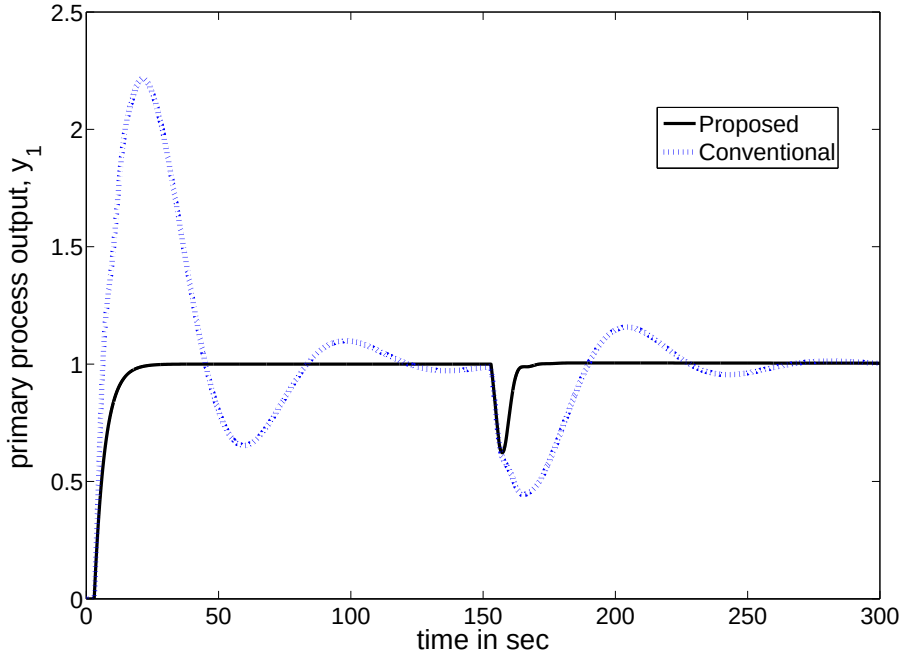

Figure 5.10: Nominal process outputs for example 5.2

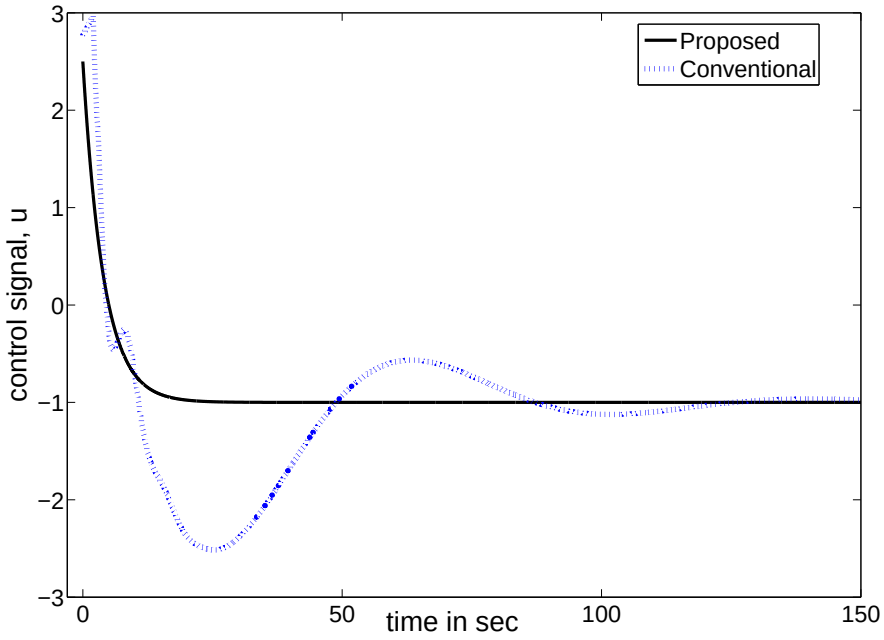

Figure 5.11: Nominal process inputs for example 5.2

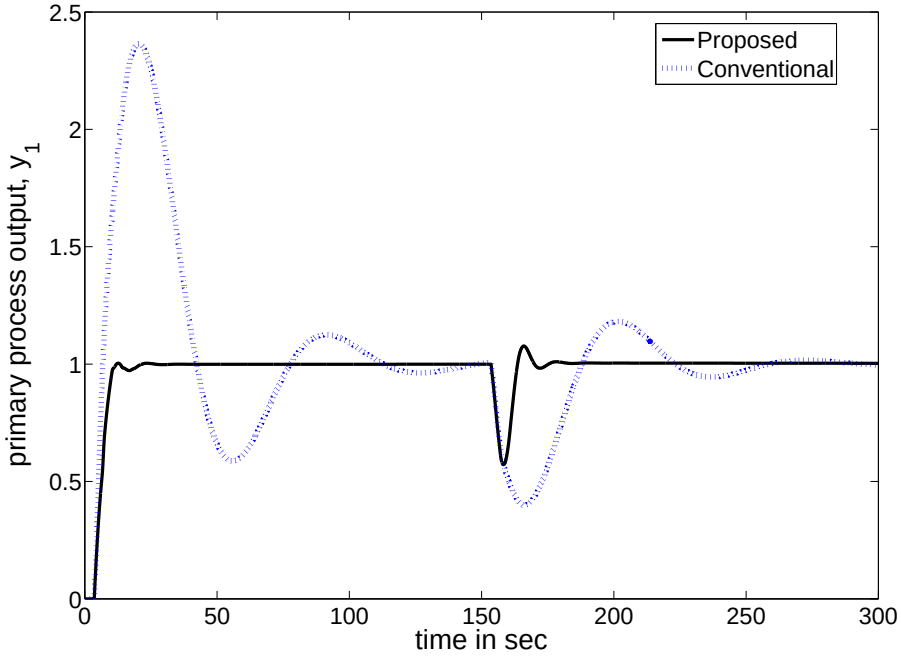

Figure 5.12: Perturbed process outputs for example 5.2

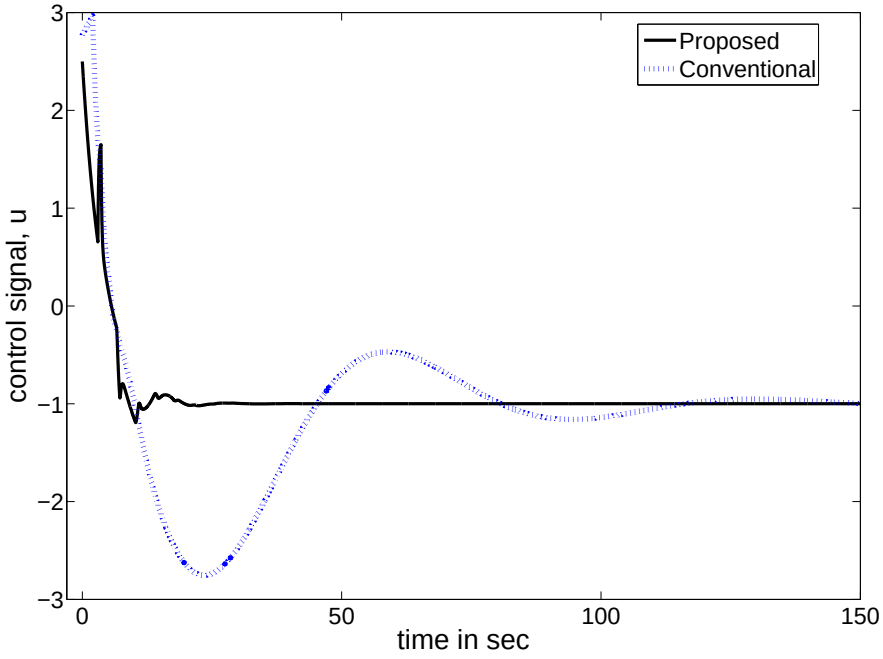

Figure 5.13: Perturbed process inputs for example 5.2

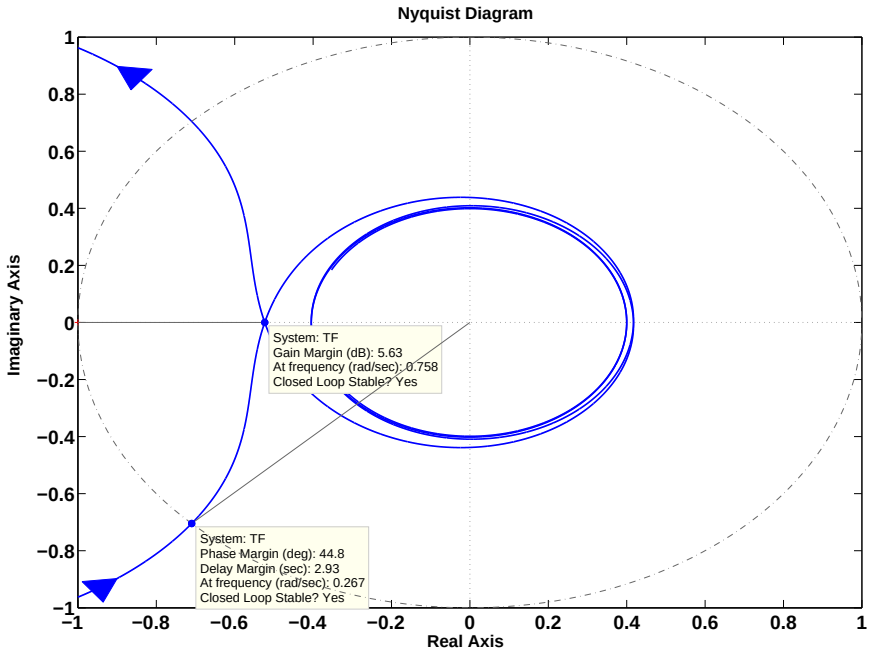

(a) Nyquist plot for $k_1 = 1$, $\tau_1 = 10$, $\theta_1 = 3$

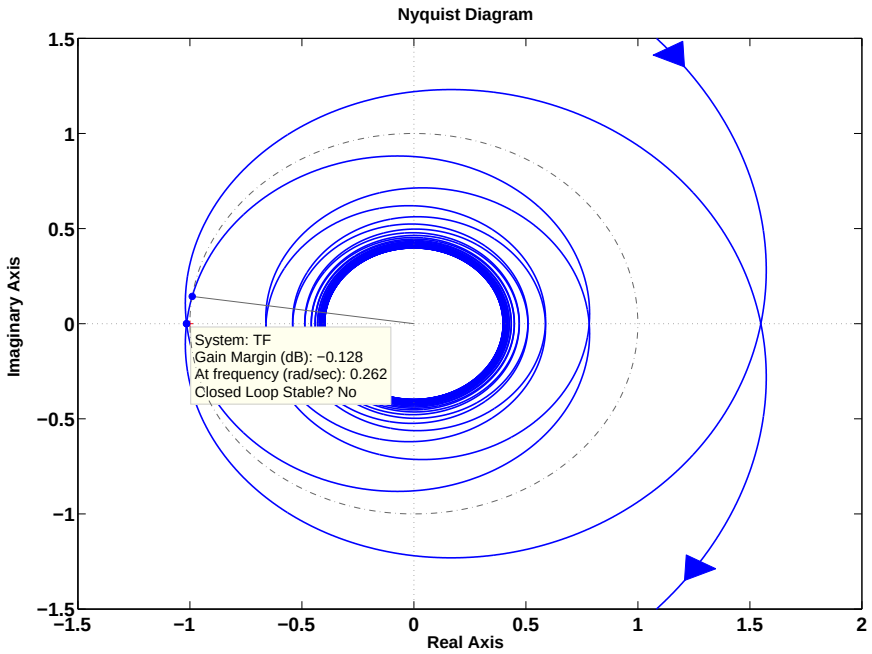

(b) Nyquist plot for $k_1 = 1$, $\tau_1 = 10$, $\theta_1 = 30$

Figure 5.14: Stabilization of G_{p1} for example 5.2

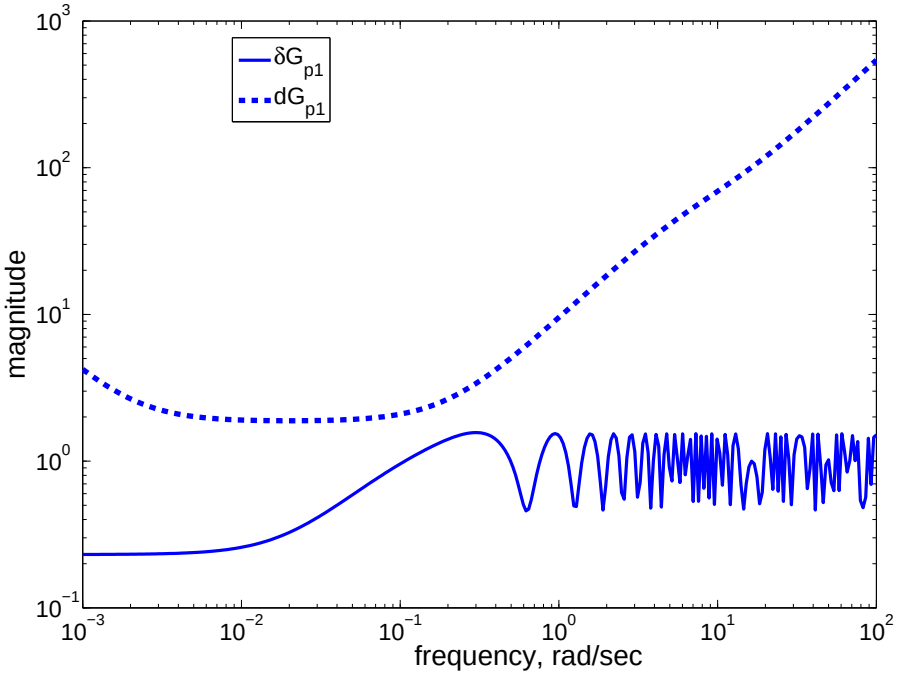

Figure 5.15: Magnitude plots for modeling error (dashed line) and uncertainty norm bound (solid line) under perturbation of +30% in k_1, θ_1 and −30% in τ_1 for example 5.2

It can be observed from Figure 5.15, that the proposed structure and design method give robust control performances.

Example-5.3: Let the primary and secondary process (load disturbance) transfer functions be $G_{p1}(= G_{d1}) = \frac{2e^{-2s}}{s}$ and $G_{p2}(= G_{d2}) = \frac{4e^{-s}}{s+1}$, respectively [81]. For the proposed method, the parameters of disturbance rejection controllers are $K_{c2} = 0.2677$, $T_{i2} = 3.1796$, $T_{d2} = 0.1317$, $K_{c1} = 0.195$, $T_{i1} = 9.9246$ and $T_{d1} = 0.6486$. The setpoint filter ($G_{cs} = (s+2)/(4s+2)$) is obtained after choosing $\lambda_{cs} = \theta_m = 2$. For conventional cascade scheme, the controllers parameters $K_{c2} = 0.2827$, $K_{c1} = 0.5556$ and $T_{i1} = 6.4$ are obtained using ZN tuning method. A unit step setpoint and a load disturbance $d = -0.1$ are introduced at $t = 0$ and 60 sec, respectively. The responses of the closed-loop system for these controller settings are given in Figure. 5.16 for the process with time delay equal to the nominal value ($\theta_m = \theta_1$) and for changes of +20% (i.e.$\theta_m = 2$ and $\theta_1 = 2.4$).

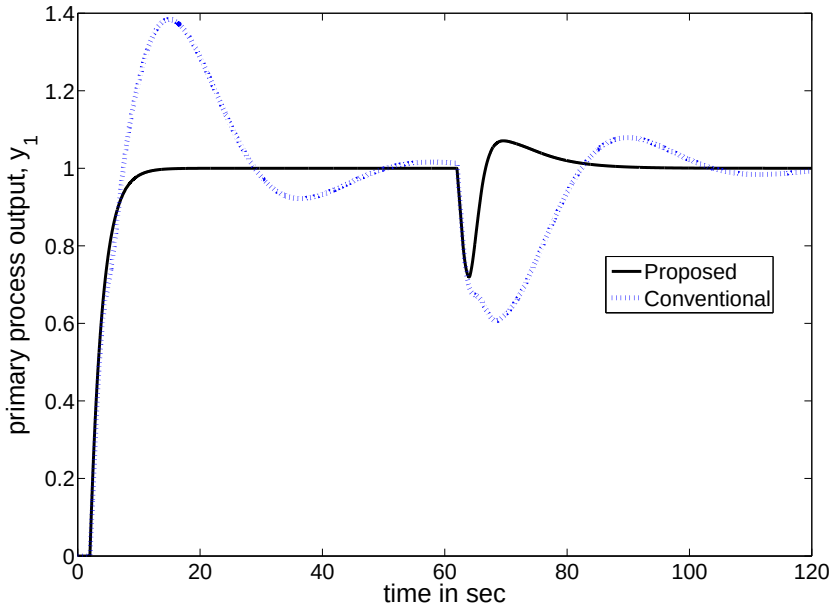

(a) Nominal responses

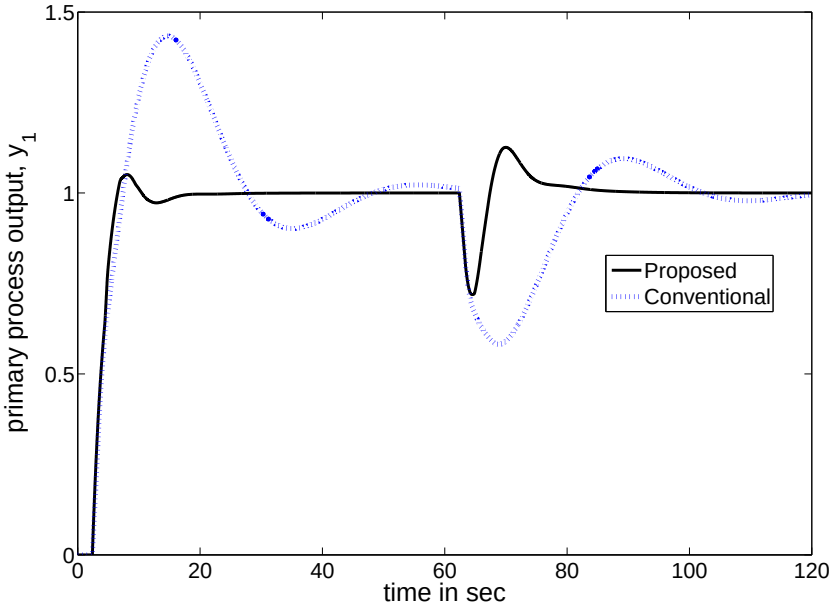

(b) Perturbed responses

Figure 5.16: Responses for example 5.3

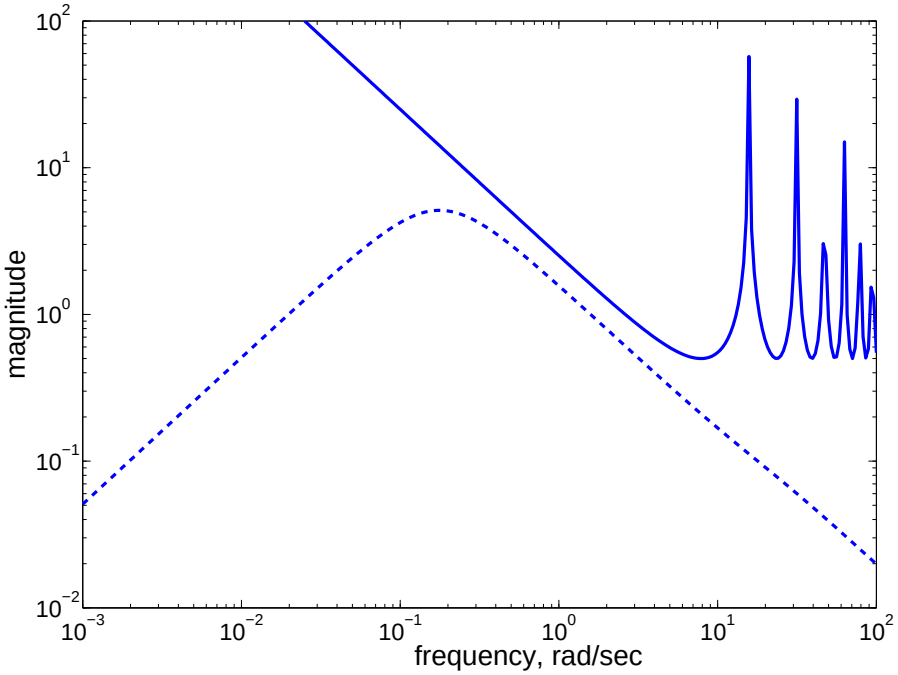

(a) Magnitude plots for complimentary sensitivity function (dashed line) and uncertainty norm bound (solid line) under perturbations of +20% in θ_1

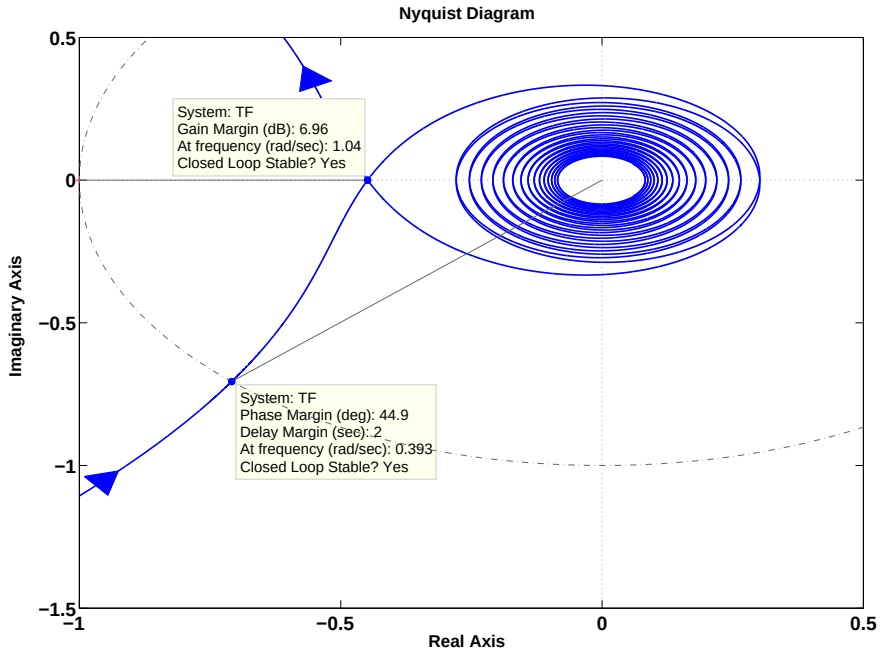

(b) Stabilization of G_{p1}

Figure 5.17: Magnitude plot and Nyquist plot for example 5.3

The magnitude plots of the complementary sensitivity function and the uncertainty (uncertainty

of +20% in θ_1) are considered for robustness analysis and are shown in Figure. 5.17(a). From Figure. 5.17(a), it is clear that the proposed PID settings give robust performance. Also, the primary and secondary processes are stabilizable by the proposed PID controllers as $\theta_{n1} = 2 > 0$ and $\theta_{n2} = 1 > 0$. The Nyquist plot shown in Figure.5.17(b) indicates a stable closed-loop.

Example-5.4: Consider the transfer functions $G_{p1} = G_{d1} = \frac{e^{-0.7s}}{s^2}$ and $G_{p2} = G_{d2} = \frac{e^{-0.3s}}{s+1}$. For the proposed method, the disturbance rejection controller settings are $K_{c2} = 3.565$, $T_{i2} = 0.8559$, $T_{d2} = 0.07943$, $K_{c1} = 0.3769$, $T_{i1} = 8.859$ and $T_{d1} = 2.132$. Taking $\lambda_{cs} = 2.85\theta_m$ results in $G_{cs} = \left(s^2+1\right)\Big/(2s+1)^2$. For the conventional cascade structure, the secondary loop controller is $K_{c2} = 2.9443$ which is obtained by ZN tuning method and the PID parameters of primary controller obtained by SIMC [94] are $K_{c1} = 0.04332$, $T_{i1} = 5.6$ and $T_{d1} = 5.6$.

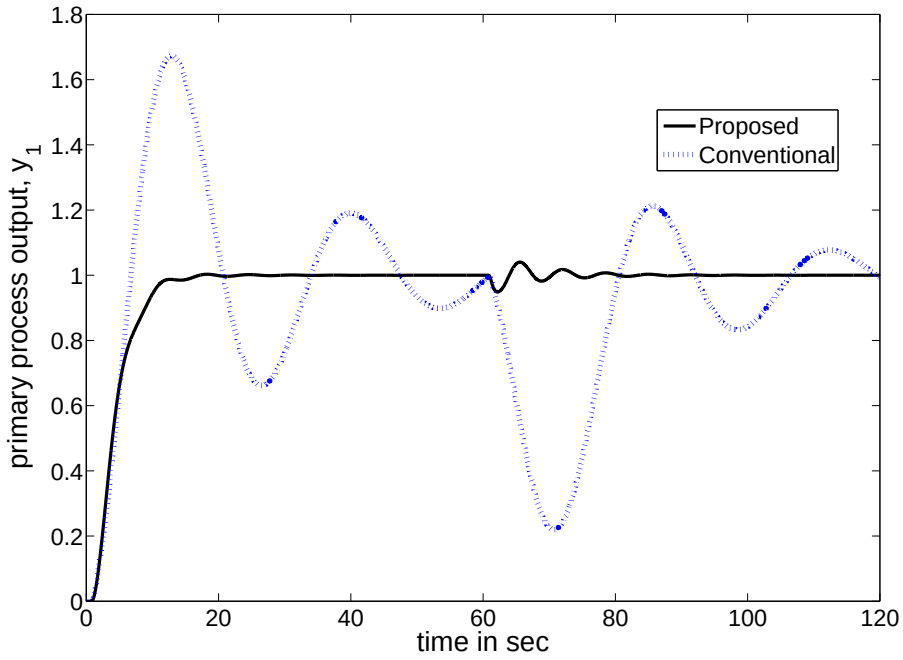

Figure 5.18: Nominal process outputs for example 5.4

A unit step setpoint input at $t = 0$ and a load disturbance $d = -0.2$ at $t = 60$ sec are introduced. The closed-loop responses for nominal system is shown in the Figure.5.18. Now, suppose that there exists a +15% perturbation in the primary process and load disturbance time delays, the perturbed system responses are shown in Figure. 5.19.

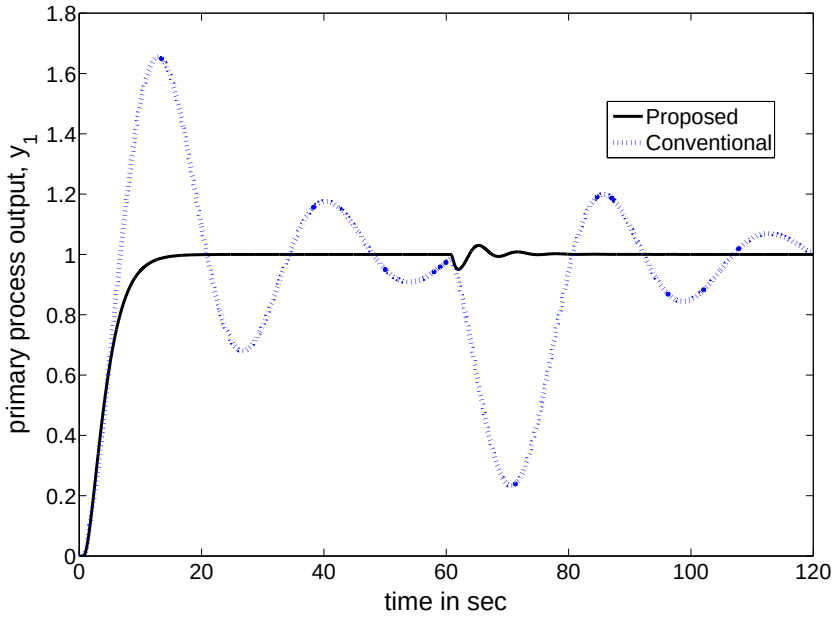

Figure 5.19: Perturbed process outputs for example 5.4

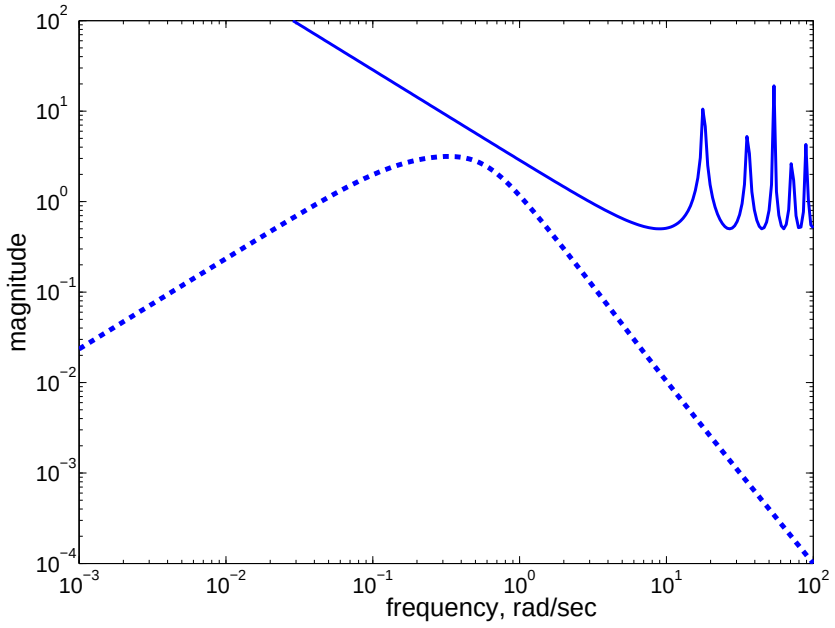

Figure 5.20: Magnitude plots for complimentary sensitivity function (dashed line) and uncertainty norm bound (solid line)under perturbations of +50% in θ_1 for example 5.4

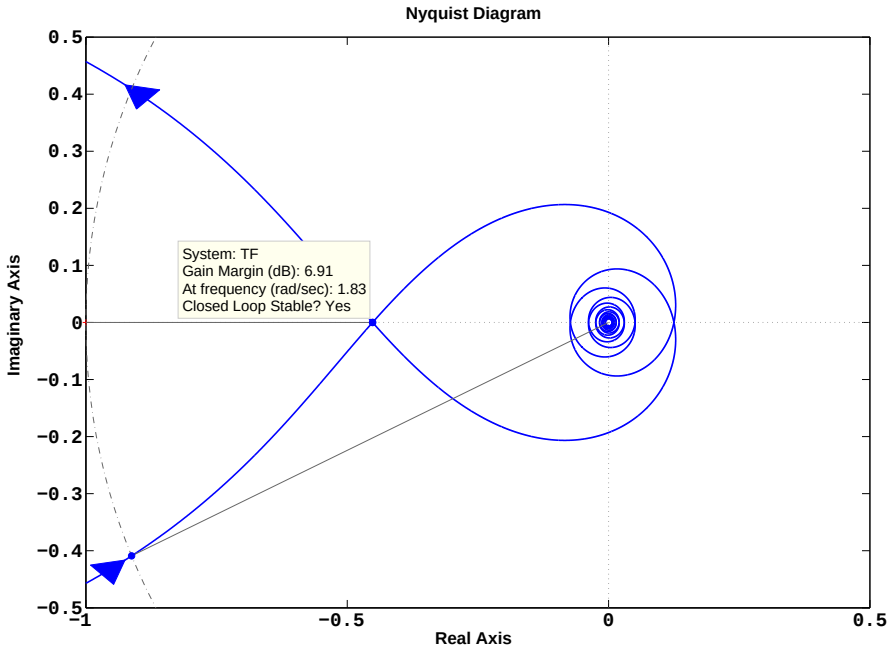

Figure 5.21: Nyquist plot for example 5.4

The performance indices (Table 5.6 and 5.7) of proposed method are smaller than those of conventional scheme. For analyzing the robustness conditions, an uncertainty of +50% in primary process and load disturbance time delays is considered. The magnitude plots of the complementary sensitivity function and the uncertainty bound are shown in Figure. 5.20. The normalized time delay, θ_{n1} is 0.7 which is greater than 0. From the stabilizability condition in Table 5.4, it confirms that the primary process is stabilizable by the proposed PID controller. The Nyquist plot shown in Figure. 5.21 indicates a stable closed-loop.

Example-5.5: This example has the process and load disturbance transfer functions $G_{p1} = G_{d1} = \frac{4e^{-14.69s}}{(21.62s+1)(11.34s+1)}$, $G_{p2} = G_{d2} = \frac{0.57e^{-8s}}{20s+1}$. Choice of $\lambda_{cs} = 0.136\theta_m$ gives $G_{cs} = \frac{245.17s^2+32.96s+5}{4(2s+1)^2}$. The disturbance rejection controller settings are $K_{c2} = 4.6916$, $T_{i2} = 23.4233$, $T_{d2} = 1.7926$, $K_{c1} = 0.2911$, $T_{i1} = 56.9154$ and $T_{d1} = 6.9099$ using (5.31) and Table 5.2. For the conventional cascade structure, the controllers settings obtained using ZN tuning method are $K_{c2} = 4.0235$, $K_{c1} = 0.1392$, $T_{i1} = 7.0133$ and $T_{d1} = 1.6832$. A unit step setpoint and a load disturbance $d = -0.1$ are introduced at $t = 0$ and 80 sec, respectively. The response of the nominal closed-loop system for these controller settings is given in Figure. 5.22(a).

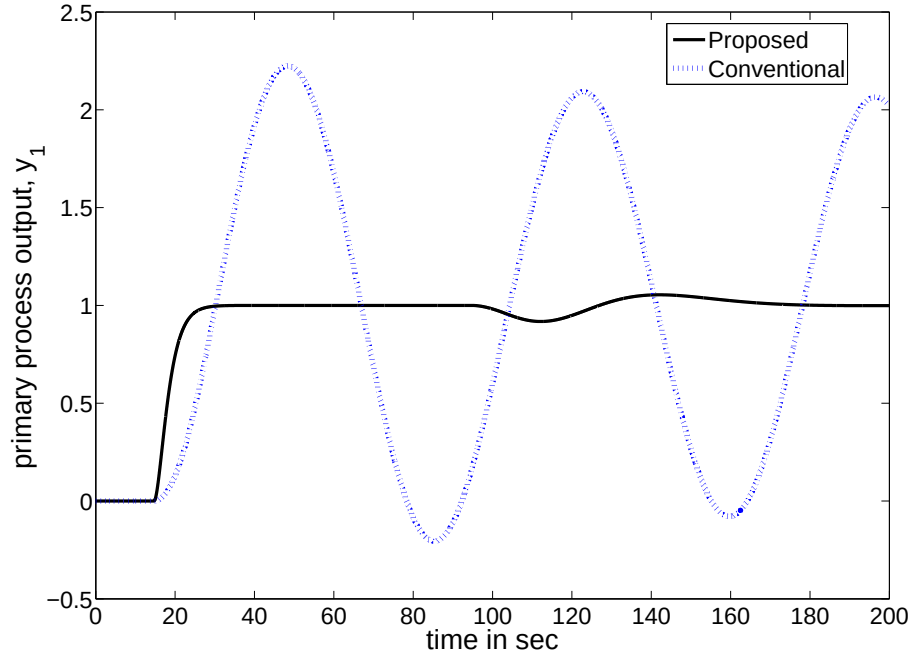

(a) Nominal responses

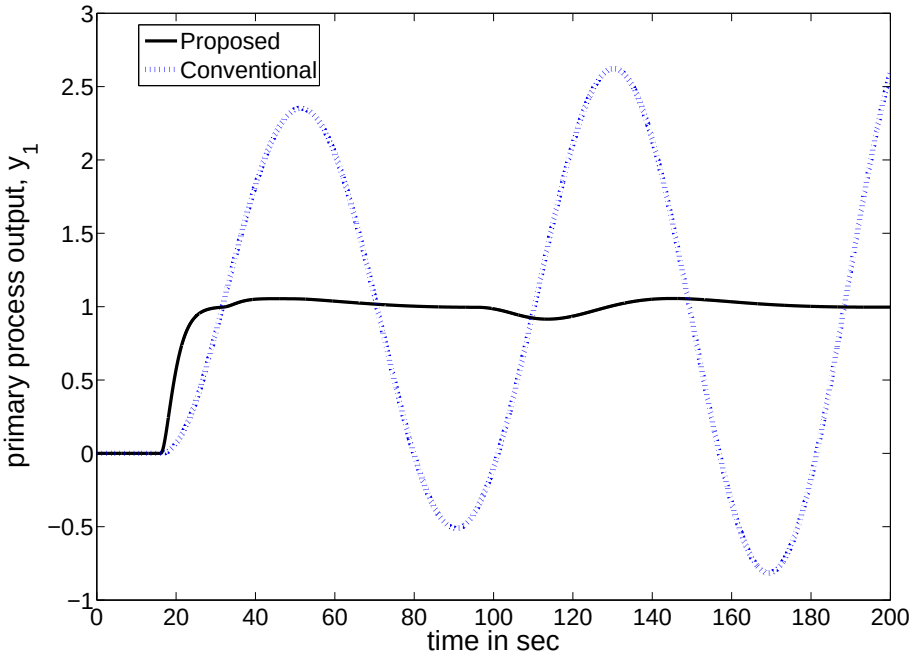

(b) Perturbed responses

Figure 5.22: Responses for example 5.5

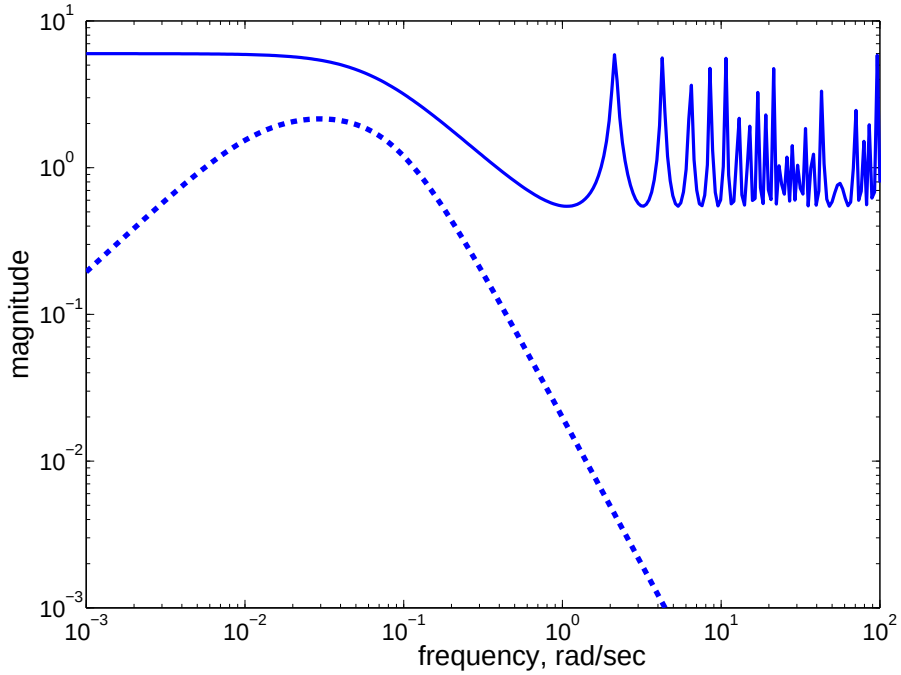

(a) Magnitude plots for complimentary sensitivity function (dotted line) and uncertainty norm bound (solid line)under perturbations of +20% in k_1 and θ_1

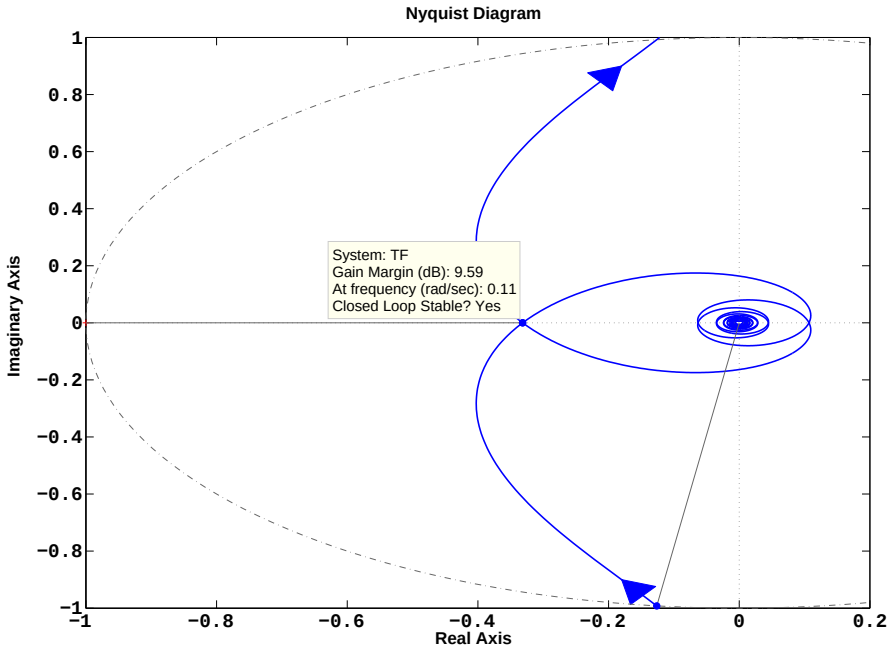

(b) Stabilization of G_{p1}

Figure 5.23: Magnitude plot and Nyquist plot for example 5.5

The robust closed-loop response for +10% change in θ_1 is shown in Figure. 5.22(b). Magnitude

plots of the complementary sensitivity function and an uncertainty of +20% in k_1 and θ_1 are considered for further analysis of robust stability conditions. The corresponding responses are plotted and are shown in Figure. 5.23(a). Since $\theta_{n1} = 0.6795 > \sqrt{1 + (11.34/21.62)^2} - (11.34/21.62) - 1$, it confirms from Table 5.4 that the primary process is stabilizable by the proposed PID controller. The Nyquist plot shown in Figure. 5.23(b) indicates a stable closed-loop.

Table 5.8: Maximum of sensitivity function

	Scheme	M_{s2}	M_{s1}
Example-5.1	Proposed	2.34	1.09
	Rao et al.	3.28	2.28
	Lee et al.	2.85	1
Example-5.2	Proposed	1.53	1.89
	Conventional	1.99	4.09
Example-5.3	Proposed	1.86	1.89
	Conventional	2.04	2.56
Example-5.4	Proposed	2.09	3.22
	Conventional	2.12	4.98
Example-5.5	Proposed	2.02	1.61
	Conventional	2.10	9.26

Remark 3. *The maximum sensitivity values for all the examples are given in the Table 5.8. For the proposed design method, the M_s values for the inner and the outer loops are either close to or within 1 and 2. Thus, using the proposed method better performance and robustness can be achieved.*

5.7 Conclusions

An improved parallel cascade control scheme for controlling stable, unstable and integrating processes with time delay has been introduced. The proposed scheme, which has only two controllers and a setpoint filter, is simple to use as the parameters of disturbance rejection controllers are expressed in terms of the process model parameters. The proposed structure combines the merits of the parallel cascade structure and the modified Smith predictor. Also, the setpoint response decouples from the regulatory response in the nominal case. The simulation results indicate that the designs are relatively robust to parameter variations. A significant improvement in the closed-loop performance is obtained when compared to some existing parallel cascade control methods.

6

A New Parallel Cascade Control Scheme for Unstable Delay Processes

Contents

Resume

In this chapter a new parallel cascade control scheme is proposed for controlling stable and unstable processes with delay. The proposed control structure has only two controllers. The inner and outer loop controllers are designed based on IMC approach and desired complementary sensitivity function, respectively. One of the main feature of the proposed structure is that the primary process output completely tracks the primary setpoint in the nominal system. Simulation results are given to show the efficacy of the proposed design method.

The work presented in this chapter is published [133].

6.1 Introduction

Disturbance rejection is the major concern in the design of process control systems. In parallel cascade control, the secondary loop dynamics should be much faster than the primary loop because the disturbances entering in to the secondary loop should be rejected immediately so that it reduces steady state error in the primary loop. The design of parallel cascade control for regulatory response and a method for selection of secondary measurement under different disturbances were addressed by [43] and [44], respectively. [45] used a conventional feedback controller in the secondary loop and an IMC controller in the primary loop. [48] proposed an analytical method of PID controller design for parallel cascade control taking into account the interaction between primary and secondary control loops. The design of parallel cascade control systems has attracted relatively less attention despite the clear benefits of the parallel cascade control and its wide range applications in process industries. If a long time delay exists in the outer loop, the cascade control may not give satisfactory closed-loop responses to setpoint changes. To overcome this problem, many researchers ([41], [96], [42], [100]) use a dead time compensator scheme in the outer loop of the series cascade control system. Recently, [49] proposed a parallel cascade control structure (consists of three controllers and a filter) in which they have used a dead time compensator in the outer loop. The structure proposed by [48] consists of two controllers and two filters. Till date, most of the published works on parallel cascade control strategies are for control of stable processes. In this chapter, further results are presented for a new parallel cascade control structure and controller design for controlling unstable process with time delay. For easy in plant operation, a simple structure with less number of controllers is desirable. This chapter shows how effective control can be achieved for both long time delay and unstable processes with only

two controllers.

For clear interpretation, the proposed cascade control structure has been addressed in Section 6.2. The controller design procedures are explained in Section 6.3. The simulation results are provided in Section 6.4 followed by the conclusions at the end.

6.2 A new parallel cascade control structure

The proposed parallel cascade control structure (shown in Fig. 6.1) has two controllers, namely, G_{c1} and G_{c2}. G_{c2} in the inner loop stabilizes the process by rejecting the disturbances entering the inner loop. Unlike the conventional parallel cascade control structure, the proposed structure uses the outer loop controller G_{c1} in the feedback path. Although, G_{c1} is primarily meant for load disturbance rejection, it also takes part in stabilizing the unstable process in the outer loop. $G_{p1} = \tilde{G}_{p1}e^{-\theta_1 s}$ and $G_{p2} = \tilde{G}_{p2}e^{-\theta_2 s}$ are the transfer functions of the primary and secondary processes respectively. $G_{m1} = \tilde{G}_{m1}e^{-\theta_{m1} s}$ and $G_{m2} = \tilde{G}_{m2}e^{-\theta_{m2} s}$ are the transfer functions of the primary and secondary process models respectively. G_{d1} and G_{d2} are the transfer functions of the disturbances for primary and secondary loops respectively. The overall outer loop process transfer function is

$$G_p = \tilde{G}_p e^{-\theta_p s} = G_{c2}G_{p1} = G_{c2}\tilde{G}_{p1}e^{-\theta_1 s} \tag{6.1}$$

and

$$G_m = \tilde{G}_m e^{-\theta_m s} \tag{6.2}$$

is the transfer function of the overall outer loop process model. The closed-loop transfer function relating the primary process response (y_1) to the reference (r_1) can be written as

$$\frac{y_1}{r_1} = \frac{G_{c2}G_{p1}\left(1 + G_{c1}\tilde{G}_m e^{-\theta_m s}\right)}{\tilde{G}_m\left(1 + G_{c1}G_{c2}G_{p1} + G_{c2}G_{p2} - G_{c2}G_{m2}\right)} \tag{6.3}$$

where $\tilde{G}_m e^{-\theta_m s} = G_m$ is the transfer function model of the overall process dynamics. Similarly, the closed-loop transfer function relating the primary process output (y_1) to the disturbance input d is given by

$$\frac{y_1}{d} = \frac{G_{d1}\left(1 + G_{c2}G_{p2} - G_{c2}G_{m2}\right) - G_{d2}G_{c2}G_{p1}}{1 + G_{c1}G_{c2}G_{p1} + G_{c2}G_{p2} - G_{c2}G_{m2}} \tag{6.4}$$

Based on the assumption that the model used perfectly matches the process dynamics, (6.3) and (6.4) reduce to

$$\frac{y_1}{r_1} = e^{-\theta_m s} \tag{6.5}$$

and

$$\frac{y_1}{d} = \frac{G_{d1} - G_{d2}G_{c2}G_{p1}}{1 + G_{c1}G_{c2}G_{p1}} \tag{6.6}$$

respectively. It concludes from (6.5) that the primary process output follows the setpoint input and

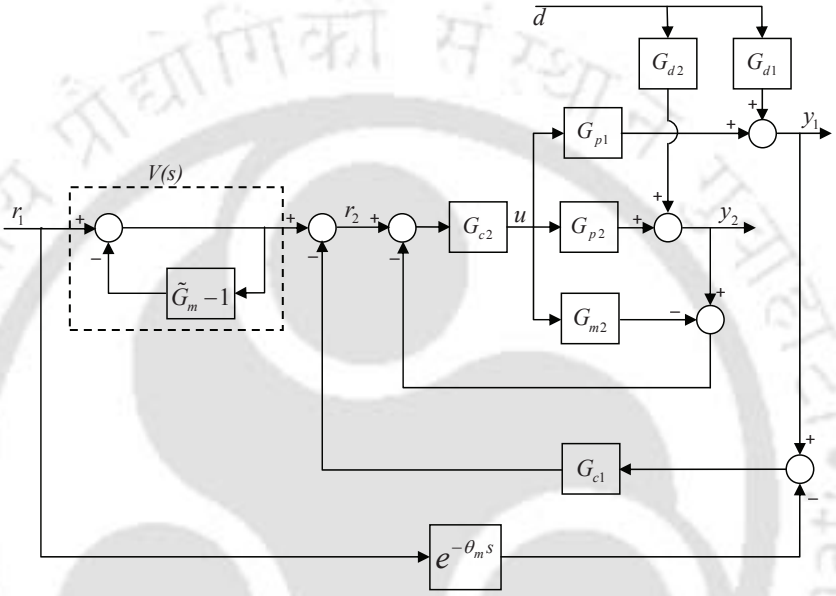

Figure 6.1: Proposed parallel cascade control structure

the closed-loop system is always stable under the nominal condition. Also, from (6.5) and (6.6), it is evident that the new structure decouples the servo response from the regulatory response for the nominal system.

6.2.1 Process models

In practice, in the case of parallel cascade control, the inner loop process has no or a negligible time delay while the outer loop process has a large time delay compared to the inner loop. Generally, in the industrial applications, the dynamics of secondary process is stable and that of the primary process is stable or unstable. Therefore, the inner loop process transfer function is assumed to be a first order plus time delay(FOPTD):

$$G_{p2} = \frac{k_2 e^{-\theta_2 s}}{\tau_2 s + 1} \tag{6.7}$$

The outer loop process transfer functions are assumed in the following form

$$G_{p1} = \frac{k_1 e^{-\theta_1 s}}{\tau_1 s + 1} \tag{6.8}$$

for a FOPTD process and

$$G_{p1} = \frac{k_1 e^{-\theta_1 s}}{\tau_1 s - 1} \tag{6.9}$$

for an unstable first order plus time delay (UFOPTD) process.

6.3 Controller design procedures

The design methods for the controllers (G_{c1} and G_{c2}) are explained in this section in details.

6.3.1 Design of the inner loop controller, G_{c2}

The secondary loop controller is designed based on internal model control (IMC) principles [91]. The inner loop is referred to as IMC since the plant model G_{m2} appears in the control structure. The inner loop process model G_{m2} is given by

$$G_{m2} = \frac{k_{m2} e^{-\theta_{m2} s}}{\tau_{m2} s + 1} \tag{6.10}$$

According to the IMC controller design, decomposing the process model into two parts results in

$$G_{m2}(s) = G_{m2M}(s) G_{m2A}(s) \tag{6.11}$$

where G_{m2M} contains the invertible portion of the model and G_{m2A} contains all the non-invertible portion. The invertible portions are the part of the model with stable poles.

The ideal IMC controller is the inverse of the invertible portion of the process model i.e.

$$G_{c2i} = G_{m2M}^{-1} \tag{6.12}$$

In order to make the IMC controller proper, it is necessary to introduce a low-pass filter ($f_{c2} = \frac{1}{(\lambda_2 s+1)^n}$) with a steady state gain of 1. Where λ_2 is the filter time constant and the index n should be selected to make the IMC controller realizable.

Now, the secondary loop controller G_{c2} is given by

$$G_{c2} = G_{c2i} f_{c2} = \frac{\tau_{m2} s + 1}{k_{m2} (\lambda_2 s + 1)} \tag{6.13}$$

where λ_2 is the adjustable tuning parameter. The response speed is determined by the parameter λ_2.

In order to achieve good control performance, the inner loop should be faster than the outer loop. The smaller the value of λ_2 the better the performance of the parallel cascade control system. The value of λ_2 should be selected such that satisfactory closed-loop responses can be achieved. On the basis of simulation studies based on the MATLAB toolbox, the suggested range for λ_2 are $0.1\theta_m - 0.8\theta_m$ for small time delay processes, $0.001\theta_m - 0.09\theta_m$ for large time delay and unstable processes.

6.3.2 Design of the outer loop controller, G_{c1}

Based on the nature of the primary process and load disturbance transfer functions, the desired closed-loop complementary sensitivity function is chosen and correspondingly the controller is designed. In fact, for all the cases PID controller in series with lead/lag compensator is obtained. The detailed design procedure is explained below.

The loop transfer function for the outer loop is given by

$$L_1(s) = G_{c1}G_{c2}G_{p1} \tag{6.14}$$

The nominal complementary sensitivity function of the outer loop for disturbance rejection is

$$T_{d_1} = \frac{L_1(s)}{1 + L_1(s)} = \frac{G_{c1}G_{c2}G_{p1}}{1 + G_{c1}G_{c2}G_{p1}} \tag{6.15}$$

By following a simple calculation, we get

$$G_{c1} = \frac{T_{d_1}}{1 - T_{d_1}} \times \frac{1}{G_{c2}G_{p1}} \tag{6.16}$$

6.3.2.1 For FOPTD primary process:

If the primary process dynamics is $G_{p1} = k_1 e^{-\theta_1 s}/(\tau_1 s + 1)$, in order to get the desired closed-loop performances, the closed-loop complementary sensitivity function is written as

$$T_{d_1} = \frac{1}{(\lambda_1 s + 1)^2} e^{-\theta_m s} \tag{6.17}$$

From (6.8), (6.13), (6.16) and (6.17), we get

$$G_{c1} = \frac{k_2 (\lambda_2 s + 1)(\tau_1 s + 1)}{k_1 (\tau_2 s + 1)\left[(\lambda_1 s + 1)^2 - e^{-\theta_m s}\right]} \tag{6.18}$$

Using (1, 2) Padé approximation for the time delay (i.e. $e^{-\theta_m s} = (6-2s\theta_m)/(6+4s\theta_m+s^2\theta_m^2)$) reduces (6.18) as

$$G_{c1} = \frac{k_2(\lambda_2 s+1)(\tau_1 s+1)(6+4\theta_m s+s^2\theta_m^2)}{k_1(\tau_2 s+1)\left[(\lambda_1 s+1)^2(6+4\theta_m s+s^2\theta_m^2)-(6-2\theta_m s)\right]} \tag{6.19}$$

After following a simple calculation, we get

$$G_{c1} = \frac{k_2(\lambda_2 s+1)(\tau_1 s+1)(6+4\theta_m s+s^2\theta_m^2)}{k_1 s\left[x_4 s^4+x_3 s^3+x_2 s^2+x_1 s+x_0\right]} \tag{6.20}$$

where $x_4 = \tau_2\lambda_1^2\theta_m^2$, $x_3 = \lambda_1^2\theta_m^2 + 2\tau_2\lambda_1\theta_m^2 + 4\tau_2\lambda_1^2\theta_m$, $x_2 = 4\lambda_1^2\theta_m + 6\tau_2\lambda_1^2 + 2\lambda_1\theta_m^2 + \tau_2\theta_m^2 + 8\tau_2\lambda_1\theta_m$, $x_1 = 6\lambda_1^2 + \theta_m^2 + 8\lambda_1\theta_m + 6\tau_2\theta_m + 12\tau_2\lambda_1$ and $x_0 = 6\theta_m + 12\lambda_1$.

(6.20) can be approximated as a PID controller in series with lead/lag compensator in the form of

$$G_{c1} = K_c\left(1+\frac{1}{T_i s}+T_d s\right)\left(\frac{a_2 s^2+a_1 s+1}{b_4 s^4+b_3 s^3+b_2 s^2+b_1 s+1}\right) \tag{6.21}$$

where

$$\begin{cases} K_c = \frac{6k_2(\tau_1+\lambda_2)}{k_1 x_0},\ T_i = \tau_1+\lambda_2,\ T_d = \frac{\tau_1\lambda_2}{\tau_1+\lambda_2} \\ a_2 = \frac{\theta_m^2}{6},\ a_1 = \frac{2\theta_m}{3} \\ b_4 = \frac{x_4}{x_0},\ b_3 = \frac{x_3}{x_0},\ b_2 = \frac{x_2}{x_0},\ b_1 = \frac{x_1}{x_0} \end{cases} \tag{6.22}$$

6.3.2.2 For UFOPTD primary process:

In order to reject the step load disturbances injected into the primary loop process, an asymptotic constraint

$$\lim_{s\to 1/\tau_1}(1-T_{d_1}) = 0 \tag{6.23}$$

should be satisfied so that the closed-loop internal stability can be achieved. The desired closed-loop complementary sensitivity function is proposed as

$$T_{d_1} = \frac{\beta_1 s+1}{(\lambda_1 s+1)^3}e^{-\theta_m s} \tag{6.24}$$

where β_1 is a positive number and λ_1 is a tuning parameter for obtaining the desirable closed-loop performances of the outer loop. Substitution of (6.24) in (6.23) results in

$$\beta_1 = \tau_1\left[\left(\frac{\lambda_1}{\tau_1}+1\right)^3 e^{\theta_m/\tau_1}-1\right] \tag{6.25}$$

From (6.9), (6.13), (6.16) and (6.24), we get

$$G_{c1} = \frac{k_2 \left(\lambda_2 s + 1\right) \left(\tau_1 s - 1\right) \left(\beta_1 s + 1\right)}{k_1 \left(\tau_2 s + 1\right) \left[\left(\lambda_1 s + 1\right)^3 - \left(\beta_1 s + 1\right) e^{-\theta_m s}\right]} \tag{6.26}$$

Using (1, 2) Padé approximation for the time delay term of (6.26) gives

$$G_{c1} = \frac{k_2 \left(\lambda_2 s + 1\right) \left(\tau_1 s - 1\right) \left(\beta_1 s + 1\right) \left(6 + 4\theta_m s + \theta_m^2 s^2\right)}{k_1 \left(\tau_2 s + 1\right) \left[\begin{array}{l} \left(\lambda_1 s + 1\right)^3 \left(6 + 4\theta_m s + \theta_m^2 s^2\right) - \\ \left(\beta_1 s + 1\right) \left(6 - 2\theta_m s\right) \end{array}\right]} \tag{6.27}$$

After following a simple calculation, we get

$$\begin{aligned} G_{c1} = & -\frac{6k_2(\lambda_2+\beta_1)}{k_1 m_0} \left(1 + \frac{1}{(\lambda_2+\beta_1)s} + \frac{\lambda_2\beta_1}{(\lambda_2+\beta_1)} s\right) \\ & \times \frac{1 + 2\theta_m s/3 + \theta_m^2 s^2/6}{\left(1 + x_1 s + x_2 s^2 + x_3 s^3 + x_4 s^4 + x_5 s^5\right)/(-\tau_1 s + 1)} \end{aligned} \tag{6.28}$$

where $x_1 = m_1/m_0$, $x_2 = m_2/m_0$, $x_3 = m_3/m_0$, $x_4 = m_4/m_0$, $x_5 = m_5/m_0$, $m_0 = 18\lambda_1 + 6\theta_m - 6\beta_1$, $m_1 = \theta_m^2 + 12\lambda_1\theta_m + 2\beta_1\theta_m - 6\tau_2\beta_1 + 6\tau_2\theta_m + 18\tau_2\lambda_1 + 18\lambda_1^2$, $m_2 = 3\lambda_1\theta_m^2 + 6\lambda_1^3 + 12\tau_2\lambda_1\theta_m + 12\lambda_1^2\theta_m + 2\tau_2\beta_1\theta_m + \tau_2\theta_m^2 + 18\tau_2\lambda_1^2$, $m_3 = 4\lambda_1^3\theta_m + 3\tau_2\lambda_1\theta_m^2 + 3\lambda_1^2\theta_m^2 + 6\tau_2\lambda_1^3 + 12\tau_2\lambda_1^2\theta_m$, $m_4 = 4\tau_2\lambda_1^3\theta_m + \lambda_1^3\theta_m^2 + 3\tau_2\lambda_1^2\theta_m^2$ and $m_5 = \tau_2\lambda_1^3\theta_m^2$.

(6.28) can be expressed in the form of a PID controller in series with lead/lag compensator as

$$G_{c1} = K_c \left(1 + \frac{1}{T_i s} + T_d s\right) \left(\frac{a_2 s^2 + a_1 s + 1}{b_3 s^3 + b_2 s^2 + b_1 s + 1}\right) \tag{6.29}$$

where

$$\begin{cases} K_c = -\frac{6k_2(\beta_1+\lambda_2)}{k_1 m_0},\ T_i = \beta_1 + \lambda_2,\ T_d = \frac{\beta_1\lambda_2}{\beta_1+\lambda_2} \\ a_1 = \frac{2\theta_m}{3},\ a_2 = \frac{\theta_m^2}{6} \\ b_1 = x_1 + \tau_1,\ b_2 = x_2 + b_1\tau_1,\ b_3 = x_3 + b_2\tau_1 \end{cases} \tag{6.30}$$

The filter parameters b_1, b_2 and b_3 are obtained by the following method. The parameter b_1 is obtained by taking first derivative of the term $\left(1 + x_1 s + x_2 s^2 + x_3 s^3 + x_4 s^4 + x_5 s^5\right)/(-\tau_1 s + 1)$ and substituting $s = 0$. Similarly, the second derivative of the said term and substition of $s = 0$ gives the expression for b_2 and so on [100].

The tuning of the control parameter λ_1 aims at the trade-off between nominal performance of the closed-loop and its robust stability. That is, decreasing λ_1 improves the disturbance rejection performance of the closed-loop but degrades its robust stability in the presence of process uncertainty. In contrast, increasing λ_1 tends to strengthen the robust stability of the closed-loop but degrades its

disturbance rejection performance. On the basis of simulation studies based on the MATLAB toolbox, it is observed that the initial value of λ_1 is equal to overall process time delay. The suggested range of the tuning parameter is $\lambda_1 = 0.09\theta_m - \theta_m$ for FOPTD process, $\lambda_1 = 0.5\theta_m - 1.2\theta_m$ for the UFOPTD process.

Remark 4. *From the following block diagram, the closed-loop transfer function $V(s)$ can be obtained as*

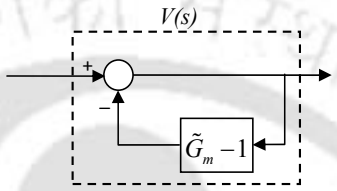

$$V(s) = \frac{1}{\tilde{G}_m} = \frac{1}{G_{c2}\tilde{G}_{p1}} \tag{6.31}$$

G_{c2} is a function of the tuning parameter λ_2 in turn $V(s)$ is also a function of λ_2. It is to be noted that $V(s)$ primarily helps in improving the overall servo tracking performance of the closed-loop system.

6.3.3 Performance

To evaluate the closed-loop performance, we consider two popular performance specifications based on integral error such as IAE and ISE.

To evaluate the manipulated input, we compute the total variation (TV) of the input $u(t)$ which should be as small as possible. The TV is a good measure of smoothness of a signal [94].

6.4 Simulation results

In this section, to illustrate the usefulness of the proposed cascade control structure and design procedure, three typical simulation examples are presented.

Example 6.1: Consider the process and disturbance transfer function models [48] given by $G_{p1} = G_{d1} = e^{-4s}/(20s+1)$ and $G_{p2} = G_{d2} = 1/(10s+1)$. Taking $\lambda_2 = 0.5$, the inner loop controller is obtained as $G_{c2} = (10s+1)/(0.5s+1)$. Choosing the primary controller parameter as $\lambda_1 = 0.5\theta_m$ and using the design formulae (6.22), the parameters of G_{c1} are obtained as $K_c = 2.5625$, $T_i = 20.5$, $T_d = 0.4878$, $a_2 = 2.6667$, $a_1 = 2.6667$, $b_4 = 13.3333$, $b_3 = 28$, $b_2 = 24.3333$ and $b_1 = 12.1667$.

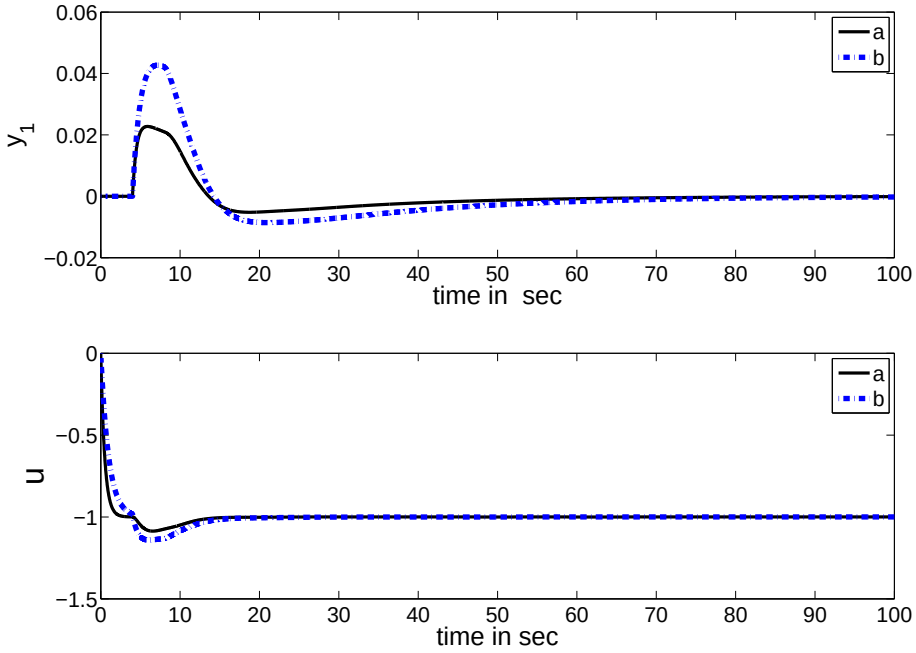

Figure 6.2: Nominal responses for example 6.1: (a) Proposed, (b) Lee et al.

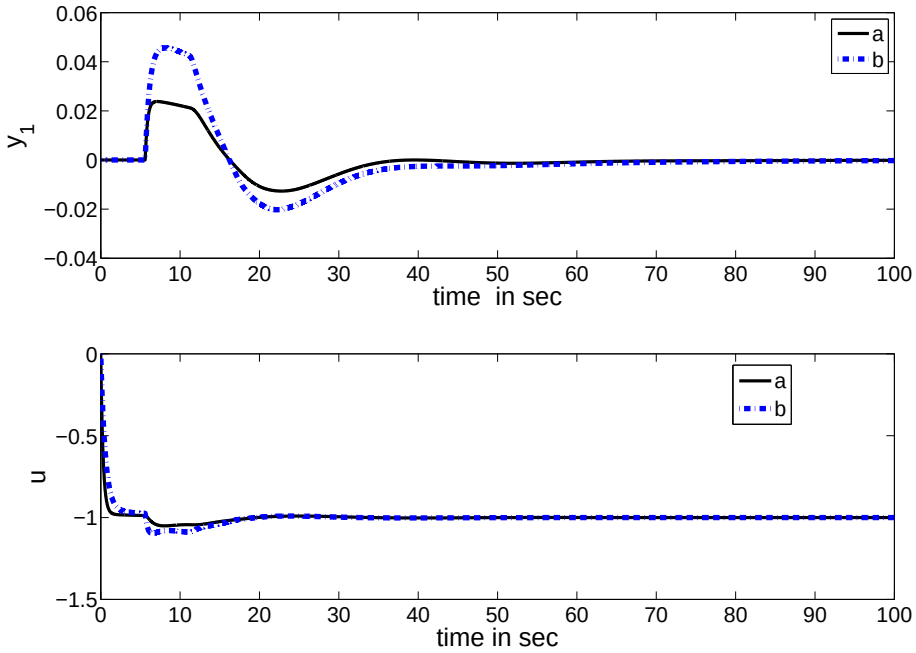

Figure 6.3: Perturbed responses for example 6.1: (a) Proposed, (b) Lee et al.

Table 6.1: Performance specifications for regulatory responses

	Scheme	Nominal System			Perturbed system		
		IAE	ISE	TV	IAE	ISE	TV
Example-6.1	Proposed	0.2799	0.003	1.1732	0.3542	0.0049	1.1276
	Lee et al.	0.5251	0.0104	1.2817	0.6549	0.0164	1.2394
Example-6.2	Proposed	63.86	6.158	894.84	94.47	9.048	911.12
	Lee et al.	70.39	7.073	1.492E4	105.8	10.04	1.085E4
	Rao et al.	108	10.9	1.071E3	116.3	13.12	1.074E3
Example-6.3	Proposed	1.614	0.1118	2.4369	1.615*	0.118*	2.599*
					1.633†	0.107†	2.329†
					2.164‡	0.189‡	3.257‡

(*)-10% change in θ_1 and τ_1, (†)$+10\%$ change in θ_1 and τ_1 and (‡)$+10\%$ change in θ_1 and -10% in τ_1

With these controller settings, the performances of the closed loop system are evaluated by introducing a unit step load disturbance at time $t = 0$. For comparison, the method proposed by [48] is considered. The closed-loop primary responses for these controllers setting are shown in Figure 6.2. In the present work, a $+40\%$ perturbation in the primary process time delay and -40% in the primary and secondary process time constants have been considered and the corresponding responses are shown in Figure 6.3. The control signals (u) are also shown in Figure 6.2 and Figure 6.3. As the proposed method gives low TV (see Table 6.1), the control action variation is comparatively smooth . For quantitative comparison, IAE and ISE (for regulatory responses) performance indices are considered here. It is observed from the Table 6.1 that the proposed method gives low IAE and ISE values. It is evident from the simulation results that the proposed method yields robust and superior control performances.

Example 6.2: Consider the following liquefied petroleum gas (GPL) splitter model studied by [49]

$$G_{p1} = \frac{-0.0067e^{-300s}}{105.8s+1}, \quad G_{d1} = \frac{0.05843e^{-300s}}{115.5s+1}$$

$$G_{p2} = \frac{-5.217}{101.6s+1}, \qquad G_{d2} = \frac{44.15}{109.5s+1}$$

Taking $\lambda_2 = 0.5$ results in $G_{c2} = (101.6s+1)/(-2.608s-5.217)$. By choosing $\lambda_1 = 0.1\theta_m$, the parameters of G_{c1} are obtained as $K_c = 229.92$, $T_i = 106.3$, $T_d = 0.4976$, $a_2 = 15000$, $a_1 = 200$, $b_4 = 3810000$, $b_3 = 342300$, $b_2 = 10874$ and $b_1 = 179.1$.

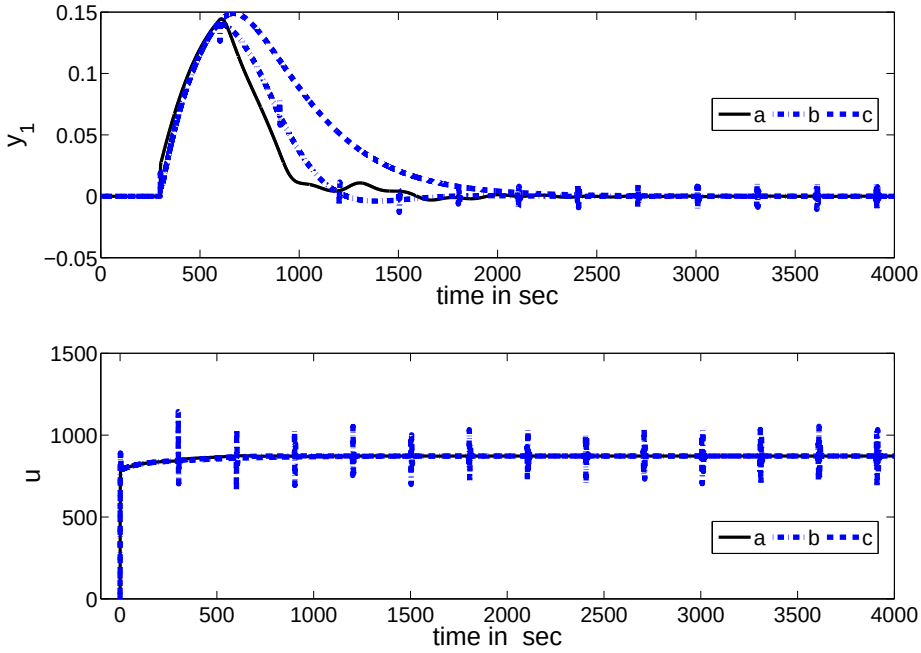

Figure 6.4: Nominal responses for example 6.2: (a) Proposed, (b) Lee et al., (c) Rao et al.

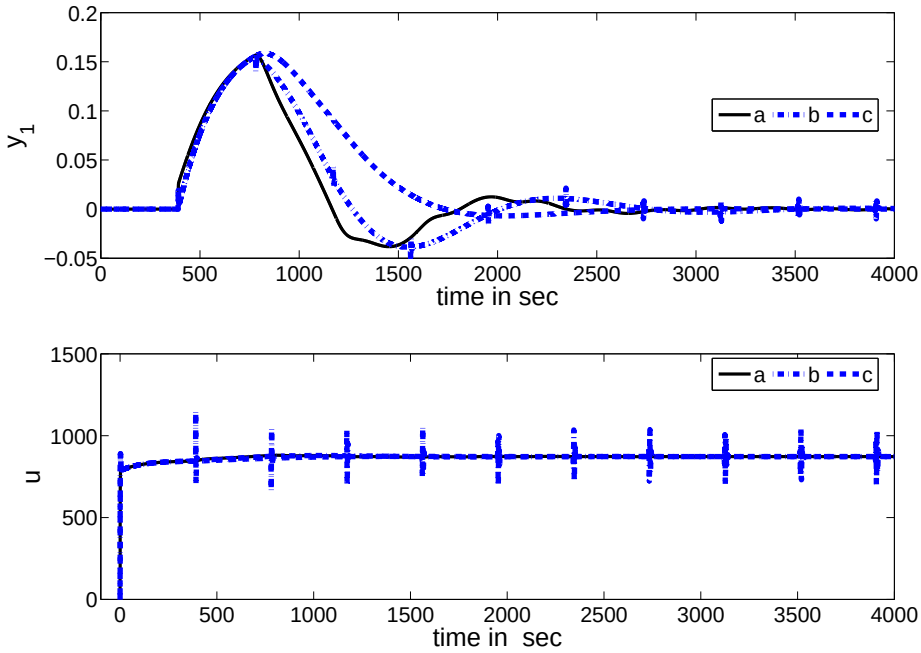

Figure 6.5: Perturbed responses for example 6.2: (a) Proposed, (b)Lee et al., (c)Rao et al.

With these controller settings a step load input of magnitude 100 at $t = 0$ is introduced and the corresponding closed-loop responses are shown in Figure 6.4. To investigate the robustness of the proposed controller, a perturbation of +30% in the primary process and load disturbance time delays is considered and the closed-loop performances are given in Figure 6.5. From the simulation results, it is seen that [48] method produces spikes in a regular interval (see Figure 6.4 and Figure 6.5). It can be observed (see Table 6.1) that the proposed method gives smaller performance indices compared to that of [49] and [48]. Also, it gives better performances for disturbance rejection.

Example 6.3: Consider a cascade control system with the following primary and secondary process and load disturbance transfer functions $G_{p1} = G_{d1} = e^{-4s}/(20s - 1)$ and $G_{p2} = G_{d2} = 2e^{-2s}/(20s + 1)$, respectively. By choosing $\lambda_1 = \theta_m$ and using the design formulae (6.30), the parameters of G_{c1} are obtained as $K_c = 7.1580$, $T_i = 22.2317$, $T_d = 0.02$, $a_2 = 2.6667$, $a_1 = 2.6667$, $b_3 = 48.6843$, $b_2 = 40.8994$ and $b_1 = 21.9240$. The inner loop controller is obtained as $G_{c2} = (20s + 1)/(0.04s + 2)$. With these controller settings a unit step load disturbance is introduced at time $t = 0$.

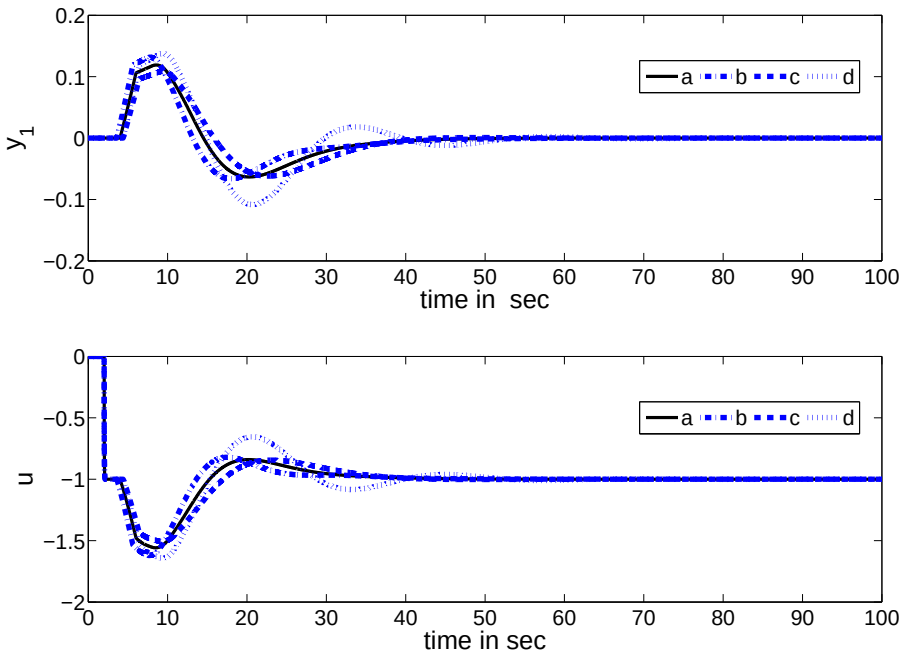

Figure 6.6: Regulatory responses for example 6.3: (a) Nominal, (b) perturbation of -10% in θ_1 and τ_1, (c) perturbation of $+10\%$ in θ_1 and τ_1 and (d)perturbation of $+10\%$ in θ_1 and -10% in τ_1

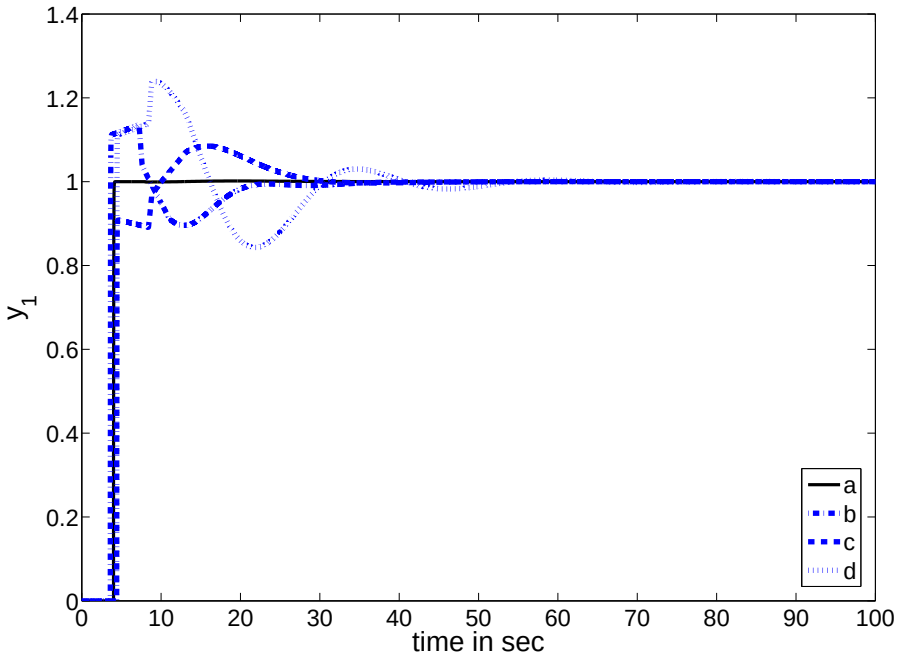

Figure 6.7: Servo responses for example 6.3: (a) Nominal, (b) perturbation of -10% in θ_1 and τ_1, (c) perturbation of $+10\%$ in θ_1 and τ_1 and (d)perturbation of $+10\%$ in θ_1 and -10% in τ_1

The corresponding closed-loop responses are shown in Figure 6.6. To illustrate the robustness to parameter variations, perturbations of $+10\%$ in the primary process time delay and -10% in the primary process time constant and again $\pm 10\%$ in the primary process time delay and in the primary process time constant have been considered and the corresponding closed-loop responses and control signals are shown in Figure 6.6. The servo responses for perfect and perturbed systems are shown in Figure 6.7. It is evident from the simulation results that the proposed cascade scheme gives robust closed-loop performances in terms of the servo tracking and the load disturbance rejection.

6.5 Conclusions

In this chapter, the problem of controlling stable and unstable time delayed processes has been tackled by proposing a new parallel cascade control structure. One of the important features of the proposed structure is that it decouples the servo response from the regulatory response in the nominal case. The comparative analysis shows that with less number of controllers, the proposed scheme gives improved closed-loop performances. It is shown that both nominal and robust control performances are obtained with the designed controllers.

7

A New Control Scheme for PID Load Frequency Controller of Power Systems

Contents

Resume

One of the most important subjects in electric power systems is load frequency control (LFC) problem. In practice LFC systems use simple PI controllers. However, since the PI controllers usually are unable to obtain good dynamic behavior against various load changes and operating conditions, a new control structure with a PID load frequency controller for power systems is presented in this chapter. The control strategy is based on the desired complementary sensitivity function. The PID controller parameters are obtained by expanding the controller transfer function using a Laurent series. Relay based identification technique is adopted to estimate the power system dynamics. Initially, the PID controller is designed for single-area power system, then it is extended to multi-area case. The simulation results indicate that the proposed control scheme works well and it is robust to changes in the parameters of the power systems and to bounded disturbances acting on the systems.

The work presented in this chapter is published in [134].

7.1 Introduction

The active power and frequency control is referred to as load frequency control (LFC) which has been used as an effective ancillary service in power systems for many years [135]. Several papers have been published to address the LFC [50, 51, 136]. For large scale power systems with interconnected areas, LFC is important to keep the system frequency and the inter-area tie-line power as near to the scheduled values as possible. In addition, the LFC has to be robust against unknown external disturbances and system model and parameter uncertainties. Many control strategies for load frequency control in power systems had been proposed by researchers over the past decades [60, 67, 68, 104, 137–148]. This extensive research is due to the fact that LFC constitutes an important function of power system operation where the main objective is to regulate the output power of each generator at prescribed levels while keeping the frequency fluctuations within predetermined limits. Most of the reported works of the LFC problem have been tested for their robustness against large step load change. However, very few of the published researches deal with parameter uncertainties. In this chapter, a design method for the LFC PID is proposed, which is able to consider uncertainties in power systems. Even though many advanced control theories have been established, most industrial controllers still use conventional applications such as PI or PID. PID controllers are preferred due to their simple structures, robustness, applicability over a wide range and easy in implementation on analog or digital platform [149]. We

especially pay attention in modeling of the power system dynamics using relay feedback identification method and PID controller design for the developed model. In the proposed method, a Laurent series has been used in order to derive the expression for the controller's parameters.

For clear interpretation, the proposed control structure is presented in Section 7.2. The modeling of power system dynamics, controller design, simulation results and robustness analysis for single-area power system are given in Section 7.3. Multi-area power system is addressed in Section 7.4 followed by the conclusions in Section 7.5.

7.2 Proposed control structure

The proposed control structure for LFC is shown in Figure 7.1 which has only one controller (G_c). Unlike the conventional LFC control structure, the proposed structure uses the controller G_c in the feedback path. Although, G_c is primarily meant for load disturbance rejection, it also takes part in stabilizing the oscillatory process in the loop. G represents the transfer function of overall plant. θ_m is the time delay part and G_m is the transfer function of the delay free part of the plant model. The

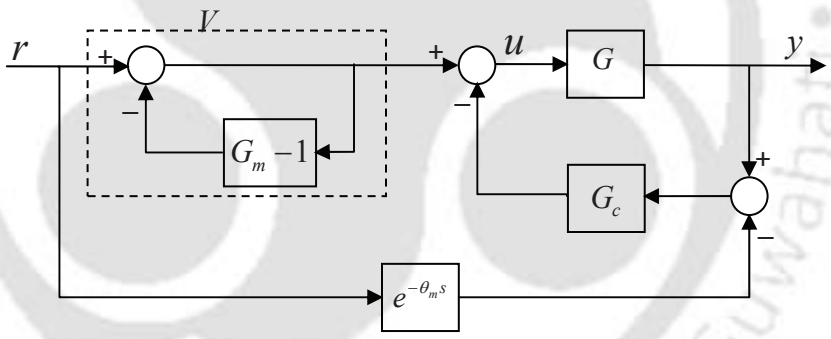

Figure 7.1: Proposed control structure

closed-loop transfer function relating the output (y) to the reference (r) can be written as

$$\frac{y}{r} = \frac{G + GG_cG_me^{-\theta_m s}}{G_m\left(1 + GG_c\right)} \tag{7.1}$$

When the model used exactly matches the plant dynamics, (7.1) reduces to

$$\frac{y}{r} = e^{-\theta_m s} \tag{7.2}$$

(7.2) indicates the system output can reach the setpoint value just after the process time delay. It is to be noted that the block V primarily helps in improving the overall servo performance of the closed-loop system. It is popularly known that for LFC design, the load disturbance rejection is more important than the setpoint response [145]. Therefore, the controller G_c has been designed mainly for power system load disturbances.

7.3 Single-area power system

7.3.1 Modeling of power system dynamics

A linear model of a single-area power system is shown in Figure 7.2, in which a single generator is supplying power to a single-area. In the present work, non-reheat turbine (NRT) and reheat turbine

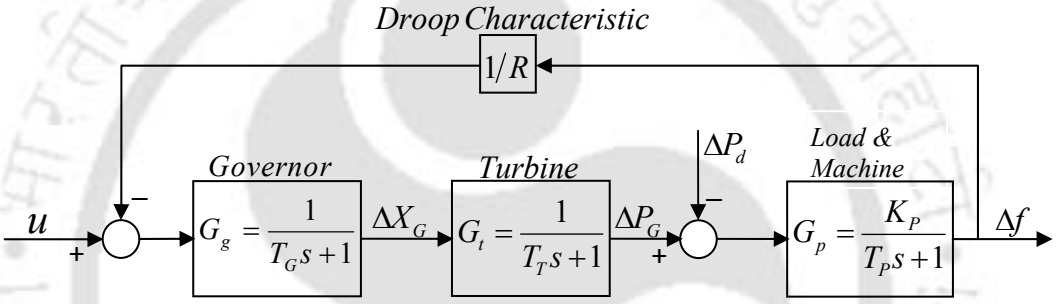

Figure 7.2: Block diagram of a single-area power system

(RT) are considered for LFC modeling. The plant model used for LFC without droop characteristics is

$$G = G_g G_t G_p \tag{7.3}$$

where G_g, G_t and G_p are the dynamics of the governor, turbine and load & machine, respectively. The governor dynamics $G_g = \frac{1}{T_G s+1}$ and the Load and machine dynamics, $G_p = \frac{K_p}{T_p s+1}$. Non-reheat turbines are first-order units. The dynamics of the non-reheat turbine is represented as $G_t = \frac{1}{T_T s+1}$. Reheat turbines are modeled as second-order units, since they have different stages due to high and low steam pressure. The transfer function of the reheat turbine is in the form of $G_t = \frac{cT_r s+1}{(T_r s+1)(T_T s+1)}$ where T_r stands for the low pressure reheat time and c is the portion of the power generated by the reheat turbine in the total generated power.

The plant model used for LFC with droop characteristic is

$$G = \frac{G_g G_t G_p}{1 + G_g G_t G_p / R} \tag{7.4}$$

For LFC, G generally results in higher order plant models which may be inconvenient for controller design. Therefore, these higher order models are approximated by lower order transfer functions with time delay using relay based identification method [99]. (7.3) and (7.4) can be represented by the second order transfer function model

$$G = \frac{k e^{-\theta_m s}}{(T_1 s + 1)(T_2 s + 1)} \tag{7.5}$$

Its state space equations in the Jordan canonical form become

$$\dot{x}(t) = Ax(t) + bu(t - \theta_m) \tag{7.6}$$

$$y(t) = cx(t) \tag{7.7}$$

where

$$A = \begin{bmatrix} \frac{-1}{T_1} & 0 \\ 0 & \frac{-1}{T_2} \end{bmatrix}; b = \begin{bmatrix} 1 \\ 1 \end{bmatrix}; c = \frac{k}{T_1 - T_2} \begin{bmatrix} 1 & -1 \end{bmatrix}.$$

When a relay test is performed with a symmetrical relay of height $\pm h$, then the expression for the limit cycle output for $0 \leq t \leq \theta_m$ is

$$y(t) = ce^{At} x(0) + cA^{-1}\left(e^{At} - I\right) bh \tag{7.8}$$

Let the half period of the limit cycle output be τ. Then the expression for the limit cycle output for $\theta_m \leq t \leq \tau$ is

$$y(t) = ce^{A(t-\theta_m)} x(\theta_m) - cA^{-1}\left(e^{A(t-\theta_m)} - I\right) bh \tag{7.9}$$

The condition for a limit cycle output can be written as

$$y(0) = cx(0) = -y(\tau) = 0 \tag{7.10}$$

Substitution of $t = \tau$ in (7.9) and use of (7.8) gives the initial value of the cycling states

$$x(0) = \left(I + e^{A\tau}\right)^{-1} A^{-1}\left(2e^{A(\tau-\theta_m)} - e^{A\tau} - I\right) bh \tag{7.11}$$

When t_p is the time instant at which the positive peak output occurs and $t_p \geq \theta_m$, then the expression

of the peak output A_p becomes

$$A_p = c\left(e^{A(t_p-\theta_m)}x\left(\theta_m\right) - A^{-1}\left(e^{A(t_p-\theta_m)} - I\right)bh\right) \tag{7.12}$$

and the expression for the peak time becomes

$$t_p = \theta_m + \frac{T_1T_2}{T_1 - T_2}\ln\left(\frac{1+e^{-\tau/T_1}}{1+e^{-\tau/T_2}}\right) \tag{7.13}$$

Substitution of A, b and c in (7.11) and (7.12) give

$$T_1\left(1+e^{-\tau/T_2}\right)\left(2e^{-(\tau-\theta_m)/T_1} - e^{-\tau/T_1} - 1\right) - T_2\left(1+e^{-\tau/T_1}\right)\left(2e^{-(\tau-\theta_m)/T_2} - e^{-\tau/T_2} - 1\right) = 0 \tag{7.14}$$

$$A_p = kh\left(2\left(1+e^{-\tau/T_1}\right)^{\frac{-T_1}{T_1-T_2}}\left(1+e^{-\tau/T_2}\right)^{\frac{T_2}{T_1-T_2}} - 1\right) \tag{7.15}$$

(7.13), (7.14) and (7.15) are solved simultaneously to estimate θ_m, T_1 and T_2 from the measurements of τ, A_p and t_p. The steady state gain k is assumed to be known a priori or can be estimated from a step signal test. Care has been taken to solve the set of non-linear equations so that convergence may not take place to a false solution.

7.3.2 Design of the controller, G_c

For easy implementation of PID controller, G_c is considered in the following form

$$G_c = K_c\left(1 + \frac{1}{T_is} + \frac{T_ds}{\varepsilon T_ds + 1}\right) \tag{7.16}$$

where the derivative filter constant is typically fixed by the manufacture [125] and $\varepsilon = 0.1$ throughout the chapter. In the proposed control structure shown in Figure 7.1, the nominal complementary sensitivity function for load disturbance rejection can be obtained as

$$T = \frac{GG_c}{1+GG_c} \tag{7.17}$$

In order to reject a step change in load of power system, the asymptotic constraint

$$\lim_{s\to-\frac{1}{T_1},-\frac{1}{T_2}}(1-T) = 0 \tag{7.18}$$

should be satisfied so that the closed-loop internal stability can be achieved. The desired closed-

loop complementary sensitivity function is proposed as

$$T = \frac{\left(\alpha_2 s^2 + \alpha_1 s + 1\right)}{(\lambda s + 1)^4} e^{-\theta s} \tag{7.19}$$

where λ is a tuning parameter for obtaining the desirable performance of the power system. α_1 and α_2 can be obtained from (7.18) and (7.19) as $\alpha_1 = \frac{T_1^2\left(\left(1-\frac{\lambda}{T_1}\right)^4 e^{-\theta/T_1}-1\right)-T_2^2\left(\left(1-\frac{\lambda}{T_2}\right)^4 e^{-\theta/T_2}-1\right)}{T_2-T_1}$ and $\alpha_2 = T_2^2\left(\left(1-\frac{\lambda}{T_2}\right)^4 e^{-\theta/T_2}-1\right) + T_2\alpha_1$. Using (7.17) and (7.19) , we get

$$G_c = \frac{(T_1 s + 1)(T_2 s + 1)\left(\alpha_2 s^2 + \alpha_1 s + 1\right)}{k\left[(\lambda s + 1)^4 - e^{-\theta s}\left(\alpha_2 s^2 + \alpha_1 s + 1\right)\right]} \tag{7.20}$$

The resulting controller G_c does not have a standard PID controller form. Therefore, in order to produce the desired disturbance rejection controller, the following procedure is employed. G_c can be approximated by an approximation series in a complex plane, by expanding it near vicinity of zero. Laurent series has been used for approximation instead of Taylor or MacLaurin series (where terms with s^0, s^1, and s^2 appear), Laurent series has been chosen (because the controller is given by (7.16), where terms with s^0, s^{-1}, and s^1 appear, the series no longer belongs to the Taylor or Maclaurin type, but becomes Laurent type, with other coefficients as zeros) because it addresses complex coefficients that are important especially to investigate the behavior of functions near singularity. A practical desired disturbance rejection controller should possess an integral characteristic to eliminate any system output deviation arising from load disturbances. Therefore, let

$$G_c = \frac{f(s)}{s} \tag{7.21}$$

or

$$G_c = \frac{\gamma(s)}{s(1 + \beta s)} \tag{7.22}$$

Now, expanding G_c in the vicinity of zero by Laurent series

$$G_c = \frac{1}{s(\beta s + 1)}\left(\cdots + \gamma(0) + \gamma'(0)s + \frac{\gamma''(0)s^2}{2!} + \cdots\right) \tag{7.23}$$

The parameters of G_c obtained from (7.16) and (7.23)

$$\begin{cases} K_c = \gamma'(0) \\ \frac{K_c}{T_i} = \gamma(0) \\ K_c T_d = \frac{\gamma''(0)}{2!} \end{cases} \tag{7.24}$$

where $\gamma(0) = f(0)$, $\gamma'(0) = \beta f(0) + f'(0)$, $\gamma''(0) = 2\beta f'(0) + f''(0)$,
$f(0) = 1/k\,(4\lambda - \alpha_1 + \theta_m)$, $f'(0) = \frac{T_1\theta_m + T_2\theta_m + \left(\theta_m^2/2\right) - T_2\alpha_1 + 4\alpha_1\lambda - \alpha_1^2 + \alpha_2 + 4T_1\lambda - T_1\alpha_1 - 6\lambda^2 + 4T_2\lambda}{k\left(16\lambda^2 - 8\alpha_1\lambda + 8\theta_m\lambda + \alpha_1^2 - 2\theta_m\alpha_1 + \theta_m^2\right)}$ and

$$f''(0) = \frac{\left(\begin{array}{l} 48\theta_m\alpha_2\lambda + 72\theta_m\alpha_1\lambda^2 - 24\theta_m\alpha_2\alpha_1 + 48\theta_m^2\alpha_1\lambda + 24T_2\lambda\theta_m^2 + 48T_2\lambda\alpha_2 \\ +6T_2\theta_m^3 + 48\alpha_2\lambda^2 + 48T_2\lambda\theta_m\alpha_1 - 12T_2\alpha_2\alpha_1 + 264T_1\lambda^2\alpha_1 \\ -24T_1T_2\alpha_1\theta_m - 96T_1\alpha_1^2\lambda + 24T_1\lambda\theta_m^2 + 48T_1\lambda\alpha_2 + 12T_1T_2\theta_m^2 \\ +48T_1\lambda\theta_m\alpha_1 + 12T_1T_2\alpha_1^2 + 96T_1T_2\theta_m\lambda + 192T_1T_2\lambda^2 - 72T_2\lambda^2\theta_m \\ -96T_2\alpha_1^2\lambda - 96T_1T_2\alpha_1\lambda - 48\theta_m\alpha_1^2\lambda + 6T_1\theta_m^3 - 48\alpha_2\lambda\alpha_1 \\ +264T_2\lambda^2\alpha_1 + 12T_2\alpha_1^3 + 12\theta_m\alpha_1^3 + 12\alpha_2^2 + \theta_m^4 \\ -12T_1\alpha_2\alpha_1 + 12T_2\theta_m\alpha_2 - 288T_2\lambda^3 - 288T_1\lambda^3 - 240\alpha_1\lambda^3 \\ +12T_1\theta_m\alpha_2 + 12T_1\alpha_1^3 - 72\theta_m^2\lambda^2 - 48\theta_m\lambda^3 - 12\theta_m^2\alpha_1^2 \\ +240\lambda^4 - 6T_2\theta_m^2\alpha_1 - 6T_1\theta_m^2\alpha_1 - 12T_1\theta_m\alpha_1^2 + 72\lambda^2\alpha 1^2 \\ -72T_1\lambda^2\theta_m - 8\theta_m^3\lambda + 2\theta_m^3\alpha_1 + 12\theta_m^2\alpha_2 - 12T_2\theta_m\alpha_1^2 \end{array}\right)}{\left(\begin{array}{l} 384k\lambda^3 - 288k\alpha_1\lambda^2 + 288k\theta_m\lambda^2 + 72k\lambda\alpha_1^2 - 144k\lambda\theta_m\alpha_1 \\ +72k\theta_m^2\lambda - 6k\alpha_1^3 + 18k\theta_m\alpha_1^2 - 18k\theta_m^2\alpha_1 + 6k\theta_m^3 \end{array}\right)}$$

Thus, K_c, T_i and T_d can be obtained from (7.24).

7.3.3 Simulation results for single-area power system

Consider a power system with a non-reheated turbine and a reheated turbine studied by Tan [104]. The model parameters are

Non-reheated turbine: $K_P = 120$, $T_P = 20$, $T_T = 0.3$, $T_G = 0.08$, $R = 2.4$

Reheated turbine: $K_P = 120$, $T_P = 20$, $T_T = 0.3$, $T_G = 0.08$, $R = 2.4$, $T_r = 4.2$ and $c = 0.35$

The Nyquist plots of the identified and actual models for the non-reheat turbine without droop (NRTWD) are shown in Figure 7.3 to illustrate the accuracy of the identification method. By

Table 7.1: Identified models and controller settings

	Identified model	Controller parameters
NRTWD	$\frac{120e^{-0.4626s}}{(28.4952s+1)(0.2202s+1)}$	$K_c = 1.0326, T_i = 1.2116, T_d = 0.3420$
NRTD	$\frac{250e^{-0.05s}}{2.028s^2+12.765s+106.2}$	$K_c = 1.4978, T_i = 1.1481, T_d = 0.1574$
RTWD	$\frac{120e^{-0.541s}}{(23.2137s+1)(0.9057s+1)}$	$K_c = 3.6317, T_i = 1.0998, T_d = 0.4828$
RTD	$\frac{235.3e^{-0.035s}}{1.79s^2+16.9s+100}$	$K_c = 6.164, T_i = 3.1934, T_d = 0.1882$

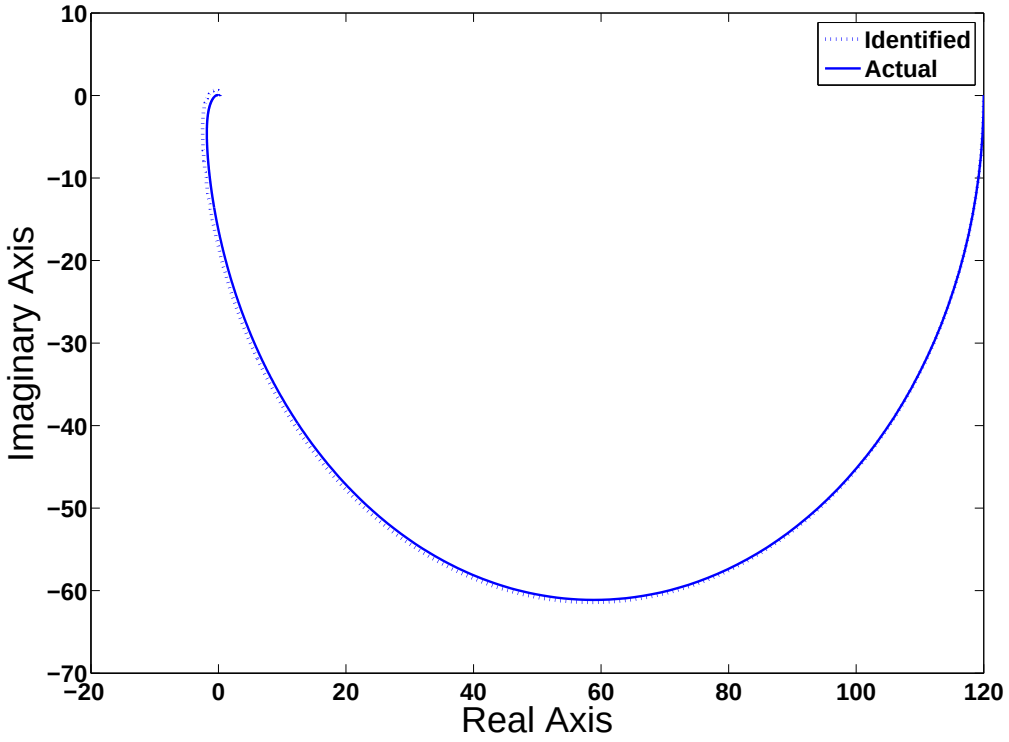

Figure 7.3: Nyquist plots for the power system with NRTWD

selecting suitable value of λ and β, the controller settings (see Table 7.1) for the power system with non-reheated and reheated turbines can be obtained using (7.24).

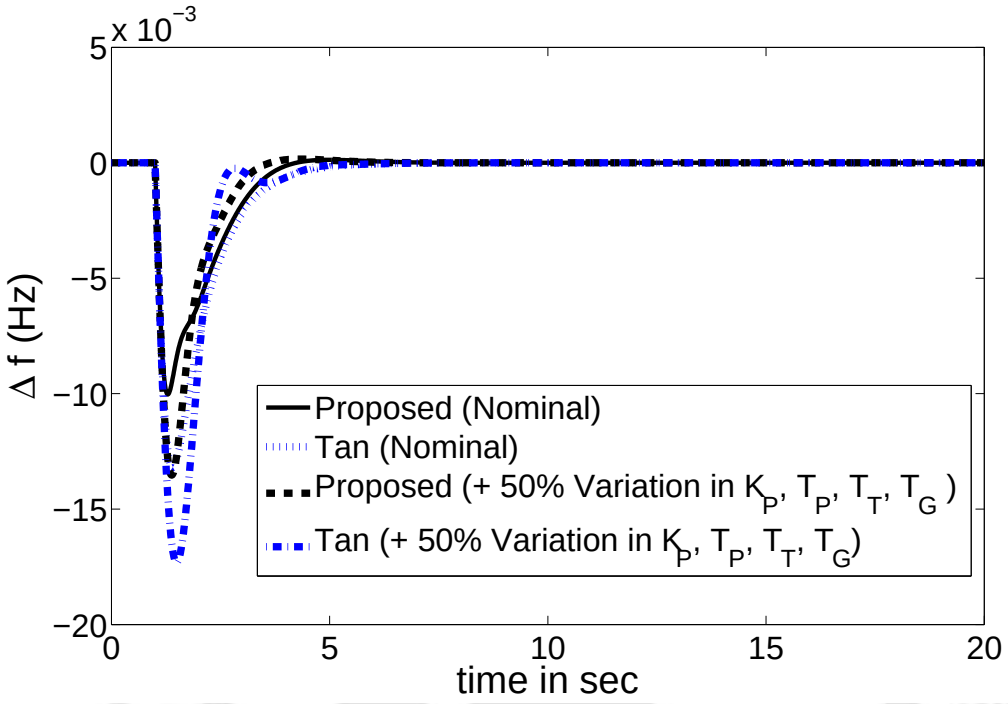

Figure 7.4: Frequency deviation for NRTWD

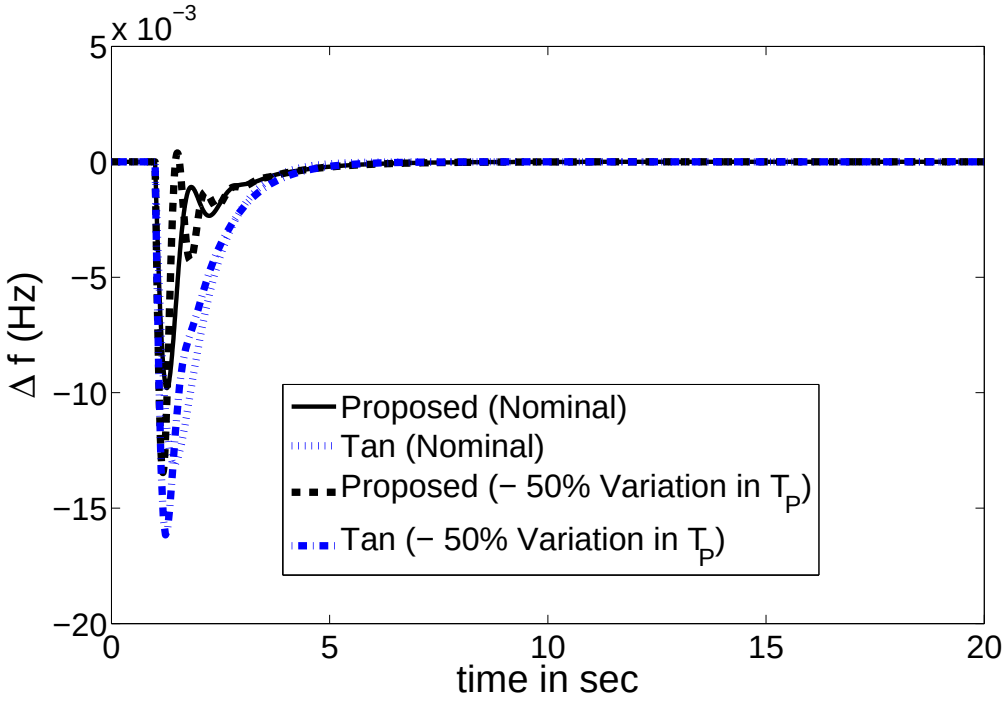

Figure 7.5: Frequency deviation for NRTD

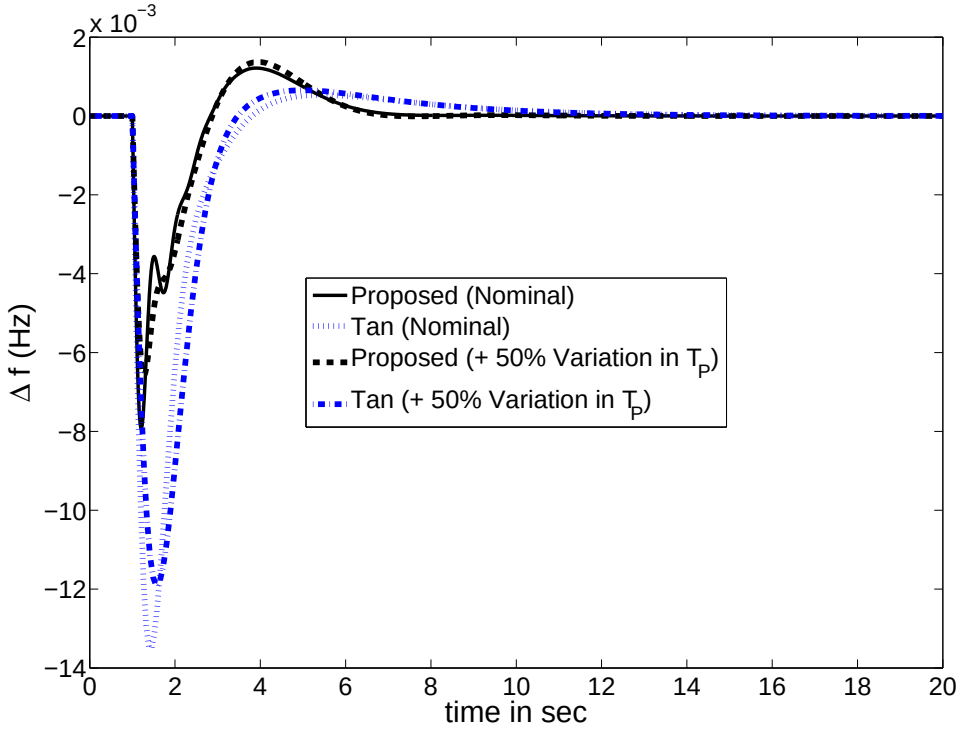

Figure 7.6: Frequency deviation for RTWD

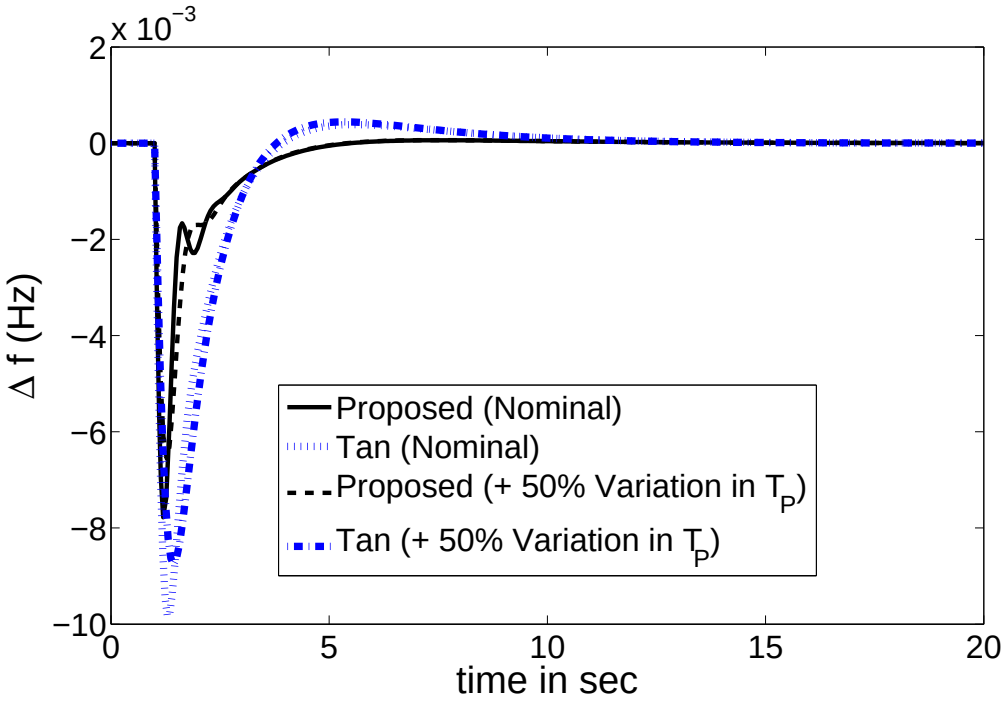

Figure 7.7: Frequency deviation for RTD

By the help of simulation study, $\lambda = 0.13$ and $\beta = 0.012$ for NRTWD, $\lambda = 0.11$ and $\beta = 1$ for NRTD, $\lambda = 0.05$ and $\beta = 0.0035$ for RTWD and $\lambda = 0.1$ and $\beta = 3$ for RTD. Figure (7.4-7.7) show the frequency changes of the power system following a load demand $\Delta P_d = 0.01$. The stability robustness is tested by changing the parameters (K_P, T_P, T_T, T_G) of the system by $\pm 50\%$. From the simulation results, it is evident that the proposed method gives improved performance than Tan's method.

7.3.4 Robustness analysis

When modeling a high-order power systems, the model and parameter approximations can not be avoided. A study of robustness analysis is an important task in LFC design because no mathematical model of a system will be a perfect representation of the actual system. If the controller tuning is too tight, the closed-loop system may become unstable with a small mismatch in the system parameters. Now, we will examine the closed-loop stability property of the proposed controller design with some mismatch in the plant parameters. Kharitonov's theorem is used for the robustness analysis considering parametric uncertainties in the plant parameters. Now, consider the parameters of the non-reheated turbine without or with droop characteristic as discussed in the previous section. The parameters (K_P, T_P, T_T and T_G) variation of 30% and 20% are considered simultaneously for NRTWD and NRTD, respectively. The closed-loop characteristic equation of the system is given by

$$1 + GG_c = 0$$

For NRTWD, the closed-loop polynomial in terms of K_P, T_P, T_T and T_G is given by

$$\begin{aligned}
&K_P K_c + (T_i + K_P K_c T_i + \varepsilon K_P K_c T_d)\, s + (\varepsilon T_i T_d + T_P T_i + T_G T_i + T_T T_i + \varepsilon K_P K_c T_i T_d + K_P K_c T_i T_d)\, s^2 \\
&+ (\varepsilon T_P T_i T_d + T_G T_P T_i + T_T T_P T_i + T_G T_T T_i + \varepsilon T_G T_i T_d + \varepsilon T_T T_i T_d)\, s^3 \\
&+ (\varepsilon T_G T_P T_i T_d + T_G T_T T_P T_i + \varepsilon T_G T_T T_i T_d + \varepsilon T_T T_P T_i T_d)\, s^4 + \varepsilon T_G T_T T_P T_i T_d s^5 = 0
\end{aligned}$$

The four Kharoitonov polynomials

$$K_1(s) = 357.9498 + 449.4338s + 435.6944s^2 + 54.0864s^3 + 2.5926s^4 + 0.0575s^5$$

$$K_2(s) = 664.7639 + 834.6629s + 234.6047s^2 + 29.1234s^3 + 4.8148s^4 + 0.1067s^5$$

$$K_3(s) = 664.7639 + 449.4338s + 234.6047s^2 + 54.0864s^3 + 4.8148s^4 + 0.0575s^5$$

$$K_4(s) = 357.9498 + 834.6629s + 435.6944s^2 + 29.1234s^3 + 2.5926s^4 + 0.1067s^5$$

for NRTWD and

$$K_1(s) = 260.918 + 388.6268s + 130.7567s^2 + 19.8579s^3 + 0.9999s^4 + 0.0126s^5$$

$$K_2(s) = 391.377 + 582.9403s + 87.1711s^2 + 13.2386s^3 + 1.4998s^4 + 0.0188s^5$$

$$K_3(s) = 391.377 + 388.6268s + 87.1711s^2 + 19.8579s^3 + 1.4998s^4 + 0.0126s^5$$

$$K_4(s) = 260.918 + 582.9403s + 130.7567s^2 + 13.2386s^3 + 0.9999s^4 + 0.0188s^5$$

for NRTD.

Table 7.2: The roots of Kharitonov polynomials for NRTWD

$K_1(s)$	$K_2(s)$	$K_3(s)$	$K_4(s)$
$-0.56 + j0.8632$	-0.9119	$-0.1682 + j0.4189$	-1.602
$-0.56 - j0.8632$	-0.292	$-0.1682 + j0.4189$	-0.6671
-0.702	$-0.0131 + j0.1537$	$-0.1628 + j0.0614$	$-0.0063 + j0.0743$
$-0.0318 + j0.0332$	$-0.0131 - j0.1537$	$-0.1628 - j0.0614$	$-0.0063 + j0.0743$
$-0.0318 - j0.0332$	-0.0253	-0.014	-0.0502

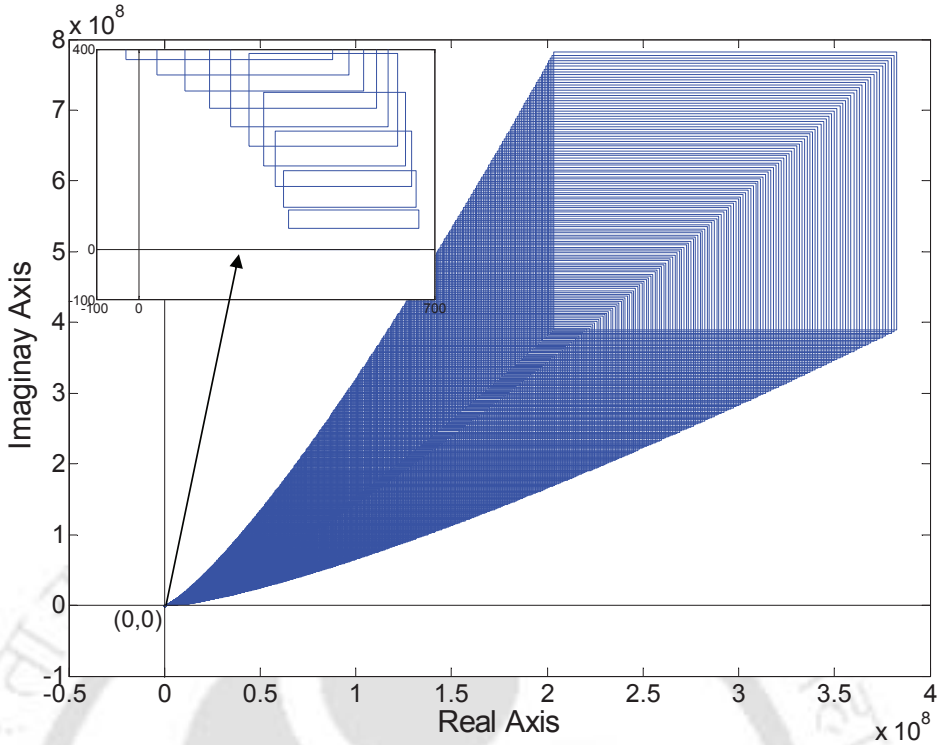

Figure 7.8: Kharitonov's rectangles for the NRTWD

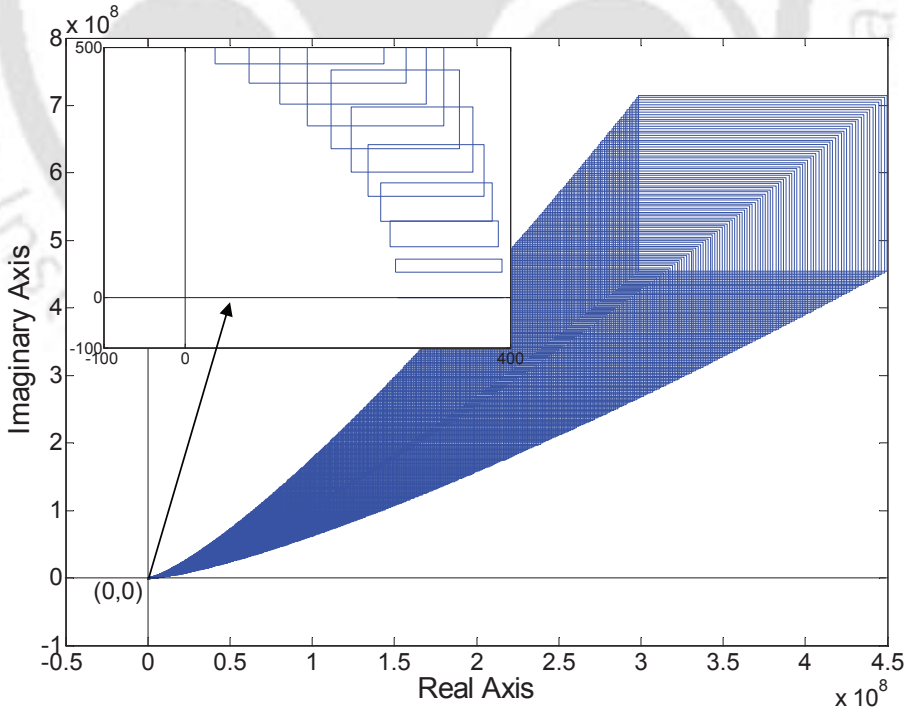

Figure 7.9: Kharitonov's rectangles for the NRTD

Table 7.3: The roots of Kharitonov polynomials for NRTD

$K_1(s)$	$K_2(s)$	$K_3(s)$	$K_4(s)$
-1.0912	-1.3406	-0.7835	-1.9953
$-0.161 + j0.1225$	$-0.0044 + j0.1417$	$-0.054 + j0.2093$	-0.1495
$-0.161 - j0.1225$	$-0.0044 - j0.1417$	$-0.054 + j0.2093$	$-0.032 + j0.092$
-0.0575	-0.1259	-0.0919	$-0.032 - j0.092$
-0.0188	-0.0142	-0.0096	-0.0255

The coefficients of Kharitonov polynomials for NRTWD and NRTD are checked for Hurwitz condition. It is observed that all the roots of the Kharitonov polynomials (see Table 7.2 and 7.3) have negative real part i.e. all roots are in the left half of the complex plane. From the Figure 7.8 and Figure 7.9, it is clear that Kharitonov rectangles move about the origin in counter-clockwise sense in order to have the monotonic phase increase property of Hurwitz polynomials. The graph is zoomed to show what is happening in the neighborhood of the point $(0, 0)$. Since the origin is excluded from the Kharitonov rectangles (Figure 7.8 and Figure 7.9) it is concluded that the closed-loop control system is robustly stable. By following a similar procedure as above the robustness analysis considering parametric uncertainties in the plant parameters for RTWD and RTD can be checked.

7.4 Multi-area power system

A multi-area power system comprises areas that are interconnected by high voltage transmission lines or tie-lines. The trend of frequency measured in each control area is an indicator of the trend of the mismatch power in the interconnection and not in the control area alone [150]. In case of a decentralized power system, area frequency and tie-line power interchange vary as power load demand varies randomly. The objectives of decentralized LFC are to minimize the transient deviations of these variables and to ensure their steady state errors to be zero. When dealing with the LFC problem of power systems, unexpected external disturbances, parameter uncertainties and the model uncertainties pose big challenges for controller design. For N control areas (Figure 7.10), the total tie-line power change between area 1 and other areas is

$$\Delta P_{tiei} = \sum_{\substack{j=1 \\ j \neq i}}^{N} \Delta P_{tieij} = \frac{1}{s} \left[\sum_{\substack{j=1 \\ j \neq i}}^{N} T_{ij} \Delta f_i - \sum_{\substack{j=1 \\ j \neq i}}^{N} T_{ij} \Delta f_j \right]$$

The balance between connected control areas is achieved by detecting the frequency and tie line power deviations to generate the area control error (ACE) signal, which is in turn utilized in the control strategy as shown in Figure 7.10. The ACE for each control area can be expressed as a linear combination of tie-line power change and frequency deviation.

$$ACE_i = B_i \Delta f_i + \Delta P_{tiei} \tag{7.25}$$

where B_i is the frequency bias coefficient. The LFC system in each control area of an interconnected (multi-area) power system should control the interchange power with the other control areas as well as its local frequency. The plant model for multi-area power system is given by

$$G_i = B_i \frac{G_{gi} G_{ti} G_{pi}}{1 + G_{gi} G_{ti} G_{pi} / R_i}$$

For the tuning of multi-area LFC, the same procedure can be followed as in single-area LFC tuning. Therefore, LFC of each area can be tuned independently.

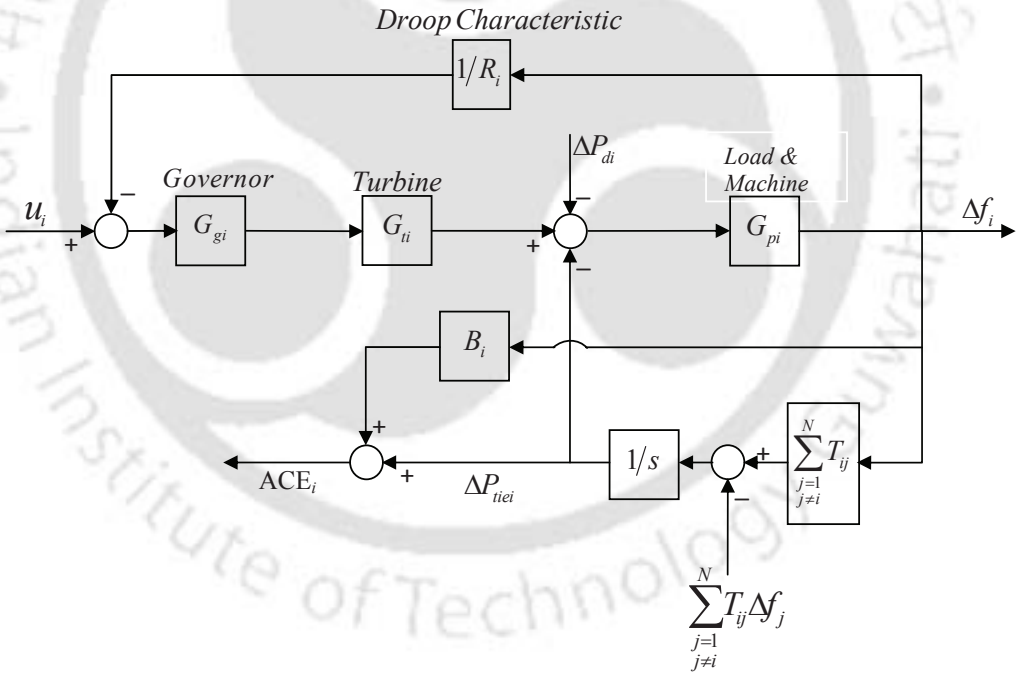

Figure 7.10: Block diagram representation of control area i

7.4.1 Simulation results for four area power systems

The simplified diagram of a four area power systems is shown in Figure 7.11. In the simulation results, area 1, area 2 and area 3 are denoted as the area with reheat unit, and area 4 is denoted as the area with non-reheat unit.

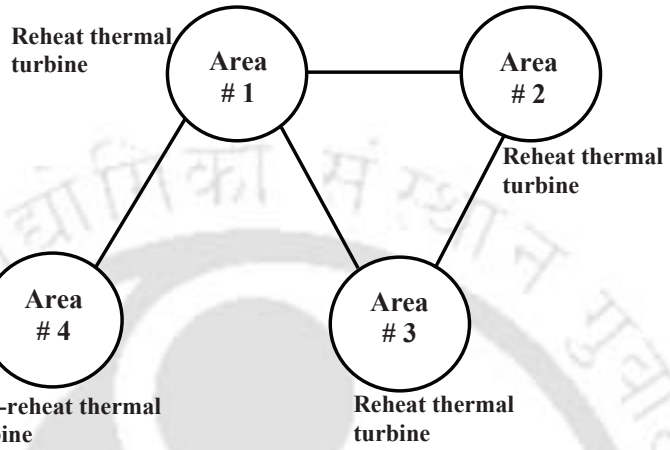

Figure 7.11: Simplified diagram of a four area power systems

The parameters of the non-reheat and reheat units in different areas are chosen as

Nominal parameters for area 1, area 2 and area 3: $T_{P1} = T_{P2} = T_{P3} = 20$, $T_{T1} = T_{T2} = T_{T3} = 0.3$, $T_{G1} = T_{G2} = T_{G3} = 0.2$, $K_{P1} = K_{P2} = K_{P3} = 120$, $R_1 = R_2 = R_3 = 2.4$, $T_{r1} = T_{r2} = T_{r3} = 20$ and $c_1 = c_2 = c_3 = 0.333$

Nominal parameters for area 4: $K_{P4} = 120$, $T_{P4} = 20$, $T_{T4} = 0.3$, $T_{G4} = 0.08$, $R_4 = 2.4$

The synchronizing constants are $T_{12} = T_{23} = T_{31} = T_{41} = 0.0707$ and the frequency bias constants are $B_1 = B_2 = B_3 = B_4 = 0.425$. The identified model for reheat unit with droop characteristic is obtained as $G = \frac{0.9965e^{-0.5s}}{0.72s^2+1.7s+1}$ and that for non-reheat unit with droop is same as that of given in Table 7.1. By choosing $\lambda = 0.7$ and $\beta = 0.35$, the controller settings for area 1, area 2 and area 3 are $K_c = 1.1895$, $T_i = 1.9090$ and $T_d = 0.5454$. Similarly, the controller parameters for area 4 are $K_c = 1.9822$, $T_i = 0.5242$ and $T_d = 0.1756$ by taking $\lambda = 0.1$ and $\beta = 0.35$.

To show the performance of the decentralized PID controller, a step load $\Delta P_{d1} = 0.01$ is applied to Area 1 at $t = 5$ sec, followed by a step load $\Delta P_{d3} = 0.01$ to Area 3 at $t = 100$ sec. Figure 7.12 and Figure 7.13 illustrate the frequency errors of the four different areas. Figure 7.14 and Figure 7.15 show the tie-line power errors of the four areas. From the simulation results, it can be seen that the

frequency errors, and tie-line power deviations have been driven to zero by proposed controller in the presence of power load changes.

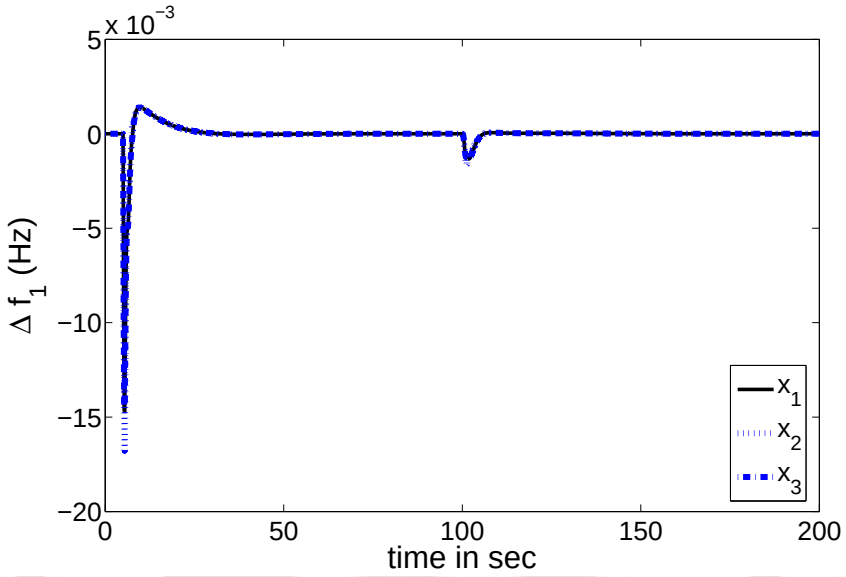

(a)

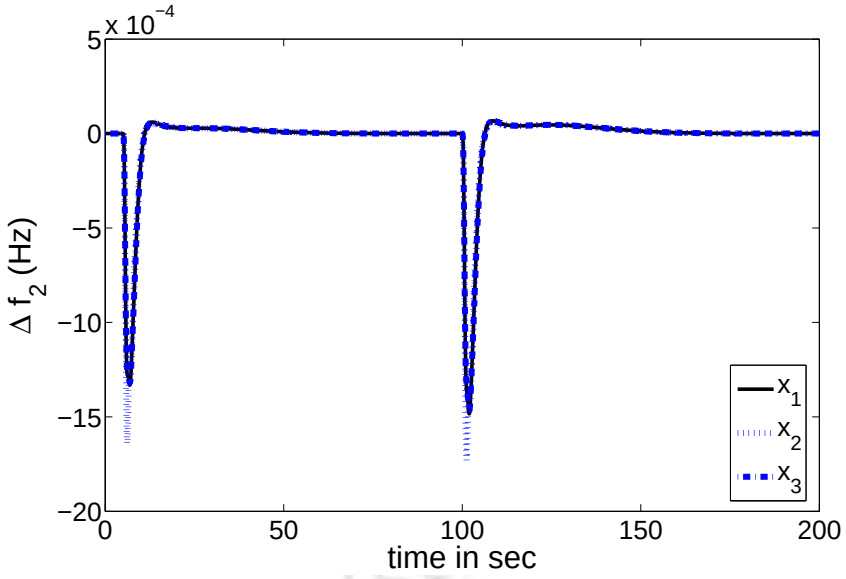

(b)

Figure 7.12: Frequency deviation for Multi-area power systems (a) Area 1, (b) Area 2: (x_1) Nominal, (x_2) +50% Variation in K_P and T_P and (x_3) -50% Variation in K_P and T_P

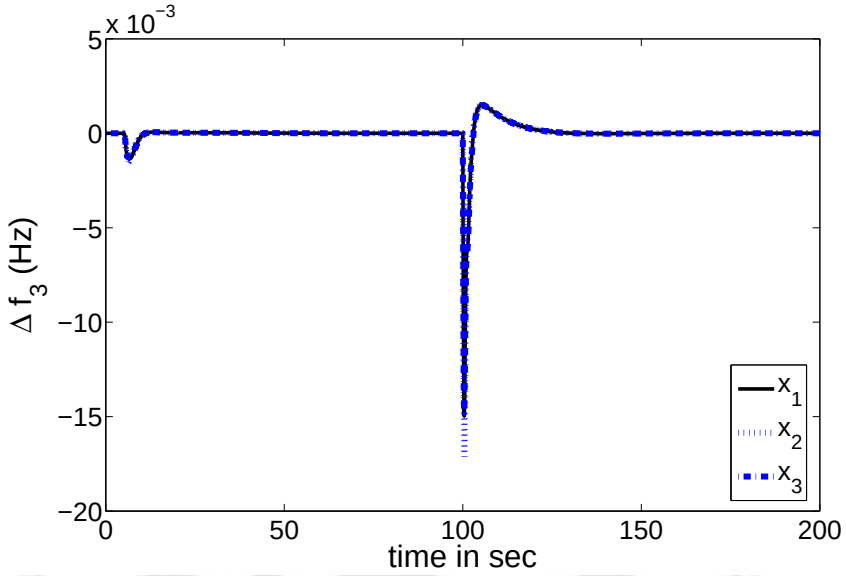

(a)

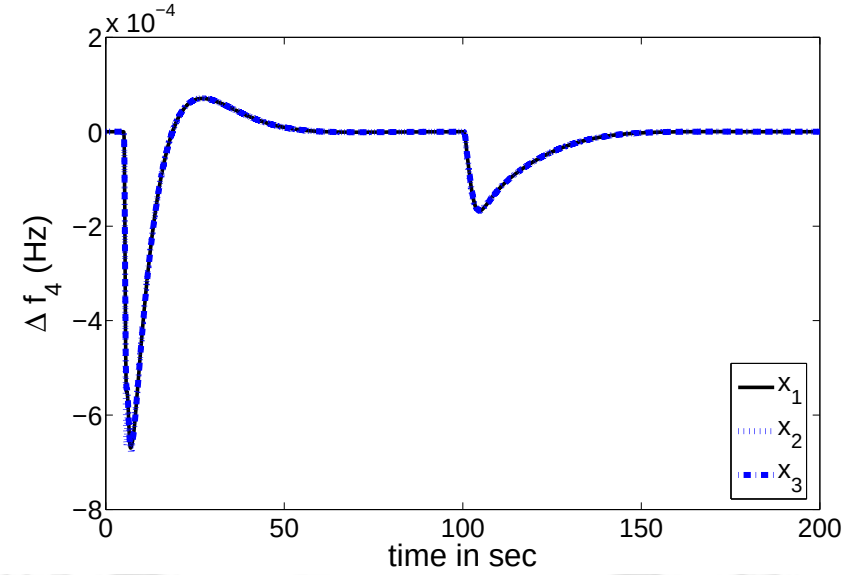

(b)

Figure 7.13: Frequency deviation for Multi-area power systems (a) Area 3, (b) Area 4: (x_1) Nominal, (x_2) +50% Variation in K_P and T_P and (x_3) -50% Variation in K_P and T_P

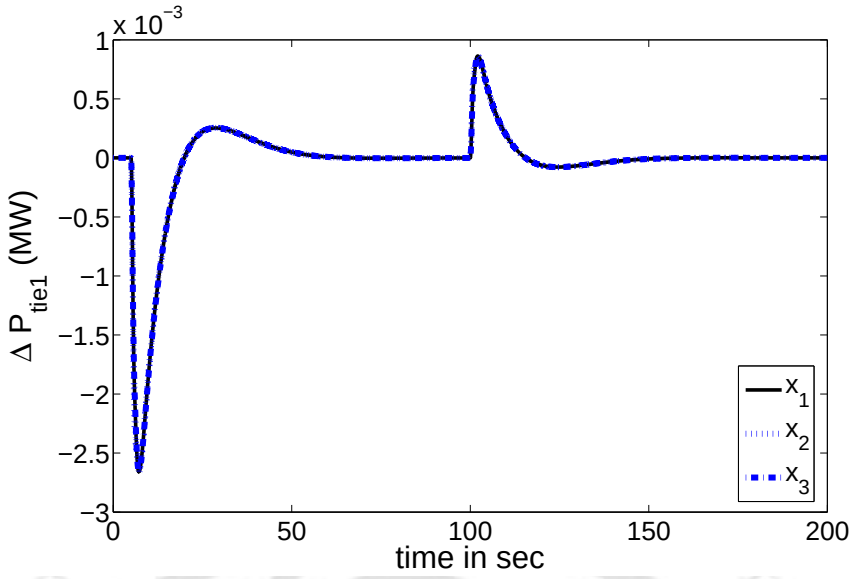

(a)

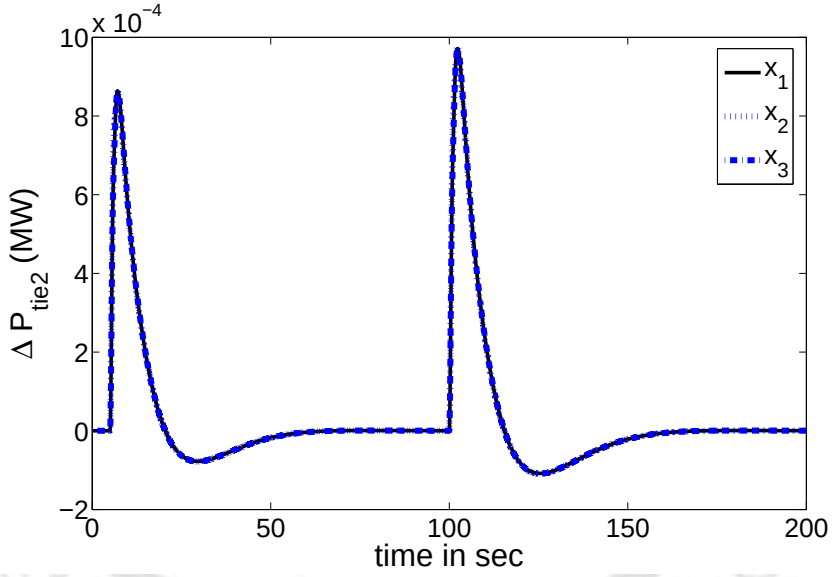

(b)

Figure 7.14: Tie Line Power deviation for Multi-area power systems (a) Area 1, (b) Area 2: (x_1) Nominal, (x_2) +50% Variation in K_P and T_P and (x_3) -50% Variation in K_P and T_P

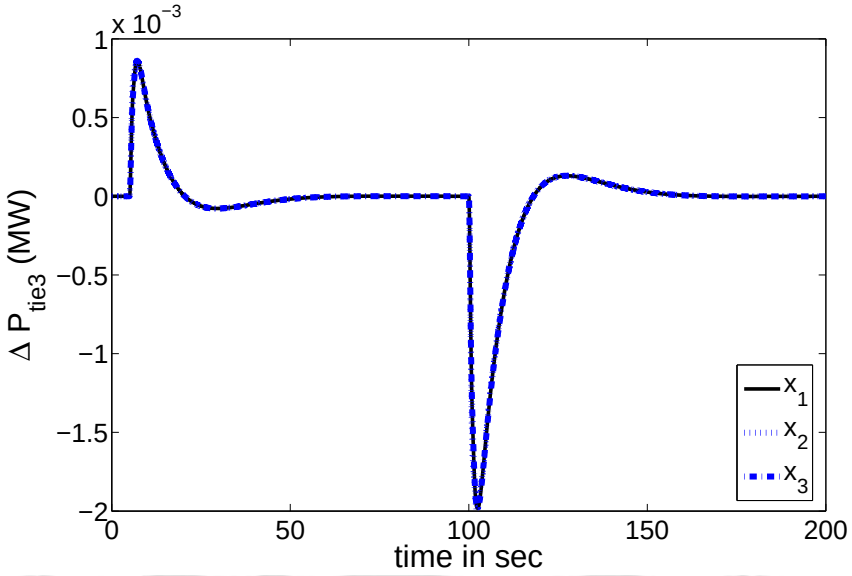

(a)

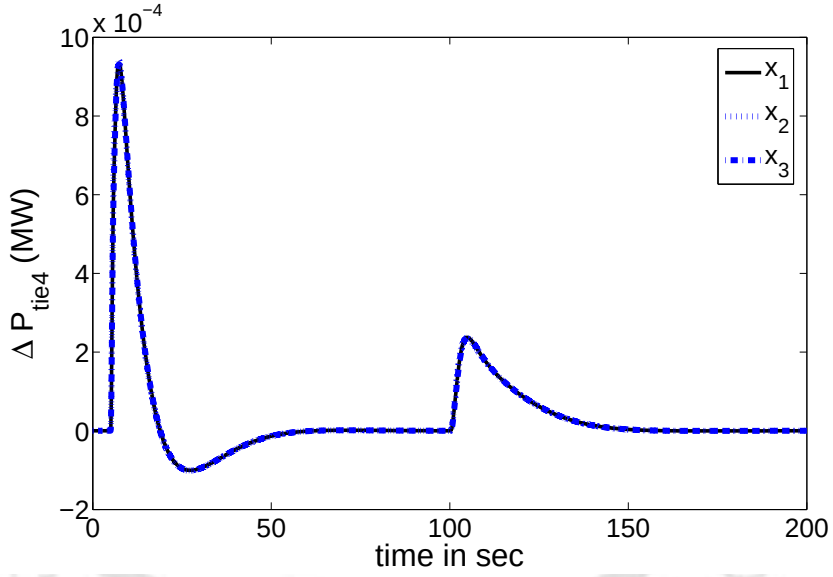

(b)

Figure 7.15: Tie Line Power deviation for Multi-area power systems (a) Area 3, (b) Area 4: (x_1) Nominal, (x_2) +50% Variation in K_P and T_P and (x_3) -50% Variation in K_P and T_P

In order to test the robustness of the controller, the variations of the parameters of the non-reheat and reheat units in the four areas are assumed to be ±50% of their nominal values. However, the controller parameters are not changed with the variations of the system parameters. Figure 7.12 and Figure 7.13 illustrate the frequency errors of four areas with the variant parameter values. Figure 7.14 and Figure 7.15 show the tie-line power errors of the four areas with the variant parameter values. From the simulation results, it can be seen that despite such large parameter variations, the system

responses do not show notable differences from the nominal values. Therefore the simulation results demonstrate the robustness of proposed controller against system parameter variations. It is observed that the proposed decentralized PID controller achieves better damping for frequency and tie-line power flow deviations in all the four-areas.

7.5 Conclusions

The LFC characteristics of a single-area power system with non-reheat and reheat turbines have been studied. A relay feedback test has been conducted to estimate the parameters of the power system. The robustness of the LFC is tested using Kharitonov's theorem. The results show that the proposed PID controller with a new structure gives a better performance than recently reported method. The proposed method is applied to a four-control area power system and tested with different plant parameters uncertainty scenarios.

8

Conclusions and Future Work

Contents

8.1 Concluding remarks

Most work of the thesis are focused on the modified Smith predictor, control structures and controller design for time delay processes. In this thesis, several new results are obtained for control system design that improve the performance and robustness. Briefly, the results are summarized as follows:

A. Design of Modified Smith Predictor Controllers

A two-degree-of-freedom modified Smith control scheme is investigated for enhanced control performance of stable, integrating and unstable time delay processes. The proposed scheme is also capable of successfully controlling non-minimum phase stable processes. The two controllers in the scheme are well placed to tune from the setpoint and disturbance. The setpoint and load disturbance responses can each be tuned conveniently by a single control parameter. Guidelines are provided for selecting the tuning parameter. The tuning rule for the scheme enables convenient design of disturbance rejection controller with superior regulatory performance, as well as easy trade-off between system robustness and performance.

B. Enhanced Series Cascade Control Structure for Unstable Delay Processes

The modified Smith predictor has been used in the outer loop of cascade control structure in order to have the best merits of the Smith predictor as well as cascade control scheme. The proposed control structure has two main advantages: firstly, it is very effective when the system is subjected to load disturbances and outer loop plants with large time delay. Secondly, the controllers for servo and regulatory responses can be tuned independently. It is verified using Kharitonov's theorem that the proposed controllers are robust and stable.

C. Improved Series Cascade Control Structure for Integrating Delay Processes

A new series cascade control structure is presented to tackle the problem of controlling a class of integrating delay processes. The primary advantages of the proposed control structure are: firstly, it suppresses the load disturbance and compensates the dead time and secondly, the servo response decouples the regulatory response in nominal case. A simulation study of the control design on commonly encountered processes has verified the effectiveness of the proposed scheme.

D. Modified Smith Predictor based Parallel Cascade Control Structure

A parallel cascade control in the enhanced modified Smith predictor structure for controlling stable, unstable and integrating processes with time delay is proposed. The new parallel cascade control structure possesses only two controllers and a setpoint filter. The disturbance rejection controllers are designed by adjusting the slope of the Nyquist curve at gain crossover frequency. The stabilization, robustness analysis and performances of time delay processes have been investigated. Simulation results show that the proposed design method outperforms some conventional and recently reported methods.

E. A New Parallel Cascade Control Scheme for Unstable Delay Processes

A novel parallel cascade control structure is presented for controlling stable and unstable processes with time delay. The comparative analysis shows that with less number of controllers, the proposed scheme gives improved closed-loop performances. It is shown that both nominal and robust control performances are obtained with the designed controllers. Simulation examples are given to demonstrate the value of the proposed control method.

F. A New Control Scheme for PID Load Frequency Controller of Power Systems

A new control structure for Load frequency controller of power systems is investigated. In order to estimate the parameters of the power system, a relay feedback test has been conducted. The simulation results show that the proposed PID controller with a new structure gives a better performance than reported methods.

8.2 Suggestions for further work

There are several ways in which the work in this thesis can be extended and further investigated. Some of them are enumerated as follows.

- In Chapter 2, the controllers are designed for stable, unstable and integrating processes but it will be more interesting if the proposed analysis can be extended to other class of processes like under-damped and RHP zero.

- The autotuning approach is very important in industrial practice as no mathematical model of the process is required and also the Smith predictor strategy is commonly used for processes

with large time delays. The modified Smith predictor scheme in Chapter 2 can be extended to have a relay feedback automatic tuning method to provide a controller for processes with long dead time.

- For the modified Smith predictor, many tuning formulas for linear PID controllers are given for process control. However, there has been no systematic tuning rules proposed for non-linear PID controllers so far, even for stable process control. It is possible to generate the nonlinear PID controller settings via some non-linear approaches such as genetic algorithm or adaptive neural networks.

- It will be interesting if the modified Smith predictor for periodic disturbance rejection can be proposed.

- The proposed control structures and control laws are limited to continuous domain. It will be more interesting if discrete implementation is considered.

- The thesis is restricted to single-input single-output systems. However, all of the techniques used in the thesis can be readily extended to square multi-input multi-output systems. Further extension to non-square systems is more challenging, and appropriately left for future work.

- The genetic algorithm, PSO, ACO, BFA or fractional-PID controller design methods can be used for the control structures.

- The proposed series and parallel cascade control structures can be extended to non-minimum phase stable and unstable systems.

- The LFC-PID problem can be extended to power system with communication delays in deregulated power environment.

A

Supplementary Materials

Contents

A.1 Detailed explanation for the statement 'x_1 always gives a negative value'of 3.3.1

In order to ensure the controller parameters in (3.28) to be positive, $x_1 < 0$.

The expression for x_1 is

$$x_1 = 6\theta_2 + 12\lambda_2 - 6\alpha_2 \tag{A-1}$$

Now, we can write

$$\frac{x_1}{6\theta_2} = \left(1 + \frac{2\lambda_2}{\theta_2} - \frac{\alpha_2}{\theta_2}\right) < 0 \tag{A-2}$$

or,

$$1 + \frac{2\lambda_2}{\theta_2} < \frac{\alpha_2}{\theta_2} \tag{A-3}$$

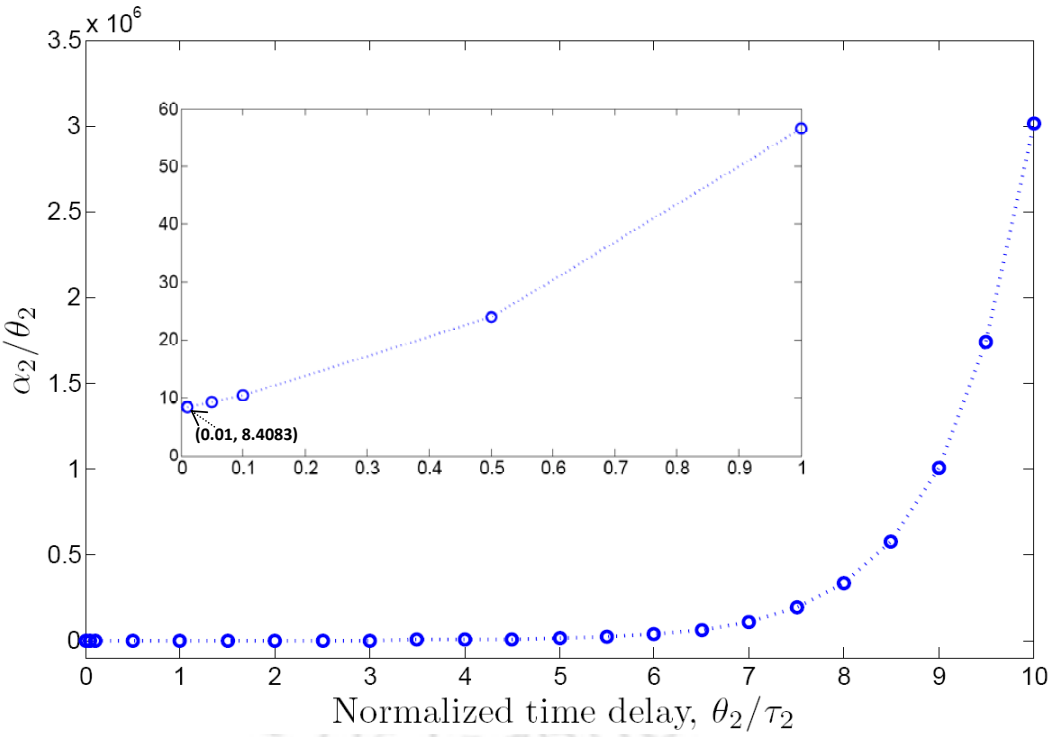

Figure f-1: Plot for α_2/θ_2 versus θ_2/τ_2

The suggested range of the tuning parameter λ_2 is $1.5\theta_2 - 3.6\theta_2$. For the upper limit of λ_2, (A-3) gives $\alpha_2/\theta_2 > 8.2$. For every value of α_2/θ_2 to be greater than 8.2, x_1 is always negative.

(3.23) can be written as

$$\frac{\alpha_2}{\theta_2} = \frac{\tau_2}{\theta_2}\left[\left(1 + \frac{\lambda_2}{\tau_2}\right)^2 e^{\theta_2/\tau_2} - 1\right] \tag{A-4}$$

For the smaller value of normalized time delay i.e. $\theta_2/\tau_2 = 0.01$, (A-4) gives $\alpha_2/\theta_2 = 8.4083$. Similarly, for the larger value of normalized time delay (i.e. $\theta_2/\tau_2 > 1$), say $\theta_2/\tau_2 = 10$, $\alpha_2/\theta_2 = 3015423.067$.

From the Figure f-1, it is clear that the graph starts from the point $(0.01, 8.4083)$ which indicates $\alpha_2/\theta_2 > 8.2$ and thus, x_1 is always negative irrespective of any value of normalized time delay. This is also true for the other values of λ_2.

A.2 An alternate method to get the filter parameters (d_{f1} and d_{f2}) of 3.3.2

An alternate method to get the filter parameters (d_{f1} and d_{f2}) of the primary controller G_{cd1} is by using the Taylor series expansion. From (3.4) and (3.39), d_{f1} and d_{f2} can be obtained on equating $\left(1 + d_{f1}s + d_{f2}s^2\right)$ and $\left(1 + l_1 s + l_2 s^2 + l_3 s^3 + l_4 s^4\right)/(1 - \tau_1 s)$. Thus,

$$\begin{aligned}\left(1 + d_{f1}s + d_{f2}s^2\right) &= \left(1 + l_1 s + l_2 s^2 + l_3 s^3 + l_4 s^4\right)/(1 - \tau_1 s) \\ &= \left(1 + l_1 s + l_2 s^2 + l_3 s^3 + l_4 s^4\right)(1 - \tau_1 s)^{-1}\end{aligned} \tag{A-5}$$

Expanding $(1 - \tau_1 s)^{-1}$ using Taylor series, (A-5) becomes

$$\left(1 + d_{f1}s + d_{f2}s^2\right) = \left(1 + l_1 s + l_2 s^2 + l_3 s^3 + l_4 s^4\right)\left(1 + \tau_1 s + \tau_1^2 s^2 + \tau_1^3 s^3 + \cdots\right) \tag{A-6}$$

Neglecting the higher degrees of s

$$1 + d_{f1}s + d_{f2}s^2 = 1 + (l_1 + \tau_1)\, s + \left(l_2 + \tau_1 l_1 + \tau_1^2\right) s^2 \tag{A-7}$$

From (A-7), we get $d_{f1} = l_1 + \tau_1$ and $d_{f2} = l_2 + d_{f1}\tau_1$ which are exactly same as that in (3.39).

A.3 Detailed explanation for the statement 'm_1 always gives a negative value'of 3.3.2

In order to ensure the controller parameters in (3.39) to be positive, $m_1 < 0$.

The expression for m_1 is given by

$$m_1 = 6\theta_m + 18\lambda_1 - 6\alpha_1 \tag{A-8}$$

Now, we can write

$$\frac{m_1}{6\theta_m} = \left(1 + \frac{3\lambda_1}{\theta_m} - \frac{\alpha_1}{\theta_m}\right) < 0 \tag{A-9}$$

The above expression can also be written as

$$1 + \frac{3\lambda_1}{\theta_m} < \frac{\alpha_1}{\theta_m} \tag{A-10}$$

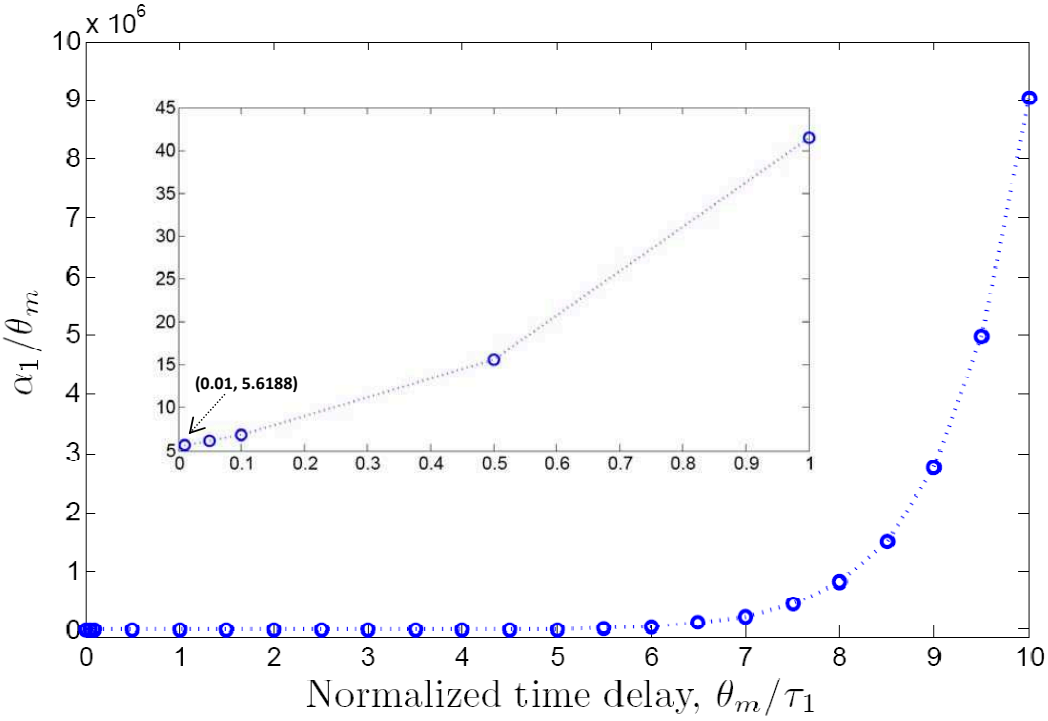

Figure f-2: Plot for α_1/θ_m versus θ_m/τ_1

The suggested range of the tuning parameter λ_1 is $0.5\theta_m - 1.5\theta_m$. For the upper limit of λ_1, (A-10) gives $\alpha_1/\theta_m > 5.5$. For every value of α_1/θ_m to be greater than 5.5, m_1 is always negative.

(3.34) can be written as

$$\frac{\alpha_1}{\theta_m} = \frac{\tau_1}{\theta_m}\left[\left(1 + \frac{\lambda_1}{\tau_1}\right)^3 e^{\theta_m/\tau_1} - 1\right] \tag{A-11}$$

For the smaller value of normalized time delay i.e. $\theta_m/\tau_1 = 0.01$, (A-11) gives $\alpha_1/\theta_m = 5.6188$. Similarly, for the larger value of normalized time delay (i.e. $\theta_m/\tau_1 > 1$), say $\theta_m/\tau_1 = 10$, $\alpha_1/\theta_m = 9022040.29$.

From the Figure f-2, it is clear that the graph starts from the point $(0.01, 5.6188)$ i.e. $\alpha_1/\theta_m > 5.5$ which concludes m_1 is always negative irrespective of any value of normalized time delay. This is also true for the other values of λ_1.

A.4 Use of orthogonality property of H_2 norm in (2.18)

Let V be an inner product space.

Two non zero vectors x, y ∈ V are said to be orthogonal if their product is zero: $\langle x, y\rangle = 0$. It will be then noted that $x \perp y$ [93].

x and y are orthogonal if $\|\mathrm{x} + \mathrm{y}\|_2^2 = \|x\|_2^2 + \|y\|_2^2$. Now, (2.18) can be written as

$$\|W(s)\,(1 - Y_r(s))\|_2^2 = \left\| \frac{1}{s}\left[\frac{P_{nn}(\theta s)}{P_{nn}(-\theta s)} - 1 - \frac{kG_{cs}(s)}{(\tau_1 s \pm 1)(\tau_2 s + 1) + k} + 1 \right] \right\|_2^2$$

$$\|W(s)\,(1 - Y_r(s))\|_2^2 = \left\| \frac{P_{nn}(\theta s) - P_{nn}(-\theta s)}{sP_{nn}(-\theta s)} + \frac{[(\tau_1 s \pm 1)(\tau_2 s + 1) + k] - kG_{cs}(s)}{s\,[(\tau_1 s \pm 1)(\tau_2 s + 1) + k]} \right\|_2^2$$

Using Orthogonality property, we get

$$\|W(s)\,(1 - Y_r(s))\|_2^2 = \left\| \frac{P_{nn}(\theta s) - P_{nn}(-\theta s)}{sP_{nn}(-\theta s)} \right\|_2^2 + \left\| \frac{[(\tau_1 s \pm 1)(\tau_2 s + 1) + k] - kG_{cs}(s)}{s\,[(\tau_1 s \pm 1)(\tau_2 s + 1) + k]} \right\|_2^2$$

A.5 Detailed derivation for (3.44) of the section 3.5

Determinant of the systems,

$$\Delta = (1 + G_m)\,(1 + G_{p2}G_{p1}G_{cd1} + G_{p2}G_{cd2} + G_{m2}G_{cd2}G_{p2}G_{p1}G_{cd1})$$

Now,

$$\begin{aligned} \prod_{i=1}^{8} p_i(s) &= p_1(s)p_2(s)p_3(s)p_4(s)p_5(s)p_6(s)p_7(s)p_8(s) \\ &= g_1(s)g_2(s)g_3(s)\gamma(s)\gamma(s)\gamma(s)\gamma^2(s) \\ &= g_1(s)g_2(s)g_3(s)\gamma^5(s) \end{aligned}$$

Therefore,

$$\begin{aligned} & p_c(s) = \Delta \prod_{i=1}^{8} p_i(s) \\ & = \left[1 + \tfrac{\delta^2(s)}{\gamma^2(s)}\right]\left[1 + \tfrac{\delta(s)}{\gamma(s)}\tfrac{\delta(s)}{\gamma(s)}\tfrac{f_2(s)}{g_2(s)} + \tfrac{\delta(s)}{\gamma(s)}\tfrac{f_3(s)}{g_3(s)} + \tfrac{\delta(s)}{\gamma(s)}\tfrac{f_3(s)}{g_3(s)}\tfrac{\delta(s)}{\gamma(s)}\tfrac{\delta(s)}{\gamma(s)}\tfrac{f_2(s)}{g_2(s)}\right] g_1(s)g_2(s)g_3(s)\gamma^5(s) \\ & = \left[\tfrac{\gamma^2(s)+\delta^2(s)}{\gamma^2(s)}\right]\left[1 + \tfrac{\delta^2(s)}{\gamma^2(s)}\tfrac{f_2(s)}{g_2(s)} + \tfrac{\delta(s)}{\gamma(s)}\tfrac{f_3(s)}{g_3(s)} + \tfrac{\delta^3(s)}{\gamma^3(s)}\tfrac{f_3(s)}{g_3(s)}\tfrac{f_2(s)}{g_2(s)}\right] g_1(s)g_2(s)g_3(s)\gamma^5(s) \\ & = \left[\tfrac{\gamma^2(s)+\delta^2(s)}{\gamma^2(s)}\right]\left[\tfrac{\gamma^3(s)g_2(s)g_3(s)+\gamma(s)\delta^2(s)f_2(s)g_3(s)+\gamma^2(s)\delta(s)f_3(s)g_2(s)+\delta^3(s)f_2(s)f_3(s)}{\gamma^3(s)g_2(s)g_3(s)}\right] \\ & \times g_1(s)g_2(s)g_3(s)\gamma^5(s) \\ & = \left[\gamma^2(s) + \delta^2(s)\right]\left[\gamma^3(s)g_2(s)g_3(s) + \gamma(s)\delta^2(s)f_2(s)g_3(s) + \gamma^2(s)\delta(s)f_3(s)g_2(s) + \delta^3(s)f_2(s)f_3(s)\right] g_1(s) \end{aligned}$$

Bibliography

[1] K. Gu, V. L. Kharitonov, and J. Chen, *Stability of Time-Delay Systems*. Birkhäuser, Berlin, 2003.

[2] K. Gu and S. I. Niculescu, "Survey on recent results in the stability and control of time-delays systems," *J. Dyn. Syst. Meas. Control*, vol. 125, pp. 158–165, 2003.

[3] S. I. Niculescu, *Delay Effects on Stability: A Robust Control Approach*. Springer-Verlag, Heidelberg, Germany, 2001.

[4] J. P. Richard, "Time-delay system: an overview of some recent advances and open problems," *Automatica*, vol. 39 (10), pp. 1667–1694, 2003.

[5] R. Vilanova and A. Visioli, Eds., *PID Control in the Third Millennium: Lessons Learned and New Approaches*. Springer, 2012.

[6] K. Watanabe and M. Ito, "A process-model control for linear systems with delay," *IEEE Trans. Automatic Control*, vol. 26 (6), pp. 1261–1269, 1981.

[7] T. Hägglund, "An industrial dead-time compensating PI controller," *Control Eng. Practice*, vol. 4, pp. 749–756, 1996.

[8] O. J. M. Smith, "A controller to overcome dead time," *ISA J.*, vol. 6, pp. 28–33, 1959.

[9] ——, "Closer control of loops with dead time," *Chem. Eng. Progr.*, vol. 53, pp. 217–219, 1957.

[10] A. Z. Manitius and A. W. Olbrot, "Finite spectrum assignment problem for systems with delays," *IEEE Trans. Autom. Control*, vol. 24 (4), pp. 541–553, 1979.

[11] T. Hägglund, "A predictive PI controller for processes with long dead-time delay," *IEEE Control Syst. Mag.*, vol. 12, pp. 57–60, 1992.

[12] A. Ingimundarson and T. Hägglund, "Performance comparison between PID and dead-time compensating controllers," *J. Process Control*, vol. 12, pp. 887–895, 2002.

[13] J. E. Normey-Rico, C. Bordons, and E. F. Camacho, "Improving the robustness of dead-time compensating PI controllers," *Control Eng. Practice*, vol. 5, pp. 801–810, 1997.

[14] I. L. Chien, S. C. Peng, and J. H. Liu, "Simple control method for integration processes with long deadtime," *J. of Process Control*, vol. 12 (3), pp. 391–404, 2002.

[15] M. R. Stojic, M. S. Matijevic, and L. S. Draganovic, "A robust Smith predictor modified by internal models for integrating process with dead time," *IEEE Trans. Automatic Control*, vol. 46 (8), pp. 1293–1298, 2001.

[16] I. Kaya, "IMC based automatic tuning method for PID controllers in a Smith predictor configuration," *Computers & Chemical Engineering*, vol. 28 (3), pp. 281–290, 2004.

[17] T. Takehara, T. Kunitake, H. Hashimoto, and F. Harashima, "The control for the disturbance in the system with time delay," in *International workshop on Advanced Motion Control, AMC, vol. 1, pp. 349-353*, 1996.

[18] Q. G. Wang, H. Q. Zhou, Y. S. Yang, and Y. Zhang, "Modified Smith predictor design for periodic disturbance rejection," in *5th Asian Control Conference, vol. 2, pp. 1145-1150*, 2004.

[19] K. J. Åström, C. C. Hang, and B. C. Lim, "A new Smith predictor for controlling a process with an integrator and long dead-time," *IEEE Trans. Automatic Control*, vol. 39, pp. 343–345, 1994.

[20] M. R. Mataušek and A. D. Micić, "A modified Smith predictor for controlling a process with an integrator and long dead time," *IEEE Trans. Automatic Control*, vol. 44, pp. 1199–1203, 1996.

[21] ——, "On the modified Smith predictor for controlling a process with an integrator and long dead time," *IEEE Trans. Automatic Control*, vol. 44 (8), pp. 1603–1606, 1999.

[22] J. E. Normey-Rico and E. F.Camacho, "A unified approach to design dead-time compensators for stable and integrative processes with dead time," *IEEE Trans Automat Control*, vol. 47(2), pp. 299–305, 2002.

[23] Q. C. Zhong and J. Normey-Rico, "Control of integral processes with dead-time. part 1: disturbance observer-based 2 dof control scheme," *Control Theory Appl., IEE Proc.*, vol. 149 (4), pp. 285–290, 2002.

[24] Q. C. Zhong and H. X. Li, "2-degree-of-freedom proportional-integral-derivative type controller incorporating the Smith principle for processes with dead time," *Ind. Eng. Chem. Res.*, vol. 41, pp. 2448–2454, 2002.

[25] Q. C. Zhong, "Control of integral processes with dead time part 3: dead beat disturbance response," *IEEE Trans. Autom. Control*, vol. 48 (1), pp. 153–159, 2003.

[26] A. S. Rao, V. S. R. Rao, and M. Chidambaram, "Setpoint weighted modified smith predictor for integrating and double integrating processes with time delay," *ISA Transactions*, vol. 46, pp. 59–71, 2007.

[27] S. Majhi and D. P. Atherton, "Obtaining controller parameters for a new smith predictor using autotuning," *Automatica*, vol. 36, pp. 1651–1658, 2000.

[28] Y. Lee, J. Lee, and S. Park, "PID controller tuning for integrating and unstable processes with time delay," *Chem. Eng. Sci*, vol. 55, pp. 3481–3493, 2000.

[29] ——, "IMC-based control system design for unstable process," *Ind. Eng. Chem. Res.*, vol. 41, pp. 4288–4294, 2002.

[30] W. Tan, H. J. Marquez, and T. Chen, "IMC-based design for unstable processes with time delays," *J. Process Control*, vol. 13, pp. 203–213, 2003.

[31] X. Lu, Y. S. Yang, Q. G. Wang, and W. X. Zheng, "A double two-degree-offreedom control scheme for improved control of unstable delay processes," *J. Process Control*, vol. 15(5), pp. 605–614, 2005.

[32] T. Liu, W. Zhang, and D. Gu, "Analytical design of two-degree-of-freedom control scheme for open-loop unstable processes with time delay," *J. Process Control*, vol. 15 (5), pp. 559–572, 2005.

[33] A. S. Rao, V. S. R. Rao, and M. Chidambaram, "Simple analytical design of modified smith predictor with improved performance for unstable first-order plus time delay (foptd) processes," *Ind. Eng. Chem. Res.*, vol. 46(13), pp. 4561–4571, 2007.

[34] A. S. Rao and M. Chidambaram, "Analytical design of modified Smith predictor in a two-degrees-of-freedom control scheme for second order unstable processes with time delay," *ISA Transactions*, vol. 47, pp. 407–419, 2008.

[35] G. Stephanopoulos, *Chemical Process Control: An Introduction to Theory and Practice*. New Jersey: Prentice Hall, 1984.

[36] W. Luyben, "Parallel cascade control," *Ind. Eng. Chem. Fundam.*, vol. 12, pp. 463–467, 1973.

[37] R. G. Franks and C. W. Worley, "Quantitive analysis of cascade control," *Ind. Eng. Chem.*, vol. 48(6), pp. 1074–1079, 1956.

[38] M. Zhuang and D. P. Atherton, "Optimum cascade PID controller design for SISO systems," in *CONTROL'94, 21-24 March*, 1994.

[39] F. S. Wang, W. S. Juang, and C. T. Chan, "Optimal tuning of PID controllers for single and cascade control loops," *Chem. Eng. Commun.*, vol. 132, pp. 15–34, 1995.

[40] Y. H. Lee, S. W. Park, and M. Y. Lee, "PID controller tuning to obtain desired closed loop responses for cascade control systems," *Ind. Eng. Chem. Res.*, vol. 37 (5), pp. 1859–1865, 1998.

[41] I. Kaya, "Improving performance using cascade control and a smith predictor," *ISA Transactions*, vol. 40, pp. 223–234, 2001.

[42] S. Uma, M. Chidambaram, and A. S. Rao, "Enhanced control of unstable cascade processes with time delays using a modified smith predictor," *Ind. Eng. Chem. Res.*, vol. 48, pp. 3098–3111, 2009.

[43] C. C. Yu, "Design of parallel cascade control for disturbance rejection," *AIChE J*, vol. 34(11), pp. 123–128, 1988.

[44] S. H. Shen and C. C. Yu, "Selection of secondary measurement for parallel cascade control," *AIChE J*, vol. 36(8), pp. 1347–1352, 1990.

[45] D. Semino and A. Brambilla, "An efficient structure for parallel cascade control," *Ind. Eng. Chem. Res.*, vol. 35, pp. 1845–1852, 1996.

[46] M. Pottmann, M. A. Henson, B. A. Oginnaike, and J. S. Schwaber, "A parallel control strategy abstracted from the baroreceptor reflex," *Chem. Eng. Sci.*, vol. 51(6), pp. 931–945, 1996.

[47] J. Chen, S. C. Huang, and Y. Yea, "Achievable performance assessment and design for parallel cascade control systems," *J Chem Eng Japan*, vol. 38(3), pp. 188–201, 2005.

[48] Y. Lee, M. Skliar, and M. Lee, "Analytical method of PID controller design for parallel cascade control," *J. Process Control*, vol. 16, pp. 809–818, 2006.

[49] A. S. Rao, S. Seethaladevi, S. Uma, and M. Chidambaram, "Enhancing the performance of parallel cascade control using smith predictor," *ISA Transactions*, vol. 48, pp. 220–227, 2009.

[50] N. Jaleeli, L. S. VanSlyck, D. N. Ewart, L. H. Fink, and A. G. Hoffmann, "Understanding automatic generation control," *IEEE Transactions on Power Systems. Vol. 7, No. 3, August 1992*, vol. 7 (3), pp. 1106–1122, 1992.

[51] H. Shayeghi, H. Shayanfar, and A. Jalili, "Load frequency control strategies: A state-of-the-art survey for the researcher," *Energy Conversion and Management*, vol. 50, pp. 344–353, 2009.

[52] O. I. Elgerd and C. Fosha, "Optimum megawatt-frequency control of multiarea electric energy systems," *IEEE Trans. Power Apparatus & Systems*, vol. 89 (4), pp. 556–563, 1970.

[53] C. Fosha and O. I. Elgerd, "The megawatt-frequency control problem: a new approach via optimal control," *IEEE Trans. Power Apparatus & Systems*, vol. 89 (4), pp. 563–577, 1970.

[54] P. Reddoch, T. T. Julich, and E. Tacker, "Model and performance functional for load frequency control in interconnected power systems," in *IEEE Conf Decision and Control*, 1971.

[55] M. Aldeen, "A fresh approach to the LQR problem with application to power systems," in *Proc International Power Engineering Conf.*, 1993.

[56] Q. P. Ha, "A fuzzy sliding mode controller for power system load frequency control," in *IEEE Second Conf Knowledge-Based Intelligent Systems*, 1998.

[57] J. Kanniah, S. C. Tripathy, O. P. Malik, and G. S. Hope, "Microprocessor-based adaptive load-frequency control," *Generation, Transmission and Distribution, IEE Proc C*, vol. 131 (4), pp. 121–128, 1984.

[58] I. Vajk, "Adaptive load-frequency control of the hungarian power system," *Automatica*, vol. 21 (2), pp. 129–137, 1985.

[59] K. Yamashita and H. Miyagi, "Multivariable self-tuning regulator for load frequency control system with interaction of voltage on load demand," *Control Theory Appl., IEE Proc. D*, vol. 138 (2), pp. 177–183, 1991.

[60] C. T. Pan and C. M. Liaw, "An adaptive controller for power system load frequency control," *IEEE Transactions on Power Systems*, vol. 4 (1), pp. 122–128, 1989.

[61] C. S. Indulkar and B. Raj, "Application of fuzzy controller to automatic generation control," *Electric Mach Power Systems*, vol. 23 (2), pp. 209–220, 1995.

[62] D. K. Chaturvedi, P. S. Satsangi, and P. K. Kalra, "Load frequency control: A generalised neural network approach," *Electr Power Energy Systems*, vol. 21, pp. 405–415, 1999.

[63] M. L. Kothari, J. Nanda, D. P. Kothari, and D. Das, "Discrete-mode automatic generation control of a two-area reheat thermal system with new area control error," *IEEE Trans Power Syst*, vol. 4 (2), pp. 730–738, 1989.

[64] S. Velusami and I. A. Chidambaram, "Design of decentralized biased dual mode controllers for load-frequency control of interconnected power systems," *Electr Power Components Syst*, vol. 34 (10), pp. 1057–1075, 2006.

[65] O. P. Malik, A. Kumar, and G. S. Hope, "A load frequency control algorithm based on a generalized approach," *IEEE Trans Power Syst*, vol. 3 (2), pp. 375–382, 1988.

[66] R. G. Rao and S. I. Ahson, "Control of interconnected power systems using two-level methods," *Int J Control*, vol. 34 (6), pp. 1195–1205, 1981.

[67] A. Rubaai and V. Udo, "Self-tuning load frequency control : Multilevel adaptive approach," *IEE Proc.-Gener. Transm. Distrib.*, vol. 141 (4), pp. 285–290, 1994.

[68] A. Khodabakhshian and R. Hooshmand, "A new PID controller design for automatic generation control of hydro power systems," *Electrical Power and Energy Systems*, vol. 32, pp. 375–382, 2010.

[69] R. J. Abraham, D. Das, and A. Patra, "Automatic generation control of an interconnected hydrothermal power system considering superconducting magnetic energy storage," *Int J Electr Power Energy Syst*, vol. 29 (8), pp. 571–579, 2007.

[70] Y. Wang, R. Zhou, and C. Wen, "Robust load frequency controller design for power systems," *IEE Proc Generat Transmis Distribut*, vol. 140 (1), pp. 11–16, 1993.

[71] ——, "New robust adaptive load frequency control with system parametric uncertainties," *IEE Proc Generat Transmis Distribut*, vol. 141 (3), pp. 184–190, 1994.

[72] K. J. Åström and T. Hägglund, *PID controllers: Theory, Design, and Tuning*. Instrument Society of America, Research Triangle Park, NC, 1995.

[73] W. L. Luyben, *Process modeling, simulation and control for chemical engineers*. McGraw-Hill International Editions. New York, 1990.

[74] K. Ogata, *Mordern control Engineering, 2nd edition*. Prentice Hall, Engle-wood Cliffs, NJ, 1990.

[75] W. K. Ho and W. Xu, "PID tuning for unstable processes based on gain and phase-margin specifications," *IEE proc. Control Theory Appl.*, vol. 145 (5), pp. 392–396, 1998.

[76] J. H. Park, S. W. Sung, and I. Lee, "An enhanced PID control strategy for unstable processes," *Automatica*, vol. 34 (6), pp. 751–756, 1998.

[77] G. J. Silva, A. Datta, and S. P. Bhattacharyya, *PID controllers for time-delay systems*. Birkhäuser, Boston., 2004.

[78] D. Chen and D. E. Seborg, "PI/PID controller design based on direct synthesis and disturbance rejection." *Ind. Eng. Chem. Res.*, vol. 41, pp. 4807–4822, 2002.

[79] I. Kaya, N. Tan, and D. P. Atherton, "Improved cascade control structure for enhanced performance," *J. Process Control*, vol. 17, pp. 3–16, 2007.

[80] T. Liu, W. Zhang, and D. Gu, "IMC-based control strategy for open-loop unstable cascade processes," *Ind. Eng. Chem. Res.*, vol. 44, pp. 900–909, 2005.

[81] I. Kaya and D. P. Atherton, "Use of smith predictor in the outer loop for cascaded control of unstable and integrating processes," *Ind. Eng. Chem. Res.*, vol. 47, pp. 1981–1987, 2008.

[82] S. Uma, M. Chidambaram, A. S. Rao, and C. K. Yoo, "Enhanced control of integrating cascade processes with time delays using modified Smith predictor," *Chemical Engineering Science*, vol. 65, pp. 1065–1075, 2010.

[83] D. G. Padhan and S. Majhi, "Modified Smith predictor and controller for time delay processes," *IET Electronics Letters*, vol. 47(17), pp. 959 – 961, 2011.

[84] ——, "A two-degree-of-freedom control scheme for improved performance of unstable delay processes," in *IEEE ICECE, 18-20 December, Dhaka, Bangladesh*, 2010.

[85] ——, "Modified smith predictor and controller for stable and unstable processes," in *4th International Conference CERA09, 19-21 February, IIT Roorkee, India*, 2010.

[86] F. Furukawa and E. Shimemura, "Predictive control for systems with time delay," *Int. J. Control*, vol. 37(2), pp. 399–412, 1990.

[87] A. D. Paor, "A modified smith predictor and controller for unstable processes with time delay," *Int. J. Control*, vol. 41(4), pp. 1025–1036, 1985.

[88] A. D. Paor and R. Egan, "Extension and partial optimization of a modified smith predictor and controller for unstable processes with time delay," *Int. J. Control*, vol. 50 (4), pp. 1315–1326, 1989.

[89] I. Kaya, "Obtaining controller parameters for a new PI-PD smith predictor using autotuning," *J. Process Control*, vol. 13, pp. 465–472, 2003.

[90] T. Liu, Y. Z. Cai, D. Y. Gu, and W. D. Zhang, "New modified smith predictor scheme for integrating and unstable processes with time delay," *IEE Proc Control theory Appl.*, vol. 152(2), pp. 238–246, 2005.

[91] M. Morari and E. Zafiriou, *Robust process control*. Prentice Hall, Englewood Cliffs, 1989.

[92] Y. Lee, S. Oh, and S. Park, "Enhanced control with a general cascade control structure," *Ind. Eng. Chem. Res.*, vol. 41, pp. 2679–2688, 2002.

[93] K. Zhou and J. C.Doyle, *Essentials of Robust Control*. Prentice Hall, Upper Saddle River, 1998.

[94] S. Skogestad, "Simple analytic rules for model reduction and PID controller tuning," *J. Process Control*, vol. 13, pp. 291–309, 2003.

[95] O. Camacho, R. Rojas, and W. García-Gabín, "Some long time delay sliding mode control approaches," *ISA Transactions*, vol. 46, pp. 95–101, 2007.

[96] I. Kaya, "A new smith predictor and controller for control of processes with long dead time," *ISA Transactions*, vol. 42, pp. 101–110, 2003.

[97] ——, "Two-degree-of-freedom IMC structure and controller design for integrating processes based on gain and phase-margin specifications," *IEE Proc Control Theory Appl*, vol. 151(4), pp. 401–407, 2004.

[98] C. C. Hang, Q. G. Wang, and L. S. Cao, "Self-tuning smith predictors for processes with long dead time," *Int. J. Adaptive Signal Proc.*, vol. 9, pp. 255–270, 1995.

[99] S. Majhi and D. P. Atherton, "Modified smith predictor and controller for processes with time delay," *IEE Proc. Control Theory Appl.*, vol. 146(5), pp. 359–366, 1999.

[100] D. G. Padhan and S. Majhi, "Modified smith predictor based cascade control of unstable time delay processes," *ISA Transactions*, vol. 51, pp. 95–104, 2012.

[101] M. L. Luyben and W. L. Luyben, *Essentials of Process Control*. McGraw-Hill, 1997.

[102] D. E. Seborg, T. F. Edgar, and D. A. Mellichamp, *Process Dynamics and Control*. John Wiley & Sons, 2004.

[103] H. P. Huang, I. L. Chien, and Y. C. Lee, "Simple method for tuning cascade control systems," *Chem. Eng. Commun.*, vol. 165, pp. 89–121, 1998.

[104] W. Tan, "Unified tuning of PID load frequency controller for power systems via IMC," *IEEE Trans. on Power systems*, vol. 25 (1), pp. 341–350, 2010.

[105] T. Liu, D. Y. Gu, and W. D. Zhang, "Decoupling two-degree-of-freedom control strategy for cascade control systems," *J Process Control*, vol. 15(2), pp. 159–167, 2005.

[106] M. Vajta, "Some remarks on Padé-approximations," *3rd TEMPUS-INTCOM Symposium, Veszprém, Hungary*, pp. 1–6, September 9–14, 2000.

[107] Q. G. Wang, T. H. Lee, and J. B. He, "Internal stability of interconnected systems," *IEEE Transactions on Automatic Control*, vol. 44(3), pp. 593–596, 1999.

[108] S. Dasgupta, "Kharitonov's theorem revisited," *Systems and Control Letters*, vol. 11 (4), pp. 381–384, 1988.

[109] B. R. Barmish, "A generalization of kharitonov' s four-polynomial concept for robust stability problems with linearly dependent coefficient perturbations," *IEEE Transactions on Automatic Control*, vol. 34(2), pp. 157–165, 1989.

[110] H. Chapellat, M. Dahleh, and S. P. Bhattacharyya, "Robust stability under structured and unstructured perturbations," *IEEE Transactions on Automatic Control*, vol. 35(10), pp. 1100–1108, 1990.

[111] H. Chapellat and S. P. Bhattacharyya, "A generalization of kharitonov's theorem: Robust stability of interval plants," *IEEE Transactions on Automatic Control*, vol. 34(3), pp. 306–311, 1989.

[112] S. P. Bhattacharyya, H. Chapellat, and L. H. Keel, *Robust control: The parametric approach.* Prentice Hall, 1995.

[113] D. G. Padhan and S. Majhi, "Enhanced cascade control for a class of integrating processes with time delay," *ISA Transactions (http://dx.doi.org/10.1016/j.isatra.2012.08.004 (Article in Press))*, 2012.

[114] K. K. Tan, T. H. Lee, and R. Ferdous, "Simultaneous online automatic tuning of cascade control for open loop stable processes," *ISA Transactions,*, vol. 39, pp. 233–242, 2000.

[115] S. Song, W. Cai, and Y. G. Wang, "Auto-tuning of cascade control systems," *ISA Transactions*, vol. 42, pp. 63–72, 2003.

[116] M. V. Sadasivarao and M. Chidambaram, "PID controller tuning of cascade control systems using genetic algorithm," *J. Indian Inst. Sci.*, vol. 86, pp. 343–354, 2006.

[117] A. Visioli and A. Piazzi, "An automatic tuning method for cascade control systems," in *Proceedings of the IEEE International Conference on Control Applications Munich, Germany, October 4-6*, 2006.

[118] O. Arrieta, R. Vilanova, and P. Balaguer, "Procedure for cascade control systems design: Choice of suitable PID tunings," *Int. J. of Computers, Communications & Control*, vol. III(3), pp. 235–248, 2008.

[119] V. M. Alfaro, R. Vilanova, and O. Arrieta, "Robust tuning of two-degree-of-freedom (2-DoF) PI/PID based cascade control systems," *J. of Process Control*, vol. 19, pp. 1658–1670, 2009.

[120] W. Zhang, Y. Xi, G. Yang, and X. Xu, "Design PID controllers for desired time-domain or frequency-domain response," *ISA Transactions*, vol. 41, pp. 511–520, 2002.

[121] S. Majhi and D. P. Atherton, "Autotuning and controller design for processes with small time delays," *IEE Proceedings Control Theory and Applications*, vol. 146 (5), pp. 415–425, 1999.

[122] W. Tan, K. Liu, and P. K. S. Tam, "PID tuning based on loop-shaping H_∞ control," *IEE Proceedings - Control Theory and Applications*, vol. 145 (6), pp. 485–490, 1998.

[123] D. G. Padhan and S. Majhi, "An improved parallel cascade control structure for processes with time delay," *J. of Process Control*, vol. 22, pp. 884–898, 2012.

[124] A. Karimi, D. Garcia, and R. Longchamp, "PID controller tuning using Bode's integrals," *IEEE Trans Control Syst Technol*, vol. 11(6), pp. 812–821, 2003.

[125] A. O'Dwyer, *Handbook of PI and PID Controller Tuning Rules.* Imperial College Press, 2nd Edition, 2006.

[126] K. J. Åström, "Limitations on control system perfromance," *Eur J. Control*, vol. 6(1), pp. 2–20, 2000.

[127] C. Xiang, Q. G. Wang, X. Lu, L. A. Nguyen, and T. H. Lee, "Stabilization of second-order unstable delay processes by simple controllers," *J. Process Control*, vol. 17, pp. 675–682, 2007.

[128] S. C. Lee, Q. G. Wang, and C. Xiang, "Stabilization of all-pole unstable delay processes by simple controllers," *J. Process Control*, vol. 20, pp. 235–239, 2010.

[129] J. E. Normey-Rico and E. F. Camacho, *Control of dead-time processes.* Springer-Verlag London Limited, 2007.

[130] H. Panagopoulos, K. J. Åström, and T. Hägglund, "Design of PID controllers based on constrained optimisation," *IEE Proc.-Control Theory Appl.*, vol. 149 (1), pp. 32–40, 2002.

[131] J. G. Ziegler and N. B. Nichols, "Optimal setting for automatic controllers," *Trans. ASME*, vol. 65, pp. 433–444, 1943.

[132] S. Majhi and D. P. Atherton, "Online tuning of controllers for an unstable FOPDT process," *IEE Proc.-Control Theory Appl.*, vol. 147(4), pp. 421–427, 2000.

[133] D. G. Padhan and S. Majhi, "Synthesis of PID tuning for a new parallel cascade control structure," in *IFAC Conference on Advances in PID Control PID'12, 28-30 March, Brescia, Italy*, 2012.

[134] ——, "A new control scheme for pid load frequency controller of single-area and multi-area power systems," *ISA Transactions (http://dx.doi.org/10.1016/j.isatra.2012.10.003 (Article in Press))*, 2012.

[135] P. Kundur, *Power System Stability and Control*. New York: McGraw-Hill, 1994.

[136] Ibraheem, P. Kumar, and D. P. Kothari, "Recent philosophies of automatic generation control strategies in power systems," *IEEE Trans on power systems*, vol. 20 (1), pp. 346–357, 2005.

[137] P. Agathoklis and M. H. Hamza, "Comparison of three algorithms for load frequency control," *Electric Power Systems Research*, vol. 7, pp. 165–172, 1984.

[138] G. Aly, Y. L. Abdel-Magid, and M. A. Wali, "Load frequency control of interconnected power systems via minimum variance regulators," *Electric Power Systems Research*, vol. 7, pp. 1–11, 1984.

[139] Y. M. Park and K. Y. Lee, "Optimal decentralized load frequency control," *Electric Power Systems Research*, vol. 7, pp. 279–288, 1984.

[140] A. Rubaai and V. Udo, "An adaptive control scheme for load-frequency control of multiarea power systems part I. identification and functional design," *Electric Power Systems Research*, vol. 24, pp. 183–188, 1992.

[141] ——, "An adaptive control scheme for load-frequency control of multiarea power systems part II. implementation and test results by simulation," *Electric Power Systems Research*, vol. 24, pp. 189–197, 1992.

[142] C. Chang and W. Fu, "Area load frequency control using fuzzy gain scheduling of PI controllers," *Electric Power Systems Rescarch*, vol. 42, pp. 145–152, 1997.

[143] G. Ray, A. Prasad, and G. Prasad, "A new approach to the design of robust load-frequency controller for large scale power systems," *Electric Power Systems Research*, vol. 51, pp. 13–22, 1999.

[144] S. Hosseini and A. Etemadi, "Adaptive neuro-fuzzy inference system based automatic generation control," *Electric Power Systems Research*, vol. 78, pp. 1230–1239, 2008.

[145] A. Khodabakhshian and M. Edrisi, "A new robust PID load frequency controller," *Control Engineering Practice*, vol. 16, pp. 1069–1080, 2008.

[146] W. Tan, "Tuning of PID load frequency controller for power systems," *Energy Conversion and Management*, vol. 50, pp. 1465–1472, 2009.

[147] ——, "Decentralized load frequency controller analysis and tuning for multi-area power systems," *Energy Conversion and Management*, vol. 52, pp. 2015–2023, 2011.

[148] W. Tan and Z. Xu, "Robust analysis and design of load frequency controller for power systems," *Electric Power Systems Research*, vol. 79, pp. 846–853, 2009.

[149] R. C. Panda, "Synthesis of PID tuning rule using the desired closed-loop response," *Ind. Eng. Chem. Res.*, vol. 47, pp. 8684–8692, 2008.

[150] H. Bevrani, *Robust Power System Frequency Control*. Springer, 2009.